

UNIVERSITY OF NOTTINGHAM

School of Biosciences

**Control of Wheat Tillering by Nitrogen Availability:
The Case of Strigolactones**

by

Petros Sigalas

Thesis submitted to the University of Nottingham for the degree of
Doctor of Philosophy

July 2022

UNIVERSITY OF NOTTINGHAM

School of Biosciences

Doctor of Philosophy

Control of Wheat Tillering by Nitrogen Availability:
The Case of Strigolactones

By Petros Sigalas

Abstract

Primary plant responses to nutrient-deficient conditions include changes in root and shoot architecture. Above-ground plant architecture is shaped by modulating tillering patterns. Tillering is known to be regulated by the interaction between three classes of phytohormones: auxin, cytokinins (CKs) and strigolactones (SLs). Gene expression analysis showed that nitrogen (N) limitation systematically induced the SL biosynthetic genes in the root and the basal nodes of wheat, whereas N resupply quickly reversed the induction of SL biosynthetic genes. This observation raised questions about the functionality of SLs under N-limiting conditions. Although many studies have focused on the transcriptional and hormonal changes that govern N limitation response in roots, fewer studies have focused on the molecular pathways involved in tillering modulation by N limitation during vegetative plant growth in wheat. RNA-sequencing and phytohormonal analysis in basal nodes of N-limited wheat plants showed that N limitation strongly induced bud dormancy and affected many metabolic and hormonal pathways, including changes in the expression of many N-response master regulators, strong suppression of CK biosynthesis and changes in sugar partitioning and utilization. In addition, the SL metabolic pathway was among the top enriched pathways under N limitation, implying that SLs may be involved in coordinating morphological, physiological, and transcriptional changes in response to N status. To test this hypothesis, a *Tad17* SL-deficient mutant was generated using lines from the hexaploid wheat TILLING population. The phenotypic response of *Tad17* mutants and transcriptomic analysis in the basal nodes showed that SLs are required but are not necessary for tiller inhibition by N limitation. SLs affected CK metabolic genes and CK levels in the basal nodes, however, the lack of SLs was not sufficient to suppress the N limitation mediated decline in CK levels, which contributed to tiller suppression under N limitation. However, lack of SL biosynthesis and imbalance in tillering regulation affected plant adaptation to N-limiting conditions. *Tad17* mutant showed changes in resource allocation between root and shoot, N remobilization and the regulation of master regulators of N-response, suggesting that SLs are required for the fine-tune regulation of the N limitation transcriptional network. The genetic information and the results presented regarding the role of SLs in wheat growth and development set the foundation for and highlighted the potential of manipulation of SL metabolism in order to improve wheat architecture or nutrient use efficiency for increasing wheat crop productivity.

Acknowledgements

Firstly, I would like to thank my principal supervisor, Malcolm Hawkesford, for giving me this opportunity, supporting and guiding me throughout this journey and through hard times, giving me access to unlimited resources and for showing me his trust from the first day. Thank you, Malcolm, for everything and for keeping showing your trust in me and allowing me to develop further as a scientist. Of course, would like to acknowledge Peter Buchner, who was always there whenever I needed his help and for passing me down his many years of molecular biology experience. In addition, I would like to thank Steve Thomas for his excellent guidance and advice in the generation of wheat mutant lines. I also wish to thank my university supervisor, Malcolm Bennett, for being a very nice advisor and always very inspiring and motivating.

I would also like to thank everyone in Hawkesford's group for making the 4.5 years of my PhD enjoyable. Thank you all for welcoming me to the group from the first day. Of course, special thanks to the "special field force" – Andrew, March, David, Nicolas and many others over the years – for helping me with my field trials under rain or the hot sun. I hope I have paid back all your hard work! In addition, I would like to thank Yongfang Wan for her company in the lab and also for kindly performing for me the *in situ* hybridization. Huge thanks also to Keywan Hassani-Pak and his bioinformatics team for introducing me to the world of transcriptomics, helping me to become a more independent bioinformatic user and helping me resolve every problem I faced with my RNA-seq data. I would also like to thank Andy Phillips for his advice on the wheat mutant generation and for providing me with *Tad14* mutant seeds.

I would also like to acknowledge Groupe Roullier for fully funding this PhD project and helping me make my dream possible. I would like to personally thank Frank Jamois, Mustapha Arkoun and Jean-Claude Yvin for their contribution to the project and for showing their trust. My time at the Centre Mondial de l'Innovation Roullier in Saint-Malo was one of my PhD highlights, so thank you for your hospitality and this opportunity. For sure, I will miss our enjoyable dinners after each in-person meeting.

Many thanks to my family, Dad, Mum and sister Evangelia for their support not only during my PhD but since the first day of my life. No matter how hard it was for them to see me moving abroad, they never stopped supporting and caring about me. Also, thanks to my friends – Thanasis and Giannis – who, despite the distance, helped me keep my sanity and for our endless discussion about our hobby. In addition, thanks to Lisa, who, without realizing it, helped me fulfil my social need during the writing-up period.

Lastly and foremost, I would like to thank my partner, Marilou, for believing in me since the first day I applied for the PhD, for being by my side and giving me strength all those years, and of course, for proofreading all my reports and my thesis. All this work belongs to us! Now it is your time to make your dream come true!

Declaration of original authorship

Declaration: I confirm that this work was conducted by me and the use of all material from other sources has been properly and fully acknowledged.

Petros Sigalas

Table of Contents

Abstract	i
Acknowledgements	iii
Declaration of original authorship	v
Table of Contents	vii
List of Figures	xv
List of Tables	xxii
Abbreviations.....	xxiv
Chapter 1 Introduction	1
1.1. A Tale of a Growing Tiller	1
1.1.1 Tillering Pattern	2
1.1.2 Tiller Formation	3
1.1.3 Tillering Cessation.....	10
1.1.4 Tiller Abortion/Senescence	12
1.1.5 Tiller Fertility.....	14
1.2. A Brief History of Strigolactones	16
1.1.6 Strigolactone Biosynthesis.....	18
1.1.7 Strigolactone Transport	22
1.1.8 Strigolactone Perception and Signalling.....	26
1.1.9 TB1-dependent Action of SLs in Tillering Control.....	27
1.1.10 TB1-independent Action of SLs in Tillering Control	28
1.3. Tillering Control by Nitrogen Limitation	31
1.1.11 Nitrogen Availability as a Signal	32
1.1.12 Cytokinins as Signal under N Limitation	34
1.1.13 Strigolactones as Signal under N Limitation	39

1.1.14 Auxin as Signal under N Limitation.....	41
1.4. Thesis Objectives.....	43
Chapter 2 Materials and Methods	45
2.1 Hydroponic Experiments.....	45
2.1.1 Hydroponic Culture	45
Hydroponic System 1	45
Hydroponic System 2	45
2.1.2 Nutrient Solution Composition.....	46
2.1.3 Experimental Design: N Limitation and N Induction Time Course Analysis	47
2.1.4 Experimental Design: N and P Limitation Transcriptional Changes	49
2.1.5 Experimental Design: Involvement of SL in Regulating Tiller Suppression under N Limitation.....	49
2.1.6 Experimental Design: Effect of Microalgae-based Biostimulant on Wheat Growth and Development	51
2.2 Phenotyping and Sampling.....	52
2.2.1 Tiller Counting.....	52
2.2.2 Fresh and Dry Weight	52
2.2.3 Chlorophyll Content – SPAD	52
2.2.4 Tissue Harvesting/Sampling	52
2.3 Molecular Biology.....	53
2.3.1 DNA Extraction	53
2.3.2 RNA Extraction.....	53
TRizol Extraction Method	54
Hot Phenol Extraction Method	55
Other RNA extraction Methods	56
2.3.3 Nucleic Acid Determination.....	56

2.3.4 cDNA Synthesis	56
2.3.5 Polymerase Chain Reaction (PCR)	57
2.3.6 PCR Product Purification	58
2.3.7 Gel Electrophoresis.....	58
2.3.8 Genotyping	59
Genotyping by Sequencing	59
Kompetitive Allele Specific PCR (KASP) Genotyping.....	60
2.3.9 Real-Time qPCR.....	61
2.3.10 Real-Time qPCR Data Analysis	61
2.3.11 High-throughput RNA-sequencing	62
2.4 Bioinformatic Analysis.....	64
2.4.1 Identifying Wheat Orthologue Genes	64
2.4.2 Sequence Alignment and Phylogenetic Analysis.....	64
2.4.3 Primer Design	64
Homoeologue-Specific Primers.....	64
Quantitative reverse-transcription PCR Primers	65
2.4.4 RNA-sequencing Workflow.....	66
2.5 Metabolomic Analysis	69
2.5.1 Cytokinin Extraction.....	69
2.5.2 Other Phytohormone Extraction	69
2.5.3 UHPLC-MS/MS.....	70
2.5.4 Sugar Analysis	71
2.6 Chemical Analysis	71
2.6.1 Total Nitrogen Analysis.....	71
2.6.2 Elemental Analysis.....	71
2.7 Wheat TILLING Mutant Generation	72

2.7.1 Screening of EMS Mutagenized Lines.....	72
2.7.2 Plant Material and Growth Conditions.....	72
2.7.3 Wheat Crossing.....	73
2.8 Statistical Analysis	74
2.9 Data Availability.....	75
Chapter 3 Transcriptional Regulation of Strigolactone Biosynthesis, Perception and Signalling by Plant Nitrogen Supply	77
3.1 Introduction.....	77
3.1.1 Background	77
3.1.2 Chapter Objectives	78
3.2 Results	79
3.2.1 Identification of Wheat Homoeologue Genes Involved in SL Biosynthesis, Perception and Signalling	79
3.2.2 Effect on N Limitation on Wheat Tillering	84
3.2.3 Time-course Analysis of SL Biosynthetic and Perception Gene Expression in Root in Response to N Limitation	86
3.2.4 Time-course Analysis of SL Biosynthetic and Perception Gene Expression in Basal Nodes in Response to N Limitation	89
3.2.5 Transcriptional Response of SL Biosynthetic and Perception Genes in Root to N Resupply.....	92
3.2.6 Expression Pattern of Wheat <i>MAX1</i> Genes in Root and Basal Nodes.....	95
3.3 Discussion	98
3.3.1 SL Biosynthesis and Signalling Genes Regulated by N Supply.....	98
3.3.2 <i>TB1</i> Induction by N Limitation in Wheat	100
3.3.3 Distinct Expression Profiles of Wheat <i>MAX1</i> genes	101
Chapter 4 Transcriptional and Phytohormonal Changes in Basal Nodes of Wheat Grown under Low Nitrogen and Low Phosphorus Conditions	105

4.3.2 Tissue-specific Regulation of SL Biosynthetic and Signalling Genes by Nutritional Signals.....	160
Chapter 5 Generation and Functional Characterisation of a Strigolactone-deficient Mutant.....	163
5.1 Introduction.....	163
5.1.1 Background.....	163
5.1.2 Carotenoid Cleavage Oxygenase/Dioxygenase.....	163
5.1.3 Expression Pattern of <i>TaD17</i> in Wheat.....	166
5.1.4 Targeting Induced Local Lesions in Genomes (TILLING).....	168
5.1.5 Chapter Objectives.....	169
5.2 Results.....	170
5.2.1 Identification of Wheat Candidate Genes for the Generation of an SL-deficient Mutant.....	170
5.2.2 Identification of Mutations within <i>TaD17</i> Homoeologous Sequences.....	171
5.2.3 Identification of Conserved Amino Acid Residues in Wheat D17/CCD7...	173
5.2.4 Genotyping of the M4 Generation.....	177
5.2.5 Design and Optimisation of KASP Assays for the Targeted Mutation Sites.....	180
5.2.6 Stacking of <i>TaD17</i> Mutant Alleles.....	182
5.2.7 BC1F2 <i>Tad17</i> Mutants Showed Increased Tillering Phenotype.....	185
5.2.8 Phenotyping of <i>Tad17</i> Mutant under High and Low N Conditions.....	187
5.2.9 RNA-sequencing in Basal Nodes of the <i>Tad17</i> Mutant under High and Low N Conditions.....	191
5.2.10 Transcriptional Changes in Basal Nodes of <i>Tad17</i> Compared to WT Revealed Greater Changes under N Limiting Conditions.....	193
5.2.11 Validation of RNA-sequencing Results.....	196

5.2.12 Functional Annotation Enrichment Analysis of the Transcriptional Changes in <i>Tad17</i> Basal Nodes.....	197
5.2.13 <i>Tad17</i> Mutants Showed Suppression of Genes Involved in Photosynthesis	202
5.2.14 Transcriptional Response of SL Metabolic Genes in Basal Nodes of <i>Tad17</i>	203
5.2.15 Response of <i>DRM</i> Genes and <i>TB1</i> in Basal Nodes of <i>Tad17</i> Mutant	206
5.2.16 SLs Affect Tre6P and Sugar Signalling Genes in Basal Nodes	209
5.2.17 <i>Tad17</i> Showed Altered Expression of Amino Acid Metabolism Genes, Predominately of Gln and Asn.....	211
5.2.18 N-limited <i>Tad17</i> Showed Significant Changes in N-responsive Genes ...	213
5.2.19 Functional Annotation Enrichment Analysis of N-responsive Genes Affected in <i>Tad17</i>	215
5.2.20 SLs Affected the Transcriptional Regulation of CK Metabolic and Signalling Genes to N Limitation.....	219
5.2.21 SLs are Required for Nutrient and Carbohydrate Remobilization under N-limiting Conditions.....	221
5.2.22 SLs affect the Transcriptional Response of GA Biosynthetic Genes to N Limitation.....	225
5.2.23 Interaction Between SL and IAA under N-limiting Conditions	226
5.2.24 SLs Control the Expression of Different N-response Master Regulators	228
5.2.25 Cytokinin Analysis in Basal Nodes of <i>Tad17</i> Mutant under High and Low N Conditions.....	231
5.2.26 Sugar Analysis in Crown of <i>Tad17</i> Mutant under High and Low N Conditions	233
5.2.27 Elemental Analysis in Root and Shoot of <i>Tad17</i> Mutant under High and Low N Conditions	235

5.3 Discussion	238
5.3.1 Mutant D17/CCD7 Protein Functionality	238
5.3.2 Is <i>Tad17</i> Mutant SL-deficient?.....	239
5.3.3 <i>TaD17</i> Is Involved in Tillering Regulation in Wheat.....	241
5.3.4 SLs Are Required But Are Not the Only Signal Controlling Tillering in Response to N Availability	248
5.3.5 SLs Affect Resource Allocation under N-limiting Conditions	249
5.3.6 SL and CK Interaction.....	252
Chapter 6 General Discussion	257
6.1 Introduction.....	257
6.2 Future Perspective	257
6.2.1 Shoot Architecture.....	257
6.2.2 Plant Response to Nutrient-limiting Conditions.....	259
6.2.3 Strigolactone Structural Diversity.....	262
Appendix A: RT-qPCR Primer Efficiency Test	265
Appendix B: Differential Gene Expression Analysis R Script (DESeq2)	266
Appendix C: List of Orthologous SL-related Sequences	272
Appendix D: Selected Differentially Expressed Genes under Low N	275
Appendix E: <i>Tad17</i> Mutant RNA-sequencing Supplementary Data	280
Appendix F: RNA-seq Validation Test	282
Appendix G: Additional GO and KEGG Enrichment Analysis.....	283
Appendix H: Expression of <i>TaNIGT1</i> in Basal Nodes and Root of <i>Tad17</i>	284
Appendix I: Phenotype of <i>Tad17</i> (BC1F3) and <i>Tad14</i> (BC3F3) triple knock-out Mutant in Three Different N Levels	285
References	287

List of Figures

Chapter 1

Figure 1.1: Growth stages and tillering dynamics in a winter wheat crop.....	3
Figure 1.2: Two current models of the hormonal regulation of lateral bud outgrowth. (A) Second messenger model. (B) Canalization model.....	4
Figure 1.3: Different roles of the main hormonal signals at different stages of bud outgrowth.	6
Figure 1.4: Model integrating hormonal and sugar availability control of bud outgrowth.	9
Figure 1.5: The many roles of SLs as rhizosphere signals and as plant hormones.....	17
Figure 1.6: Structures of characteristic naturally occurring SLs.	19
Figure 1.7: SL biosynthetic pathway. (A) The compartmentalisation of SL biosynthetic pathway. (B) Steps downstream of CL for the biosynthesis of canonical and non-canonical SLs.	22
Figure 1.8: Schematic illustration of grafting experiments conducted in <i>A. thaliana</i> SL biosynthesis mutants proving that SLs act as long-distance signals.	24
Figure 1.9: SL perception and signalling pathway.	28
Figure 1.10: Simplified CK biosynthetic pathway.	35

Chapter 2

Figure 2.1: Different hydroponic culture systems used in the hydroponic experiments.	46
Figure 2.2: Experimental timeline of N limitation and N induction hydroponic experiments.	48
Figure 2.3: Schematic representation of WT and <i>Tad17</i> mutant lines used in the hydroponic experiment.	50
Figure 2.4: Example of gel electrophoresis of total RNA.	59

Figure 2.5: Schematic illustration of the RNA sequencing workflow starting from the sampled material until the differential gene expression analysis.....	68
---	----

Chapter 3

Figure 3.1: Phylogenetic analysis of wheat D17 and D10 proteins.	80
Figure 3.2: Phylogenetic analysis of wheat MAX1 homologs.....	82
Figure 3.3: Phylogenetic analysis of wheat D53 proteins.....	83
Figure 3.4: Effect of N limitation on wheat tillering..	86
Figure 3.5: Time-course analysis of the gene expression levels of SL biosynthetic (<i>TaD27</i> , <i>TaD17</i> , <i>TaD10</i> , <i>TaMAX1a1</i> , <i>TaMAX1a2</i> , <i>TaMAX1c</i> and <i>TaMAX1d</i>) and perception genes (<i>TaD3</i> and <i>TaD14</i>) in root of wheat 0, 4, 8 and 12 days after N limitation (0.1 mM N) compared to high N treatment (10 mM N)..	88
Figure 3.6: Time-course analysis of the gene expression levels of SL biosynthetic (<i>TaD27</i> , <i>TaD17</i> , <i>TaD10</i> , <i>TaMAX1a1</i> , <i>TaMAX1a2</i> , <i>TaMAX1c</i> and <i>TaMAX1d</i>) and perception genes (<i>TaD3</i> and <i>TaD14</i>) in the basal node (0.5 cm of main shoot base) of wheat 0, 4, 8 and 12 days after N limitation (0.1 mM N) compared to high N treatment (10 mM N)..	90
Figure 3.7: Time-course analysis of the gene expression levels of transcription factors <i>TaTB1</i> and <i>TaGT1</i> in the basal node (0.5 cm of main shoot base) of wheat 4, 8 and 12 days after N limitation (0.1 mM N) compared to high N treatment (10 mM N).....	91
Figure 3.8: Time-course analysis of the gene expression levels of SL biosynthetic (<i>TaD27</i> , <i>TaD17</i> , <i>TaD10</i> , <i>TaMAX1a1</i> , and <i>TaMAX1d</i>) and signalling genes (<i>TaD3</i> and <i>TaD14</i>) in the root of wheat before (0h), 24h and 72h after the N resupply.....	94
Figure 3.9: Expression data of wheat <i>MAX1</i> genes from RNA-seq experiments in root and basal nodes.	97

Chapter 4

Figure 4.1: Effect of N and P limitation on wheat tillering..	110
Figure 4.2: Principal component analysis based on the differential gene expression analysis results of N and P limitation effect in the basal node.....	113

Figure 4.3: Volcano plot of the differential gene expression analysis of the effect of (A) N and (B) P limitations compared to the control.....	114
Figure 4.4: RNA-seq validation test results.....	115
Figure 4.5: GO term enrichment analysis of the differentially expressed genes in the basal node of wheat grown under N limitation for 8 days.....	117
Figure 4.6: GO term enrichment analysis of the differentially expressed genes in the basal node of wheat grown under P limitation for 8 days.	118
Figure 4.7: KEGG pathway enrichment analysis of the differentially expressed genes (Top) by N limitation and (Bottom) by P limitation in the basal node of wheat grown under the respective nutrient limitation for 8 days.	120
Figure 4.8: Percentage of expressed TFs that were significantly DE in N-deficient basal nodes per TF family.....	129
Figure 4.9: Heatmap of differentially expressed transcription factors in the basal node of wheat grown under N limitation for 8 days based on the RNA-seq data.	131
Figure 4.10: Heatmap of differentially expressed SL- and CK-related genes in the basal node of wheat grown under N limitation for 8 days based on the RNA-seq data. ...	136
Figure 4.11: Heatmap of differentially expressed ABA- and auxin-related genes in the basal node of wheat grown under N limitation for 8 days based on the RNA-seq data.	138
Figure 4.12: Heatmap of differentially expressed other hormone-related genes in the basal node of wheat plants grown under N limitation for 8 days based on the RNA-seq data.	140
Figure 4.13: Heatmap comparison of SL biosynthetic and signalling gene transcript levels in the basal node of wheat grown under N and P limitation for 8 days based on the RNA-seq data.	142
Figure 4.14: Gene expression levels of SL biosynthetic (<i>TaD27</i> , <i>TaD17</i> , <i>TaD10</i> , <i>TaMAX1a1</i> , <i>TaMAX1a2</i> , <i>TaMAX1c</i> and <i>TaMAX1d</i>) and signalling genes (<i>TaD3</i> and	

<i>TaD14</i>) in the root of wheat grown under N and P limitation for 8 days based on RT-qPCR data.....	144
Figure 4.15: Heatmap comparison of analysed phytohormones in roots, basal node and shoot of wheat grown under N and P limitation for 8 days.	150
Figure 4.16: Summary of changes observed in the basal nodes of N-limited plants, which might be associated with tiller suppression and the general plant adaptation to N-limiting conditions.....	153

Chapter 5

Figure 5.1: Simplified biosynthetic pathway of the main apocarotenoid signalling molecules, SLs and ABA.	165
Figure 5.2: <i>In situ</i> hybridization analysis of <i>TaD17</i> in root and the basal node of wheat.	167
Figure 5.3: Position of the selected mutations within the genomic sequence of <i>TaD17</i> homoeologues.	173
Figure 5.4: Nucleotide and amino acid sequence alignment of the WT <i>TaD17</i> homoeologues with the corresponding selected loss-of-function mutant lines.	173
Figure 5.5: Protein alignment of members of the CCD/CCO family from various plant species, including <i>TaD17-2A</i> , <i>-2B</i> and <i>-2D</i>	175
Figure 5.6: (A) Predicted overall structure and (B) active site of <i>TaD17-2A</i> (<i>D17/CCD7</i>) enzyme.....	177
Figure 5.7: Gel electrophoresis of gradient PCR products for the identification of the best annealing temperature for each pair of primers.	178
Figure 5.8: (A) <i>Cad1738</i> , (B) <i>Cad1271</i> and (C) <i>Cad0880</i> genotyping by sequencing results.....	179
Figure 5.9: Designed KASP assays for genotyping of the selected mutant alleles. ...	181
Figure 5.10: Allelic discrimination plots for the designed KASP assays using samples with known genotypes (positive controls) for testing the efficiency and specificity of the KASP assay.	182

Figure 5.11: Followed crossing scheme to stack the selected <i>Tad17</i> mutant alleles in one individual plant..	184
Figure 5.12: Number of shoots at ear emergence and number of ears at final harvest per plant in triple <i>Tad17</i> mutants (aabbdd) and WT segregant lines (AABBDD).	186
Figure 5.13: Phenotype of <i>Tad17</i> TILLING mutant lines from two different BC1F2 populations.	187
Figure 5.14: Images of 3-week-old representative plants of triple <i>Tad17</i> mutants (aabbdd) in comparison to WT segregant (AABBDD) grown under high N (10 mM) or low N (0.1 mM) conditions for 12 days.	188
Figure 5.15: Phenotypic responses of triple <i>Tad17</i> mutants (aabbdd) to N supply compared to WT segregant plants (AABBDD).	190
Figure 5.16: Principal component analysis based on the differential gene expression analysis results of genotype (<i>Tad17</i> , WT) and N treatment (High N, Low N) effects.	192
Figure 5.17: Volcano plot of the differential gene expression analysis of the effect of <i>Tad17</i> knock-out (A) under high N and (B) under low N conditions and N limitation effect in (C) WT segregant and (D) <i>Tad17</i> mutant.	195
Figure 5.18: RNA-seq validation test results.	196
Figure 5.19: Molecular Function (MF) GO term enrichment analysis of the differentially expressed genes in the basal node of <i>Tad17</i> mutant (aabbdd) compared to WT segregant (AABBDD).	199
Figure 5.20: Biological Process (BP) GO term enrichment analysis of the differentially expressed genes in the basal node of <i>Tad17</i> mutant (aabbdd) compared to WT segregant (AABBDD).	200
Figure 5.21: KEGG pathway enrichment analysis of the differentially expressed genes in the basal node of <i>Tad17</i> mutant (aabbdd) compared to WT segregant (AABBDD).	201

Figure 5.22: Transcriptional regulation of SL-related genes in the basal node of <i>Tad17</i> mutant (aabbdd) and WT segregant (AABBDD) grown under high N (10 mM) or low N (0.1 mM) conditions for 8 days based on the RNA-seq data.....	205
Figure 5.23: Expression of <i>TB1</i> and <i>DRM</i> genes in the basal node of <i>Tad17</i> mutant (aabbdd) and WT segregant grown under high N (10 mM) or low N (0.1 mM) conditions for 8 days.....	208
Figure 5.24: Heatmap of selected differentially expressed genes involved in Tre6P and carbohydrate metabolism and sugar signalling in the basal node of <i>Tad17</i> mutant (aabbdd) and WT segregant grown under high N (10 mM) or low N (0.1 mM) conditions for 8 days.....	210
Figure 5.25: Heatmap of differentially expressed genes involved in Gln and Asn metabolism in the basal node of <i>Tad17</i> mutant (aabbdd) and WT segregant grown under high N (10 mM) or low N (0.1 mM) conditions for 8 days.	213
Figure 5.26: Effect of SLs on the transcriptional regulation of N-responsive genes.	215
Figure 5.27: (A) Biological Process (BP) GO term and (B) KEGG enrichment analysis of the differentially expressed N-responsive genes in the basal node of <i>Tad17</i> mutant under low N conditions.....	218
Figure 5.28: Heatmap of differentially expressed genes involved in CK biosynthesis, homeostasis and signalling in the basal node of <i>Tad17</i> mutant (aabbdd) grown under low N (0.1 mM) conditions for 8 days.....	221
Figure 5.29: Heatmap of various N-responsive transporters significantly differentially expressed in the basal node of <i>Tad17</i> mutant (aabbdd) grown under low N (0.1 mM) conditions for 8 days.....	223
Figure 5.30: Heatmap of significantly differentially expressed genes involved in GA metabolism in the basal node of <i>Tad17</i> mutant (aabbdd) grown under low N (0.1 mM) conditions for 8 days.....	226
Figure 5.31: Heatmap of differentially expressed genes involved in Trp and IAA biosynthesis, IAA homeostasis, transport and signalling in the basal node of <i>Tad17</i> mutant (aabbdd) grown under low N (0.1 mM) conditions for 8 days.	228

Figure 5.32: Heatmap of genes encoding master regulators (TF) of N response which were found to be differentially expressed in the basal node of <i>Tad17</i> mutant (aabbdd) grown under low N (0.1 mM) conditions for 8 days.....	231
Figure 5.33: CK concentration in the basal node of triple <i>Tad17</i> mutant (aabbdd) and WT segregant grown on high N (10 mM) or low N (0.1 mM) conditions for 8 days (18 DAS).....	233
Figure 5.34: Sugar content (Glc, Fru, sucrose and starch) in the crown of 3-week-old triple <i>Tad17</i> mutant (aabbdd) and WT segregant grown on high N (10 mM) or low N (0.1 mM) conditions for 12 days.....	234
Figure 5.35: Macronutrient concentration (N, P, K and S) in root and shoot of triple <i>Tad17</i> mutant (aabbdd) and WT segregant grown on high N (10 mM) or low N (0.1 mM) conditions for 8 days (18 DAS).	237
Figure 5.36: Protein alignment of the <i>T. aestivum</i> proteins sequences of D17/CCD7-2A, -2B and -2D and the mutant protein of the selected TILLING lines Cad1738, Cad1271 and Cad0880.	239

Appendix

Figure S1: RT-qPCR primer efficiency test by using a dilution series of cDNA from root and shoot total RNA samples. Efficiency was calculated based on the slope of the standard curve.	265
Figure S2: Sample distance matrix based on the differential gene expression analysis performed by DESeq2.	281
Figure S3: Validation test of RNA-seq results in <i>Tad17</i> basal nodes under two different N levels.....	282
Figure S4: Biological Process (BP) GO term and KEGG enrichment analysis per cluster (1-4) of the differentially expressed N-responsive genes in the basal node of <i>Tad17</i> mutant under low N conditions.....	283
Figure S5: Expression of wheat orthologues of NIGT1 in the basal node and root of <i>Tad17</i> mutant (aabbdd) and WT segregant grown under high N (10 mM) or low N (0.1 mM) conditions for 8 days.	284

Figure S6: Number of shoots of <i>Tad17</i> SL-deficient (BC1F3) and <i>Tad14</i> SL-insensitive mutants (BC3F3) grown under three different N regimes (Low, Mid and High N) compared to the respective WT segregant lines.....	285
---	-----

List of Tables

Chapter 2

Table 2.1: Primer sequences for each of the three homoeologues of <i>TaD17</i> and optimized PCR parameters used for genotyping of the mutant lines by sequencing.	57
Table 2.2: Reagent used for Q5 polymerase PCR reaction setup.....	58
Table 2.3: Primer sequences used for KASP genotyping.	61
Table 2.4: Primer sequences of genes used as reference genes for relative gene expression analysis.	62
Table 2.5: Experimental details of next-generation RNA-sequencing projects.....	63
Table 2.6: Forward and reverse primer sequences designed and used for the gene expression analysis by RT-qPCR.....	66

Chapter 4

Table 4.1: RNA-sequencing raw data analysis statistics.	112
Table 4.2: Concentration of different CKs (pg/mg) in the root, basal node and shoot of wheat grown under Control (10 mM N and 1 mM P), Low N (0.1 mM N) and Low P (0.01 mM P) conditions.....	147
Table 4.3: ABA, PA, DPA and IAA concentration (pg/mg) in the root, basal node and shoot of wheat grown under Control (10 mM N and 1 mM P), Low N (0.1 mM N) and Low P (0.01 mM P) conditions.	148

Chapter 5

Table 5.1: Summary of the available hexaploid wheat TILLING mutants in the protein-coding region of SL core biosynthetic genes, <i>TaD27</i> , <i>TaD17</i> and <i>TaD10a</i>	171
---	-----

Table 5.2: Mutant line IDs with a stop-gained mutation in the protein-coding region of *TaD17* homoeologues..... 172

Appendix

Table S1: List of gene accession numbers (GeneID) of SL biosynthetic (D27, D17 and D10) orthologous protein sequences used for the phylogenetic analysis. 272

Table S2: List of gene accession numbers (GeneID) of MAX1 orthologous protein sequence used for the phylogenetic analysis..... 273

Table S3: List of gene accession numbers (GeneID) of SL perception (D3, D14) and signalling (D53, TB1) orthologous protein sequences used for the phylogenetic analysis..... 274

Table S4: Selected differentially expressed genes in the basal node of wheat grown under N limitation for 8 days based on the RNA-seq data..... 275

Table S5: RNA-sequencing raw data analysis statistics 280

Abbreviations

1'-OH-MeCLA - hydroxymethyl-carlactonoate	CL - carlactone
4DO - 4-deoxyorobanchol	CLA - carlactonoic acid
5DS - 5-deoxystrigol	CO - CONSTANS
AAO - abscisic-aldehyde oxidase	cwINV - cell wall invertase
AAP - amino acid permease	cZ - cis-zeatin
AAT - amino acid transporter	D - DWARF
ABA - abscisic acid	DAS - days after sowing
ABC - ATP-binding cassette	DE - differentially expressed
ABF - abscisic acid-responsive element binding factors	DEPC – diethyl pyrocarbonate
ACT - actin	DHZ - dihydro-zeatin
Ala - alanine	DPA - dihydrophaseic acid
AMF - arbuscular mycorrhizal fungi	DRM - DORMANCY-ASSOCIATED PROTEIN-LIKE
ANOVA - analysis of variance	DW - dry weight
AP2 - APETALA2	EMS - ethyl methanesulfonate
Asn - asparagine	FC - fold change
ASN - asparagine synthetase	FC1 - FINE CULM 1
Asp - aspartic acid	FPK - fructokinase
ASPG - asparaginase	FRET - fluorescence resonant energy transfer
ATL – amino acid transporter-like	Fru - fructose
BP - biological process	GAs - gibberellins
BR - brassinosteroid	Glc - glucose
BRC1 - BRANCHED 1	Gln - glutamine
C - carbon	Glu - glutamic acid
CCD - carotenoid cleavage dioxygenase	GO - gene ontology
CCO - carotenoid cleavage oxygenase	GOGAT - glutamate synthase
cdNA - complementary DNA	GS - glutamine synthetase
CDS - protein-coding region	GT1 - GRASSY TILLER 1
CKs - cytokinins	HC - high-confidence
CKX - CYTOKININ OXIDASE/DEHYDROGENASE	HD-ZIP - homeodomain leucine zipper
	HHO - HRS1 HOMOLOG

HK - His-protein kinase
HP - His-containing phosphotransferase protein
HTD1 - HIGH TILLERING AND DWARF 1
IAA - indole-3-acetic acid
IGL - indole-3-glycerol phosphate lyase
IGPS - indole-3-glycerol phosphate synthase
Ile - isoleucine
iP - N⁶-(Δ^2 -isopentenyl)adenine
iPA - isopentenyl adenosine
IPA1 - IDEAL PLANT ARCHITECTURE 1
IPT - adenosine phosphate isopentenyl transferase
JA - jasmonic acid
KASP - kompetitive allele-specific PCR
KO - KEGG Orthology
LBD - LATERAL ORGAN BOUNDARIES
LBO - LATERAL BRANCHING OXYDOREDUCTASE
LC - low-confidence
Leu - leucine
LGS1 - LOW GERMINATION STIMULANT1
LN2 - liquid nitrogen
LOG - LONELY GUY
LSD - Fisher's least significant difference
MAX - MORE AXILLARY MERISTEM
Me-CLA - methyl-carlactonoate
Met - methionine
MF - molecular function
MOC1 - monoculm 1
N - nitrogen
NCED - 9-cis-epoxycarotenoid dioxygenase
NF-Y - Nuclear Factor Y
NGR5 - N-mediated tiller growth response
NGS - Next-Generation Sequencing
NH₄⁺ - ammonium
Nhd1 - N-mediated heading date 1
NIGT1 - NITRATE-INDUCIBLE GARP-TYPE TRANSCRIPTIONAL REPRESSOR 1
NiR - nitrite reductase
NLP - NIN-like protein
NO₃⁻ - nitrate
NPF - nitrate transporter 1/peptide family
NR - nitrate reductase
NRQ - Normalized Relative Quantity
NRT2 - high-affinity nitrate transporters
NUE - nitrogen use efficiency
P - phosphorus
PA - phaseic acid
padj – p-value adjusted for multiple comparisons
PATS - polar auxin transport system
PCR - polymerase chain reaction
PDR1 - PLEIOTROPIC DRUG RESISTANCE1
Phe - phenylalanine
phyB - phytochrome B
PIN - PIN-FORMED
PNR - primary nitrate response
PP2Cs - protein phosphatases 2C
R: FR - red to far-red ratio
RNA-seq - RNA-sequencing

RR - response regulator

RT-qPCR - quantitative reverse-transcription PCR

SAURs - SMALL AUXIN UPREGULATED RNAs

SCF - Skp1-Cullin-F-box

SD1 - Semidwarf 1

SDH - succinate dehydrogenase

SE - standard error

SLs - strigolactones

SMXL - SUPPRESSOR OF MAX2 1-LIKE

SNP - single nucleotide polymorphism

SnRK1 - sucrose non-fermented kinase 1

SOC - SUPPRESSOR OF CONSTANS

SPL - SQUAMOSA promoter-binding protein-like

SPS - sucrose phosphate synthase

SPS - sucrose-phosphate synthase

SUC - sucrose synthetase

SuSy - sucrose synthase

SUT - sucrose transporter

SWEET - Sugars will eventually be exported transporters

TB1 - TEOSINTE BRANCHED1

TCA - tricarboxylic acid

TF - transcription factor

TILLING - Targeting Induced Local Lesions in Genomes

tin - tiller inhibition

TPM - transcripts per million mapped reads

TPP - trehalose-6-phosphate phosphatase

TPS - trehalose-6-phosphate synthase

Tre6P - trehalose 6-phosphate

TS - tryptophan synthase-related protein

TSA1 - tryptophan synthase

tZ - trans-zeatin

UHPLC-MS/MS - Ultra-high performance liquid chromatography-tandem mass spectrometry

UPS - ureide permease

Val - valine

VP14 - Viviparous14

WT – wild-type

Chapter 1 Introduction

1.1. A Tale of a Growing Tiller

Tillering is an important agronomical trait in cereal crops such as wheat (*Triticum spp.*), barley (*Hordeum vulgare*) and rice (*Oryza sativa*) as it affects key traits, such as canopy formation, which impacts on the photosynthetic capacity. The number of tillers determines the number of spikes per unit area, which along with the number of spikelets per spike and the grain size, comprise the main yield components in cereal crops (Slafer et al., 1996, Slafer et al., 2014). Despite negative correlations between wheat yield components, several studies have shown an increase in yield with increasing spike population, underlining the importance of the manipulation of tiller development and survival in cereals (Bulman and Hunt, 1988, Harasim et al., 2016). In addition, in the early developmental stages, adequate tillering improves canopy light interception by affecting ground coverage, while it also improves competition against weeds. However, excessive tillering may result in yield reduction due to ineffective use of available resources, a phenomenon that is especially apparent under stress conditions (Kebrom et al., 2012). For instance, under water-limiting conditions, reduced-tillering *tiller inhibition (tin)* wheat lines have been shown to perform better and achieve higher yields (Mitchell et al., 2013). Under stress conditions, low tillering appears to ensure more assimilates per plant for spike formation and grain filling, leading to heavier spikes and larger grains. Another example in which a low tillering phenotype is accompanied by higher productivity is modern maize (*Zea mays*) compared to its ancestor, *teosinte*, which is highly branched (Doebley et al., 2006).

Naturally, plants have developed mechanisms to interpret a plethora of environmental stimuli and control overall plant architecture in such a way as to optimise their growth. As a result, tillering is influenced by various environmental and agronomic factors. For instance, planting density strongly affects tillering pattern (Darwinkel, 1978). This mechanism is driven by the competition of neighbouring plants for photosynthetically active radiation through a mechanism controlled by the red to far-red ratio (R: FR)

signalling pathway (Finlayson et al., 2010). In high plant densities, plants tend to form fewer tillers, while individually cultivated plants develop a more bushy phenotype.

Additionally, tillering is strongly influenced by mineral nutrient availability and, more specifically, by nitrogen (N) and phosphorus (P) levels, which are limiting factors for plant growth. During early developmental stages, both macro-nutrient deficiencies negatively affect tiller formation, resulting in a lower number of shoots per unit area, while nutrient limitation at later stages can lead to a high tiller death rate. In contrast, the application of N fertiliser stimulates lateral shoot formation and increases the tiller survival rate.

1.1.1 Tillering Pattern

In wheat, tillering starts when the third or fourth leaf of the main stem has emerged, while successive tillers are outgrown one phyllochron¹ later. The onset of tillering depends on growing conditions and the sowing date. Autumn sown wheat tends to form tillers earlier, whereas in late sown wheat, tillering starts once the temperature rises after the winter. Tillers that are derived from the leaf axils located at the base of the main shoot are called primary tillers. Secondary tillers can be formed from the base of the primary tiller, and those give rise to higher-order tillers (McMaster, 2005). During vegetative growth, the number of tillers rapidly increases until the transition of the plants to the reproductive phase. During stem elongation that follows, the number of tillers declines and stabilises before ear emergence (**Figure 1.1**) (Fraser et al., 1982). Thus, depending on the growing conditions, only a fraction of the developed tillers will form an ear and contribute directly to the grain yield.

Taken together, it is apparent that there are critical developmental processes and stages that determine tillering and tiller contribution to the final yield, namely *tiller formation*, *tillering cessation*, *tiller abortion-senescence* and *tiller fertility*. The main factors and signals affecting those stages will be presented in the following sections, while emphasis will be given to the signals controlling tiller formation in relation to nutrient availability.

¹ As phyllochron is defined the time between the appearance of two successive leaves (McMaster, 2005).

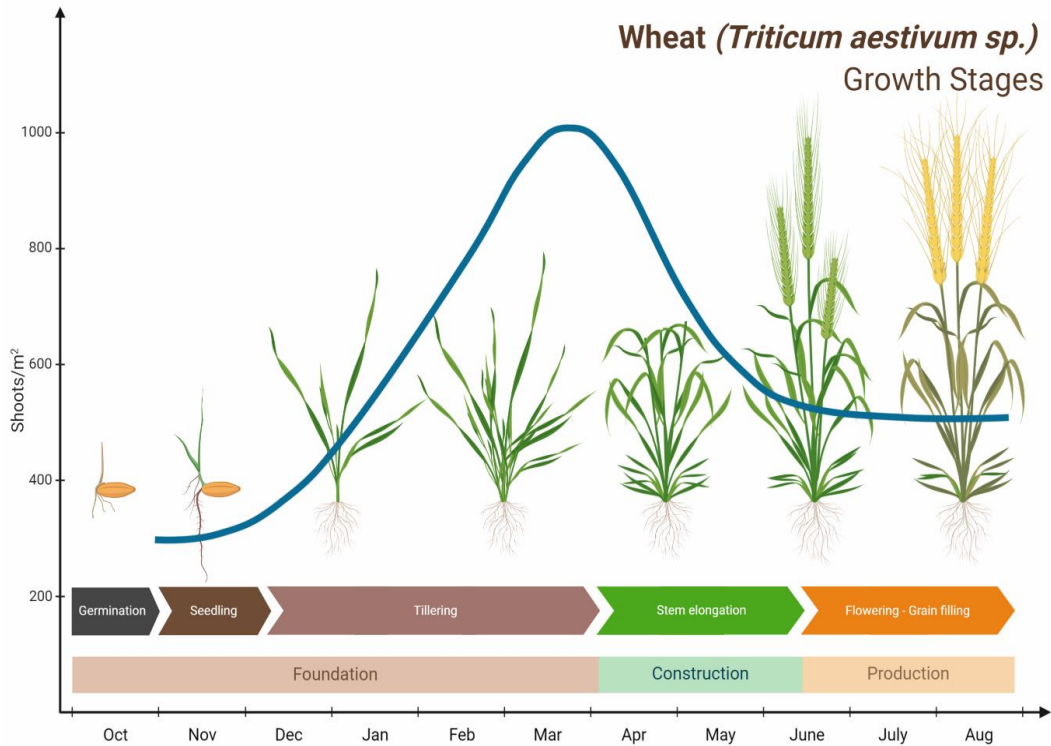
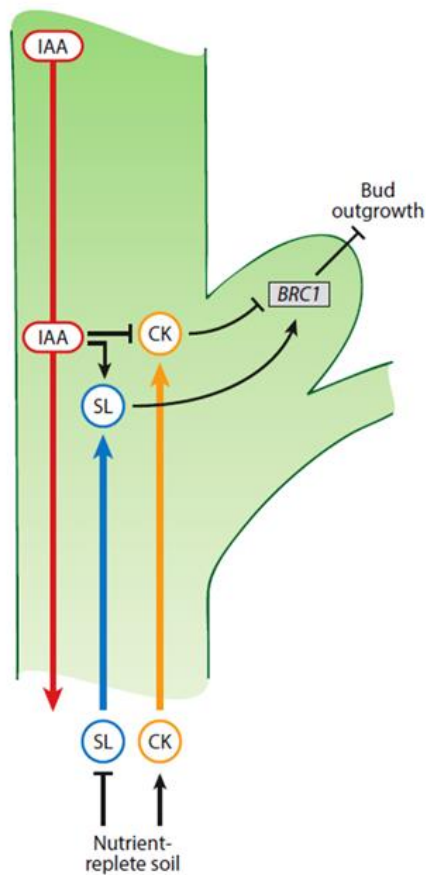


Figure 1.1: Growth stages and tillering dynamics in a winter wheat crop. The blue line represents the number of shoots per unit area over the winter wheat growing season. Illustration created with BioRender and inspired by Slafer et al. (2014).

1.1.2 Tiller Formation

Tiller formation can be divided into two distinct steps: i) axillary bud formation and ii) bud outgrowth (Kebrom et al., 2013, McSteen and Leyser, 2005). Axillary bud formation refers to the initiation of the vegetative lateral meristems. The formation of the axillary buds is mainly controlled genetically and constitutes the tillering capacity, which exhibits great variation between species and cultivars. On the other hand, bud outgrowth is regulated by different internal and external signals (Domagalska and Leyser, 2011). In summary, the fate of a formed bud is determined by complex interactions between hormonal, developmental and environmental cues. This enables plants to adjust their development and, in particular, their architecture according to the available resources. As a consequence, the tiller number is ranked at the highest end of plasticity among the cereal yield components, which makes it a challenging trait to study (Sadras and Slafer, 2012).

A. Second messenger



B. Canalization

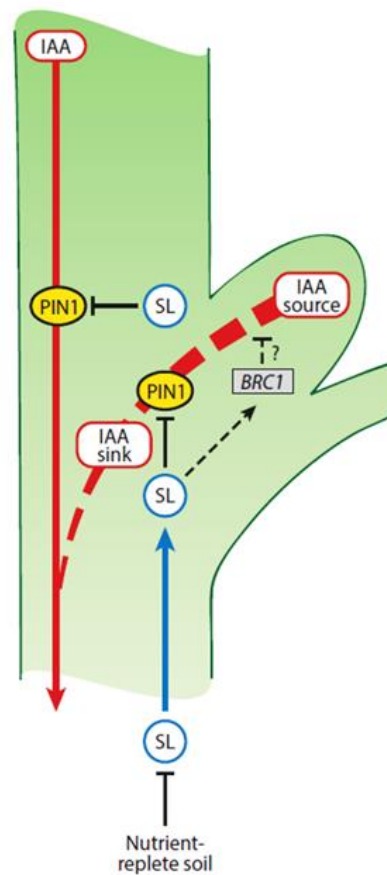


Figure 1.2: Two current models of the hormonal regulation of lateral bud outgrowth. (A) Second messenger model. According to this model, auxin inhibits bud outgrowth by controlling the levels of CKs and SLs. CKs act as positive, whereas SLs as negative regulators of tillering. An important element of this model is the bud-specific transcription factor *BRC1* (orthologue of *TB1/FC1*) which acts as a negative regulator of tillering. CKs and SLs act antagonistically, suppressing and inducing the expression of *BRC1*, respectively. **(B) Canalization model.** Based on this model, auxin moving into the stem inhibits lateral buds from exporting auxin and developing their own PATS, which is required for bud outgrowth. SLs negatively affect PIN1 activity, impairing the capacity of lateral buds for auxin transport. According to both models, phytohormones play an essential role in the coordination of lateral branching according to nutrient availability. Figure modified from Waters et al. (2017) with permission from the publisher².

Bud outgrowth is mainly controlled by complex interactions between plant hormones; however, the exact mechanism is not fully elucidated to date. Briefly, the phytohormones auxin, cytokinins (CKs) and, more recently, strigolactones (SLs) have been identified as key players involved in the control of bud outgrowth. The role of

² Modified from Annual Review of Plant Biology, Vol. 68, M. T. Waters, C. Gutjahr, T. Bennett, D. C. Nelson, Strigolactone Signaling and Evolution, 291-32, Copyrights (2017), with permission from Annual Reviews, <http://www.annualreviews.org>.

auxin as a suppressor of tillering/branching has been known for many years due to its involvement in the phenomenon of apical dominance (Thimann and Skoog, 1933). Auxin has been shown to act indirectly by suppressing bud outgrowth without entering the bud. Currently, there are two suggested models to explain shoot branching regulation and the inhibitory role of auxin (**Figure 1.2**) (Waters et al., 2017). The first model, namely the *second messenger model*, suggests that auxin controls bud outgrowth by regulating the levels of two other hormones, CKs and SLs. More specifically, auxin suppresses CK levels, whereas it induces SL biosynthesis. An important component of the second messenger model is the transcription factor TEOSINTE BRANCHED1 (TB1)/ BRANCHED 1 (BRC1)/ FINE CULM 1 (FC1), a negative regulator of bud outgrowth. CKs suppress the expression of *TB1*, whereas SLs lead to the accumulation of *TB1* (**Figure 1.2A**). Based on the second model, known as the *canalization model*, apical-derived auxin inhibits bud outgrowth by preventing axillary buds from establishing their polar auxin transport system (PATs), which is important for bud activation (**Figure 1.2B**) (Domagalska and Leyser, 2011). This model is applied in dicotyledonous species; however, there are indications that the apical dominance and the effect of auxin are not so apparent in monocotyledonous plants, especially during the vegetative growth stage (Kebrom, 2017). Finally, sugar availability has been shown to play an important role in lateral branching control (Barbier et al., 2015b, Kebrom, 2017). It has been proposed that all these components of the regulatory pathway may act at different stages of bud outgrowth, as it is summarized in **Figure 1.3** (Barbier et al., 2019).

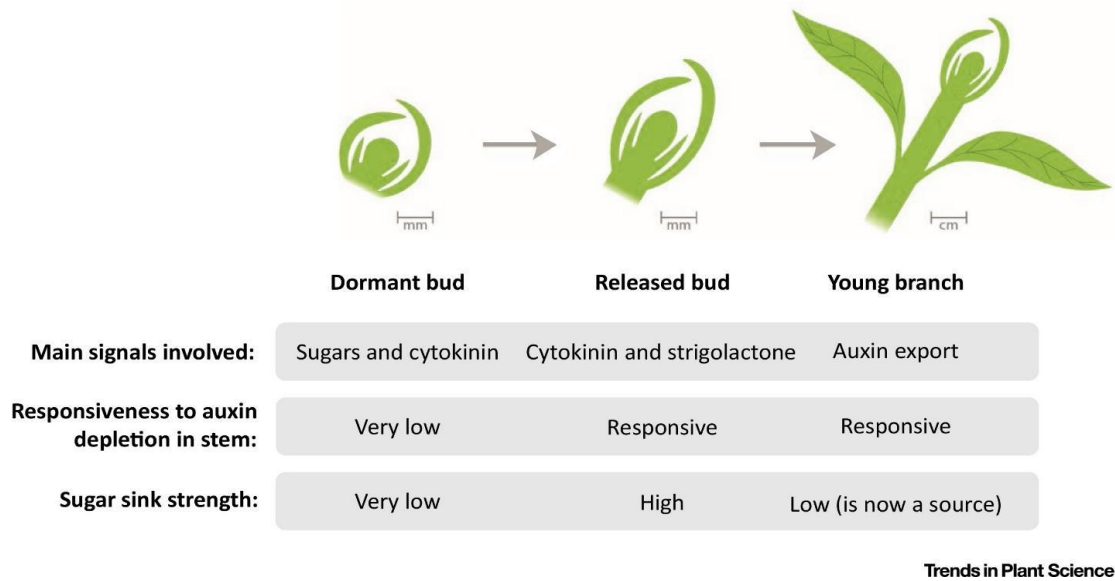


Figure 1.3: Different roles of the main hormonal signals at different stages of bud outgrowth. Figure reprinted from Bardier et al. (2019) with permission from the publisher³.

CKs are a class of phytohormones involved in many aspects of plant development, including cell division, root and shoot growth, nutritional responses and senescence (Kiba et al., 2013, Sakakibara et al., 2006). In relation to shoot branching, CKs act antagonistically to auxin by promoting bud outgrowth. CKs seem to promote tillering by partially affecting the levels of the transcription factor *TB1/BRC1* or/and by promoting the auxin transport capacity of the lateral buds (Barbier et al., 2019). In addition, the levels of CKs have been associated with the positive effect of N fertilizers on lateral branching. In rice, it has been previously reported that N induces tillering and stimulates CK biosynthesis (Sakakibara et al., 2006, Ding et al., 2014). The application of nitrate promotes the expression of CK biosynthetic genes in nodes of rice plants leading to higher levels of CK. Similar results have also been reported in *Arabidopsis thaliana* (Arabidopsis) (Takei et al., 2004a, Miyawaki et al., 2004).

More recent studies in both monocotyledons and dicotyledons revealed that SLs play an essential role in the suppression of tillering. As has been shown by many studies, *TB1/BRC1* is one of the downstream targets of the SL signalling pathway, which is positively regulated by SLs (section 1.2.4). Moreover, SLs have also been reported to

³ Reprinted from Trends in Plant Science, Vol. 24, No. 3, Francois F. Barbier, Elizabeth A. Dun, Stephanie C. Kerr, Tinashe G. Chabikwa, Christine A. Beveridge, An Update on the Signals Controlling Shoot Branching, 220-236, Copyright (2019), with permission from Elsevier.

affect auxin transport, suggesting that SLs might additionally control tillering via a TB1-independent pathway (section 1.2.5). In many species, SL biosynthesis has been associated with low P conditions, as P limitation induces SL production and exudation, leading to the suppression of lateral bud outgrowth (Umehara et al., 2010, Kohlen et al., 2011, Yoneyama et al., 2007b, Yoneyama et al., 2007a, López-Ráez et al., 2008). There are some indications that SLs are also involved in the suppression of tillering under low N, but this is not well established (de Jong et al., 2014, Yoneyama et al., 2012, Luo et al., 2018b). Furthermore, another target of the SL signalling pathway has been found to be *CYTOKININ OXIDASE/DEHYDROGENASE* (CKXs) in rice, providing new insights into the molecular interaction between SLs and CKs. SLs were found to control CK catabolism by inducing the expression of *OsCKX9* in the nodes of rice plants leading to lower levels of CKs (Duan et al., 2019b).

The bud-specific transcription factor, TB1/BRC1, is considered the key target element of this hormone signalling pathway since CKs suppress, whereas SLs promote its expression (Wang et al., 2015a). The role of TB1 seems to be conserved among monocotyledons and dicotyledons, given that in several species, the expression of *TB1* orthologues is correlated with the suppression of lateral bud outgrowth (Aguilar-Martínez et al., 2007, Takeda et al., 2003, Choi et al., 2012, Lewis et al., 2008). In many species, *tb1/brc1/fc1* mutants have a highly branched phenotype, further supporting TB1 as a negative regulator of bud outgrowth. Apart from phytohormones, *TB1* is responsive to other signals; hence it has been suggested to act as a key hub for integrating hormonal, developmental and environmental signals to control tillering (Wang et al., 2019c). However, some studies have demonstrated that TB1/BRC1 is not the only mechanism that controls tiller bud outgrowth since, in *brc1* mutants, some buds remain dormant, while *brc1* mutants also respond to signals affecting branching. Furthermore, in highly branched SL mutants of *Arabidopsis*, the expression of *BRC1* was found to be increased without leading to lateral branching inhibition (Seale et al., 2017). Hence, Walker and Bennett (2018) suggested a model according to which *TB1/BRC1* expression controls the activation potential of the bud by other signals (Walker and Bennett, 2018).

Apart from phytohormones, sugar availability has been shown to have an effect on bud outgrowth. Exogenously supplied sucrose has been found to release buds from dormancy by affecting transcript levels of *TB1/BRC1*. Therefore it has been suggested that *TB1* expression is also controlled by plant energy status (Mason et al., 2014). Studies in other species, such as wheat and sorghum (*Sorghum bicolor*), have linked sugar levels in the buds with tillering (Kebrom et al., 2012, Kebrom and Mullet, 2016, Kebrom, 2017). In addition, sucrose triggers lateral bud outgrowth in *Arabidopsis* (Barbier et al., 2015a), while dormant buds of different herbaceous and woody plant species (including *Arabidopsis*) show a typical sugar starvation response (Tarancón et al., 2017), demonstrating that bud outgrowth is also regulated by sugar availability. Sugars are known to play a pivotal role in plant growth and development since, through glycolysis, they provide the energy and carbon required for protein synthesis and growth. As a result, one possible mechanism of action of sugar control over bud outgrowth is attributed to sugar nutritional value. However, experiments have shown that the sucrose effect on branching is independent of its nutritional value. More specifically, experiments with non-metabolised sucrose analogues resulted in suppression of *BRC1* and triggered branching, suggesting that sucrose functions also as a signal affecting developmental decision making leading to bud outgrowth (Barbier et al., 2015b). However, the exact mechanism is not fully understood. Trehalose 6-phosphate (Tre6P) has been proposed to play a regulatory role since it is known to act as a signal of sucrose availability (Figuroa et al., 2016, Yadav et al., 2014). In fact, a positive correlation between sucrose and Tre6P has been found, while the increase in Tre6P levels has been correlated with bud outgrowth (Fichtner et al., 2017). In *Arabidopsis*, changes in Tre6P levels affected branch formation, indicating that Tre6P is involved in branching regulation. In addition to that, many genes involved in Tre6P have been found to be affected in dormant buds (Kebrom and Mullet, 2016, Tarancón et al., 2017). Tre6P might regulate bud outgrowth by interacting with sucrose non-fermented kinase 1 (SnRK1). SnRK1 is a master regulator of energy status, which, when activated, represses growth by controlling downstream genes involved in sugar utilization and growth arrest. Tre6P is thought to inhibit SnRK1 under high sugar

availability resulting in the diversion of metabolic reprogramming towards growth (Fichtner and Lunn, 2021).

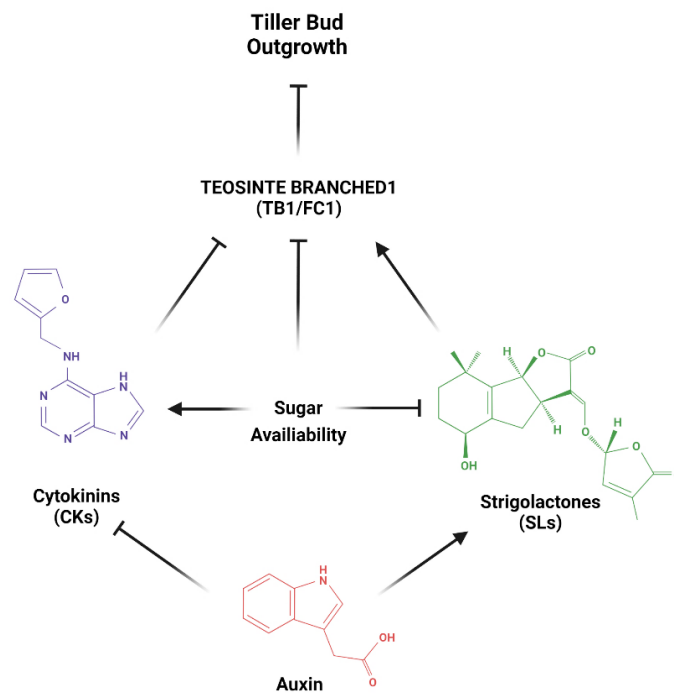


Figure 1.4: Model integrating hormonal and sugar availability control of bud outgrowth. This model is based on the second messenger model of bud outgrowth regulation. CKs promote tillering, and SLs suppress tillering by affecting the expression of TB1/BRC1/FC1. Auxin suppresses tillering by suppressing CKs and inducing SLs. Sugar availability affects tillering by directly suppressing the expression of TB1/BRC1/FC1 and by affecting the levels of CKs but also the SL signalling. Illustration created with BioRender.

Other signals that have been associated recently with the regulation of tillering, and especially with the N-mediated regulation of bud outgrowth, are amino acids. Amino acids represent one of the main forms of N in plants and can be transported systemically, acting as signals of N availability (Barbier et al., 2019). In fact, the levels of asparagine (Asn) and glutamine (Gln) have been associated with tillering in monocotyledons. Asn and Gln deficiency in transgenic plants lacking biosynthetic genes results in decreased tillering in rice (Ohashi et al., 2018, Ohashi et al., 2015a). In addition, increased levels of Gln have been found to promote tillering in sorghum (Urriola and Rathore, 2015). It has been suggested that Gln may affect tillering by affecting the biosynthesis of CKs, as Gln and CK biosynthesis are closely related (Ohashi et al., 2017, Kamada-Nobusada et al., 2013).

1.1.3 Tillering Cessation

The maximum number of tillers on a wheat plant is dependent on the duration of the tillering phase, since the prolonged tillering phase leads to a higher number of tillers. Tillering usually stops after the transition of the main stem from vegetative to reproductive development, which is known as floral initiation, followed by the elongation of the stem. More specifically, during floral initiation, the leaf primordia stop initiating, and the spikelet primordia start to differentiate. This transition from the juvenile to the reproductive phase in winter wheat is mainly controlled by temperature, vernalization requirements and photoperiod (Trevaskis et al., 2007). Spikelet development and subsequent stem elongation are highly energy-consuming processes leading to changes in source-sink status at the whole plant level, resulting in the inhibition of bud outgrowth. Kebrom et al. (2012) reported that in the *tin1* mutant, the inhibition of bud outgrowth is caused mainly by the precocious stem elongation of the main culm leading lateral buds to sugar deficiency (Kebrom et al., 2012). In addition, after the onset of floral initiation, changes in the levels of bioactive gibberellins (GAs) have been reported in cereals. It is well known that GAs are involved in the internode elongation in cereals and the transition from the vegetative phase to the floral phase (Rameau et al., 2015). In fact, upon floral initiation, the expression of *GA2ox1*, which catalyses the deactivation of GAs, is significantly downregulated at the base of the plant allowing active GAs to reach lateral buds. In contrast, during vegetative growth, *GA2ox1* is highly expressed, ensuring low levels of GAs. GAs have been shown to also negatively affect bud outgrowth by affecting the expression of *TB1* (Lo et al., 2008). Another component of the tillering regulatory pathway that has been associated with developmental changes is miRNA156. miRNA156 is known to regulate the expression of SQUAMOSA promoter-binding protein-like 14 (SPL14) transcription factor (wheat orthologue SPL17). Many members of the SPL transcription factor family have been shown to be involved in both vegetative and reproductive development, shaping plant architecture (Liu et al., 2016, Xie et al., 2006). SPL14 controls the transcriptional activation of *TB1*, and it is closely linked with the SL signalling mechanism (Lu et al., 2013). Overexpression of miRNA156 leads to the delayed cessation of tillering, as has been shown in rice (Xie et al., 2006).

However, cessation of tillering is not only associated with the switch to the reproductive phase, as plants have developed other adaptation mechanisms that allow them to control tillering based on external signals. The main external signal involved in the early cessation of tillering is light quality, which is associated with plant density. Plants grown in high sowing density tend to form fewer tillers mainly due to early cessation of tillering, as the tiller formation rate remains unaffected (Evers et al., 2006, Sparkes et al., 2006). Thereby, it has been shown that cessation of tillering is photomorphogenetically regulated, and the main signal of this regulatory pathway is the R: FR. In dense canopies, R: FR is low due to the absorption of red and blue wavelength by the surrounding vegetation, while far-red is reflected. High R: FR in the base of the canopy is associated with delayed tillering cessation (Xie et al., 2016). According to Evers et al. (2006), tiller formation stopped at a particular value of leaf area index (0.59) associated with 0.25-0.3 R: FR ratio, which has been suggested as a threshold below which tiller appearance ceased regardless of the development stage. In sorghum, the inhibition of bud outgrowth under low R: FR has been correlated with upregulation of *TB1* and *GRASSY TILLER 1 (GT1)*, both acting as suppressors of tillering (Kebrom et al., 2006, Kebrom et al., 2013). In wheat, a recent RNA-seq study on *phytochrome B (phyB)* null mutant, which behaves as growing in low R: FR conditions due to the absence of functional PhyB, revealed that under shading conditions, auxin and ethylene biosynthesis is induced (Pearce et al., 2016). The upregulation of auxin levels can be involved in the suppression of tillering under shading conditions. Among other transcription factors, the *phyB*-null mutant showed a significant upregulation of *GT1*, known as a negative regulator of tillering (Pearce et al., 2016). Whipple et al. (2011) also reported that *GT1* is involved in tillering regulation by shading signals in maize (Whipple et al., 2011).

N nutrition is among the environmental cues that affect the transition from the vegetative to reproductive phase by controlling flowering time (Vidal et al., 2014, Luo et al., 2020). In fact, N limitation often induces flowering, whereas excess N supply extends vegetative growth and delays flowering (Vidal et al., 2014). In rice, late flowering has been associated with an increase in tiller number (Leng et al., 2020). This observation is probably due to the prolonged vegetative stage allowing a wider time

window for tiller formation. On the other hand, N limitation results in the induction of flowering as an escape mechanism for plants to produce seeds and complete their life cycle. N effect on floral initiation and flowering has been suggested to involve the GA pathway (Liu et al., 2013, Gras et al., 2018). Liu et al. (2013) showed that low N availability leads to higher levels of GA in Arabidopsis, while a decrease in GA levels was recorded under high N supply. In addition, the expression of the *CONSTANS (CO)* gene is also induced by N limitation, supporting that low N supply induces flowering, as CO promotes flowering. Nitrate has also been shown to act as a signal directly in the apical meristem affecting the expression of *SUPPRESSOR OF CONSTANS (SOC1)*, which is an important integrator of signals controlling flowering (Olas et al., 2019). In the same study, it was also shown that *SOC1* is required for the N-mediated regulation of flowering. More recently, Zhang et al. (2021) found that the gene *N-mediated heading date-1 (Nhd1)* is involved in the regulation of flowering by N status, as *nhd1* rice mutants showed delayed flowering and less sensitivity to flowering control by N supply (Zhang et al., 2021). However, other studies in monocotyledonous and dicotyledonous species have shown that severe N deficiency can delay flowering. Therefore, it has been demonstrated in both Arabidopsis and rice that flowering response to N availability is described by a U-shape curve as both severe N limitation and excess N supply delay flowering (Lin and Tsay, 2017, Sun et al., 2021). Based on this response, the prolonged vegetative period under high N supply can contribute to the higher number of tiller/branches formed under high N supply. However, this does not apply under severe N deficiency, where both flowering and tiller formation is suppressed, suggesting that the decrease in tiller number is mainly attributed to tiller bud outgrowth suppression rather than to the impact of N limitation on tiller cessation and floral transition. In field-grown wheat, N fertilization has been reported to increase the maximum number of tillers, but this effect is mainly attributed to the increase in the rate of tiller appearance rather than the duration of tillering (Alzueta et al., 2012).

1.1.4 Tiller Abortion/Senescence

At tiller cessation, plants reach the maximum number of tillers which coincides with the start of stem elongation (**Figure 1.1**). Soon the number of tillers per unit area

declines until ear emergence. The maximum tiller number varies between cultivars and is strongly influenced by plant density and plant nutrition. N fertilization increases the maximum number of tillers mainly by affecting the development of higher-order tillers. However, only a fraction of the developed tillers will form an ear (fertile tillers) and directly contribute to grain yield, whereas the rest will senesce. In general, the mortality rate is higher in the late formed tillers, which correspond to high-order tillers (secondary, tertiary etc.) (Fraser et al., 1982). In spring wheat, tiller abortion varies between cultivars, season, growing conditions and nutrient supply and ranges between 90 and 20% (Sharma, 1995). Studies have shown that there is a positive correlation between the maximum tiller number and tiller mortality, which means that a high tiller number leads to higher mortality (Alzueta et al., 2012). Some studies have shown a positive correlation between the maximum number of tillers and the number of ears per unit area, one of the main yield components. Although there is a strong correlation between the ear number and grain yield, there is a weak correlation between the maximum number of tillers and grain yield. This is mainly because excessive tillering can sometimes lead to yield reduction. Whether unfertile tillers are beneficial or can lead to yield reduction remains an open question. The answer to that question is not simple since it depends on the growing conditions. Non-surviving tillers can be beneficial if nutrients such as N and fixed carbon are redistributed to other parts of the plants after their death (Palta et al., 2007). If this mechanism is effective unfertile tillers can be considered a pool of assimilates and nutrients at the early stages. Nevertheless, carbon and nutrient redistribution is not always effective, and thereby high mortality rate can lead to yield reduction, a phenomenon which is apparent under water stress conditions (Berry et al., 2003).

The main reason for tiller abortion is the competition in the plant community for available resources. Late-formed tillers fail to compete with the main shoot and primary tillers, as the latter are strong sinks of carbohydrates. Again, tiller senescence has been associated with light quality and R: FR ratio. Data from winter wheat field trials indicate that tiller death starts at a relatively constant critical level of R: FR of 0.2-0.4 (Sparkes et al., 2006). This can partially explain why tiller mortality is higher when the maximum number of tillers has been reached. In addition, N fertilization has been

reported to reduce tiller mortality and increase the final number of ear-bearing tillers. There are indications that the high leaf N content can decrease the critical value of R:FR; hence plants are less sensitive to shading, leading to a lower tiller death rate (Sparkes et al., 2006, Evers and Vos, 2013). Consistent with this observation, N fertilization increases yield by mainly affecting the development and maturity of high-order tillers, which otherwise would have senesced (Power and Alessi, 1978).

On a physiological level, tiller senescence includes processes similar to mature leaf senescence, including decomposition of cells, degradation of cellular components and remobilization of carbon and nutrients to other parts of the plant. In senescing tillers, abscisic acid (ABA) has been found to be upregulated, whilst indole-3-acetic acid (IAA) and GA content were lower compared to actively growing stems. The changes in the hormonal levels are followed by decreased levels of ascorbic acid, the main antioxidant mechanism in plants, and a subsequent increase in the levels of lipid peroxidation products (Vasantha et al., 2012).

1.1.5 Tiller Fertility

Based on the negative impact of tiller mortality on the number of ears and the positive correlation between ear population and grain yield, it is apparent that one potential strategy to increase the grain yield could be the reduction of tiller abortion. Under conditions that cause high tiller mortality, such as N limitation or water deficit, the contribution of the tillers to the grain yield compared to the contribution of the main stem is low. In contrast, under high N availability or sufficient water supply, the yield that is attributed directly to tillers increases (Elhani et al., 2007, Power and Alessi, 1978). However, it is notable that grain yield and its components are not consistent among tillers. High-order tillers exhibited lower grain yield per spike than the main shoot and the first two primary tillers. In fact, the number of fertile spikelets is lower in late-formed tillers; hence they produce fewer grains per spike. This observation suggests that there might be differences in floret development during spike initiation among tillers. Li et al. (2001) showed that the main shoot and the first two primary tillers revealed a similar pattern of floret initiation and maximum floret number, which under favourable growing conditions, led to similar contributions to grain yield (Li et

al., 2001). In contrast, in the same study, it was shown that as tiller order increases, floret fertility deteriorates. The low light intensity that high-order tillers receive during inflorescence development due to the superior tillers impacts spikelet initiation and decreases the number of grains per spike (Toyota et al., 2001). It is not only the number of fertile spikes which causes lower yield but also the grain filling process that is deteriorated in late-formed tillers. Main shoot and primary tillers tend to reach higher photosynthetic rates during grain filling compared to secondary tillers. Moreover, the flag leaf senescence rate in secondary tillers is higher, suggesting differences in grain filling period among tillers (Xu et al., 2015a). Finally, the lower productivity of late-formed tillers can also be attributed to their short growth period compared to the main stem and primary tillers, since the maturation of the tillers is synchronous in cereals, whereas tiller initiation and development are asynchronous (Wang et al., 2017).

1.2. A Brief History of Strigolactones

Strigolactones (SLs) are a group of terpenoid lactones found in most land species and play an important role as signalling molecules in the rhizosphere, while they are involved in many aspects of plant growth and development (**Figure 1.5**). SLs had been identified initially as compounds that stimulate the germination of *Striga sp* seeds, a parasitic weed commonly known as witchweed, after which they were named (Cook et al., 1966). Strigol was the first identified SL in root exudates of *Gossypium hirsutum* (cotton). Strigol was soon identified in the root exudates of other plant species, such as *S. bicolor* and *Z. mays* (Siame et al., 1993). Orobanchol was another type of SLs which was identified in the root exudates of *Trifolium pratense* (red clover), which stimulates the germination of *Orobancha minor* seeds, another type of parasitic plant (Yokota et al., 1998). Those observations clearly demonstrated that SLs act as a signal utilized by the parasitic plant in such a way that they have increased chances of survival. However, the fact that plants release SLs in the rhizosphere without having any beneficial effect raised many evolutionary questions as to why plants produce a signal that facilitates parasitisation.

The answer to the above question came partially in 2005 when another type of SLs, 5-deoxystrigol (5DS), was identified to be involved in the cross-talk between plants and arbuscular mycorrhizal fungi (AMF) (Akiyama et al., 2005). In fact, 5DS promotes the hyphal branching of AMF, positively affecting the colonization of the roots by the AMF. The mutualistic relationship between AMF and plants has great ecological importance since plants provide AMF with photoassimilates in return for water and inorganic nutrients such as P and N. In addition, AMF establishment has also been shown to improve plant tolerance to abiotic and biotic stress (Begum et al., 2019). The observation that P limitation and, to a lesser extent, N limitation induce SL exudation strengthened the idea that SLs act as a rhizosphere signal under nutrient limiting conditions facilitating the AMF establishment, thus increasing nutrient acquisition. However, the role of SLs in AMF symbiosis did not fully elucidate the role of SLs because non-mycorrhizal plants, such as *Arabidopsis*, also produce and exude SLs in the rhizosphere.

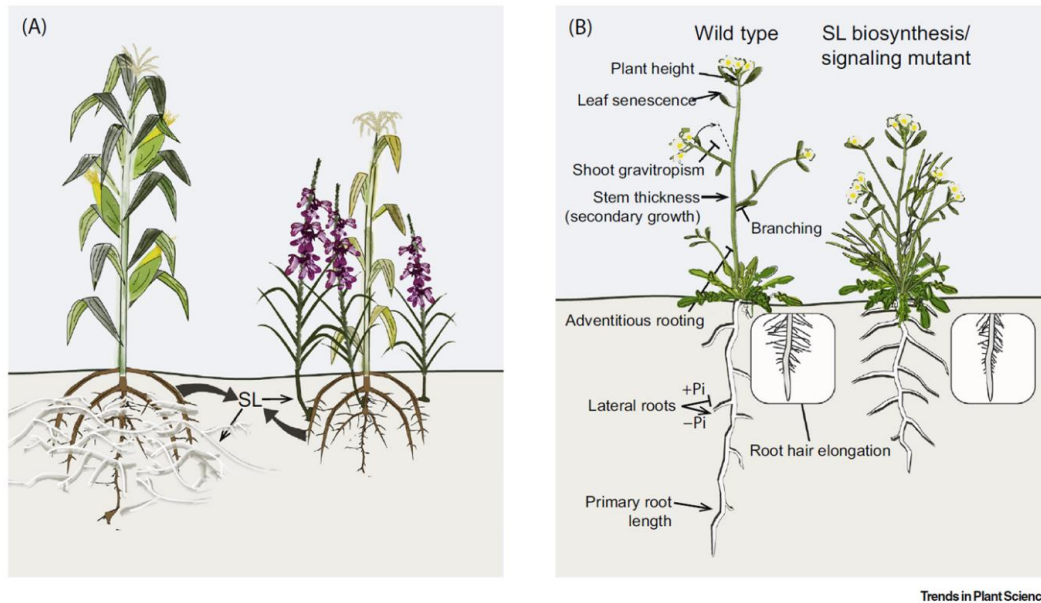


Figure 1.5: The many roles of SLs as rhizosphere signals and as plant hormones. (A) Plants release SLs in the rhizosphere, where they act as signals involved in the cross-talk between plants and AMF (left). SLs stimulate the germination of parasitic plants *Striga* sp. and *Orobanche* sp. **(B)** SLs have been found to act as plant hormones regulating many aspects of plant growth and development. SLs mainly act as inhibitors of lateral branching; therefore, SL biosynthesis or signalling mutants show a highly branched phenotype. They are also involved in shoot gravitropism, leaf senescence, plant height, stem thickness and adventitious root formation. In below-ground tissues, SLs control primary and lateral root growth and root hair elongation. Figure reprinted from Chesterfield et al. (2020) with permission from the publisher⁴.

As a matter of fact, in 2008, SLs were identified as key hormones for the regulation of lateral branching, acting as branching inhibitors (Gomez-Roldan et al., 2008, Umehara et al., 2008). Several high branching/tillering mutants from various plant species, such as *more axillary meristem (max)* in *Arabidopsis* and *dwarf (d)* in rice, led to the discovery that SLs play a central role in the modulation of above-ground plant architecture. More specifically, *max4/d10* and *max3/d17* showed reduced levels of SL production and highly branched/tillering phenotypes. The phenotype of those mutants could be rescued by the application of GR24, a synthetic SL analogue. Similar results have been reported by Lin et al. (2009) in *d27* rice mutants, indicating that D27, D17 and D10 are part of the SL biosynthetic pathway (Lin et al., 2009). On the other

⁴ Reprinted from Trends in Plant Science, Vol. 25, No. 11, Rebecca J. Chesterfield, Claudia E. Vickers, Christine A. Beveridge, Translation of Strigolactones from Plant Hormone to Agriculture: Achievements, Future Perspectives, and Challenges, 1087-1106, Copyright (2020), with permission from Elsevier.

hand, the highly branched phenotype of *max2/d3* and *d14* could not be rescued by exogenous application of GR24, while those mutants accumulated high levels of endogenous SLs. These observations indicated that both D14 and D3 might be involved in SL perception and signalling rather than in biosynthesis. Since their identification as branching inhibitors, SLs have been shown to be involved in many aspects of plant growth and development, such as in regulating root architecture, senescence, stem elongation and many more, as summarized in **Figure 1.5B** (Chesterfield et al., 2020). Furthermore, SLs have been linked to plant nutritional status, mainly to P and less to N. More recent studies have also focused on the involvement of SL in biotic and abiotic stress responses, highlighting the importance of SLs in plant growth and resilience.

1.1.6 Strigolactone Biosynthesis

SLs are terpenoid lactones derived from the carotenoid biosynthetic pathway (Matusova et al., 2005). Since the discovery of strigol, more than 30 different SLs have been identified in plants, which are classified as *canonical* and *non-canonical* SLs based on their chemical structure (Yoneyama and Brewer, 2021). Canonical SLs are the most well-studied class and consist of a fourth methyl butanolide ring (D ring) connected with a three-ring structure (ABC ring) via an enol-ether bridge (**Figure 1.6**). Canonical SLs are further divided into strigol- or orobanchol-type based on the stereochemistry of the C ring. In contrast, in non-canonical SLs, the D ring is connected via an enol-ether bridge to various groups instead of the ABC ring. The type of synthesised SLs varies between plant species (Yoneyama and Brewer, 2021). Some plants, such as *Arabidopsis* and maize, produce a blend of canonical and non-canonical SLs. In addition, there is variability between species in relation to the type of canonical SL produced. In fact, in rice, only orobanchol-type has been detected, whereas maize mainly produces strigol-type (Wang and Bouwmeester, 2018). Both types of canonical SLs have been reported in *Nicotiana tabacum* (tobacco) and sorghum. In addition, in tobacco, it has been reported that the ratio between strigol- and orobanchol-type varies between different cultivars.

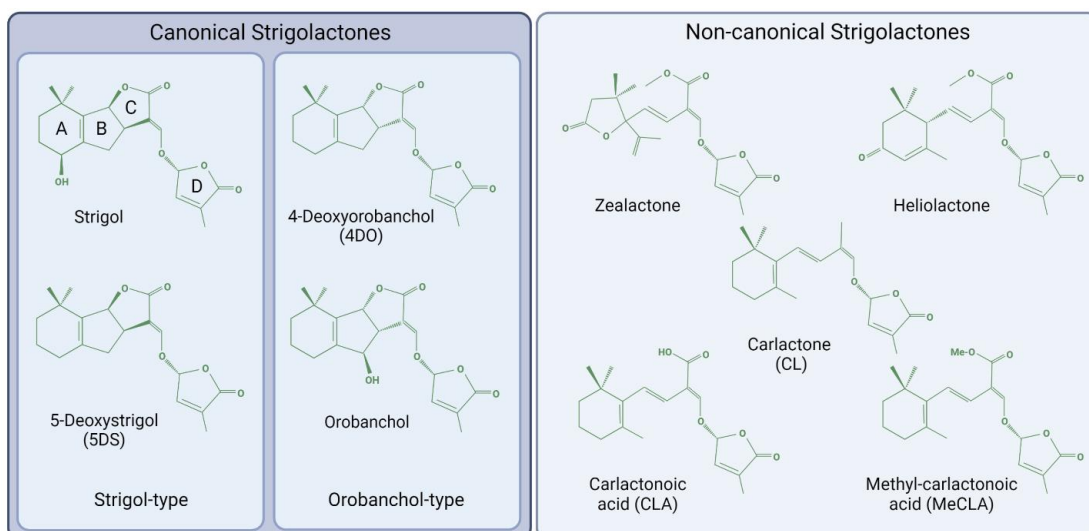


Figure 1.6: Structures of characteristic naturally occurring SLs. Based on their chemical structure SLs are classified into canonical and non-canonical. Canonical SLs consist of an ABC-ring connected with a D-ring via an enol-ether bond. Based on the stereochemistry of the C-ring are further divided into strigol- and orobanchol-type. In non-canonical SLs, the presence of the D-ring and enol-ether bond is conserved, while ABC-ring is replaced by various groups leading to a large structural diversity. Illustration created with BioRender.

The first step of SL biosynthesis is catalysed by β -carotene isomerase, DWARF27 (D27), an iron-containing enzyme that catalyses the conversion of all-trans- β -carotene into 9-cis- β -carotene (Alder et al., 2012). The function of D27 is an important step of SL biosynthesis, as it has been shown from *d27* highly branched mutants. However, there are some indications that chemical isomerization occurs at low rates, which can compensate for the isomerase activity of D27. Subsequently, carotenoid cleavage dioxygenase 7 (CCD7) encoded by *MAX3* and *D17* in Arabidopsis and rice, respectively, catalyses the cleavage of 9-cis- β -carotene to 9-cis- β -apo-10'-carotenal. The latter is then converted into carlactone (CL) by another member of the carotenoid cleavage dioxygenase family, CCD8 encoded by *AtMAX4* in Arabidopsis and *OsD10* in rice. Seto et al. (2014) showed that CL is used for the biosynthesis of 4-deoxyorobanchol (4DO) and orobanchol, indicating that CL is an intermediate of SLs biosynthesis (Seto et al., 2014). The multi-step production of CL from β -carotene, as described above, takes place in the plastid (**Figure 1.7A**). Subsequently, CL is exported in the cytosol, where it is used as a precursor for both canonical and non-canonical bioactive SLs. The biosynthesis of bioactive SLs from CL is predominantly catalysed by members of the cytochrome P450 CYP711 subfamily. More specifically, in Arabidopsis, CYP711A1 encoded by *MAX1* converts CL to carlactonoic acid (CLA) (Abe et al., 2014). The

diversity of produced bioactive SLs in different species is attributed to steps downstream of CLA. CLA is a non-canonical SL-like compound which does not interact with D14, the receptor protein of the SL signalling pathway, whereas methylcarlactonoate (Me-CLA) possesses this ability indicating that the latter is biologically active in suppressing shoot branching (Abe et al., 2014). In addition, Me-CLA is a non-canonical SLs that is considered an important intermediate for the biosynthesis of other non-canonical SLs, since it has a similar chemical structure to other non-canonical SLs found in plants, including zealactone found in maize and heliolactone produced by *Helianthus annuus* (Mashiguchi et al., 2021) (**Figure 1.6**). In fact, in *Arabidopsis*, Me-CLA has been found to be the substrate of an oxidoreductase-like enzyme encoded by *LATERAL BRANCHING OXYDOREDUCTASE (LBO)*, which converts Me-CLA to an unknown product that also acts as a branching inhibitor (Brewer et al., 2016). Yoneyama et al. (2020) found the product of the LBO is hydroxymethylcarlactonoate (1'-OH-MeCLA), while the function of LBO was found to be conserved in both maize and sorghum (Yoneyama et al., 2020a). For many years the enzymatic conversion of CLA to Me-CLA had remained unknown. Recently, Wakabayashi et al. (2021) found that a SABATH methyltransferase catalyses the conversion of CLA to Me-CLA in *Arabidopsis* (Wakabayashi et al., 2021). This finding indicated that other SABATH methyltransferases might play an important role in the biosynthesis of other non-canonical SLs.

However, in monocotyledonous species, the pathway downstream of CL remains elusive. Although most of the dicot species have only one *MAX1* homologue, monocotyledons have multiple CYP711 *MAX1* genes in their genome. In fact, five different *MAX1* homologues have been found in the rice genome, while maize and sorghum have three and four homologues, respectively. It has been suggested that different *MAX1* homologues have different substrate specificity and catalyse distinct reactions. Zhang et al. (2014) showed that Os900 converts CL to 4DO, and subsequently, Os1400 converts 4DO to orobanchol (Zhang et al., 2014). Nevertheless, it was found later that both Os900 and Os1400 catalyse the conversion of CL to CLA (Yoneyama et al., 2018a). Therefore, a classification of *MAX1* homologues into three categories, based on their main activity, was suggested by Yoneyama et al. (2018): A1

type converting CL to CLA, A2 type converting CL to CLA and CLA to 4DO and A3-type being involved in both conversion of CL to CLA and 4DO to orobanchol. Therefore, based on this classification, *Os900* is classified as A2-type CYP711A and *Os1400* as A3-type. As a result, CLA is considered an intermediate for the biosynthesis of orobanchol-type of SLs. *Os1500*, which is phylogenetically close to *Os900* and *Os1400*, has not shown any enzymatic activity, which has been attributed to a premature stop codon (Yoneyama et al., 2018a). Less is known about the enzymatic activities of other MAX1 homologues in rice, especially of *Os1900* and *Os5100*. More recently, a new biosynthetic pathway of canonical SL biosynthesis was identified in sorghum. More specifically, *SbMAX1a* was found to convert CL to 18-hydroxy-CLA. The latter is used as a substrate by a sulfotransferase encoded by *LOW GERMINATION STIMULANT 1 (LGS1)*, which is probably involved in the biosynthesis of 5DS and 4DO (Wu and Li, 2021). *LGS1* had been previously linked to the resistance of some sorghum cultivars to *Striga sp.*, indicating that it is indeed involved in SL biosynthesis and exudation (Gobena et al., 2017). More recent studies have also highlighted the role of the CYP722C subfamily of P450, members of which seem to be responsible for the structural diversity in canonical SLs acting downstream of MAX1s (Mashiguchi et al., 2021). However, the non-canonical SL biosynthetic pathways remain elusive in monocotyledonous plants.

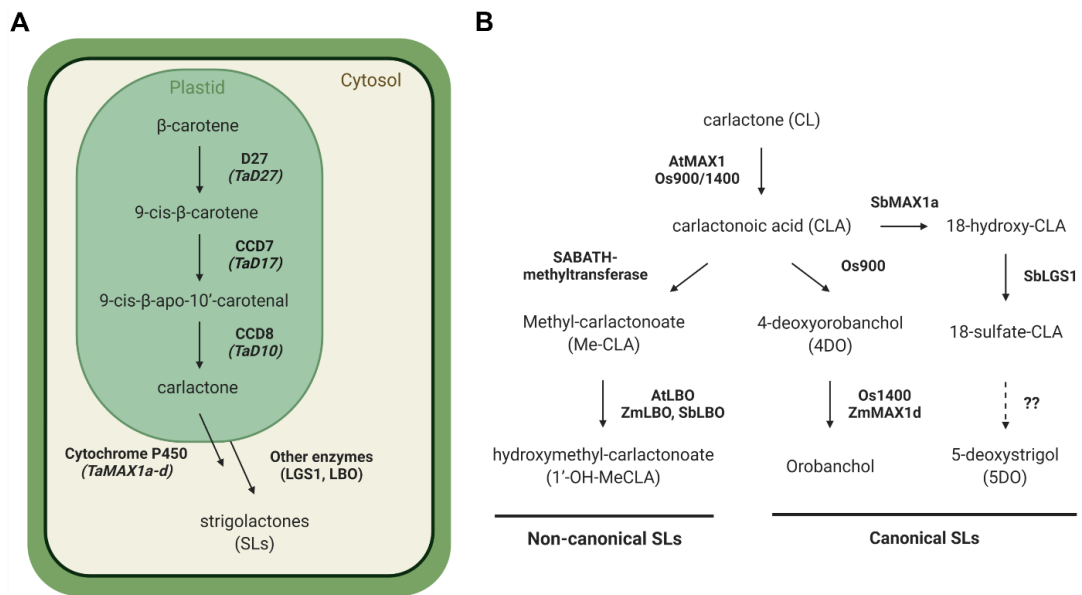


Figure 1.7: SL biosynthetic pathway. (A) The compartmentalisation of SL biosynthetic pathway. The multi-step production of carlactone (CL) from all-trans- β -carotene takes place in the plastids and is considered the core biosynthetic pathway. The sequential reactions are catalysed by D27, CCD7 (D17), and CCD8 (D10) enzymes. CL is then exported into the cytosol, where it is converted into bioactive SLs, mainly by members of CYP711A (MAX1) members and other enzymes such as LBO and LGS1. **(B) Steps downstream of CL for the biosynthesis of canonical and non-canonical SLs.** Structural diversity in naturally occurring SL is attributed to steps downstream of CL. CL is converted to CLA by MAX1 in *A. thaliana*. CLA is used as a precursor for both the biosynthesis of canonical and non-canonical SLs. SABATH methyltransferase was recently found to convert CLA to Me-CLA, which in turn is used by LBO for the biosynthesis of 1'-OH-MeCLA. In *O. sativa*, both Os900 and Os1400 convert CL to CLA. CLA is used as a substrate by Os1900 for the production of 4-deoxyorobanchol. The latter is then converted to orobanchol by Os1400. Recently, in *S. bicolor*, MAX1a was found to catalyze the conversion of CLA to 18-hydroxy-CLA, which is converted to 18-sulfate-CLA by SbLGS1 as part of the 5-DO biosynthetic clade. Illustration created with BioRender.

1.1.7 Strigolactone Transport

The dual role of SLs as rhizosphere signals and plant hormones suggests the presence of a transport system facilitating the exudation of SLs in the rhizosphere and their systemic transport to control plant architecture. SL biosynthesis is strongly induced in roots of P- and N-deficient plants; therefore, it has been hypothesized that SLs act as long-distance signals coordinating shoot architecture to the nutrient availability sensed by roots. The acropetally transport of SLs has been confirmed by different grafting experiments in dicotyledonous plants. The highly branched phenotype of SL-deficient mutants (*max4*, *max1*) can be rescued by grafting their shoots to wild-type roots (Sorefan et al., 2003, Booker et al., 2004). However, the same experiments also

showed that locally synthesised SLs in shoots are sufficient for controlling lateral branching, as wild-type shoots did not form more branches when grafted in SL-deficient roots (**Figure 1.8**).

More dedicated grafting experiments with different combinations of SL biosynthetic mutants have provided more insights into which forms of SL are transported from root to shoot (reviewed by Mashiguchi et al., 2021). CL, which is the precursor of bioactive SLs, has been shown to be transmittable since highly branched *max4* mutants can be rescued when grafted in *max1* roots (Booker et al., 2005). CL is the product of *max4* and the substrate of *max1*, therefore, root synthesized CL can be transported acropetally and control shoot branching. Consistent with this observation, *d27* mutants were rescued by grafting *max1* roots, whereas *d27* shoots remained highly branched when *max4* roots were used (Lin et al., 2009, Waters et al., 2012). Therefore, only CL and compounds downstream of CL can be transported over long distances. Further experiments showed that apart from CL, Me-CLA can also be transported from root to shoot, suppressing lateral branching in *max1* shoots. In addition, WT roots grafted in *lbo* shoots could also rescue the *lbo* phenotype, indicating that even the product of LBO is transmittable long-distance (Brewer et al., 2016).

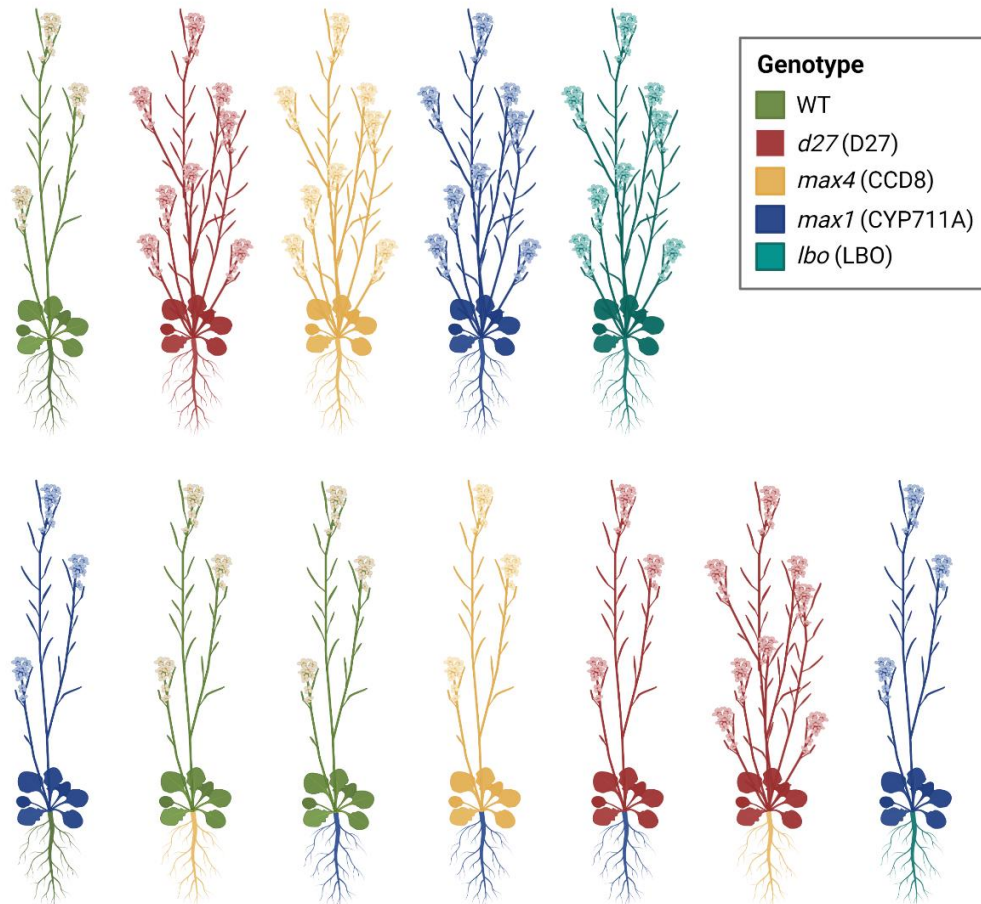


Figure 1.8: Schematic illustration of grafting experiments conducted in *A. thaliana* SL biosynthesis mutants proving that SLs act as long-distance signals. The highly branched phenotype of *max1* mutant could be rescued after grafting WT root onto *max1* shoot. In addition, SLs are also locally synthesised in shoots, given that grafting of *max4* or *max1* roots in WT shoots did not affect the number of lateral shoots. *d27* and *max4* mutant phenotype could be rescued when *max1* roots were grafted, but grafting of *max4* root onto *d27* did not affect the branch number, suggesting that only CL is transmittable. Finally, grafting *lbo* root to *max1* shoot reduces the number of formed branched, indicating that Me-CLA can also be transported from root to shoot. The illustration was inspired by Domagalska and Leyser, 2011 and created in Biorender.

Even though the above observation clearly demonstrated that SLs act as long-distance signals, the mechanism of SL distribution within the plant remains elusive. Initially, Kohler et al. (2011) reported that the upregulation of SL biosynthesis in roots under P limitation is accompanied by an increase in the amount of orobanchol and other SL-like compounds in xylem sap of *Arabidopsis* (Kohlen et al., 2011). Lower levels of SLs were detected on the xylem sap of SL-deficient mutants, supporting the idea that SLs are transported through the xylem. However, contradictory results were later

presented by Xie et al. (2015), who did not detect any SL compound in the xylem sap of *Arabidopsis* (Xie et al., 2015b). The absence of detected SL was also consistent in all the plant species included in this study, including rice, sorghum and *Solanum lycopersicum* (tomato). In line with the absence of SLs in the xylem sap, experiments in rice showed that isotope-labelled SLs are indeed transported from root to shoot, but they were not detected in xylem sap (Xie et al., 2015b). Thus, it has been speculated that long-distance transport of SLs is mainly facilitated by cell-to-cell transport rather than through the xylem; therefore, the presence of transporters facilitating SL transport is required (Borghi et al., 2015).

Our understanding of SL transporters is limited, especially in plants like *Arabidopsis* and rice. PLEIOTROPIC DRUG RESISTANCE 1 (PDR1) was the first reported SL transporter found in *Petunia hybrida* (petunia), which acts as a cellular exporter of SLs (Kretschmar et al., 2012). PDR1 is a member of the ATP-binding cassette (ABC) transporter family, members of which play important roles in various phytohormone transport (Borghi et al., 2015). Reduced levels of SLs were detected in a *pdr1* mutant, along with reduced colonisation of roots by AMF, an indication that they are involved in exporting SLs to the rhizosphere. Furthermore, it was shown that the *PDR1* is mainly expressed in the root tip, and *PDR1* expression overlaps with the expression of SL biosynthetic genes (Sasse et al., 2015). Furthermore, based on the subcellular localisation of PDR1, a dual role was suggested to be involved in loading synthesised SLs in the apoplast and exporting SLs to the rhizosphere. Apart from the roots, expression of *PtPDR1* was also detected by GUS-staining in shoots near the lateral buds (Kretschmar et al., 2012). In addition, *pdr1* mutants, apart from the lower levels of SLs in root exudates, had an increased branching phenotype. Combining those two observations, Kretschmar et al. (2012) speculated that PDR1 might deliver acropetally transported SLs to developing buds and suppress their outgrowth. However, more recent studies revealed that PDR1 is involved in short-distance transport of SLs, and root-to-shoot transport does not appear to be directly dependent on PDR1 (Shiratake et al., 2019). The authors suggested that long-distance transport of SLs might involve other unidentified transporters or involves SL precursors that are not substrates of PDR1. The orthologue of PDR1 in tobacco was also shown to be involved in SL transport

(Xie et al., 2015a), however, no SL transporter has been reported in Arabidopsis or rice. ABCG59 from *Medicago truncatula*, which is a close orthologue of PtPDR1, has also been found to be involved in SL secretion affecting root mycorrhization (Banasiak et al., 2020).

1.1.8 Strigolactone Perception and Signalling

Among the highly branched mutants which led to the initial discovery of SLs as negative regulators of lateral branching, *max2* and *d3* in Arabidopsis and rice, respectively, did not respond to exogenous applied GR24, suggesting that MAX2/D3 are part of the SL perception and signalling pathway (Gomez-Roldan et al., 2008, Umehara et al., 2008). Subsequently, another highly branched mutant, *d14*, was also found to be SL-insensitive, revealing the second possible component of the SL perception and signalling pathway in rice (Arite et al., 2009). Several studies demonstrated that *D14* encodes an α/β -hydrolase protein, which acts as the receptor protein of SL signals (Shabek et al., 2018, Yao et al., 2016). In the presence of SLs, D14 binds and hydrolyses SLs. This reaction results in the formation of a covalently linked intermediate molecule and triggers conformational changes in D14 proteins. Those changes allow D14 to interact with F-box protein D3 (MAX2 in Arabidopsis). D3 is part of the Skp1-Cullin-F-box (SCF) E3 ubiquitin ligase complex (SCF^{D3}) responsible for the ubiquitination and proteasomal degradation of targeted proteins. In rice, the D53 nuclear repressor protein has been shown to be the target of the D14- SCF^{D3} complex (Zhou et al., 2013). D53 is degraded after the application of GR24 in a D14-SCF^{D3}-dependent manner (Jiang et al., 2013). Therefore, in the presence of SLs, D53 is degraded, and the expression of downstream genes repressed by D53 is released (**Figure 1.9**). Similarly, in Arabidopsis, SL signalling relies on the degradation of SUPPRESSOR OF MAX2 1-LIKE 6, 7 and 8 (SMXL6, 7, 8), which are the functional orthologous proteins of D53 (Wang et al., 2015b, Soundappan et al., 2015).

D53 repressor has been found to control its own transcription forming a feedback loop regulation in rice. Thereby, in the presence of SLs, *D53* transcription is induced, whereas, in the absence of SLs, *D53* is suppressed (Song et al., 2017). More recently, in Arabidopsis, SMXL6 was shown to directly bind to the promoters of *SMXL6*, *7*, *8* and

negatively regulate their transcription, demonstrating an autoregulation model of *SMXL6, 7, 8* transcript abundance (Wang et al., 2020b).

1.1.9 TB1-dependent Action of SLs in Tillering Control

As it has been shown in different SL-deficient or -insensitive mutants in many species, one of the main roles of SLs as phytohormones is to control lateral branching/tillering. There are several lines of evidence that this regulation is mediated solely through D53. In fact, *d53* mutants with a gain-of-function mutation, which constantly suppresses the SL signalling pathway, have increased branched phenotype and are insensitive to GR24 treatment (Zhou et al., 2013). In addition, *smxl6/7/8* mutants in Arabidopsis displayed a decreased branching phenotype, whereas they rescued the phenotype of SL-deficient and -insensitive mutants (Wang et al., 2015b). D53 contains an ethylene-responsive element binding factor-associated amphiphilic repression motif, which is known to be involved in the interaction with TOPLESS/TOPLESS Related transcriptional co-repressors (Ma et al., 2017). As a result, D53 has been suggested to act as a transcriptional repressor inhibiting the transcription of downstream genes. In rice, it has been shown that D53 can physically interact with SPL14 encoded by *IDEAL PLANT ARCHITECTURE 1 (IPA1)*. *IPA1/SPL14* belongs to a gene family, QUAMOSA Promoter-Binding Protein-like transcription factors, the members of which are involved in both vegetative and reproductive development, shaping the plant architecture. Loss-of-function *ipa1* mutants show a high tillering phenotype suggesting that IPA1 controls the transcription of genes that control tillering (Song et al., 2017). Biochemical and genetic studies demonstrated that IPA1 binds the promoter region of *TB1* and controls its expression. Therefore, it was proposed that the SL signalling pathway controls tillering by affecting the expression of *TB1/BRC1/FC1* via D53-SPL14 (Song et al., 2017). In agreement, Liu et al. (2017) found that wheat D53 could physically interact with TaSPL17, the wheat orthologue of OsSPL14, and control the transcriptional activation of *TaTB1* (Liu et al., 2017). In fact, *TB1/BRC1* expression is repressed in SL-insensitive mutants (Soundappan et al., 2015). In contrast, constitutive upregulation of *TB1/BRC1* has been found in *d53* rice mutants and in *smxl6, 7, 8 max2* quadruple Arabidopsis mutant, supporting the hypothesis that *TB1/BRC1* is a downstream target of SL signalling (Wang et al., 2015b, Soundappan et al., 2015). Similarly, rice *tb1/fc1* mutants

are insensitive to externally applied SLs, indicating that TB1 is required for the inhibition of tillering by SLs (Minakuchi et al., 2010). In Arabidopsis, a strong downregulation of *BRC1* has been reported in *max* mutants, while Brewer et al. (2015) reported that *brc1* mutants are insensitive to GR24 (Brewer et al., 2015). In rice, IPA1 interacts with D53 and is involved in the feedback regulation of *D53* expression (Song et al., 2017) (**Figure 1.9**). However, in Arabidopsis, it has been recently shown that SMXL6 directly binds *SMXL6*, *7*, *8* promoter regions, controlling their expression without interacting with other TFs, indicating a divergence in the mechanism of SL signalling between monocotyledons and dicotyledons (Wang et al., 2020b).

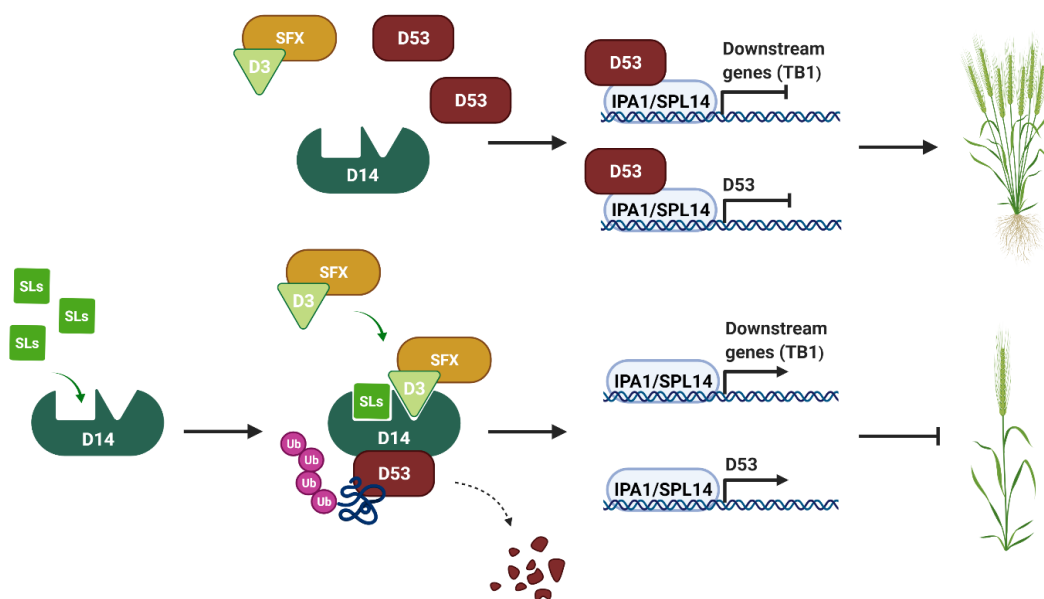


Figure 1.9: SL perception and signalling pathway. SL signalling pathway consists of D14 receptor protein, D3 F-box protein and D53 transcriptional repressor. In the absence of SLs, D53 interacts with IPA1/SPL14 transcription factor and represses the expression of downstream genes. In the presence of SL, SLs bind to D14, leading to conformational changes of D14, allowing interaction of D14 with F-box protein D3. D53 is targeted by the D14- SCF^{D3} complex leading to the ubiquitination and degradation of D53. Degradation of D53 releases the transcription of downstream genes. *TB1* is likely to be one of the downstream targets of the SL signalling pathway. *D53* transcription is controlled by D53, forming a typical negative feedback regulation. Illustration created in Biorender.

1.1.10 TB1-independent Action of SLs in Tillering Control

Despite the fact that SL action via regulating *TB1* expression is widely accepted, there are several lines of evidence supporting a parallel mechanism of lateral branching/tillering controls by SLs (Bennett et al., 2016). Firstly, the role of

TB1/BC1/FC1 in grasses has not been proven to be widely applicable. Even though the application of GR24 suppresses lateral branching in wild-type rice plants, transcript levels of *OsFC1* were not found to be upregulated. Similarly, *TB1/FC1* expression is not suppressed in SL mutants, as anticipated (Arite et al., 2007). Moreover, rice SL-deficient mutants formed more tillers than *fc1/tb1* mutants, suggesting the presence of a parallel mechanism of tiller suppression by SLs other than TB1 (Minakuchi et al., 2010). Similarly, recent and more detailed studies in *Arabidopsis* revealed that branching could be suppressed by GR24 even in *brc1* mutants, while *brc1 brc2* double mutants show less branching than SL signalling mutants (Seale et al., 2017). Consequently, there may be regulatory mechanisms operating in the SL-mediated inhibition of lateral branching other than TB1/BRC1/FC1. The model that can explain the TB1-independent regulation of tillering by SLs is based on the principle of the auxin transport canalization model (**Figure 1.3B**), according to which SLs suppress tillering by affecting PAT (Bennett et al., 2006, Prusinkiewicz et al., 2009). PAT is generally correlated with shoot branching in many species. In favour of the effect of SLs on PAT, Lin et al. (2009) reported on the characterization of the *d27* rice mutant that *d27* plants showed lower polar auxin transport than wild-type (Lin et al., 2009). In *Arabidopsis*, SLs dampen auxin transport, hence increasing the competition between the bud for establishing their own auxin canalization to the main stem, which is important for bud activation (Bennett et al., 2006, Crawford et al., 2010). In particular, SLs impair bud activation by triggering the rapid removal of the auxin efflux carrier PIN-FORMED 1 (PIN1) from the plasma membrane of the cell in the stem (Shinohara et al., 2013). More recently, van Rongen et al. (2019) demonstrated that in *Arabidopsis*, SLs control branching by affecting auxin transport and this effect is independent of TB1/BRC1. More specifically, the *pin3 pin4 pin7* triple mutant was able to rescue the highly branched phenotype of SL-deficient mutants, whereas the highly branched phenotype of the *brc1* mutant was not affected (van Rongen et al., 2019). Furthermore, there is evidence that CK can also act at least partly independently of TB1 by affecting the auxin transport capacity of the buds by affecting the accumulation of PIN3, 4 and 7, leading to higher auxin polar transport between lateral bud and main stem in *Arabidopsis* (Waldie and Leyser, 2018). Whether the regulation of lateral branching is facilitated in

a TB1-dependent manner or via affecting auxin transport, or those mechanisms co-exist and work in parallel in a fine-tune regulation of plant architecture has not been elucidated since both *BRC1* and PINs auxin efflux carriers are downstream targets of the SL and CK pathways in Arabidopsis (Bennett et al., 2016).

1.3. Tillering Control by Nitrogen Limitation

Plant growth and development rely on inorganic nutrient availability, which strongly impacts on agronomic plant productivity. N and P are among the mineral nutrients which most strongly limit plant growth and productivity. Plants, as sessile organisms, have developed different strategies to cope with low N availability. These changes include changes in root and shoot architecture which enables plants to adjust their architecture in such a way to optimize the use of available resources. Under N-limiting conditions, overall plant growth is suppressed, and more biomass is allocated to roots, while lateral root growth is induced to explore more soil for available N and increase nutrient capture (Oldroyd and Leyser, 2020). This shift in biomass accumulation is usually reflected in the root: shoot ratio, which is low under ample N supply, whereas it is increased under nutrient-limiting conditions, as root growth is induced at the expense of shoot growth (Oldroyd and Leyser, 2020). Plant adaptation to nutrient-limiting conditions also includes changes in shoot architecture, including suppression of secondary shoot formation. Both N and P limitations lead to a significant reduction in the number of formed tillers. Luo et al. (2017) showed that N limitation in rice affects the number of tillers per plant by inhibiting tiller bud outgrowth rather than affecting the initiation of tiller buds (Luo et al., 2017). Therefore, under nutrient-limiting conditions, developed buds remain dormant and can be activated when growing conditions become more favourable. Bud dormancy is known to be controlled by various signals such as phytohormonal balance, sugar availability, etc., as described in section 1.1.2. The response to N-limiting conditions requires not only a sensing mechanism but also local and long-distance signals to coordinate plant growth at a whole plant level. Therefore, it has been suggested that N may regulate tiller bud outgrowth by two different mechanisms; by regulating plant N metabolism or by regulating endogenous signals such as phytohormones, which act as long-distance signals coordinating growth at the whole plant level.

1.1.11 Nitrogen Availability as a Signal

Nitrogen is taken up by plants mainly in the form of nitrate (NO_3^-) or ammonium (NH_4^+). NO_3^- itself is known to act as a local signal triggering the primary nitrate response (PNR). PNR is triggered soon after the exposure of plants to NO_3^- and includes changes in the transcription of many genes, including genes involved in NO_3^- uptake and N assimilation, along with changes in root architecture (Zhao et al., 2018). Although the involvement of NO_3^- as signal controlling root architecture is well studied, little is known about the direct effect of NO_3^- in the modulation of shoot architecture. Dormant buds in N-deficient plants are released from dormancy after NO_3^- supply; however, this effect is more likely to be controlled by the N status of the plants rather than directly by NO_3^- . In Arabidopsis, the supply of alternative forms of N can also stimulate tillering, suggesting that the effect of NO_3^- supply is most likely to be due to the stimulation of N assimilation and the available N compounds within plants (de Jong et al., 2014). However, the type of N fertilization was found to have an effect on tillering in barley (Bauer and von Wirén, 2020). More specifically, plants supplied with NO_3^- showed a higher number of tillers compared to plants supplied with the same amount of total N, but as NO_3^- and urea or as NO_3^- and NH_4^+ . These responses were attributed mainly to the different effects of different N sources on the root-shoot translocation of CKs (Bauer and von Wirén, 2020). In the same study, external application of synthetic CKs induced tillering in plants supplied with NO_3^- but not in plants supplied with urea, suggesting that different N forms affect acropetal transport of CKs. Hydroponically grown wheat supplied with mixed N forms (NO_3^- and NH_4^+) developed more tillers than plants supplied with either N form alone (Chen et al., 1998). However, in the same study, the different effect of N forms was not attributed to the function of N forms as signals but to the different effect of N forms on phytohormone levels.

Several studies have shown that manipulation of the gene expression of different members of the nitrate transporter 1/peptide family (NPF) can modulate tillering. More specifically, overexpression of *NPF7.3* led to a higher number of tillers in rice, while the opposite effect was recorded in *NPF7.3*-RNAi lines (Fang et al., 2017). In addition, the expression of other members of the NPF family, such as *NPF7.2*, *NPF8.20*

and *NPF6.5*, have been positively associated with induced tillering in rice (Wang et al., 2018c, Fang et al., 2013, Hu et al., 2015). In fact, overexpression of *NPF7.2* in rice stimulates the expression of cell cycle genes in tiller buds leading to bud outgrowth (Wang et al., 2018c). Generally, *NPF* overexpressing lines have been shown to assimilate more N; therefore, the positive effect can be attributed to the higher levels of N compounds delivered to the developing lateral buds. In addition, altered expression of *NPFs* might trigger changes in N balance and allocation. More recently, Wang et al. (2022) showed that *OsNPF5.16* overexpression lines formed more tillers compared to the control, while the opposite phenotype was recorded in RNAi lines. Overexpression of *OsNPF5.16* resulted in elevated levels of CK, which might facilitate the tillering stimulatory effect (Wang et al., 2022b).

As mentioned above, N is mainly taken up mainly in the form of NO_3^- but roots also take up NH_4^+ and amino acids directly from the soil. Within the plants, NO_3^- and NH_4^+ are used for the biosynthesis of amino acids. Nitrogen assimilation takes place in roots and/or leaves. Gln and Asn are the main products of N assimilation, which are then used for the biosynthesis of other amino acids. Nitrate assimilation has also been shown to influence tillering. In fact, altered expression of the gene encoding rice glutamine synthetase 1.2 (*GS1.2*), which is involved in the biosynthesis of Gln, has been found to impact tillering (Ohashi et al., 2015b). Consistent with this observation, overexpression of *SbGS* stimulates tillering in sorghum (Urriola and Rathore, 2015). Further studies showed that the availability of Gln in the base of the rice shoots positively affects tiller bud outgrowth by affecting CK biosynthesis (Ohashi et al., 2017). Luo et al. (2018) reported that *asparagine synthetase 1 (asn1)* rice mutants had a significantly reduced tiller number. Although *asn1* mutants showed a reduction in the Asn content, no effect on N absorption was recorded, suggesting that Asn content is directly involved in the regulation of tillering in rice (Luo et al., 2018a).

As mentioned above, several studies have shown amino acids such as Asp and Gln play an important role in the regulation of tillering. Amino acids are the main form of N transported within the plants. Synthesised amino acids are transported from source roots or leaves to sink tissues such as developing buds. Amino acids have been suggested to act like sugars in controlling growth by acting as signalling molecules as

well as building blocks required for protein synthesis and growth. It has been previously reported that external application of low concentrations of amino acids results in stimulated tillering (Wang et al., 2019b). However, the application of a high concentration of amino acids can inhibit growth, suggesting that the effect of amino acids on growth is not only limited to their function as building blocks required for growth, but they also have important signalling roles in controlling cell metabolism and cell growth. In addition, based on studies in different species, the accumulation of certain amino acids, such as the basic amino acids (Lys and Arg), leads to tiller suppression. In both *Arabidopsis* and rice, Lys negatively affects root elongation and tiller bud outgrowth (Yang et al., 2014, Lu et al., 2018), while Lee et al. (2007) showed that accumulation of excessive amino acids leads to growth suppression (Lee et al., 2007). Amino acid transport is facilitated by different amino acid transporters. Among the different amino acid transporters present in plants, many members of the amino acid permease (AAP) family have been studied in rice, providing insights into the role of amino acid balance in tiller bud outgrowth. More specifically, suppression of *AAP5* and *AAP3* in rice has been shown to have a positive effect on tillering and grain yield by increasing the ear-bearing tillers. Amino acids determination in rice *aap5* mutant lines showed that plants have a lower content of the amino acids Lys and Arg and the neutral amino acid Val (Wang et al., 2019b). Consistent with this observation, Zhang et al., 2010 also reported that *Arabidopsis aap2* mutants had a higher number of formed branches accompanied by low amino acid content (Zhang et al., 2010a). Nevertheless, Ji et al. 2020 found that overexpression of another member of the AAP family, *OsAAP1*, positively affect tillering, whereas tiller suppression was observed in *aap1* knock-out lines. The authors suggest that *OsAAP1* might be involved in the basipetal transport of amino acids, which are required for growth (Ji et al., 2020).

1.1.12 Cytokinins as Signal under N Limitation

It has been reported in many species that CK content is correlated with N supply. In fact, in rice, the N supply stimulates the levels of CKs. CKs in roots suppress root growth, whereas in shoots, CKs control plant architecture by stimulating lateral branching/tillering and controlling other processes. Therefore, it has been suggested that systemic N response is at least partly mediated by CKs. Based on this model, N

supply stimulates CK biosynthesis in roots and shoots and the elevated levels of CKs control, in turn, plant architecture by stimulating bud outgrowth. In rice, it has been previously reported that N supply induces tillering by stimulating CK biosynthesis. Similarly, Wang et al. (2018) showed that rice lines overexpressing *OsNPF7.2*, a low-affinity nitrate transporter, showed higher uptake of N and enhanced tillering, which was accompanied by high CK content in tiller buds (Wang et al., 2018c). In addition, *gs1.2* mutants showed a strong reduction in tiller number and reduced levels of CKs in rice buds, supporting the positive correlation between N (and N metabolites such as Gln) with CK content of rice buds (Ohashi et al., 2017).

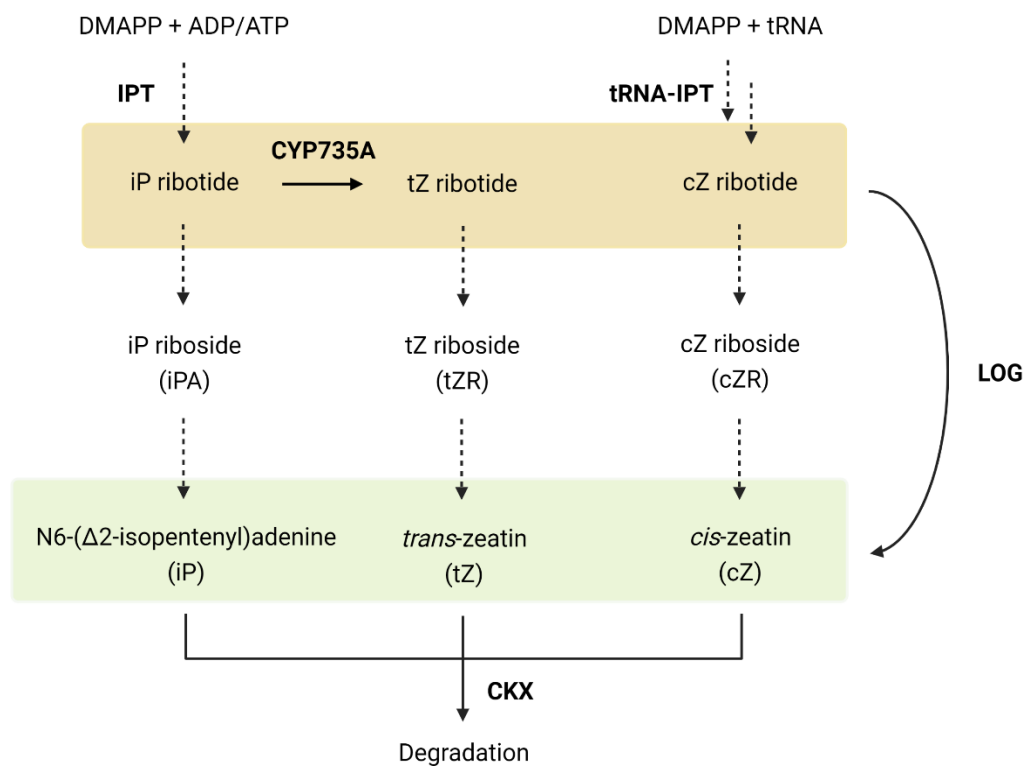


Figure 1.10: Simplified CK biosynthetic pathway. Illustration created with BioRender and inspired by Kudo et al. (2010).

The increase of CK content by N supply is achieved by the induction of the expression of CK biosynthetic genes. The primary enzyme of CK biosynthesis is adenosine phosphate isopentenyl transferase (IPT), which catalyses the biosynthesis of N6-(Δ^2 -isopentenyl) adenine (iP)-ribotide. iP-ribotide can be converted to *trans*-zeatin (tZ) ribotide by CYP735A1 or CYP735A2 (Takei et al., 2004b). The biosynthesis of the active form of CK, iP and tZ has been suggested to be controlled by two pathways, as

illustrated in **Figure 1.10** (Kudo et al., 2010). In the first pathway, ribosides are converted to the respective free base cytokinin by LONELY GUY (LOG) protein (Kurakawa et al., 2007). In the second pathway, which is also known as the two-step pathway, ribosides are formed by the dephosphorylation of the respective ribotides and are intermediates of the biosynthesis of free active CKs. However, the genes which are involved in the two-step pathway have not been identified. Essential genes for CK homeostasis are genes encoding CKX, which catalyse the irreversible degradation of active CKs. Deactivation of CK also plays an important role in controlling the levels of active CKs. CK deactivation is mediated by glycosylation catalysed by glycosyltransferases. Initially, CK biosynthesis was thought to take place only in roots, and subsequently, CKs are transported to shoots. However, recent studies have shown that *IPT* genes are also expressed in different above-ground tissues (Sakakibara, 2021). In contrast, *CYP732A* genes have been found only to be expressed in roots (Kiba et al., 2013). Finally, Kuroha et al. (2019) reported that *LOG* gene expression was also detected, not only in roots, but also in above-ground plant tissue (Kuroha et al., 2009). The different spatial variation in the expression of CK biosynthetic genes suggests that *de novo* cytokinin biosynthesis varies between different tissues, while CK activation occurs in all tissues.

The increase in CK content after N supply is mediated by the transcriptional regulation of CK biosynthesis. In fact, the expression of *IPT4* and *IPT5* in rice was induced by NO_3^- supply (Miyawaki et al., 2004, Takei et al., 2004a). Similarly, in Arabidopsis, the expression of *IPT3* is strongly induced after N supply, accompanied by higher levels of CK in root tissue (Takei et al., 2004a). Consistent with this observation, microarray analysis in roots revealed that *IPT3* and *CYP732A2* are among the N-responsive genes (Maeda et al., 2018). More specifically, for *IPT3* and *CYP732A2* transcriptional regulation has been suggested to be under the control of NIN-like protein (NLP) and Nitrate-Inducible GARP-type Transcriptional Repressor 1 (NIGT1), which are both master regulators of NO_3^- response. Takei et al. (2004) showed that CK levels were not found to be increased by N supply in *ipt3* mutants, highlighting the importance of the transcriptional regulation of *IPT* genes for the N-mediated increase in CK content. In

line with that, the repression of *IPT4* expression in rice significantly reduces CK content despite the high levels of N supply (Kamada-Nobusada et al., 2013).

More recent studies have shown that the transcriptional regulation of CK biosynthetic genes may be regulated by two different mechanisms. In the first mechanism, the expression of *IPT* genes is not regulated directly by NO_3^- but by N metabolites. More specifically, plants treated with nitrate reductase and glutamine synthetase inhibitors did not show any increase in CK levels after N supply, suggesting that CK *de novo* synthesis is controlled by N metabolites. In fact, Gln rather than NO_3^- or NH_4^+ was found to induce the expression of *IPT* genes in rice roots leading to higher levels of tZ- and iP-type of CK in both roots and shoots (Kamada-Nobusada et al., 2013). Similarly, the N-mediated induction of *IPT4* expression in rice roots was impaired in *gs2.1* loss-of-function mutant (Ohashi et al., 2017). In an alternative mechanism, in Arabidopsis, the regulation of CK biosynthetic genes has been found to be controlled by NO_3^- (Maeda et al., 2018). More recent studies have shown that *IPT3* and *CYP732A2* expression is controlled by the NLP/NIGT1 regulatory system, which is responsible for the regulation of many N-responsive genes (Maeda et al., 2018). N supply does not only stimulate the *de novo* synthesis of CK in roots but as Xu et al. (2015) demonstrated, NO_3^- supply promotes the expression of *IPT* genes locally in rice nodes, leading to higher CK content in the nodes and thereby to stimulated tillering (Xu et al., 2015b).

Apart from CK biosynthesis, CK distribution within the plant has been found to play an important role in N responses. Root synthesised CKs are transported to shoots through the xylem, acting as long-distance signals of N status. Among the different types of CK, tZR is the predominant form transported acropetally through the xylem (Hirose et al., 2008). In both barley and maize, an increase in tZR content in xylem sap has been reported after N supply (Kudo et al., 2010). In rice, all six types of CKs have been found to be upregulated by NO_3^- in xylem sap, resulting in increased CK content in both below and above-ground tissues (Song et al., 2013). All these observations suggest that CKs and predominantly tZ-type of CKs act as a signal of plant N status. The importance of the tZ-type of CK in the systemic regulation of shoot growth has been confirmed by grafting experiments in Arabidopsis. The phenotype of *cyp732a* (*cypDM*) mutant,

which does not synthesise tZ-type of CKs, was rescued when WT roots were grafted to mutant shoots (Kiba et al., 2013). The results indicated that tZ-type are transported acropetally through the xylem, while tZR is essential for the regulation of shoot growth by CK. In addition, as mentioned above, tZR is converted to tZ by LOG (Kuroha et al., 2009). Osugi et al. (2017) showed that the apical meristem activation is LOG-dependant, implying that both translocation of tZR but also the conversion of tZR to tZ locally in the shoot tissue are important for the regulation of shoot development by CKs (Osugi et al., 2017). Similarly, tZ content in the shoot was found to play an essential role in the systemic signalling of N, controlling the transcriptional reprogramming triggered by N supply (Poitout et al., 2018).

Signalling and perception of CK consist of a sensory His-protein kinase (HK), a His-containing phosphotransferase protein (HP) and a response regulator (RR) (Müller and Sheen, 2007). HKs are the receptor proteins of CK, while HPs are responsible for signal transduction. RRs are classified into two categories, type-A and type-B RRs. Type-A RRs lack a DNA recognition site, whereas type-B RRs function as transcription factors controlling the expression of downstream genes, including the expression of type-A RRs, forming a negative loop feedback regulation. Therefore, type-A RRs are CK-inducible, and their expression is positively correlated with CK content. Among the downstream genes controlled by the CK signalling pathway are transcription factors involved in shoot growth. The CK signalling pathway also controls the expression of N-related genes, indicating that CK content acts as a signal of N demand controlling the expression of N uptake and assimilation. However, several studies have shown that not all types of CKs have the same biological activity. For instance, in Arabidopsis, CK receptor proteins AHK2, 3, and 4 have been found to perceive iP and tZ, however, binding affinity varies between the different types of CKs (Sakakibara, 2021). In addition, tZ-type of CKs have been shown to strongly affect shoot growth and lateral branching compared to iP-type. Kiba et al. (2013) showed that Arabidopsis mutants lacking CYP735A1 and CYP735A2 trans-hydroxylation activity showed strong suppression of shoot development. The total CK concentration was unaffected in those mutants; however, there was a strong reduction in tZ-type of CK in both root and shoots, indicating that tZ-type, and no other CKs, are essential for shoot growth

regulation (Kiba et al., 2013). Feeding the mutant with tZ could restore the wild-type phenotype, whilst feeding with iP had no effect.

1.1.13 Strigolactones as Signal under N Limitation

SLs are a class of hormones which have been shown to act as rhizosphere signals but also as phytohormones controlling above-ground architecture, as mentioned in section 1.2. SL production and exudation have been associated with inorganic nutrient stress. Several studies have shown that P limitation strongly enhances SL levels in root and root exudates. Based on those observations, it has been suggested that under P limitation, plants which form a symbiotic relationship with mycorrhizal fungi exudate higher levels of SL in the rhizosphere to stimulate root colonization by AMF, which in turn improves inorganic P uptake (Yoneyama et al., 2012, Yoneyama et al., 2007b). Similarly, it has been found that N deficiency also induces SL levels in root exudates. Yoneyama et al. 2012 studied the SL levels under N limitation in various species and found that induction of SL levels was observed in non-legume species, including wheat. From these observations, the authors suggested that N-mediated SL production depends on plant nutrient acquisition strategy. Based on this hypothesis, non-legume plants produce more SL to facilitate AMF colonization and increase N acquisition (Yoneyama et al., 2012). However, SL exudation is not induced by low N in legume plants as they rely on rhizobacteria for N supply. Later studies demonstrated that this theory is not widely applicable, since no SL induction was found under low N conditions in tomato, which is a non-legume species. In addition, N limitation induced SL biosynthesis in *Pisum sativum* (pea), although a legume species (Foo et al., 2013). In addition, in the same study, it was demonstrated that SLs biosynthesis was not required for the regulation of nodulation in response to nutrient availability.

The observation that SL biosynthesis is induced under nutrient limiting conditions, in combination with the fact that SLs act as negative regulators of tillering, suggests SLs as good candidates for long-distance signals suppressing tillering under nutrient limiting conditions. It is well established in many species that SLs act as systemic signals, regulating tillering under low P conditions (Umehara et al., 2010, Kohlen et al., 2011). In fact, Umehara et al. (2010) demonstrated that in rice, there is a negative

correlation between the amount of SL in roots and the number of outgrowth tillers at a range of different P levels. Moreover, SL-insensitive rice mutants failed to respond to P limitation, suggesting that SLs are required for tillering regulation by P. Similar regulation was also found in Arabidopsis, suggesting that the mechanism is consistent in both monocotyledonous and dicotyledonous species.

In the same manner, based on the finding that SL production is also induced under N limiting conditions, it has been suggested that SLs might play a role in the N-mediated systemic regulation of tillering/lateral branching. In Arabidopsis, SL biosynthetic and signalling mutants formed more branches than WT plants under low N conditions; however, SL mutants still possessed the ability to respond to N limitation (de Jong et al., 2014). This suggested that the N-mediated regulation of tillering is partly dependent on SLs. Similarly, *d3* and *d14* rice mutants showed a similar response (Luo et al., 2018b). In addition, despite SL production being higher under low P conditions compared to low N, the tiller inhibition is stronger under low N, indicating that there are other systemic signals that are involved in tillering control under N-limiting conditions.

At the transcriptional level, SL biosynthetic genes have been found to be regulated locally in the basal nodes of rice plants grown under N limitation (Xu et al., 2015b). NO_3^- supply in N-deficient plants reduces the expression of SL biosynthetic genes in rice, indicating that the expression is affected by N supply. In addition, in rice, overexpression of *OsNPF7.2* resulted in higher N uptake and a higher number of outgrown tillers, with lower mRNA accumulation of SL biosynthetic genes in rice nodes. However, the exact mechanisms of transcriptional regulation of SL biosynthetic genes remain elusive. Experiments in different plants have provided some evidence regarding the signals controlling SL biosynthesis, mainly focusing on the roots. A split root experiment in sorghum showed that the expression of SL biosynthetic genes is controlled by a systemic signal and not directly by the levels of N and P (Yoneyama et al., 2015). Application of N or P in one-half of the roots led to the suppression of SL biosynthetic genes in the non-fertilized part of the root, while the N and P content of that part remained unaffected. Among the proposed signals controlling SL biosynthesis are auxin and/or CKs, as both play the role of systemic signals. Although

externally applied auxin affects SL biosynthesis in sorghum, it was found that IAA is not involved in the systemic regulation of SL biosynthesis under low N or P conditions. Some studies have correlated the suppression of SL biosynthesis under N sufficient conditions with CK content, as the application CKs suppresses the expression of SL biosynthetic genes (Xu et al., 2015b). There is a clear link between N and CK, and CKs are known to serve the role of long-distance signals of N status, as discussed in section 1.3.2. However, Yoneyama et al. (2020) tested whether CKs control SL biosynthesis under low P conditions. Based on the results from the split root experiment, CK application can indeed affect SL biosynthesis locally, but CKs were not confirmed to act as systemic signals controlling SL biosynthesis in roots (Yoneyama et al., 2020b). In contrast, Xu et al. (2015) reported that the application of synthetic CKs led to the suppression of SL biosynthetic genes *D27*, *D17* and *D10* not only locally in roots but also in basal nodes of rice (Xu et al., 2015b).

1.1.14 Auxin as Signal under N Limitation

Both CKs and SLs function as root-to-shoot signals regulating shoot branching in response to N limitation. However, there are several indications that shoot-derived signals can also be involved in tillering/branching regulation. The role of auxin in the regulation of lateral branching is well known since auxin is involved in apical dominance. Changes in auxin transport from shoot to root have been reported in response to N supply in many species. Under N-limiting conditions, IAA content has been found to be increased in the roots of many species, including Arabidopsis and maize (Kiba et al., 2010). Changes in IAA levels are important for the regulation of root architecture, whereas it has also been suggested that fluctuations in IAA movement might also play a role in tillering regulation. In Arabidopsis, the N deficiency effect on lateral branching is partly dependent on auxin (de Jong et al., 2014). Based on this study, under N-limiting conditions, each shoot apex exports more auxin, which leads to an increased amount of auxin in the PAT. Based on the transport canalization model, this increase in auxin levels in PAT can inhibit lateral bud outgrowth by preventing them from establishing their own auxin export system required for bud activation. However, this mechanism is not consistent in all plant species. More specifically, in rice, N limitation decreased the levels of IAA in the junction between shoot and roots

(the basal node) (Sun et al., 2014). In addition, the expression of *PIN1a-b*, *PIN5a*, *PIN9* and *PIN10* was downregulated under N deficiency, suggesting that auxin transport is suppressed. Similarly, Xu et al. (2015) also reported that the amount of IAA in rice nodes and buds is positively affected by N fertilization (Xu et al., 2015b). Therefore, the observation in rice showed the opposite response as the one reported in other species. However, the role of auxin in tiller inhibition under low N conditions should not be ruled out. In fact, Li et al. (2016) found that under high N supply, OsmiR393 is accumulated in tiller buds. The accumulation of miR393 was found to decrease the sensitivity of tiller buds by affecting auxin signal transduction. Therefore under high N conditions, tiller buds are less sensitive to the auxin in the PAT (Li et al., 2016).

1.4. Thesis Objectives

Tillering is an essential component of wheat architecture and an important agronomic trait as it is linked with plant productivity. Tillering is known to be regulated by many developmental and environmental factors. Phytohormones and sugar availability are among the main factors controlling bud outgrowth in response to external signals. N is among the mineral nutrients which most strongly limit plant growth and productivity. Plant adaptation to N-limiting conditions includes changes in shoot architecture, including suppression of secondary shoot/tiller formation. SLs are the most recently identified class of phytohormone being involved in the fine-tune regulation of tillering, acting as negative regulators of bud outgrowth. Several studies have linked SL production and exudation with nutrient limitations such as P and N. Although SL-related genes have been studied in other species, those genes have not been extensively studied in wheat. In addition, although SL levels are induced by N limitation in wheat root exudates, no study has focused on the transcriptional regulation of SL-related genes by N supply. Therefore, the first objective of this project was the identification of SL biosynthetic and signalling genes in wheat and to study their transcriptional response to N supply. In addition, monocotyledonous species show higher complexity in terms of *MAX1* homologue number and functionality compared to dicotyledonous species. Therefore, the spatial expression analysis of *MAX1* genes present in the wheat genome was another aim of this project.

In many species, P limitation leads to stronger SL exudation than N limitation. Therefore, it has been suggested that SL response to N limitation is attributed to lower P uptake of N-limited plants. Most of the studies have focused on root tissue, although SL biosynthetic genes are expressed and function in the basal nodes and principally in the lateral bud. Hence, an objective of this project was the comparative analysis of the N and P limitation effect on the transcription of SL metabolic genes in different tissues, including in the basal nodes.

Moreover, N limitation is known to reduce tiller number by suppressing tiller bud outgrowth. Bud dormancy is regulated by complex interactions between hormonal and nutritional signals. Recent studies have focused on the transcriptional changes that govern bud dormancy in response to different signals. However, less is known

about the signals that control bud dormancy in relation to N status. Therefore, a specific aim of this work was to study the transcriptional changes in the basal nodes under N limiting conditions that might be associated with the regulation of tillering.

The results suggested that SL biosynthesis and signalling are among the main pathways affected by N limitation, indicating that SLs might play an essential role in tillering control under N limitation. Recent studies have confirmed that SLs control tillering in wheat as *TaD27* overexpressing lines show a significantly lower number of tillers. However, in Arabidopsis and rice, it has been shown that SLs are not required for branching/tillering control by N status, as SL mutants still respond to N signals. If so, what could be the role of SL induction under N limiting conditions if not controlling tillering? Do they play another role in N response? Therefore, the final objective of this work was the generation of a wheat SL-deficient mutant and the phenotypic and transcriptomic analysis of the mutant response to N limiting conditions.

Overall, all the different objectives aim to better understand the functional role of SLs in wheat under N limitation and to examine if SLs play a different role other than suppressing tillering, such as in regulating general N response acting as a signal.

Chapter 2 Materials and Methods

2.1 Hydroponic Experiments

2.1.1 Hydroponic Culture

For the hydroponic experiments, *Triticum aestivum* plants were cultured in a custom hydroponic system in a controlled environment room or glasshouse. Seeds were surface sterilized with 1: 40 bleach solution: dH₂O (v/v) for 15 min, followed by 5-6 washes with sterilized dH₂O. Seeds were soaked in sterilized dH₂O overnight at 4 °C in the dark. Subsequently, seeds were placed in black boxes with wet filter paper to germinate (Day 0). The seed germination took place in a controlled environment room under 16 h day length and 22-18 °C. On day 4 after sowing (4 DAS), seedlings were transferred to the custom hydroponic system. In total, two similar hydroponic systems were used for the conducted experiments:

Hydroponic System 1

In hydroponic system 1, plants were grown hydroponically in Gallenkamp 228 (Sanyo, Osaka, Japan) controlled environment chamber (**Figure 2.1A**). Individual plants were grown held by foam buds on top of 1 L black pots containing the nutrient solution. The nutrient solution was aerated throughout the experiment by an aeration pump tubing system. The growing conditions were 20/10 °C day and night temperature, respectively, and 14 h day length. Lighting was provided by fluorescent bulbs at an intensity of 550 $\mu\text{mol m}^{-2} \text{sec}^{-1}$. The humidity was stable at 65% during the day and 75% during the night. To avoid any effect of the circadian clock on gene expression of the targeted genes, samplings were conducted at a similar time (if possible) and around 8-9 h after the light onset.

Hydroponic System 2

The main difference between hydroponic system 1 and system 2 was the pot size and the growing conditions. In hydroponic system 2, three plants were grown on top of 5 L black pots containing the nutrient solution under constant aeration (**Figure 2.1B**). Plants grown in the same pot were considered pseudoreplicates, and they were pooled together to form a biological replicate. The experiment was

conducted in a standard glasshouse equipped with high-pressure sodium lights (14 h day length, 20/18 °C day and night temperature, respectively).



Figure 2.1: Different hydroponic culture systems used in the hydroponic experiments: A. Hydroponic system 1: single plants were grown in 1 L black pots. Experiments were conducted in the CE chamber; **B.** Hydroponic system 2: three plants were grown in 5 L pots. The experiment was conducted in a standard glasshouse.

2.1.2 Nutrient Solution Composition

Seedlings were transferred to the hydroponic culture system at 4 DAS. To ensure good acclimatization of the plants in the hydroponic culture, plants were supplied with half-strength nutrient solution for 3 days (until 7 DAS) and then supplied with full-strength nutrient solution until sampling. The composition of the basic nutrient solution,

modified Letcombe (Drew and Saker, 1984), was 1.5 mM Ca(NO₃)₂, 5 mM KNO₃, 2 mM NaNO₃, 1.5 mM MgSO₄, 1 mM phosphate buffer solution (KH₂PO₄ – K₂HPO₄, pH 6.0), 50 μM FeNaEDTA, 0.5 μM CuCl₂, 20 μM H₃BO₃, 3.6 μM MnCl₂, 0.1 μM Na₂MoO₄ and 0.77 μM ZnCl₂. In addition, 0.25-0.5 g/L MES monohydrate (Alfa Aesar, Massachusetts, USA) was added as a pH buffer. pH was adjusted to 5.8 with KOH. The nutrient solution was renewed every 3-4 days.

The composition of the basic nutrient solution was adjusted based on the nutrient regimes used in each experiment. For the Low N treatment, plants were supplied with 0.1 mM of N in the form of KNO₃. For ionic balance in the low N nutrient solution, Ca(NO₃)₂ was replaced by CaCl₂, KNO₃ by KCl₂ and NaNO₃ by NaCl. Similarly, for the Low P treatment, plants were supplied with 0.01 mM of KH₂PO₄, while the remaining amount of KH₂PO₄ was replaced by KCL. Note that in the LowN/LowP experiment (section 2.1.4), P was supplied only as KH₂PO₄ in all the treatments instead of the phosphate buffer solution.

2.1.3 Experimental Design: N Limitation and N Induction Time Course Analysis

For both experiments, *T. aestivum* cv. Cadenza plants were hydroponically grown in the hydroponic culture system 1.

For the first experiment, exploring the effect of N limitation on the transcription of the genes of interest at different time points, a complete randomized block design with three blocks and three biological replicates per treatment combination was used. All plants received full strength nutrient solution until 10 DAS, when they were divided into two N treatments, High N (10 mM N) and Low N (0.1 mM N). The first sampling was conducted at 10 DAS and before dividing plants into the two treatments. High N and Low N treated plants were sampled 4, 8 and 12 days after the N limitation (14, 18 and 22 DAS) (**Figure 2.2A**). The selection of the time points was not random, but it was based on previous experimentation showing that those dates correspond to the dates when the first, second, third and fourth tiller bud of the main stem starts to actively grow under the given growing conditions. Tissue material from four plants was pooled together per biological replicate to ensure enough material for downstream analysis.

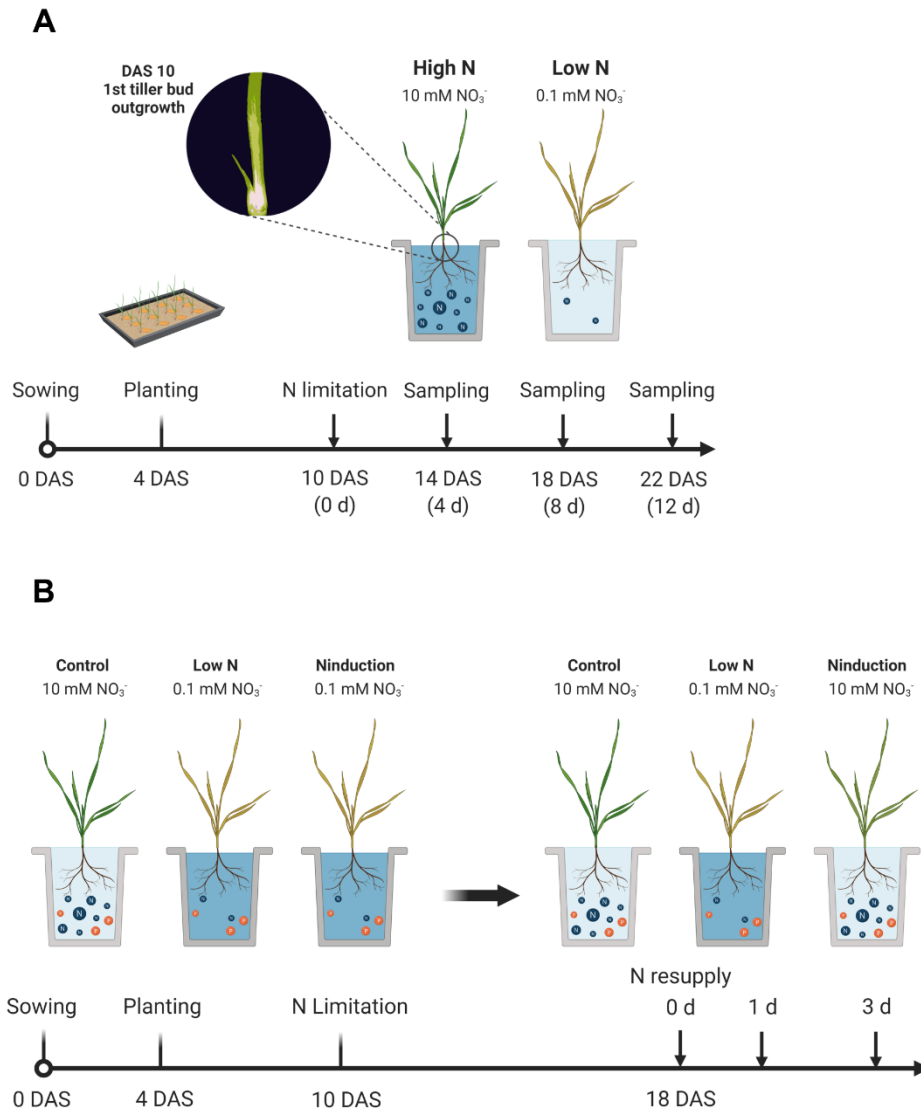


Figure 2.2: Experimental timeline of N limitation and N induction hydroponic experiments.

A. Timeline of N limitation experiment. All plants received High N nutrient solution until 10 DAS. On 10 DAS, half of the plants were provided with Low N nutrient solution containing 0.1 mM of NO_3^- . Sampling took place on 10 DAS (before the N limitation) and 4, 8 and 12 days after the N limitation. **B.** Timeline of N induction experiment. All plants received High N nutrient solution until 10 DAS when they were divided into 2 N treatments. At 18 DAS, half of the N-limited plants were provided with High N nutrient solution. Sampling took place at 18 DAS before the N resupply and 1 and 3 days after the N resupply to monitor the effect of N resupply on the gene expression of the genes of interest. The illustration was created in BioRender.

For the N induction experiment, a complete randomized block design with three blocks and three biological replicates per treatment was used. All plants received full strength nutrient solution until 10 DAS, when they were divided into two N treatments, High N (10 mM N) and Low N (0.1 mM N). At 18 DAS, half of the Low N treated plants were

resupplied with High N nutrient solution, while fresh nutrient solution was applied to the rest of the Low N and the High N treated plants. To study the effect of the N resupply on the transcription of the genes of interest, samples were taken before the resupply of N at 18 DAS (0 d), 1 day (1 d) and 3 days (3 d) after the N resupply (**Figure 2.2B**). Tissue material from two plants was pooled together per biological replicate to ensure enough material for the downstream analysis.

2.1.4 Experimental Design: N and P Limitation Transcriptional Changes

For N and P limitation experiment, *T. aestivum* cv. Cadenza plants were hydroponically grown in the hydroponic culture system 1.

A complete randomized block design with four biological replicates per treatment was used for the Low N and Low P experiment. All plants received full strength nutrient solution until 10 DAS, when they were divided into the three treatments, Control (10 mM N, 1 mM P), Low N (0.1 mM N, 1 mM P) and Low P (10 mM N, 0.01 mM P). The sampling of plant tissue took place at 18 DAS, 8 days after the introduction of plants to the respective nutrient limitation. Each biological replicate consisted of the material from six plants pooled together to ensure enough material for downstream applications. The experiment was performed twice, once for collecting sample material for the transcriptomic study and a second time for harvesting material for the phytohormonal analysis.

2.1.5 Experimental Design: Involvement of SL in Regulating Tiller Suppression under N Limitation

For this experiment, *Tad17* triple homozygous mutant (aabbdd, derived from TILLING mutant generation, see section 2.7) and wild-type (WT, AABBDD) sibling lines (also referred to as WT segregant) were grown in the custom hydroponic system 1. These sibling lines have different *TaD17* alleles, but they share many of the background mutations; thus, the comparison would be more valid. In fact, plants from two individual BC₁F₂ plants from each genotype, from two *Tad17* mutants and two WT segregant lines, were grown with three replicates per treatment (**Figure 2.3**). In other words, six biological replicates per genotype were included consisting of three biological replicates per line within the same genotype. Analysis of two segregating

lines per genotype was selected as an approach to rule out any effects caused by unlinked mutations (Uauy et al., 2017).

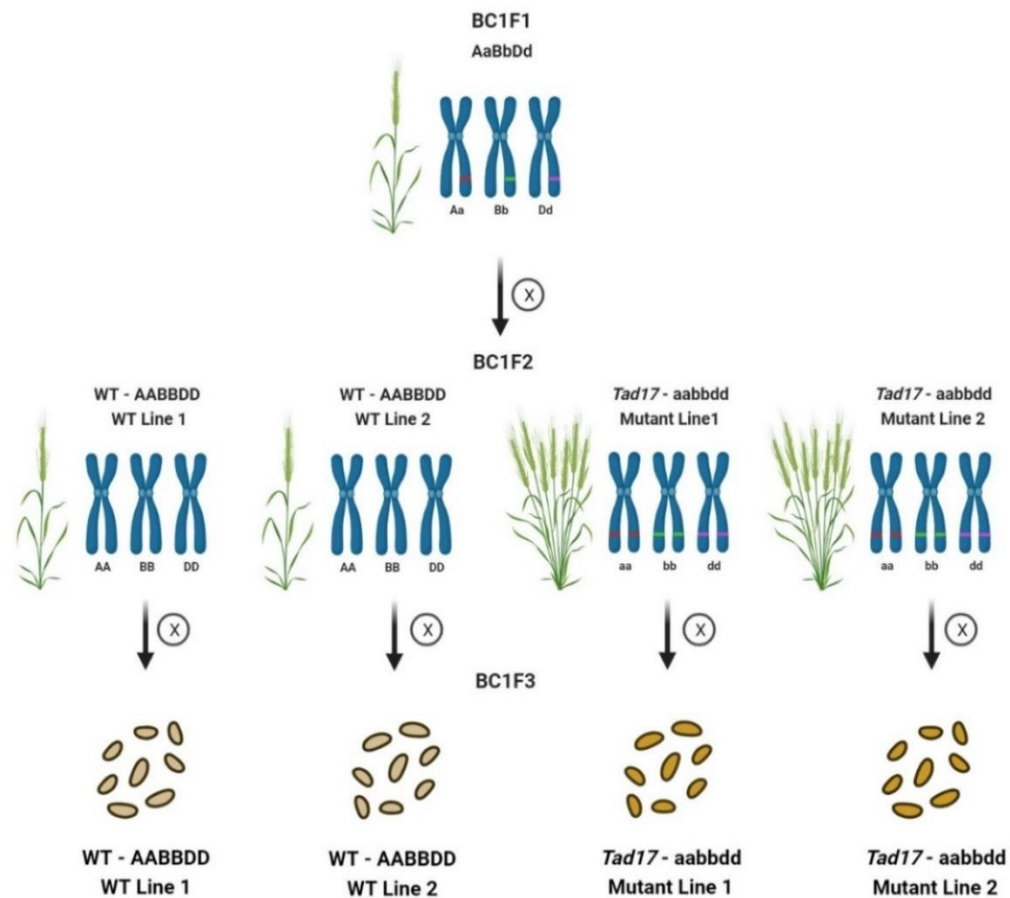


Figure 2.3: Schematic representation of WT and *Tad17* mutant lines used in the hydroponic experiment. Heterozygous BC₁F₁ plants were self-pollinated to produce a BC₁F₂ population. Triple homozygous *Tad17* mutant (aabbdd) and WT (AABBDD) sidling lines were selected in the BC₁F₂ using KASP markers. Seeds from two individuals of each genotype in the BC₁F₂ population were included in the hydroponic trial in three biological replicates per N treatment. The illustration was created in BioRender.

An incomplete Trojan square design was used for this experiment. All genotypes (WT, *Tad17*) received full strength nutrient solution until 10 DAS. At 10 DAS, half of the plants per line were supplied with Low N nutrient solution (0.1 mM N), while the rest of the plants continued receiving High N nutrient solution (10 mM N). Sampling took place at 18 DAS, 8 days after the introduction of the plants to N limitation. Each biological replicate consisted of tissue material from three plants pooled together to

ensure enough material for downstream analysis. Another sampling was conducted at 22 DAS. For the latter, a single plant was harvested per biological replicate.

2.1.6 Experimental Design: Effect of Microalgae-based Biostimulant on Wheat Growth and Development

To study the effect of the microalgae-based biostimulant on wheat growth, *T. aestivum* cv. Graham plants were hydroponically grown in the hydroponic culture system 2. Cultivar Graham was among the four wheat cultivars included in the field trial, so for consistency, it was also selected for the hydroponic trial.

The experimental design was a complete randomized block design with three blocks and three biological replicates per treatment combination. All plants received full strength nutrient solution until 14 DAS, when they were divided into four treatments: High N untreated (10 mM N, without biostimulant), High N treated (10 mM N, with biostimulant), Low N untreated (0.1 mM N, without biostimulant), Low N treated (0.1 mM N, with biostimulant). The biostimulant used was a microalgae extract-based product specifically formulated for the hydroponic culture. The biostimulant was added to the nutrient solution at a final concentration of 30 mg DW/L. The stock concentration was approximately 5% (w/v) micro-algae extract. Thereby, 3 ml of stock biostimulant was added per 5 L pot. Samples were taken 6, 24 and 72 h after the treatment application. In addition, for the long-term effect of the biostimulant, another sampling took place 18 days after the application. Tissue material from 3 plants grown in the same pot (experimental unit) was pooled together per biological replicate.

The data obtained from this experiment are not fully presented in this thesis; however, some transcriptomic data generated as part of this experiment were utilized in section 3.2.6.

2.2 Phenotyping and Sampling

2.2.1 Tiller Counting

The number of outgrown tillers per plant was recorded before each sampling point or at different time points throughout the experiment, depending on the duration of the hydroponic experiment. Only tillers that had emerged from the leaf sheath were recorded and referred to as outgrown tillers. In the N limitation time course analysis experiment, the number of primary and secondary tillers was recorded separately.

2.2.2 Fresh and Dry Weight

The total fresh weight of the whole root and shoot per plant was determined at different time points depending on the experiment. For dry weight determination, whole root and shoot samples were freeze-dried in Modulyo freeze dryer (Edwards, West Sussex, UK) for at least 2 days, and then the dry weight of each tissue was recorded.

2.2.3 Chlorophyll Content – SPAD

The chlorophyll content of leaves was measured using the SPAD-502 chlorophyll meter (Konica Minolta, Tokyo, Japan). Readings from three different positions along the examined leaf were taken, and the average value was recorded.

2.2.4 Tissue Harvesting/Sampling

The whole root system, the basal node and the remaining shoot and leaves were harvested at specific time points based on each experimental design (as described in section 2.1). In this study, the basal node is called the 0.5 cm long section from the base of the main shoot, which includes the shoot apical meristem, lateral buds and leaf meristems. After removing all the roots from the shoot, the outgrown primary tillers were also carefully removed, and 0.5 cm of the main shoot base was dissected. Samples were quickly frozen in liquid nitrogen (LN₂) and stored at -80 °C until processing.

2.3 Molecular Biology

2.3.1 DNA Extraction

For genomic DNA extraction, leaf samples (3-5 cm) were collected from wheat seedlings once their second leaf had fully emerged. Harvested leaf samples were first lyophilized overnight (16 h) in Modulyo freeze dryer (Edwards, West Sussex, UK). Subsequently, lyophilised samples were ground into a fine powder using the Geno/Grinder 2010 (SPEX SamplePrep, New Jersey, USA) using 3 mm stainless steel beads to disrupt tissues. 1 ml of the extraction buffer (100 mM TrisBase, 1 M KCl and 10 mM EDTA, pH 9.5) was added to the ground leaf tissue, followed by incubation at 65 °C for 1 h with shaking. After the incubation, 330 µL of 5 M potassium acetate pH 5.8 (KAc) were added, and the samples were mixed for 2 min in the Geno/Grinder 2010 (SPEX SamplePrep, New Jersey, USA). After centrifugation (14,000 rpm, 15 min) to pellet the cell debris, 1 ml of the supernatant was transferred in a fresh microcentrifuge tube, mixed with 550 µL of chilled isopropanol and incubated at 10 °C for 10 min. After centrifugation (14,000 rpm, 10 min, 4 °C), the supernatant was removed, and the pelleted DNA was washed with 500 µL 75% (v/v) EtOH. Finally, the air-dried pelleted DNA was dissolved in 200 µL TE (10 mM Tris-HCl pH 7.5, 0.1 mM EDTA). To ensure good suspension of the pelleted DNA, the samples were kept at 4 °C overnight. Finally, DNA was quantified and stored at -20 °C until further use.

A modified version of the above protocol was used for high-throughput DNA extraction in Abgene 96 Well 1.2 mL deep-well plates (Thermo Scientific, Waltham, USA) sealed with 96-well sealing mats (Thermo Scientific, Waltham, USA). For this purpose, volumes, incubation, and centrifugation time were adjusted accordingly.

2.3.2 RNA Extraction

Plant tissue of pooled biological replicates was ground to a fine powder under LN₂ freezing and stored at -80 °C. Basal node samples were hand-ground with pre-cooled mortar and pestle due to the small amount of the sampled tissue. Grinding of root sampled was carried out in Freezer Mill (SPEX SamplePrep, New Jersey, USA). The frozen ground plant tissue was aliquoted into 2 ml tubes and stored at -80 °C until RNA extraction.

All the solutions used for the RNA extractions had been previously treated with diethyl pyrocarbonate (DEPC, Sigma-Aldrich, Dorset, UK) to destroy any RNase activity. 1 μL of DEPC was added per 1 ml of solution. After vigorously shaking, the solution was incubated overnight at room temperature and then autoclaved.

TRizol Extraction Method

For basal node samples, RNA was extracted from approximately 100 mg of frozen tissue using TRizol reagent (Invitrogen, Waltham, USA). 1 mL of TRizol reagent was added to the frozen tissue before it thaws, followed by vortexing for 30 sec until completely homogenized. The homogenate was incubated at room temperature for 5 min and centrifuged (13.000 rpm, 10 min 4 °C) to pellet the cell debris. 1 ml of the supernatant was then transferred into a fresh 2 ml microcentrifuge tube. Next, 200 μL of chloroform was added, and the mixture was vortexed for 15 min and incubated at room temperature for 5 min. After incubation, the mixture was centrifuged (13.000 rpm, 15 min, 4 °C), and the aqueous phase (approximately 600 μL) was collected in a new 1.5 mL microcentrifuge tube. Subsequently, 1 vol isopropanol was added, and after mixing by inverting the tube, the mixture was incubated for 15 min on ice. RNA precipitation was achieved by centrifugation (13.000 rpm, 15 min, 4 °C). The RNA pellet was washed with 75% (v/v) EtOH and then recovered by centrifugation (13.000 rpm, 5 min). Finally, the supernatant was carefully removed with a pipette without disturbing the pellet, and the pelleted RNA was air-dried under the fume hood.

To ensure no DNA carryover, DNase treatment was performed by adding 150 μL of DNase master mix containing: 7 μL of 1 unit/ μL RQ1 RNase-Free DNase (Promega, Madison, USA), 15 μL DNase buffer and 128 μL $\text{H}_2\text{O}_{\text{DEPC}}$. The air-dried RNA pellet was dissolved for 30 min on ice, and the mixture was incubated for 30 min at 37 °C. After the incubation, the volume was increased to 300 μL by adding 150 μL $\text{H}_2\text{O}_{\text{DEPC}}$, followed by phenol/chloroform purification. More specifically, 1 vol of 25:24:1 phenol/chloroform/isoamyl alcohol (SIGMA-Aldrich, Dorset, UK) was added, and the mixture was then vortexed and centrifuged (13.000 rpm, 5 min). The aqueous phase was transferred to a fresh 1.5 mL microcentrifuge tube, and a further purification step was performed by adding 1 vol 24:1 chloroform/isoamyl alcohol

(SIGMA-Aldrich, Dorset, UK), vortexing and centrifugation as above. The aqueous phase was retrieved in a fresh 1.5 mL tube. RNA was precipitated by adding 3 vol EtOH absolute and 0.1 vol of 3 M NaOAc (pH 5.2) and incubated at -80 °C for 1 h or at -20 °C overnight. After centrifugation (14.000 rpm, 20 min, 4 °C), the pelleted RNA was washed with 1 ml 75% (v/v) EtOH and air-dried as described above. Finally, the air-dried RNA pellet was dissolved in 30-50 µL of RNase-free dH₂O, depending on the pellet size.

Total RNA concentration was measured using the Nanodrop 2000 spectrophotometer (Thermo Scientific, Waltham, USA) and 2 µL of each RNA sample. The quality of the extracted RNA was evaluated by running 500 ng of RNA in 1% agarose TAE-gel. Finally, the RNA samples were stored at -20 °C until further use.

Hot Phenol Extraction Method

A modified hot phenol extraction protocol was used for extracting RNA from approximately 500 mg of root tissue (Verwoerd et al., 1989). 1 mL of hot (80 °C) phenol extraction buffer was added to the frozen tissue before it thawed, followed by vortexing for 30 sec until completely homogenized. The phenol extraction buffer consisted of 1 vol phenol and 1 vol of RNA extraction buffer (0.1 M Tris/HCL, 0.1 M LiCl, 1% SDS, 10 mM EDTA, pH 8.0). After adding 500 µL of 24:1 chloroform/isoamyl alcohol (SIGMA-Aldrich, Dorset, UK), the mixture was vortexed for 30 sec and centrifuged (13.000 rpm, 5 min, 4 °C) to separate the organic and aqueous phase. The aqueous phase was transferred in a fresh 2 ml microcentrifuge tube. Subsequently, an equal volume of 24:1 chloroform/isoamyl alcohol (SIGMA-Aldrich, Dorset, UK) was added, followed by vortexing and centrifugation as above. Finally, the aqueous phase was transferred in a fresh 1.5 ml microcentrifuge tube. RNA precipitation was achieved by adding 1 vol 4 M LiCl and incubating at 4 °C overnight. RNA was pelleted by centrifugation (13.000 rpm, 20 min, 4 °C). The RNA pellet was washed with 75% (v/v) EtOH and then recovered by centrifugation (13.000 rpm, 5 min) and air-dried. DNase treatment, further phenol/chloroform RNA purification step and RNA precipitation were performed as described in the TRIzol extraction

method section. Finally, the air-dried RNA pellet was dissolved in 50 -100 μL of RNase-free dH_2O , depending on RNA pellet size.

Other RNA extraction Methods

For the samples submitted for RNA sequencing, total RNA was extracted from 100 mg of basal node tissue by using either the RNeasy Plant Mini Kit (Qiagen, Hilden, Germany) or the PureLink™ RNA Mini Kit (Invitrogen, Waltham, USA) following the manufacturer's instructions. Elution of the column was performed with 50 μL RNase-free H_2O . DNase treatment was performed by adding 100 μL of DNase master mix containing: 7 μL of 1 unit/ μL RQ1 RNase-Free DNase (Promega, Madison, USA), 15 μL DNase buffer and 78 μL $\text{H}_2\text{O}_{\text{DEPC}}$. The mixture was then incubated for 30 min at 37 °C. Further phenol/chloroform RNA purification and RNA precipitation were performed as described in the TRIzol extraction method section.

2.3.3 Nucleic Acid Determination

The concentration of the extracted nucleic acids (DNA, RNA) was measured using Nanodrop 2000 spectrophotometer (Thermo Scientific, Waltham, USA) and 2 μL of each sample. A280/A260 and A260/A230 ratios were also used to evaluate the purity of the nucleic acid. Samples were diluted to the same concentration with $\text{dH}_2\text{O}_{\text{DEPC}}$, depending on the concentration range required for downstream application.

For the more accurate quantification of the RNA samples submitted for RNA sequencing, the Qubit Broad Range Assay Kit (Invitrogen, Waltham, USA) was used. For each assay, 2 μL of RNA samples were added to 198 μL of Qubit working solution (prepared as per instructions). Qubit 2.0 Fluorometer (Invitrogen, Waltham, USA) was used for reading the samples.

2.3.4 cDNA Synthesis

First-strand complementary DNA (cDNA) was synthesized using SuperScript III Reverse Transcriptase (Invitrogen, Waltham, USA) and oligo-dT primers. 2 μg of total RNA and 1 μL of 10 mM oligo-dT primers to a final volume of 13 μL were added in a 0.5 mL PCR tube. The mixture was then mixed, centrifuged, and incubated at 70 °C for 7 min to denature the RNA. After the incubation, samples were put quickly on ice.

Subsequently, 4 μ L 5x first strand buffer, 1 μ L 0.1 M DTT, 1 μ L 10 mM dNTPs and 1 μ L Superscript III Reverse Transcriptase (Invitrogen, Waltham, USA) were added as a mix to each tube. After mixing and short centrifugation, the tubes were incubated in a PCR machine for 5 min at 20 °C, followed by 2 h at 50 °C and a final step of 15 min at 70 °C to terminate the reverse transcriptase. Synthesized cDNA was diluted 1:2 with RNase-free H₂O and stored at -20 °C.

2.3.5 Polymerase Chain Reaction (PCR)

At the initial stages of TILLING triple mutant generation, genotyping of the TILLING lines was performed by sequencing. For this purpose, standard PCR was carried out with the appropriate homoeologue-specific set of primers for the amplification of the region that contains the single nucleotide polymorphism (SNP) of interest – the mutation site. The primers used for each of the mutation sites can be found in **Table 2.1**.

Table 2.1: Primer sequences for each of the three homoeologues of *TaD17* and optimized PCR parameters used for genotyping of the mutant lines by sequencing.

Primer Name	Primer Sequence (5'→3')	Targeted Homoeologue	Annealing Temp (°C)	Q5 GC Enhancer	PCR Product (bp)
TaD17-For2A1	AGTTTACAGAGCACGCGTATAC	<i>TaD17-2A</i>	64.6	No	156
TaD17-RevA1	CACGTTCTTCATCACCTTCACG				
TaD17-ForB1	GTGTAACCTCACTGATGGCAC	<i>TaD17-2B</i>	63.8	Yes	471
TaD17-RevB1	GAAGATCAACTGAATGTTTGGC				
TaD17-ForD1	GTGGCAATTGAGCTCGACAAG	<i>TaD17-2D</i>	66	Yes	447
TaD17-RevD1	CAAATGTAGACAAAGGCGTCAAAC				

All the PCRs were performed in a Touchgene Gradient (Techne, Staffordshire, UK) PCR machine using Q5 high-fidelity proofreading DNA polymerase (New England BioLabs, Massachusetts, USA), as low base misincorporation rates are important for applications such as genotyping. The reactions were prepared following the manufacturer protocol with some modifications after optimizing the parameters for each set of primers (**Table 2.2**). Around 100-200 ng of DNA were used per 25 μ L

reaction. The PCR program used was 98 °C for 30 sec (initial denaturation), followed by 30 cycles of 98 °C for 10 sec (denaturation), 60-70 °C for 20 sec (annealing) and 72 °C for 20 sec (extension), and finally 72 °C for 2 min (final extension). The final PCR parameters used for each set of primers (annealing temperature, use of GC enhancer, etc.) varied depending on the primers' characteristics and were determined after optimization of the method by running gradient PCR in a range of different annealing temperatures (62.1-69.3 °C) and checking the amplification specificity by gel electrophoresis of the PCR product (**Table 2.1**).

Table 2.2: Reagent used for Q5 polymerase PCR reaction setup.

Q5 polymerase		
Reagent	Volume	Concentration
5X Q5 Reaction Buffer	5 µl	1x
10 mM dNTPs	0.5 µl	200 µM
10 µM Forward Primer	1.25 µl	0.5 µM
10 µM Reverse Primer	1.25 µl	0.5 µM
Template DNA	variable	100-200ng
Q5 High-Fidelity DNA Polymerase	0.25 µl	0.02 U/µl
5X Q5 High GC Enhancer (optional)	(5 µl)	(1x)
Nuclease-Free Water	to 25 µl	

2.3.6 PCR Product Purification

After the amplification of the targeted region, PCR products were purified with Wizard SV Gel and PCR Clean-Up System (Promega, Madison, USA), following the manufacturer's protocol. DNA was eluted from the column with 50 µL of DNase-free dH₂O_{DEPC}. The DNA concentration of the purified PCR product was determined using the NanoDrop 2000 spectrophotometer (Thermo Scientific, Waltham, USA)

2.3.7 Gel Electrophoresis

Gel electrophoresis was used as part of this study for either checking the extracted RNA quality or checking the PCR amplification specificity and estimating the PCR product fragment size.

Extracted RNA quality was evaluated by agarose gel electrophoresis in Tris Acetate EDTA (TAE, 40 mM Tris, 20 mM acetic acid, 1 mM EDTA). A 1% w/v agarose TAE gel was prepared, containing 1x SYBR safe DNA gel stain (Invitrogen, Waltham, USA) for staining the nucleic acids. 500 - 300 ng of RNA mixed with 1.6 μ L 6x DNA gel loading dye (Thermo Scientific, Waltham, USA) in 10 μ L dH₂O_{DEPC} final volume were loaded per well. RNA gels were usually run at 80 mV for 40 min. After the completion of the electrophoresis, the gels were visualized under UV light using the G: BOX imaging system (SYNGENE, Cambridge, UK). An example of good quality extracted RNA is shown in **Figure 2.4**.

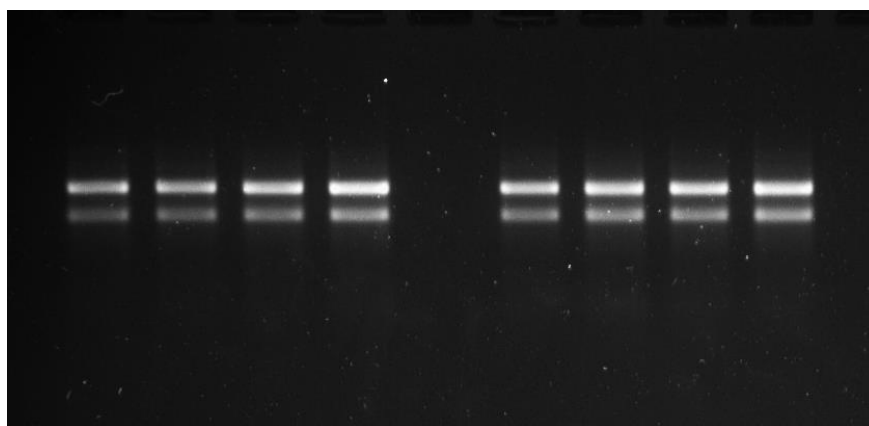


Figure 2.4: Example of gel electrophoresis of total RNA. Good quality RNA shows only two sharp bands, which correspond to 28s and 18s rRNA from top to bottom.

For the PCR product gel electrophoresis, PCR products were mixed with 1x DNA gel loading dye (Thermo Scientific, Waltham, USA) and were run in 1.2-1.5% agarose TAE gel. For the estimation of the fragment size, 100 bp DNA ladder dye (Thermo Scientific, Waltham, USA) was run alongside the PCR products. Gels were run at 100 mV for 50 min. After the completion of the electrophoresis and were visualized under UV light.

2.3.8 Genotyping

TILLING mutant lines were genotyped by either sequencing the flanking region of the site of the mutation or by using kompetitive allele-specific PCR assays.

Genotyping by Sequencing

After amplification of the region that contains the SNP of interest (section 2.3.6) and the purification of the PCR products (section 2.3.7), the PCR products were

sequenced using the TubeSeq service (Eurofins Genomics, Luxemburg, Luxemburg). The submitted samples consisted of 150-200 ng of purified PCR product in 15 μL of DNase-free H_2O and 2 μL 10 μM of the corresponding primer (final volume 17 μL). The genotype of the mutant lines was then determined by sequence alignment of the sequencing results against the sequence of wild-type Cadenza *TaD17* sequence using the Geneious 10.2.3 alignment tool (<https://www.geneious.com>).

Kompetitive Allele Specific PCR (KASP) Genotyping

For the high-throughput genotyping of the TILLING mutant lines, the KASP assay was utilized. KASP assays were performed in ABI-7500 real-time PCR system (Applied Biosystem, Massachusetts, USA) using a 10 μL reaction. Each reaction was prepared by pipetting 2 μL of extracted DNA (around 50 ng/ μL) in a white 96-well qPCR Plate (4titude, Surrey, UK) based on the pre-designed plate layout and then by adding 0.14 μL of KASP primer mix (12 μM KASP primer1, 12 μM KASP primer2, 30 μM KASP primer3 – **Table 2.3**), 2.86 μL H_2O and 5 μL PACE Low-ROX mix (3CR Bioscience, Harlow, UK) prepared as a master mix. Two negative controls ($\text{dH}_2\text{O}_{\text{DEPC}}$) were included in every plate, along with a WT Cadenza sample. The plate was sealed with adhesive qPCR seal (4titude, Surrey, UK), and after a short shaking and short centrifugation, the plate cycled in the AB-7500. The cycling program consisted by 15 min at 94 $^{\circ}\text{C}$, 10 cycles of 94 $^{\circ}\text{C}$ for 20 sec and 68 $^{\circ}\text{C}$ (-0.6 $^{\circ}\text{C}$ per cycle) for 60 sec, followed by 32-40 cycles of 94 $^{\circ}\text{C}$ for 20 sec and 62 $^{\circ}\text{C}$ for 60 sec. Finally, the plate reading was performed at 30 $^{\circ}\text{C}$ for 60 sec. The data were analysed with the allelic discrimination function for genotyping as implemented in the software ABI 7500 v2.0.6 (Applied Biosystem, Massachusetts, USA).

Table 2.3: Primer sequences used for KASP genotyping.

Primer	Primer Sequence (5'→3')	Targeted SNP	Allele
TaD17-2A KASP1	ACCCTGTGCCCCACCCTG		WT
TaD17-2A KASP2	ACCCTGTGCCCCACCCTA	Cad1738 [G/A]	Mutant
TaD17-2A KASP3	TGAGTTTACAGAGCACGCGTATAC		Common
TaD17-2B KASP1	CGAACATCCTGTGGAAATGGAAC		WT
TaD17-2B KASP2	CGAACATCCTGTGGAAATGGAAT	Cad1271 [C/T]	Mutant
TaD17-2B KASP3	CCTTCGAGGAGGACAACGG		Common
TaD17-2D KASP1	GAAGTCTGCCGGTCTGTTCC		WT
TaD17-2D KASP2	GAAGTCTGCCGGTCTGTTCT	Cad0880 [C/T]	Mutant
TaD17-2D KASP3	GATGCTCCGTGAAGAGACTGTCT		Common

2.3.9 Real-Time qPCR

The real-time qPCRs were performed in ABI-7500 real-time PCR system (Applied Biosystem, Massachusetts, USA) using the SYBR Green JumpStart kit (SIGMA-Aldrich, Dorset, UK). A pipetting scheme for the preparation of each reaction was followed to minimize pipetting mistakes and ensure repeatable results. The primer concentration in the reaction was 250 nM for both primers. More specifically, each reaction was initially prepared in a 0.5 ml microcentrifuge tube by adding 21.4 µL of master mix (11.25 µL SYBR Green JumpStart Taq ReadyMix, 0.6 µL 10 µM Forward Primer, 0.6 µM 10 µM Reverse Primer, 0.02 µL ROX and 8.93 µL H₂O_{DEPC}) and 1.1 µL of the cDNA sample. After mixing the reactions and short centrifugation, 20 µL of each reaction were pipetted into a white 96 well PCR Plate (4titude, Surrey, UK), which was sealed with adhesive qPCR seal (4titude Surrey, UK). The real-time PCR cycling parameters used were 2 min at 50 °C and 10 min at 95 °C, followed by 40 cycles of 95 °C for 15 sec and 60 °C for 60 sec. At the end of the reaction, the melting curve was recorded.

2.3.10 Real-Time qPCR Data Analysis

The real-time qPCR data were analysed with ABI 7500 v2.0.5 software (Applied Biosystem, Massachusetts, USA). The fluorescence threshold for the Ct values calculation was calculated automatically by the software or manually adjusted in the

linear phase of the amplification curve. Primer efficiency was estimated for all individual samples in each run using the linear phase of the amplification curves as calculated by LinRegPCR software (Ramakers et al., 2003).

The gene expression levels were calculated as Normalized Relative Quantity (NRQ) given by the formula $NRQ = \frac{(E_{GOI})^{-Ct_{GOI}}}{(E_{ref})^{-Ct_{ref}}}$ (Rieu and Powers, 2009). Ct_{GOI} and E_{GOI} stand for the Ct value and the average primer efficiency of the targeted gene of interest, respectively. Similarly, Ct_{ref} and E_{ref} correspond to the Ct value and the average primer efficiency of the reference gene(s). Wheat genes encoding actin3 (*TaACT3*) and succinate dehydrogenase (*TaSDH*) were used as reference genes (**Table 2.4**). Two technical replicates were used for each of the reference genes.

Table 2.4: Primer sequences of genes used as reference genes for relative gene expression analysis.

Gene Name	Gene ID	Primer Sequence (5'→3')
<i>TaACT3</i>	TraesCS5A02G124300	TaActin3-rtFor1 ATCTCGAAGGGYGAGTATGAYGAG
	TraesCS5B02G124100	
	TraesCS5D02G132200	TaActin3-rtRev1 AGAAGACCCAGACAACCTCGCAAC
<i>TaSDH</i>	TraesCS2A02G220800	TaSuccDH-rtFor1 TTTGCTCTCCGTGGTGCCTTTGG
	TraesCS2B02G246400	
	TraesCS2D02G226500	TaSuccDH-rtRev1 GAAGATGTGTAGCTCCTTGCTTGC

2.3.11 High-throughput RNA-sequencing

Extracted total RNA from basal node and root samples (section 2.3.2) was further purified with Plant RNeasy kit (Qiagen, Hilden, Germany) following the provided RNA clean-up protocol. The concentration of the purified RNA was determined by Qubit Broad Range assay (Invitrogen, Waltham, USA). 2-3 µg of RNA samples were submitted for Next-Generation Sequencing (NGS). The number of biological replicates varied among different experiments from 3 to 6 replicates per treatment combination (**section 2.1, Table 2.5**).

Prior to the library preparation, RNA integrity was assessed with RNA kit on Agilent 5300 Fragment Analyzer (Agilent Technologies, California, USA). Quality control, poly-A selection for rRNA removal, library preparation, multiplexing and sequencing was performed by Genewiz UK (Essex, UK) according to their standard workflow. Briefly, RNA library preparation was prepared using NEBNext Ultra II Library Prep Kit for Illumina following the manufacturer's protocol (NEB, Ipswich, MA, USA). Firstly, oligo-dt beads were used for mRNA enrichment, and the mRNAs were fragmented for 15 min at 94 °C. First and second strand cDNA was subsequently synthesized. Indexed adapters were ligated to cDNA fragments after adenylation of the 3' end of the cDNA fragments. Limited cycle PCR was used for library amplification. Sequencing libraries were validated using NGS Kit on the Agilent 5300 Fragment Analyzer (Agilent Technologies, California, USA) and quantified by using Qubit 4.0 Fluorometer (Invitrogen, Waltham, USA) or equivalent.

The sequencing libraries were multiplexed and loaded on the flow cell. Next-generation sequencing was performed in Illumina Novaseq 6000 platform (California, USA) with 2x150 bp pair-end configuration v1.5. Image analysis and base calling were conducted by the NovaSeq Control Software v1.7 on the NovaSeq instrument. Raw paired-end data were delivered in fastq format after de-multiplexing and standard adapter trimming by the sequencing contractor. One mismatch was allowed for index sequence identification.

Table 2.5: Experimental details of next-generation RNA-sequencing projects.

Sequencing Project No	Experiment	Tissue	Treatment Structure	No replicates per treatment
40-280905805	LowN/LowP	Nodes	Nutrient Supply (3)	4 (12)
40-382106909	<i>Tad17</i> /LowN	Nodes	Genotype (2) x NLevel (2)	6 (24)
40-460868918	LowN/APS4_1	Roots	Treatment (2) x NLevel (2)	3 (12)
40-543543449	LowN/APS4_2	Nodes	Treatment (2) x NLevel (2)	3 (12)

2.4 Bioinformatic Analysis

2.4.1 Identifying Wheat Orthologue Genes

The first step for the identification of the wheat orthologous genes of interest was to obtain the protein sequences from other model and non-model plant species, mainly from *O. sativa* cv. Japonica, *A. thaliana* and/or *H. vulgare* (where available), which had been identified in previously published data (Wang et al., 2018b, Kobae et al., 2018, Zhang et al., 2014, Liu et al., 2017). The amino acid sequences obtained were used as queries against wheat protein databases using the BLASTP tool on EnsemblPlants (Kersey et al., 2018). The protein sequences with the highest homology from the A, B and D genomes were recorded. For further confirmation of homology, the wheat sequences obtained were used for reciprocal BLASTP back to rice. The phylogenetic relationship of the identified wheat sequences was also confirmed using the Plant Compara tool → Gene tree on EnsemblPlants. The Gene Tree tool displays a phylogeny tree of homologues of any gene across different plant species.

2.4.2 Sequence Alignment and Phylogenetic Analysis

MUSCLE, as implemented in Geneious 10.2.3 software (<https://www.geneious.com>), was used for nucleotide and protein sequence alignment with the default parameters (Edgar, 2004). Phylogenetic trees were constructed based on the Neighbour-Joining method (Nei and Saitou, 1987).

2.4.3 Primer Design

The primer design tool, Primer 3 v2.3.7, as implemented in Geneious 10.2.3 (<https://www.geneious.com>), was used for designing primers used in this study.

Homoeologue-Specific Primers

Homoeologue-specific primers for the three *Tad17* homoeologues were designed as part of the *Tad17* mutant generation. More specifically, homoeologue-specific primers that amplify a region that contains the SNP of interest were designed for genotyping purposes. The optimal primer conditions were set at 58-64 °C T_m, 40-60% GC content and 18-24 bp primer size. For genotyping by sequencing, homoeologue-specific primers for each of the mutations were designed with

homoeologue specificity of at least one nucleotide at the 3' end of the primer. The homoeologue specificity of the primers was required in at least one of the primers per pair (forward or reverse). On the other hand, KASP assay primers for each of the studied SNP were manually designed. The online tool NEB Tm Calculator v1.12.0 (<https://tmcalculator.neb.com/#!/main>) was used for the calculation of primer characteristics.

Quantitative reverse-transcription PCR Primers

For gene expression analysis by quantitative reverse-transcription PCR (RT-qPCR), primers that amplify all the three homoeologues of the gene of interest were designed (**Table 2.6**). The cDNA sequences of the three homoeologues of the gene of interest were aligned and used for designing primers with the appropriate characteristic for qPCR. Regions close to the 3' end of the coding sequence with high similarity were preferred to guarantee amplification of all homoeologues. In some cases, the primers were designed manually. The online tool OligoCalc (<http://biotools.nubic.northwestern.edu/OligoCalc.html>) (Kibbe, 2007) was used for the calculation of the primer characteristics.

Each set of designed primers (forward and reverse) was tested for amplification specificity and efficiency by using a dilution series of template cDNA from different plant tissues (shoots and roots). The dilution series used was 1, 1:2, 1:4, 1:8, 1:16 and 1:32. The efficiency of each set was calculated based on the slope of the standard curve (**Appendix A**). On the other hand, the melting curve (dissociation curve) was used for evaluating the primer specificity. Primers that showed a single peak in a range of template cDNA were selected. The presence of more than one peak in the melting curve suggests unspecific amplification or primer dimers leading to unreliable results.

Table 2.6: Forward and reverse primer sequences designed and used for the gene expression analysis by RT-qPCR.

Gene	Forward Primer Sequence (5'→3')	Reverse Primer Sequence (5'→3')
<i>TaD27</i>	ACAGCAACCTCCTGAAGATGAC	AGCAAYTCACACCATAGTCCTGC
<i>TaD17</i>	CACGGCTATGTTCTTCTKGTAGAG	CCTATCTTYCTTGCATCCAACAC
<i>TaD10</i>	TGCCCAGGGACAAGTAACAC	CGACCACCGACTTGGATTCCG
<i>TaMAX1a1</i>	CTCACYGTCATCCACCTCTAC	CTTGACACCRTTCTTGAAGTTGG
<i>TaMAX1a2</i>	TCGTCATYCTCCACCTCTACC	AGATGGAATACTGGAACCTGCAGC
<i>TaMAX1c</i>	TGCAGCAGGTGAAGCTCG	TCGAAGTCGAACTGGATGGG
<i>TaMAX1d</i>	TSTACCGCCGCTACGTSTTC	GCTTGACGCCGTGCTTGAAG
<i>TaD3</i>	GGACTCAGGAAGCTCTTCATCC	TCTCYGGTGCTGGATAGTAGTC
<i>TaD14</i>	CTCGCCTAGGTTCTTGAACGAC	GACATCGCCTGGAACACCTG
<i>TaCKX3</i>	GGCTCATCCTCATCTATCCACTC	AGAATGCCAACCACGTACATCAC
<i>TaCKX4</i>	GTCGGGATGAAGCAGTACCTAG	TTCCTCCGCTCAAATGTCTCC
<i>TaTB1</i>	GACATGCTCGGCTTCGACAAG	CAGTCATGACCTCCCTGATGG
<i>TaGT1</i>	CCGAGCTCTTCGTCGTTCTC	CATGTAGTTGGTGTAGGCGTAC

2.4.4 RNA-sequencing Workflow

Unless stated otherwise, the tools used for the RNA-seq data analysis were executed in the RRes Galaxy platform (<https://galaxy.rothamsted.ac.uk/>). A schematic summary of the RNA-seq data analysis workflow can be found in **Figure 2.5**.

The RNA-sequencing (RNA-seq) raw data was received in fastq format. *FastQC v0.11.7* tool was used to assess the quality of the raw data (<http://www.bioinformatics.babraham.ac.uk/projects/fastqc/>). If required, low-quality reads and adapter sequences were removed using *Cutadapt v3.7* (Martin, 2011). In cases where the quality control showed high ribosomal RNA (rRNA) content in the raw data, the *SortMeRNA v3.2* tool was used to find and remove reads corresponding to eukaryotic rRNA (28s, 18s) (Kopylova et al., 2012). SortMeRNA tool was run on a local Linux machine. Subsequently, trimmed reads were mapped to *T. aestivum* reference genome IWGSC RefSeq v1.0 using the tool *HISAT2 v2.2.1* (Kim et

al., 2015). The *featureCounts* tool was used for assigning mapped reads to exons and counting the number of mapped reads per annotated gene using RefSeq Annotation v1.1 (Liao et al., 2013). RefSeq1.1 contains in total 107,891 high-confidence (HC) genes and 161,537 low-confidence (LC) genes. HC genes correspond to high confidence protein-coding loci with a predicted function, whereas LC genes correspond to partially supported gene models, gene fragments and gene orphans. Evidence for transcription has been found for 85% (94,114) of the HC genes, whereas LC showed much lower evidence of transcription of just 49% (Rubin et al., 2009). *DESeq2* tool was used to perform the differential gene expression analysis ($\alpha=0.01$, unless stated otherwise) by fitting the appropriate model based on each experimental design (Love et al., 2014). A prefiltering of low count genes was performed before performing differential gene expression analysis. Only genes that had at least three samples with more than five reads were included in the analysis. Significantly differentially expressed genes were retrieved by applying post hoc filtering of p-value adjusted for multiple comparisons ($p_{adj} < 0.01$ and $|\log_2FC| > 0.58$ ($FC > 1.5$), unless stated otherwise). *DESeq2* package was run in R Statistical Software (v4.1.1) on a local Windows machine. An example of the script used can be found in **Appendix B**. For the visualization of the RNA-seq data analysis, *ggplot2* v3.3.6, *heatmap* v1.0.12, *DEGreport* v1.8.2 and *EnhancedVolcano* v1.11.3 packages were used in R Statistical Software (v4.1.1).

In addition to the above workflow, raw reads were also pseudo-aligned to IWGSC RefSeq v1.0 annotation v1.1 using *kallisto* v0.46.0.4 (Bray et al., 2016), which was run in RRes Galaxy. This tool was used for calculating transcript abundance reported as transcripts per million mapped reads (TPM). A custom R script was used for calculating the gene abundance by summing the TPM of all the transcripts corresponding to the same gene ID. TPM values were used for comparing the gene expression levels of different genes since this value is normalized for both gene length and sequencing depth, allowing the comparison between different genes.

For the biological interpretation of the data, Gene Ontology (GO) enrichment analysis was performed in *g: Profiler* using the *g: GOst* tool and default parameters (statistical domain scope: only annotated genes, multiple testing correction: g: SCS algorithm,

padj < 0.05) (Raudvere et al., 2019). Only HC genes were included in the GO enrichment analysis. GO enrichment analysis results were summarized by removing redundant terms using the *REVIGO* webserver (Supek et al., 2011). Oligopeptide sequences of the differentially expressed (DE) genes were retrieved from BioMart in FASTA format. KEGG Orthology (KO) annotations for the DE genes were retrieved using the BlastKoala tool (<https://www.kegg.jp/blastkoala/>). In addition, pathway enrichment analysis was conducted in *g*:GOst tool against a custom *T. aestivum* KEGG reference containing more than 46000 wheat genes covering both KEGG pathways and BRITE hierarchies, kindly provided by Peter Buchner. Finally, *g*:Orth tool in *g*:Profiler was used for retrieving orthologue genes of the DE genes in rice and Arabidopsis.

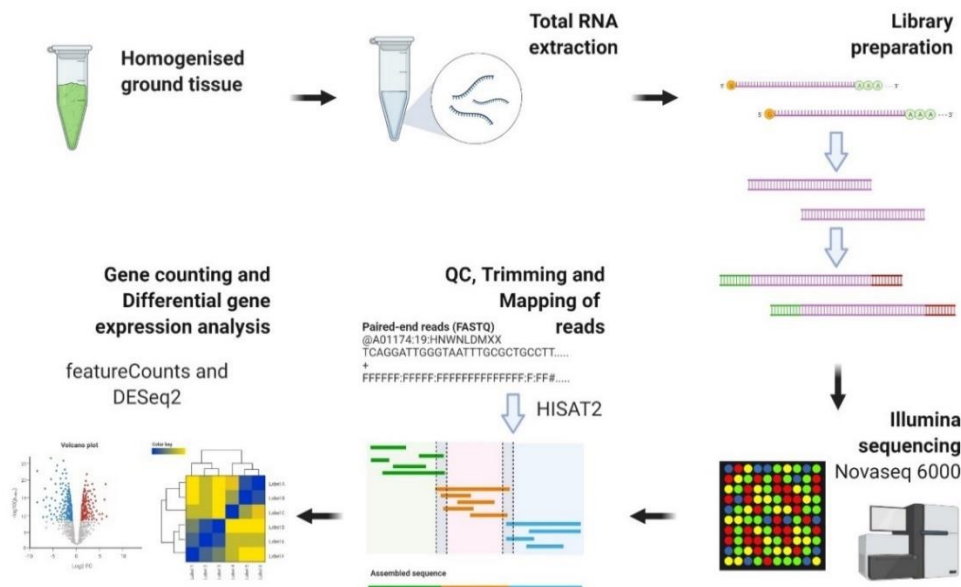


Figure 2.5: Schematic illustration of the RNA sequencing workflow starting from the sampled material until the differential gene expression analysis. Library preparation and next-generation sequencing were performed by GenewizUK (Essex, UK). Raw sequencing data were received in fastq format. Quality control of the fastq data was performed with the FASTQC tool. Trimming of low-quality reads or rRNA removal was performed if needed based on the QC output. HISAT2 tool was used for mapping reads to the *T. aestivum* reference genome RefSeqv1.0. Mapped reads were assigned to genes based on RefSeqv1.1 annotation. Differential gene expression analysis was performed with the DESeq2 tool. The illustration was created in BioRender.

2.5 Metabolomic Analysis

Harvested basal node and root tissue of pooled biological replicates were ground into fine powder in LN₂ and stored at -80 °C until extraction. All the samples were hand-ground in a pre-cooled mortar due to the small amount of sampled tissue.

2.5.1 Cytokinin Extraction

Cytokinins were extracted from 20 mg of ground plant tissue using 1 ml of extraction solution, 70:29:10 (v/v/v) methanol: H₂O: formic acid. The extraction solution also contained 0.2 ng/ml of D-iP, D-iPA, D-tZ, D-DHZ and D-DHZR as internal standards for the normalization of the variation across the samples. For better homogenization of the samples, samples were mixed in a mixer mill MM400 (Retsch, Haan, Germany) for 1 min at 30 Hz with two metal beads in each tube. Next, the samples were incubated for 30 min at 4 °C on a vortex. The supernatants were collected in a 96-deep well plate after centrifugation at full speed for 30 min at 4 °C. Subsequently, the samples were evaporated under N₂ on SPE Dry 96 (Biotage, Uppsala, Sweden). Once the evaporation was completed, the pellet was resuspended with 800 µL 2% (v/v) formic acid in ddH₂O. The following filtration and solid phase extraction were conducted using the automated system Extrahera (Biotage, Uppsala, Sweden), which allows the high-throughput processing of the samples. Isolute Filter Plates 25 µm/0.2 µm (Biotage, Uppsala, Sweden) were firstly used for the filtration of the samples, while Evolute CX express 30 mg/1 ml columns (Biotage, Uppsala, Sweden) were used for the solid-phase extraction according to the manufacturer protocol. Finally, the eluate was evaporated under N₂ on SPE Dry 96 (Biotage, Uppsala, Sweden), and the pellet was resuspended in 100 µL 0.1% (v/v) formic acid. Until injection into the system, samples were stored in the autosampler at 10 °C.

2.5.2 Other Phytohormone Extraction

For the extraction of the rest of the targeted phytohormones, a different extraction protocol was conducted. Phytohormones were extracted from 20 mg of ground plant tissue using 1 ml of extraction solution, 70:29:10 (v/v/v) methanol: H₂O: formic acid, which contained 0.8 ng/ml of D-GA1, D-GA8, D-PA, D-DPA and 0,4 ng/mL of D-ABA and D-IAA as internal standards for the normalization of the variation across the samples.

The remaining protocol was performed as described for the cytokinin extraction, apart from the solid phase extraction stage. More specifically, Evolute Express ABN 30 mg/1 mL columns (Biotage, Uppsala, Sweden) were utilized for the ultra-purification of the extracts.

2.5.3 UHPLC-MS/MS

The analysis of CKs and other phytohormones was performed by ultra-high performance liquid chromatography-tandem mass spectrometry (UHPLC-MS/MS). All the standards used were purchased from OlchemIn (Olomouc, Czech Republic). The separation and detection were accomplished using a Nexera X2 UHPLC system coupled to a Triple Quadrupole Linear Ion Trap, QTRAP 6500+ mass spectrometer (Sciex, Concord, Canada), equipped with an electrospray ionization source. 2 μ L of samples were injected and separated with a Kinetex Evo C18 column (2.1x100 mm, 2.6 μ m, Phenomenex, California, USA) at 0.7 mL/min flow rate, while the column was maintained at 40 °C. The mobile phase consisted of solvent A (H₂O: 0.1% formic acid) and solvent B (ACN: 0.1% formic acid) and a 0.7 mL/min flow rate. For cytokinins, the optimized linear gradient system was: 0-3 min, 20% B; 3-4 min, 25% B; 4-4.5 min, 100% B; 4.5-6 min, 100% B; 6-6.5 min, 2% B and 6.5-8.6 min, 2% B. For other phytohormones, the optimized linear gradient system was: 0-5 min, 60% B; 5-5.5 min, 100% B; 5.5-7 min, 100% B; 7-7.5 min, 1% B; and 7.5-9.5 min, 1% B. The analysis was performed in scheduled MRM mode in positive mode.

For the calculation of the phytohormone concentration in the sample, standard solutions were also included in the analysis. A dilution series for each of the examined phytohormones were included for the construction of the standard curve by plotting the peak area ratio (y) and the respective concentration of the compound (x). The concentration of each phytohormone was calculated based on the peak area ratio with respect to the corresponding internal standard based on the standard curve.

2.5.4 Sugar Analysis

For sugar extraction, 750 µL of 80% (v/v) EtOH were added to approximately 20 mg of lyophilized ground node sample. The homogenate was incubated at 80 °C for 30 min. Crude extracts were decanted for 15 min at room temperature, centrifuged (14,000 rpm, 10 min, 4 °C) and concentrated in a Speed Vac concentrator (Thermo Scientific, Massachusetts, USA) at 45 °C for 180 min. The pellet was resuspended in 0.75 mL of deionized water and incubated at 80 °C for 30 min. After centrifugation, the second supernatant was added to the first, concentrated, and resuspended in 0.5 mL of ddH₂O. Hexokinase, phosphoglucosomerase, and invertase were added successively to measure glucose (Glc), fructose (Fru), and sucrose, which were determined by spectrophotometry at 340 nm (SpectraMax i3x, Molecular Devices, San Jose, CA, USA).

2.6 Chemical Analysis

The whole root and shoot samples were ground into a fine powder using Freezer Mill (SPEX SamplePrep, New Jersey, USA) following the manufacturer's instructions. Samples were then lyophilized in a Modulyo freeze dryer (Edwards, West Sussex, UK) for at least 48 h or until thoroughly dried and then submitted for chemical analysis.

2.6.1 Total Nitrogen Analysis

The total N content of dried root or shoot samples was measured by the LECO CN628 combustion analyser (LECO, Stockport, UK) following the manufacturer's protocol.

2.6.2 Elemental Analysis

For analysis of major (Ca, K, Mg, Na, P, S) and trace (Cu, Fe, Mn, Mo, Zn, etc.) elements, root and shoot samples were first digested using a mixture of 85:15 (v/v) nitric acid: perchloric acid in open tube digestion block. After volatilization of the acids, the residues were dissolved in 5% (v/v) nitric acid. Sample analysis was carried out in Agilent 5900 SVDV Inductively Coupled Plasma – Optical Emission Spectrometer (ICP-OES) (Agilent Technologies UK, Stockport, UK).

2.7 Wheat TILLING Mutant Generation

2.7.1 Screening of EMS Mutagenized Lines

In silico analysis was conducted for the identification of *T. aestivum* cv. Cadenza mutant lines for SL biosynthetic genes, *TaD27*, *TaD17* and *TaD10*. Wheat TILLING population consists of 1200 hexaploid wheat lines, whose exome sequences have been sequenced and mapped to the reference genome RefSeqv1.0, leading to the identification of the point mutations induced by EMS mutagen and their predicted effect (Krasileva et al., 2017). The gene IDs of all the candidate SL biosynthetic genes were used as queries to find the available mutant lines in TILLING population by accessing the respective EnsemblPlants database (Genetic Variation → Variant table). After the identification of *TaD17* as a candidate gene for the generation of triple knock-out mutant, the protein and the genomic sequences of the *T. aestivum* cv. Cadenza and the selected mutant lines with a premature stop codon were obtained.

2.7.2 Plant Material and Growth Conditions

Four seeds of the selected mutant lines (M4 generation) were obtained from Rothamsted's TILLING population seed bank. Seeds can be ordered from UK Germplasm Resource Unit (GRU) website called SeedStor <https://www.seedstor.ac.uk/shopping-cart-tilling.php>. Seeds were surfaced sterilized with 1:40 (v/v) bleach solution: dH₂O for 15 min, followed by 5-6 washes with sterilized dH₂O. Seeds were soaked in sterilized dH₂O overnight at 4 °C in the dark and then placed in Petri dishes with moist filter paper and were cold treated (4 °C) for 2-3 days to break seed dormancy. Prior to sowing, seeds were pre-germinated in a CE room (22-18 °C and 16 h day length). Next, germinated seeds were sown in seed trays filled with Rothamsted's prescription mix compost consisting of 75% peat, 12% sterilized loam, 3% vermiculite, and 10% grit (Petersfield Products, Leicester, UK). Leaf samples were taken from each seedling for genotyping once the second leaf of the seedlings had fully emerged around 1-2 weeks after germination. Based on the genotyping results, the seedlings with the desired genotypes were then selected and transplanted into 15 cm pots containing the same compost as above. Plants were grown in a standard

glasshouse equipped with LED light. Glasshouse conditions were 18-20 °C and 15 °C during the day and night, respectively, with 16 h day length.

2.7.3 Wheat Crossing

Due to polyploidy in wheat, different mutant lines with missense mutations in all the three *TaD17* homoeologues were combined to generate a complete knock-out mutant. Soon after ear emergence, the female ears were emasculated by removing the three anthers from each of the florets. The central florets of each spikelet were removed, leaving only the two outer florets per spikelet. Subsequently, the spikelet's glumes were removed, and each of the spikelets was trimmed to allow easier anther removal without damaging the stigma. The emasculated ear was labelled and covered in a plastic bag to avoid any cross-pollination. Emasculatation was important to take place before pollen release to ensure no self-pollination, while for the same reason, all three anthers per floret should be successfully removed. 3-4 days after emasculatation, the ears were pollinated by the selected male donor plant based on the crossing scheme and the aiming genotype of the resulting progeny. After the successful pollination, premature grains were collected 16 days post pollination (or later), and they were dried at 30 °C for 5 days. Subsequently, the seeds were subjected to cold treatment (4 °C) for 3-4 days to break dormancy and were sown for germination as described above. The genotyping of the progeny was conducted by either sequencing or KASP assay, depending on the number of plants needed to be genotyped.

2.8 Statistical Analysis

Mean values and standard errors were calculated from at least three biological replicates, depending on the experimental design. The exact number of biological replicates is mentioned in each figure legend. The statistically significant effect of the treatments/factors was assessed with t-test or analysis of variance (ANOVA), depending on the experimental design. Statistical analysis was performed in GenStat statistical software package (21st edition, VSN International Ltd, Hemel Hempstead, UK) or in R Statistical Software (v4.1.1) using package *rstatix* (v0.7.0).

ANOVA was applied to all single variate data, including phenotypic data (tiller counting, root and shoot biomass), RT-qPCR gene expression data, metabolomic analysis data (phytohormone and sugar content) and chemical analysis data (macro- and micro-nutrient content). Repeated measured ANOVA was conducted for tillering data recorded in different time points in the same individuals and for SPAD dynamic data. Prior to ANOVA, assumptions for normality and homogeneity of variances were assessed using Shapiro-Wilk's normality test and Levene's test, respectively. If data were not normally distributed, data were transformed. In cases where the homogeneity of variances assumption was not met (Levene's test $p < 0.05$, as in the case of tZ content Figure 5.20), the comparison between group means was performed using a separate one-way ANOVA or t-test.

For randomised complete block designs, block structure was taken into account in the ANOVA. Following the ANOVA, Fisher's least significant difference (LSD) at 5% ($P=0.05$), calculated based on the standard error of the difference between means on the residual degrees of freedom from the ANOVA, was used to compare relevant group means. Relevant significant comparisons were reported in the figures, while LSD (5%) was also reported in each figure legend.

For the gene expression data by RT-qPCR, the Ct' values were used for the statistical analysis, $Ct' = \log_2\left(\frac{1}{NRQ}\right)$, rather than the NRQ. It has been shown that the NRQ data are not linear, and the variability across the treatments is typically too high, so the transformation of the data is required (Rieu and Powers, 2009).

For the validation of the RNA-seq data, Pearson correlation between transcript abundance values of selected genes obtained from the RNA-seq and RT-qPCR was performed in R v4.1.1 using package *ggpubr* v0.4.0.

Figures and graphs were created in GraphPad Prism v9.3.1 for Windows (San Diego, California, USA). Package *pheatmap* v1.0.12 and *ggplot2* v3.3.6 were also used in R Statistical Software (v4.1.1) for the generation of heatmaps and some figures.

2.9 Data Availability

All data supporting the findings of this study are available within the thesis. The raw data from RNA-seq experiments conducted as part of this study (**Table 2.5**) are available at ArrayExpress Archive; LowN/LowP: E-MTAB-11986; LowN/APS4_1-2: E-MTAB-11927; Tad17/LowN: Not yet available.

Chapter 3 Transcriptional Regulation of Strigolactone Biosynthesis, Perception and Signalling by Plant Nitrogen Supply

3.1 Introduction

3.1.1 Background

Nitrogen is one of the primary macronutrients required for plant growth and development. N availability is one of the main limiting factors in many agricultural and natural environments. Plant adaptation to N-limiting conditions includes strong suppression of shoot growth, including suppression of tiller bud outgrowth resulting in a decrease in tiller number. SLs are a recently identified group of phytohormones that play an essential role in suppressing lateral branching/tillering, while they also act as a rhizosphere signal. Several studies have reported elevated SL levels in root exudates in many species under nutrient-limiting conditions, suggesting that production and exudation are linked with nutrient availability, such as P and N. In fact, Yoneyama et al. (2012) reported that N limitation strongly increases the levels of SLs in the roots of many species, including wheat (Yoneyama et al., 2012). Apart from their role as rhizosphere signals under nutrient limitation facilitating root colonisation by AMF, SLs have been suggested to play a role in plant response to nutrient-limiting conditions, acting as a signal coordinating plant growth. It has been demonstrated that SLs are involved in root architectural changes triggered by N- and P-limiting conditions (Sun et al., 2014). Other studies have shown that the increased levels of SLs act as long-distance signals suppressing tillering under P deficiency (Umehara et al., 2010). Only a handful of studies, mainly in rice, have focused on the transcriptional regulation of SL biosynthetic and signalling genes in response to N availability (Xu et al., 2015b); however, there are no extensive studies on SL-related gene regulation in wheat. In addition, even in well-studied monocotyledonous plants such as rice, transcriptional studies have mainly focused on the genes involved in the core SL biosynthetic pathway, such as *D27*, *D17* and *D10*, whereas *MAX1* genes are rarely included. *MAX1* genes catalyse the steps downstream of CL, which have not been fully elucidated. There are multiple *MAX1* genes present in monocotyledons' genomes, whose

functions remain an important topic. Studies in rice, maize and sorghum have shown that different *MAX1* catalyse different steps downstream of CL and might be responsible for the large structural diversity of bioactive SLs found in plants (Yoneyama et al., 2018a, Wu and Li, 2021). Recent studies have provided insights into the phylogeny of *MAX1* genes in monocotyledonous plants, but most of the studies either did not include wheat sequences or did not include all *MAX1* genes present in wheat (Wu and Li, 2021, Marzec et al., 2020, Yoneyama et al., 2018a, Yoneyama et al., 2020a).

3.1.2 Chapter Objectives

The aim of this chapter was to identify the wheat SL biosynthetic and signalling genes in the wheat RefSeq Annotation v1.1 and study their transcriptional regulation by N supply. For that reason, the gene expression of most of the identified SL-related genes was monitored in response to N limitation and N resupply in hydroponically grown plants in both root and basal node tissue. In addition, by utilising data from different RNA-seq experiments, the tissue-specific expression and regulation of the identified *MAX1* genes were examined, providing some indications about the functionality of the different *MAX1* genes present in wheat.

3.2 Results

3.2.1 Identification of Wheat Homoeologue Genes Involved in SL Biosynthesis, Perception and Signalling

The initial step for studying the involvement of SLs in tillering regulation in wheat was to identify the wheat genes involved in different steps of SL biosynthesis, perception, and signalling. Since the role of SLs as plant hormones regulating lateral shoot formation has attracted considerable attention, SL-related genes are well characterised in species like *O. sativa* and *A. thaliana*. Therefore, for the identification of wheat genes, the protein sequences from *O. sativa* cv. Japonica were mainly used due to its close phylogenetic relationship. For phylogenetic analysis, apart from rice and Arabidopsis sequences, previously reported protein sequences from other grasses, including maize, barley, sorghum and *Brachypodium distachyon*, were also included where required.

For the identification of D27, the first enzyme of the SL biosynthetic pathway, BLASTP revealed three amino acid sequences with high similarity, sharing around 70% similarity to OsD27 (Os11t0587000) (Kobae et al., 2018). The wheat sequences obtained are encoded by homoeologous genes located on chromosomes 7A, 7B and 7D, and according to the phylogenetic analysis, they are close to Hvd27 (HORVU7Hr1G096970), previously identified in barley (Wang et al., 2018b). Therefore, TraesCS7A02G418900, TraesCS7B02G319100 and TraesCS7D02G411500 were assigned as *TaD27-7A*, *TaD27-7B* and *TaD27-7D*, respectively.

The second and third steps of SL biosynthesis are catalysed by CCD7 and CCD8 enzymes, members of the CCD family, which in rice are encoded by *OsD17* (Os04g0550600) and *OsD10* (Os01g0746400), respectively. In Arabidopsis, CCD7 and CCD8 are encoded by *AtMAX3* (AT2G44990) and *AtMAX4* (AT4G32810) genes, respectively. Three homoeologous coding sequence were identified in chromosomes 2A (TraesCS2A02G414600), 2B (TraesCS2B02G433800) and 2D (TraesCS2D02G411900), which encode proteins sharing around 77% similarity to OsD17. All three amino acid sequences show typical domains of the CCD family, suggesting that they are the most likely candidate for *TaD17-2A*, *TaD17-2B* and *TaD17-2D*. On the other hand, in total, six protein sequences were most closely related to

OsD10. The phylogenetic analysis revealed that all the identified wheat sequences were grouped closely to OsD10 and HvD10 and were divided into two distinct homoeologous subgroups (**Figure 3.1**). The protein sequences encoded by TraesCS3A02G274300, TraesCS3B02G308000, TraesCS3D02G273500 were grouped together forming subgroup a, therefore they were designated as TaD10a-3A, TaD10a-3B and TaD10a-3D, respectively. The second D10 wheat subgroup (b) consist of two genes located on chromosome 3A (TraesCS3A02G074200, TraesCS3A02G074100) and one on chromosome 3B (TraesCS3B02G088400). The high amino acid similarity of the latter protein sequences with the protein sequences of the TaD10a group suggests that they might occur due to gene duplication. Therefore, they were named *TaD10b* genes. However, *TaD10b* homoeologues are not expressed in most tissues, based on publicly available wheat gene expression data available on Wheat eFP Browser (Ramírez-González et al., 2018), whereas *TaD10a* genes were found to be expressed in various tissues. Thus, sequences of *TaD10a* homoeologues were only considered for the gene expression analysis in this study and thereafter referred to as *TaD10*.

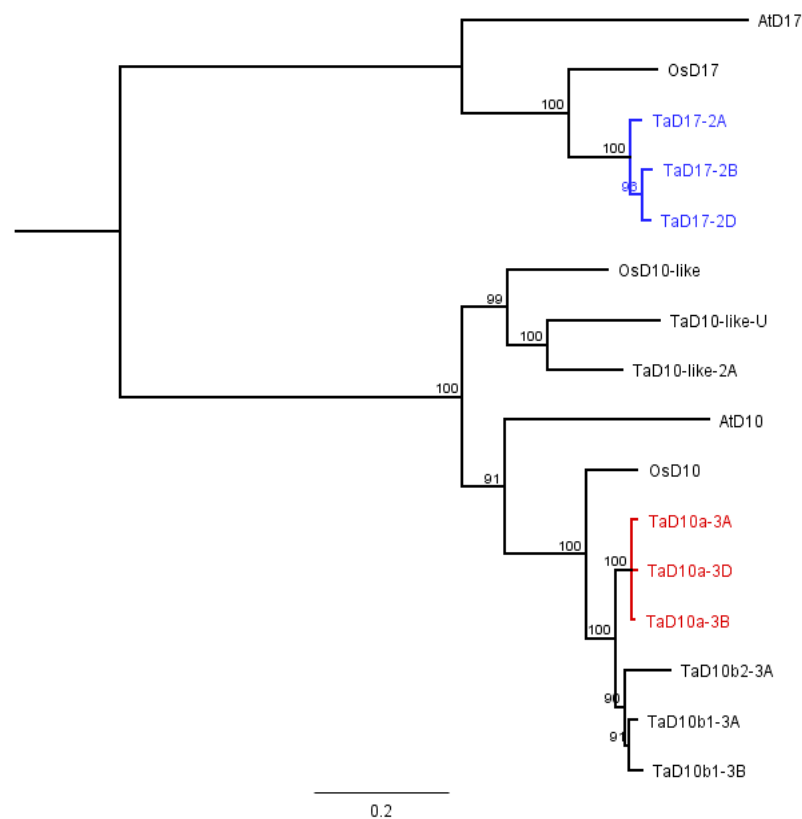


Figure 3.1: Phylogenetic analysis of wheat D17 and D10 proteins. The tree was generated using amino acid sequences of D17/MAX3 (CCD7) and D10/MAX4 (CCD8) from *O. sativa* (*Os*)

and *A. thaliana* (*At*). The tree was constructed using MUSCLE sequence alignment and the neighbour-joining method. TraesCS2A02G414600, TraesCS2B02G433800 and TraesCS2D02G411900 were assigned as *TaD17* homoeologues (in blue colour). Based on publicly available gene expression data TraesCS3A02G274300, TraesCS3B02G308000, TraesCS3D02G273500 were assigned as *TaD10a* and they were considered as functional orthologues of D10 (in red colour).

Although only one gene is present in the Arabidopsis genome encoding cytochrome P450 CYP711A known as MAX1, there are multiple homologues in grasses. More specifically, five MAX1 homologues have been identified in the rice genome (Zhang et al., 2014), while more recent studies showed that the presence of multiple MAX1 genes is a common characteristic in grasses. The number of MAX1 homologs present varies among monocotyledons. Maize has three *MAX1* genes (Yoneyama et al., 2018a), sorghum four (Wu and Li, 2021) and *B. distachyon* five (Changenet et al., 2021). To identify the *MAX1* genes present in wheat, the five OsMAX1 proteins (Os1500, Os5100, Os1900, Os900 and Os1400) were used to query wheat protein databases. In total, 13 distinct wheat amino acid sequences were retrieved. To understand the relationship of the identified proteins, a phylogenetic analysis was conducted, which included all the known MAX1 sequences from other species (**Figure 3.2**). The phylogenetic analysis revealed that *MAX1* genes from monocotyledons formed four clades (A-D). Six different wheat sequences were clustered to clade A, forming two distinct subgroups. The first subgroup of clade A consisted of three genes located on chromosome 4 (TraesCS4A02G412100, TraesCS4B02G312300, TraesCS4D02G309900) along with BdCYP711A29 and HvMAX1 (CYP711A29). The second subgroup of clade A consist of TraesCS3B02G088700, TraesCS3D02G073900 and TraesCSU02G146300 wheat genes along with SbMAX1a and BdCYP711A31. Noticeably, only sequences from wheat and *B. distachyon* were found in both subgroups of clade A, whereas none of the known rice sequences was found in clade A. Only TraesCS3A02G466400 was present in clade B, along with three of the rice MAX homologs (Os1500, Os900, Os1400) and sequences from all the monocots included in the analysis. The clade C consists of three wheat orthologues of Os1900 located on chromosome 6 (TraesCS6A02G187200, TraesCS6B02G217300, TraesCS6D02G174100). Finally, the protein sequences encoded by TraesCS7A02G360300, TraesCS7D02G362800 and TraesCS7B02G267500 fall into clade D along with Os5100. Therefore, wheat *MAX1*

homoeologues were named after the clade they fall into (*MAX1a-d*). The genes of clade A which fall into separate subclusters were named *MAX1a1* and *MAX1a2* (Figure 3.2).

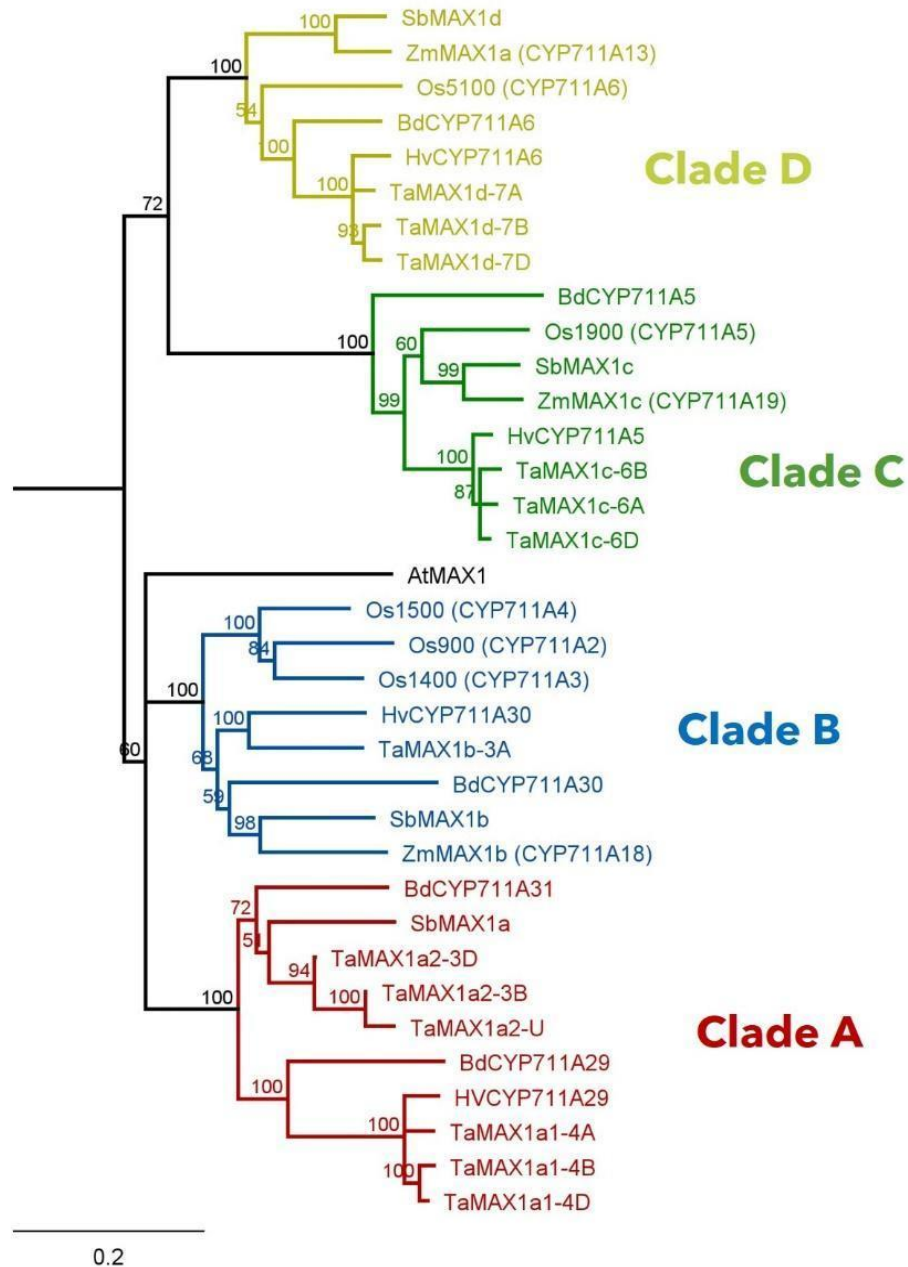


Figure 3.2: Phylogenetic analysis of wheat MAX1 homologs. The tree was generated using amino acid sequences of the cytochrome P450 CYP711A family mainly from monocotyledonous species such as *O. sativa* (*Os*), *H. vulgare* (*Hv*), *B. distachyon* (*Bd*), *S. bicolor* (*Sb*), *Z. mays* (*Zm*), while only MAX1 sequence from *A. thaliana* (*At*) was included from dicotyledonous species. The tree was constructed using MUSCLE sequence alignment and the neighbour-joining method. Different colours correspond to the four different clades identified (A-D). The accession number of sequences used for the phylogenetic analysis can be found in **Appendix C**.

For the identification of the wheat orthologues of the two main components of the SL perception pathway, the protein sequences of OsD3 (Os06t0154200) and OsD14 (Os03t0203200) were used as templates. According to the BLASTP results, the wheat proteins encoded by TraesCS7D02G106000, TraesCS7B02G008400, TraesCS7A02G110500 showed the highest identity to OsD3 (approximately 70%), hence they were assigned as *TaD3-7D*, *-7B* and *-7A*, respectively. Similarly, the proteins encoded by TraesCS4A02G046700, TraesCS4B02G258200, and TraesCS4D02G258000 shared more than 86% protein similarity with the OsD14 and were assigned as the putative *TaD14* genes.

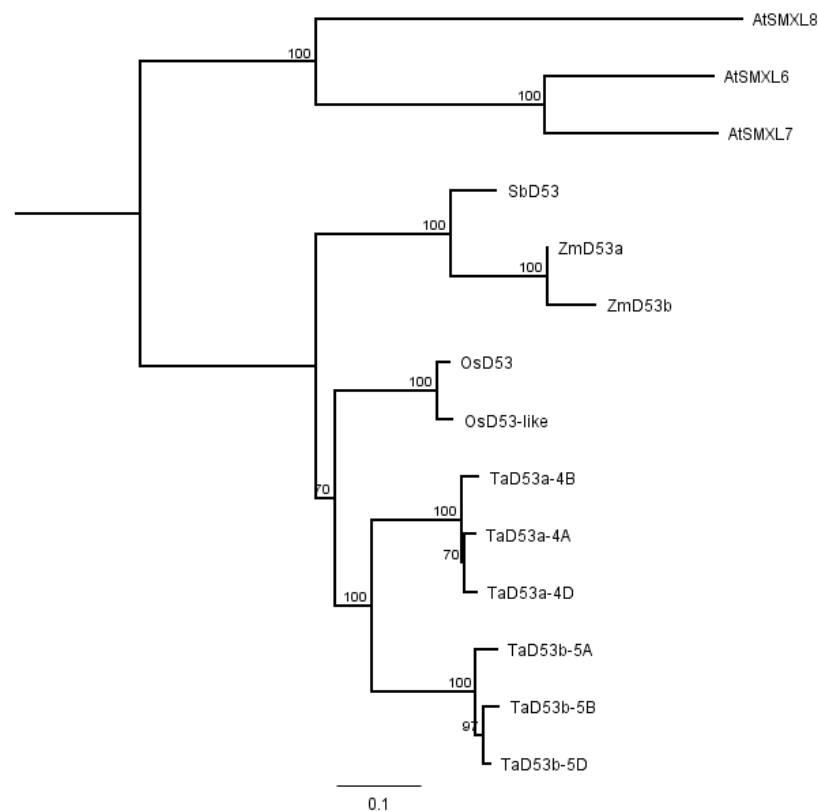


Figure 3.3: Phylogenetic analysis of wheat D53 proteins. The tree was generated using amino acid sequences of D53 from *O.sativa* (*Os*), *S.bicolor* (*Sb*) and *Z.mays* (*Zm*) and SMXL6/7/8 sequences of *A.thaliana* (*At*). The tree was constructed using MUSCLE sequence alignment and the neighbour-joining method. TraesCS4A02G182800, TraesCS4B02G135800 and TraesCS4D02G130600 were assigned as *TaD53a* homoeologues, and TraesCS5A02G155000, TraesCS5B02G153200 and TraesCS5D02G159900 were assigned as *TaD53b*.

In rice, two genes have been identified encoding D53, the main repressor of the SL signalling pathway. In Arabidopsis, AtSMXL6 (AT1G07200), AtSMXL7 (AT2G29970) and

AtSMXL8 (AT2G40130) are considered as orthologues of OsD53. Both rice sequences, OsD53 (Os11t0104300) and OsD53-like (Os12g0104300), were used as queries to identify putative wheat genes encoding D53. In total, six wheat genes were found to encode proteins with 70% similarity with both rice D53 proteins. The phylogenetic analysis showed that the identified wheat sequences form two distinct homoeologous subgroups (**Figure 3.3**). Based on publicly available wheat expression data, all six wheat genes are expressed at similar levels, so they were assigned as putative *TaD53* genes. Therefore, TraesCS4A02G182800, TraesCS4B02G135800 and TraesCS4D02G130600 were assigned as *TaD53a*. Similarly, TraesCS5A02G155000, TraesCS5B02G153200 and TraesCS5D02G159900 were named *TaD53b*.

In addition, three homoeologous wheat sequences were identified (TraesCS4A01G271300, TraesCS4B01G042700 and TraesCS4D01G040100) as putative genes encoding TB1 transcription factor, a negative regulator of tillering and an important component of the SL signalling pathway. The identified wheat sequences shared 54% similarity with OsFC1/TB1 (Os03t0706500). Thus, the respective nucleotide sequences were assigned as *TaTB1-4A*, *-4B* and *-4D*. The given nucleotide sequences are consistent with the sequences previously reported in wheat but with a different accession number (Liu et al., 2017).

3.2.2 Effect on N Limitation on Wheat Tillering

N limitation triggers many changes in root and shoot architecture, and tillering is one of the shoot architectural traits which are strongly affected by N availability. To explore the effect of N limitation on tiller formation in wheat, *T. aestivum* cv. Cadenza plants were hydroponically grown for 6 days under sufficient N supply. On 10 DAS, half of the plants were provided with low N solution (0.1 mM N), while the rest continued receiving high N nutrient solution (10 mM N). The number of outgrown tillers was recorded at 4-day intervals at 4, 8 and 12 days after the N limitation. Only the number of tillers that had emerged from the leaf sheath was recorded, and the data were presented in **Figure 3.4**. A two-way ANOVA was performed to examine the effect of N treatment and time on the number of outgrown tillers. There was a statistically significant interaction between N treatment and time on the number of outgrown

tillers ($F(2,10)=27.34$, $p<0.01$). The effect of N limitation on the different time points was examined by applying Fisher's LSD test ($LSD(5\%) = 0.68$). Overall, tillering results showed that low N supply significantly reduced the number of outgrown tillers. The effect started to be apparent 8 days after the N limitation, while the effect became more potent as time after the N limitation progressed. In fact, 12 days after the N limitation, the number of tillers in the low N treated plants was 2-fold lower than in the high N treated plants. In addition, the effect on tiller number at 22 DAS is mainly attributed to the strong suppression of N limitation on the outgrowth of secondary tillers.

To confirm the N limitation in low N plants, total N analysis was performed in the root tissue of the plants at different time points. The results showed that N concentration remained stable over time in the plants receiving high N nutrient solution, whereas the N concentration gradually decreased after the introduction of the plants to the low N conditions (2-way ANOVA, $F(2,10)=10.34$, $p<0.01$, $LSD(5\%) = 5.7$).

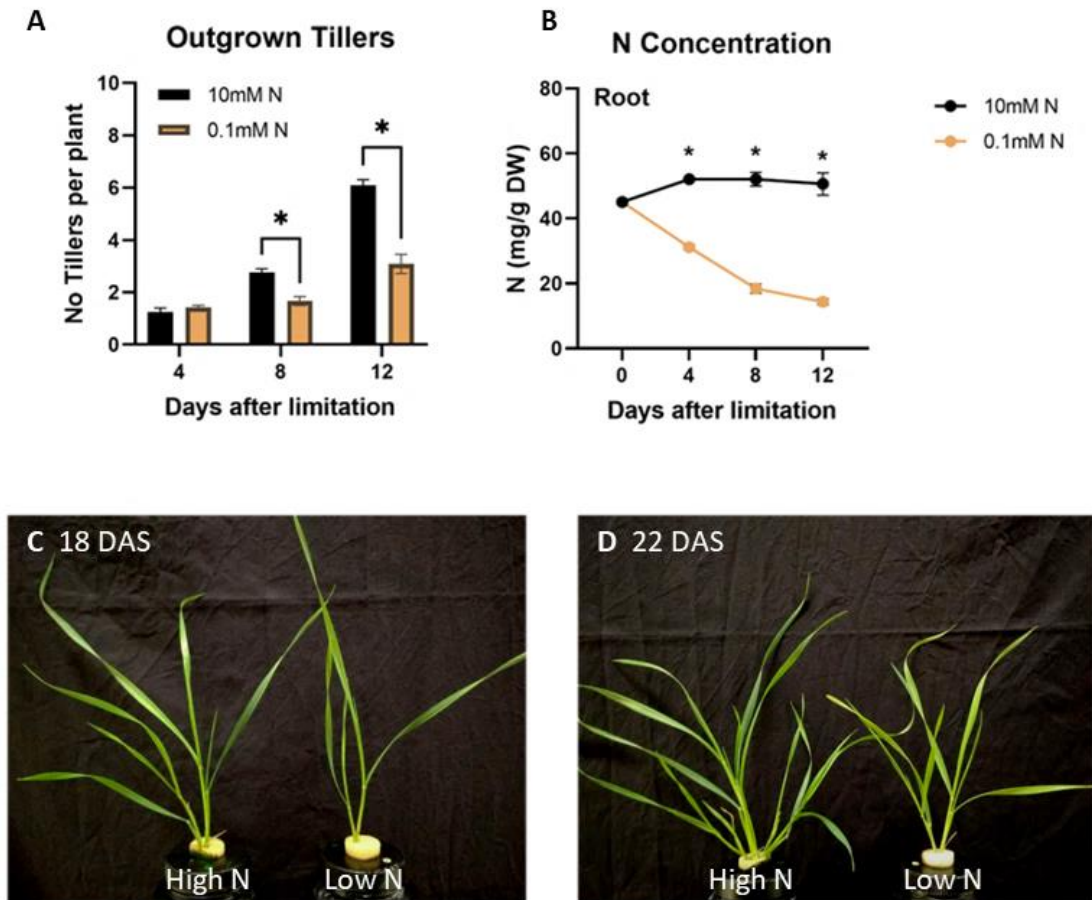


Figure 3.4: Effect of N limitation on wheat tillering. (A) Number of outgrown tillers per plant at 4, 8 and 12 days after N limitation. Values are means of three biological replicates, and error bars represent SE. Statistical analysis was conducted with 2-way ANOVA. * denotes statistically significant difference between low N and high N plants at each time point based on Fisher's LSD test ($p < 0.05$, LSD (5%) = 0.68). (B) Time-course analysis of the N concentration in the root of low N and high N treated plants. Values are means of three biological replicates, and error bars represent SE. Statistical analysis was conducted with ANOVA. * denotes statistically significant difference between low N and high N plants at each time point based on Fisher's LSD test ($p < 0.05$, LSD (5%) = 5.7). (C) and (D) representative plants grown under high N and low N conditions at 8 days (18 DAS) and 12 (22 DAS) days after N limitation, respectively.

3.2.3 Time-course Analysis of SL Biosynthetic and Perception Gene Expression in Root in Response to N Limitation

SL production in roots has been associated with inorganic nutrient stress and, more specifically, with N and P limitations. However, there was no expression data available of the SL biosynthetic and perception genes in response to N limitation in wheat. Therefore, to examine the effect of N limitation on the transcription of SL-related genes, the expression of *TaD27*, *TaD17* and *TaD10* genes was analysed by RT-qPCR in roots of plants grown under N limitation for 4, 8 and 12 days (as described in section

2.1.3). For the gene expression analysis, primers that amplify all the three wheat homologues for each gene of interest were designed; thereby, the gene expression values (NRQ) refer to the total expression of all the three homoeologues. This applies to all the genes analysed by RT-qPCR. The results were analysed by 2-way ANOVA followed by post hoc comparisons to examine the effect of N treatment at different time points. Overall, the results showed that the expression of *TaD27*, *TaD17*, and *TaD10* sharply increased over time in N-limited plants, whilst in high N treated plants, the expression of those genes remained constant at low levels.

Apart from the genes involved in the core SL biosynthetic pathway, the expression of *TaMAX1a1*, *TaMAX1a2*, *TaMAX1c* and *TaMAX1d* were also analysed. No available expression data were obtained for *TaMAX1b* due to the lack of primers suitable for RT-qPCR. The results in roots showed that *TaMAX1a1*, *TaMAX1a2* and *TaMAX1d* were strongly induced by N limitation. *TaMAX1a2* and *TaMAX1d* showed the most substantial upregulation by N limitation. In fact, both *TaMAX1a2* and *TaMAX1d* transcript levels were found to be 60-fold higher in low N roots 8 days after N limitation. In high N plants, the expression of those genes remained stable at low levels in all the three time-points examined, as also shown for the SL biosynthetic genes of the core pathway (*TaD27*, *TaD17* and *TaD10*). However, *TaMAX1c* was not found to be affected by N treatment in roots (2-way ANOVA, $F(2,10)=1.43$, $p=0.29$). In fact, no significant effect of N limitation was found at any of the time points examined. This different response of *TaMAX1c* compared to the other *TaMAX1* genes indicates that there are some differences in the regulation of *MAX1* gene expression in response to N limitation.

The gene expression results clearly demonstrated that SL biosynthetic genes are strongly induced by N limitation. To examine the response of SL perception in the same tissue, the expression of *TaD3* and *TaD14* was also analysed in roots. Unfortunately, no primers for the gene expression analysis of *TaD53* could be designed; hence *TaD53* expression was not included in the gene expression analysis by RT-qPCR. In contrast to SL biosynthetic genes, *TaD3* and *TaD14* showed significant downregulation in the root of plants grown at low N availability. Under high N conditions, increases in *TaD3*

and *TaD14* mRNA levels were observed over time, which may be developmentally related.

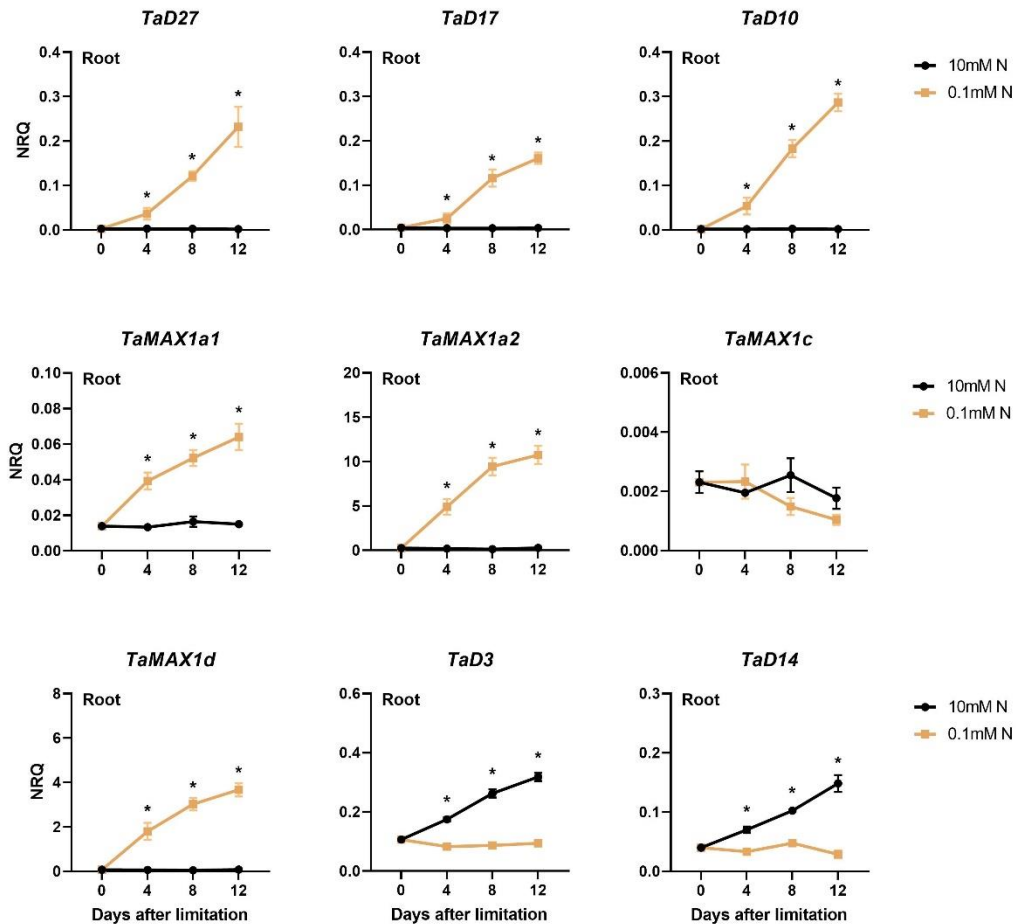


Figure 3.5: Time-course analysis of the gene expression levels of SL biosynthetic (*TaD27*, *TaD17*, *TaD10*, *TaMAX1a1*, *TaMAX1a2*, *TaMAX1c* and *TaMAX1d*) and perception genes (*TaD3* and *TaD14*) in root of wheat 0, 4, 8 and 12 days after N limitation (0.1 mM N) compared to high N treatment (10 mM N). Values are means of three biological replicates, and error bars represent SE. Statistical analysis was conducted with ANOVA on $\log_2(1/\text{NRQ})$ transformed data. * denotes a statistically significant difference in the gene expression levels between low N and high N plants at each time point based on Fisher's LSD test (*TaD27* LSD (5%) = 1.06, *TaD17* LSD (5%) = 0.81, *TaD10* LSD (5%) = 0.79, *TaMAX1a1* LSD (5%) = 0.46, *TaMAX1a2* LSD (5%) = 0.59, *TaMAX1c* LSD (5%) = 0.98, *TaMAX1d* LSD (5%) = 0.46, *TaD3* LSD (5%) = 0.20, *TaD14* LSD (5%) = 0.49).

3.2.4 Time-course Analysis of SL Biosynthetic and Perception Gene Expression in Basal Nodes in Response to N Limitation

The results in roots showed that N limitation strongly induced the expression of SL biosynthesis, while the expression of *TaD3* and *TaD14* perception genes was suppressed. Expression of SL biosynthetic genes has also been detected locally in lateral buds and basal nodes. Therefore, the expression of biosynthetic and signalling genes was examined in the basal node of wheat plants 0, 4, 8 and 12 days after N limitation. In this study, the basal node is defined as the 0.5 cm of the main shoot base, which includes the apical meristem, lateral buds, leaf meristems etc.

As observed in roots, the transcript levels of *TaD27*, *TaD17* and *TaD10* in the basal node were gradually upregulated in response to N limitation. More specifically, *TaD27* and *TaD10* were found to be significantly induced in all the time points examined. However, *TaD17* was found to be significantly upregulated from day 8 after the N limitation. *TaD10* showed the strongest upregulation in all time points. For instance, from 8 days after limitation, *TaD10* mRNA levels were found to be at least 4-fold higher in N-limited plants. In relation to *TaMAX1* genes, no significant effect of N limitation was found in the expression of *TaMAX1a1* (2-way ANOVA, $F(2,10)=0.07$, $p=0.80$). However, the transcript abundance of *TaMAX1a2* increased in response to N limitation and was significantly induced on days 8 and 12 after N limitation. *TaMAX1c* and *TaMAX1d* were found to be induced by N limitation from day 4 after N limitation onwards.

Examination of the expression of genes involved in SL perception revealed that *TaD3* was slightly induced by N limitation in the basal node, while *TaD14* showed a development-related decrease over time in both treatments. When compared to high N treatment, *TaD14* was downregulated in the N-limited plants 4 days after N limitation. No difference was observed at 8 days after N limitation, while the mRNA levels were found to increase at 12 days after limitation.

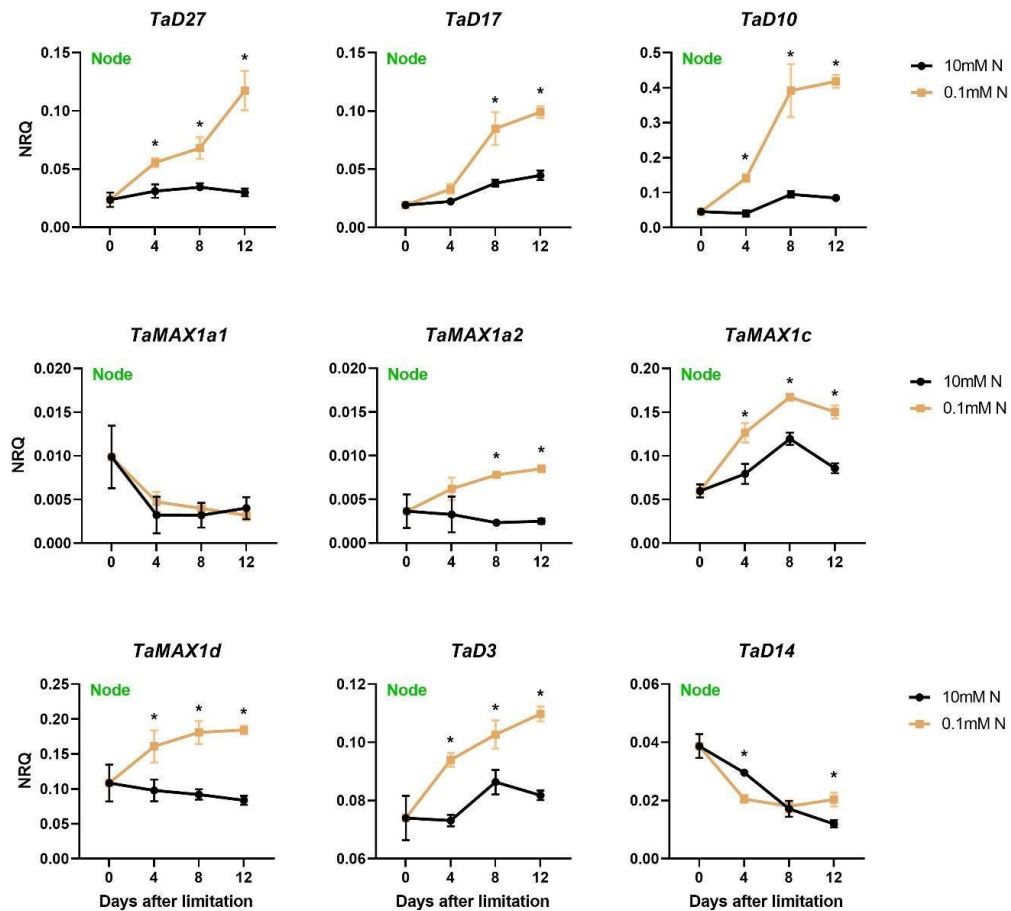


Figure 3.6: Time-course analysis of the gene expression levels of SL biosynthetic (*TaD27*, *TaD17*, *TaD10*, *TaMAX1a1*, *TaMAX1a2*, *TaMAX1c* and *TaMAX1d*) and perception genes (*TaD3* and *TaD14*) in the basal node (0.5 cm of main shoot base) of wheat 0, 4, 8 and 12 days after N limitation (0.1 mM N) compared to high N treatment (10 mM N). Values are means of three biological replicates and error bars represent SE. Statistical analysis was conducted with ANOVA in $\log_2(1/\text{NRQ})$ transformed values. * denotes statistically significant difference in the gene expression levels between low N and high N plants at each time point based on Fisher's LSD test (*TaD27* LSD (5%) = 0.56, *TaD17* LSD (5%) = 0.44, *TaD10* LSD (5%) = 0.68, *TaMAX1a1* LSD (5%) = 1.79, *TaMAX1a2* LSD (5%) = 1.25, *TaMAX1c* LSD (5%) = 0.33, *TaMAX1d* LSD (5%) = 0.49, *TaD3* LSD (5%) = 0.15, *TaD14* LSD (5%) = 0.49).

In addition, the expression of the transcription factor *TaTB1* was examined in basal node samples. TB1 is a bud-specific transcription factor involved in the suppression of tillering and has been suggested to be one of the downstream targets of the SL signalling pathway. As a result, the expression of *TaTB1* was only monitored in basal node samples and not in roots (**Figure 3.7**). Statistical analysis revealed that there is a significant main effect of N treatment on the mRNA levels of *TaTB1* ($F(1,10)=42.5$, $p<0.01$, $\text{LSD (5\%)}=0.92$). After 4 days of N limitation, the transcript levels of *TaTB1* were

increased, but no statistically significant difference was observed. However, the *TaTB1* was significantly induced following 8- and 12-days of N limitation. The induced expression of *TaTB1* correlates well with the observed phenotype, given that the effect of N limitation on tiller formation and bud outgrowth became more apparent from day 8 after N limitation. In the same tissue, the expression of another transcription factor, *TaGT1*, was also monitored. *GT1* expression has been associated with tiller suppression, and it is considered a putative downstream target of TB1. The mRNA accumulation of *TaGT1* showed a developmentally related decrease in high N treated plants over time. N supply had a strong effect on the expression of *TaGT1* in the nodes leading to a significant upregulation of *TaGT1* expression in all the time points examined ($F(1,10)=189.4$, $p<0.01$, $LSD(5\%)=0.59$).

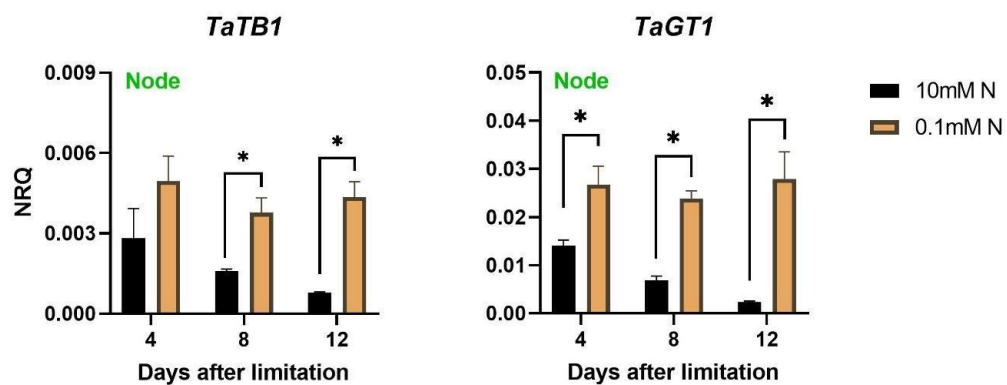


Figure 3.7: Time-course analysis of the gene expression levels of transcription factors *TaTB1* and *TaGT1* in the basal node (0.5 cm of main shoot base) of wheat 4, 8 and 12 days after N limitation (0.1 mM N) compared to high N treatment (10 mM N). Values are means of three biological replicates and error bars represent SE. Statistical analysis was conducted with ANOVA on $\log_2(1/\text{NRQ})$ transformed data. * denotes statistically significant difference in the gene expression levels between low N and high N plants at each time point based on Fisher's LSD test (*TaTB1* LSD (5%) = 0.92, *TaGT1* LSD (5%) = 0.59).

3.2.5 Transcriptional Response of SL Biosynthetic and Perception Genes in Root to N Resupply

Based on the results presented in sections 3.2.3 and 3.2.4, the expression of SL biosynthetic genes is strongly induced by N limitation in roots but also locally in the nodes. To further examine the transcriptional response of SL biosynthetic genes to N, gene expression was monitored after providing NO_3^- to N-limited plants. More specifically, wheat seedlings grown in low N conditions for 8 days were supplied with high N nutrient solution and the expression of the gene of interest was examined before, 24 and 72 h after the N resupply (**Figure 3.8**). High N and low N treated plants were also included for comparison. Although the gene expression analysis had been planned for both root and basal node tissue, data were only obtained from root samples due to quality issues with the extracted RNA from basal node samples.

Before N resupply, the expression of SL biosynthetic genes (*TaD27*, *TaD17*, *TaD10*, *TaMAX1a1* and *TaMAX1d*) was significantly higher in low N plants compared to the plants grown under high N conditions. This observation was consistent with previous results, confirming that N limitation led to strong downregulation of SL biosynthesis in roots (section 3.2.3). N resupply led to significant downregulation of all the SL biosynthetic genes included in the study within 24 h, suggesting that the regulation of the genes is controlled by N supply. In fact, a statistically significant difference based on Fisher's LSD test ($p < 0.05$) was observed for all the SL biosynthetic genes at 24 h between N-resupplied and N-limited plants. In addition, at 24 h after the N resupply, the mRNA level of *TaD27* and *TaMAX1a1* dropped to the same levels as in high N treated plants. Similarly, no significant difference was recorded between N-resupplied plants and high N plants at 72 h for *TaD10* and *TaMAX1d*.

A significant downregulation was recorded in the transcript abundance of SL biosynthetic genes at 24 h, while the expression rose again by 72 h in the N-limited plants. Despite this downregulation, the expression of SL biosynthetic genes was higher compared to high N and N resupplied plants at all time points. The observed downregulation might be related to the exchange of nutrient solution, which took place at 0 h when all the plants received a fresh nutrient solution. Therefore, at 0 h, low N plants were supplied with 1 L of 0.1 mM nutrient solution (1.4 mg of N), which

might be responsible for the observed downregulation of SL biosynthetic genes. This observation indicated that the regulation of SL biosynthetic gene expression is regulated by local signals such as by NO_3^- or by N metabolic products rather than the plant N content, given that the 0.1 mM of N cannot significantly change the N status of the plants. The transcript levels of those genes rose again at 72 h, presumably, as the small amount of NO_3^- provided was rapidly consumed.

The SL perception genes, *TaD3* and *TaD14*, were significantly downregulated in low N plants at 0 h, confirming the negative feedback regulation previously observed in roots (section 3.2.3). Both genes were induced 24 h after N resupply and found to be significantly higher compared to low N treated plants. More specifically, the mRNA levels of *TaD3* and *TaD14* rose to the same levels as in high N plants within 24 h after N resupply, while no further significant increase was observed at 72 h after the N resupply. In plants treated with low N solution, the expression of *TaD3* remained stable, whereas *TaD14* mRNA levels decreased over time. In addition, in low N roots, no effect was observed at 24 h, as observed in SL biosynthetic genes, indicating that the expression of *TaD3* and *TaD14* is not so sensitive to the N levels, but it is most likely controlled by SL levels (feedback regulation) or other factors.

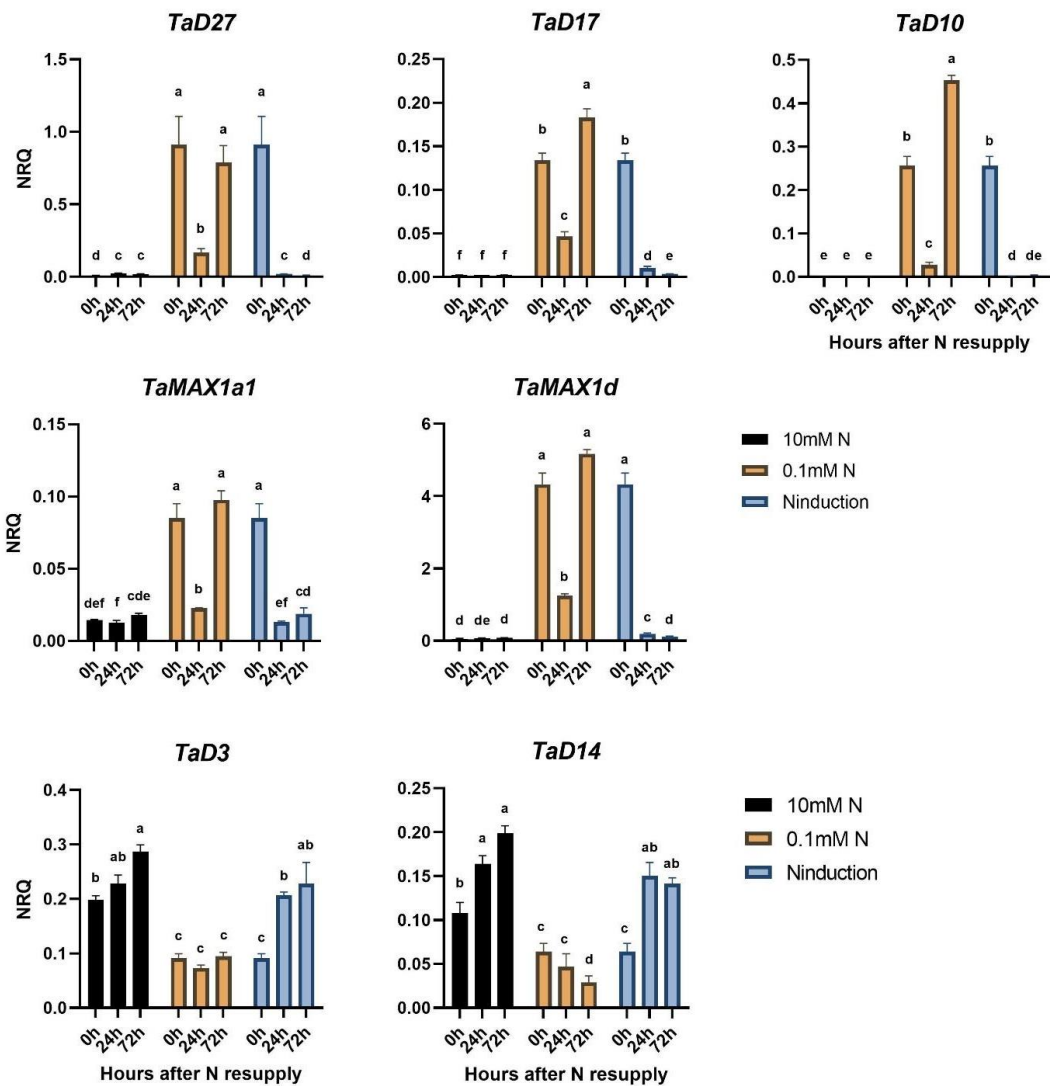


Figure 3.8: Time-course analysis of the gene expression levels of SL biosynthetic (*TaD27*, *TaD17*, *TaD10*, *TaMAX1a1*, and *TaMAX1d*) and signalling genes (*TaD3* and *TaD14*) in the root of wheat before (0h), 24h and 72h after the N resupply. Values are means of three biological replicates and error bars represent SE. Statistical analysis was conducted with an unbalanced 2-way ANOVA in $\log_2(1/\text{NRQ})$ transformed values. Different letters denote statistically significant differences in the gene expression levels between the means based on Fisher's LSD test (*TaD27* LSD (5%) = 0.85, *TaD17* LSD (5%) = 0.40, *TaD10* LSD (5%) = 0.59, *TaMAX1a1* LSD (5%) = 0.53, *TaMAX1d* LSD (5%) = 0.45, *TaD3* LSD (5%) = 0.43, *TaD14* LSD (5%) = 0.57).

3.2.6 Expression Pattern of Wheat *MAX1* Genes in Root and Basal Nodes

The time-course analysis of the SL biosynthetic and signalling genes showed that N limitation strongly induces the expression of SL biosynthetic genes in the root but also locally in the basal nodes. However, the gene expression analysis presented in sections 3.2.3 and 3.2.4 also revealed that there was a tissue-specific regulation of *MAX1* homologues in response to N supply. For instance, *MAX1a1* was found to be induced by N limitation only in roots, whereas the opposite was observed in *MAX1c*, whose transcript abundance was affected by N limitation only in the basal node. Based on that observation, it may be hypothesized that there might be a tissue-specific expression or regulation of *MAX1* genes. The expression data presented in the previous sections were relative gene expression data obtained by RT-qPCR, which did not allow for the direct comparison between the expression levels of different genes. Therefore, to examine this hypothesis, data from different RNA-seq experiments conducted as part of this project was utilised to compare the transcript abundance of the different *MAX1* genes. More specifically, the data were obtained from three independent experiments conducted in either root or basal node tissue. Root data were derived from 2 experiments, one conducted in *T. aestivum* cv. Graham at 15 DAS and 24 h after N limitation (n=3) and an experiment performed in *T. aestivum* cv. Cadenza plants at 18 DAS and 8 days after N limitation (n=6). Expression data for basal nodes were retrieved from three independent experiments. The first and the second experiment was conducted in *T. aestivum* Cadenza nodes at 18 DAS and 8 days after N limitation (n=4 and 6, respectively), while the third experiment was performed in *T. aestivum* cv. Graham nodes at 32 DAS and 18 days after N limitation (n=3). TPM values of all the 13 identified wheat *MAX1* genes were retrieved and presented as a heatmap in **Figure 3.9**. Genes with TPM values below 0.5 (TPM<0.5) were considered as low expressed.

Based on the heatmap, there was a distinct pattern of *TaMAX1s* expression distinguishing roots and basal nodes. *TaMAX1a2-U* and *TaMAX1a2-3B* are the predominant *MAX1* genes expressed in the root, showing the highest expression values among all of the *MAX1* homologues. This observation was consistent in both cultivars, although some variation was observed in the two different experiments,

probably related to the experimental condition and the different developmental conditions. In high N treated roots, the average TPM value of *TaMAX1a2-U* and *TaMAX1a2-3B* was ranging 5.96-6.43 and 5.05-11.71, respectively, depending on the experiment. However, no expression of *TaMAX1a2-3D*, which also belong to the *MAX1a2* subgroup, was observed in the roots. *TaMAX1a1* and *TaMAX1d* homoeologues were also found to be expressed in roots, but the transcript abundance was lower compared to *TaMAX1a2* genes. On average, the total mRNA levels of *TaMAX1d* homoeologues accounted for just 15% of the total *MAX1* mRNA levels, while *TaMAX1a2* accounted for 73% in N-sufficient plants. In N-limited plants, due to changes in the expression of *MAX1* genes, the total transcript abundance of *MAX1a2* homoeologues accounted for 97% of the total transcript abundance of *MAX1* genes, indicating that under N-limiting conditions, the *MAX1a2* are responsible for the biosynthesis of SLs in roots. No expression of *MAX1b-3A* and *MAX1c* homoeologues was detected in roots in either high or low N conditions in any of the cultivars, indicating that those genes are not expressed in roots.

TaMAX1c homoeologues were the predominant *MAX1* genes expressed in basal nodes. Depending on the experiment, the average TPM values of *MAX1c* homoeologues varied between 2.52-6.59 under high N conditions and between 5.12-10.66 under N-limiting conditions. In addition, *MAX1d* homoeologues were expressed in basal nodes, which accounted for 24-28% of the total *TaMAX1* transcript abundance. In some samples, low mRNA levels of *TaMAX1a1-1D* were also detected. The expression balance of *MAX1s* in basal nodes did not drastically change in response to N limitation, despite the upregulation of the genes by N limitation. No expression of *MAX1a2* homoeologues was detected in basal nodes in any of the samples included in the analysis (TPM<0.5). As observed in roots, *TaMAX1b-3A* was not found to be expressed in basal nodes.

The results demonstrated that there is a tissue-specific expression of the wheat *MAX1* genes. *MAX1a2* homoeologues are expressed only in roots, whereas *MAX1c* homoeologues are only expressed in basal nodes. *MAX1d* genes are expressed in both roots and basal nodes, but in none of the tissues were they the predominant form. Low expression of *MAX1a1* homoeologues was found in both tissues examined.

MAX1b expression was not detected in any tissue either under high or low N conditions.

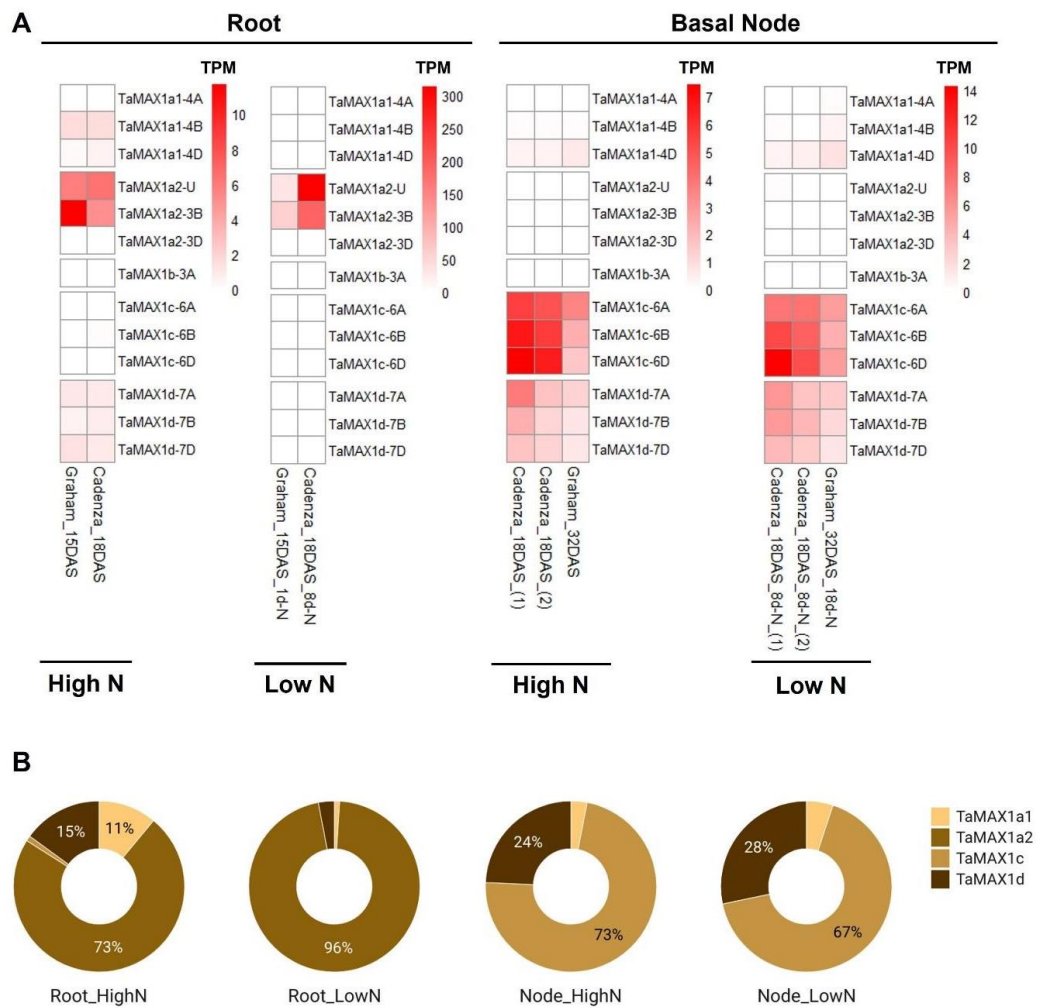


Figure 3.9: Expression data of wheat *MAX1* genes from RNA-seq experiments in root and basal nodes. (A) Heatmap comparison of wheat *MAX1* gene expression values expressed as TPM. Data were retrieved from five different RNA-seq experiments conducted as part of the project in root and basal node tissue of *T. aestivum* cv. Cadenza or Graham, grown under high N or low N conditions and at different time points (15, 18 or 32 DAS), depending on the study. The values presented are means of biological replicates (n=3-6). **(B)** Percentage of each of the *MAX1* homoeologue group expression in the total wheat *MAX1* expression in root and basal node under high N or low N conditions. The percentages presented are mean values from different experiments.

3.3 Discussion

3.3.1 SL Biosynthesis and Signalling Genes Regulated by N Supply

Nitrogen is an essential macronutrient for plant growth. Plant adaptation to N-limiting conditions includes changes in root and shoot architecture in such a way as to increase the use efficiency of available resources and maximize the chances of survival and successful reproductive development. The results presented in this study demonstrated that shoot architecture is strongly affected by N availability. N limitation strongly suppressed tiller outgrowth resulting in a reduced number of tillers per plant. As plant N levels decreased, the effect of N limitation on tillering became more apparent by affecting the formation of higher-order tillers (**Figure 3.4**). In *Arabidopsis*, branching is suppressed by the plant N status and not by the NO_3^- content of shoots, as different sources of N had the same effect on branching. This suggests that tiller suppression is controlled by systemic signals rather than by the local concentration of NO_3^- (de Jong et al., 2014).

In many species, N limitation has been found to promote SL biosynthesis and exudation. This response has also been observed in wheat under N or P limitations (Yoneyama et al., 2012). However, there are few studies focusing on the transcriptional regulation of SL biosynthetic and signalling genes by N availability. To investigate the interaction between N and SLs in wheat, the expression levels of the major biosynthetic, perception and signalling genes were monitored in roots and basal nodes of wheat grown under high and low N supply. The results showed that N limitation strongly induces the expression of the examined biosynthetic genes. Thus, it may be that the previously reported induction of SL levels under N-limiting conditions in wheat is due to the strong upregulation of SL biosynthetic genes (Yoneyama et al., 2012). Similar transcriptional regulation of *D27* and *D17* has also been reported in rice roots upon N limitation (Sun et al., 2014). Moreover, the mRNA levels of SL biosynthetic genes were found to be downregulated in roots after transferring N-limited plants to high N conditions. These findings support the conclusion that SL biosynthetic genes are tightly regulated by plant N status.

SL perception genes, *TaD3* and *TaD14*, were found to be strongly downregulated in roots of low N plants. *D3* and *D14* expression has been reported to be regulated by a negative feedback loop (Umehara et al., 2010, Sun et al., 2014, Marzec and Melzer, 2018). Therefore, this can explain the observed downregulation in low N roots and further support that N limitation leads to elevated levels of SLs by upregulating the SL biosynthetic genes.

SLs are thought to be predominantly produced in roots. However, the expression of biosynthetic genes has also been detected in lateral buds. In fact, grafting experiments in dicotyledonous species have demonstrated that locally produced SLs in shoots are sufficient to control lateral branching. According to the results presented in this chapter, expression of SL biosynthetic genes was detected in the basal nodes of wheat plants, where N limitation induced their expression, as was also observed in roots. Although *TaMAX1c* did not show any response to N level in roots, it was induced in nodes by N limitation. The opposite was true for *MAX1a1* genes, suggesting a tissue-specific regulation of those genes (further discussed in section 3.3.3). It is well established that SLs are involved in tiller suppression under P limitation in rice and Arabidopsis (Kohlen et al., 2011, Umehara et al., 2010). In fact, P limitation also induces SL biosynthesis locally in rice buds (Umehara et al., 2010). Therefore, the recorded induction of SL biosynthesis in basal nodes might contribute to tiller inhibition under N limiting conditions. Wang et al. (2018) also showed a link between N uptake and SL biosynthesis. More specifically, rice *NPF7.2* overexpressing lines showed enhanced tillering and NO_3^- uptake, while the gene expression of SL biosynthetic genes was strongly downregulated in tiller buds. The opposite effect was observed for *npf7.2* mutant lines, where the SL biosynthetic genes (*D27*, *D17* and *D10*) were suppressed in the tiller nodes within 3 h after N supply (Xu et al., 2015b). Consequently, local SL biosynthesis in nodes is regulated by N availability and possibly participates in the tiller regulation. However, de Jong et al. (2014) showed that N-mediated bud outgrowth regulation is at least partly dependent on SLs in Arabidopsis. SL mutants were found to form more branches than WT plants under low N conditions, but SL mutants could still respond to N availability. Similar results were later reported in rice *d3* and *d10* mutants (Luo et al., 2018b). However, less is known about other

roles of the elevated SL levels in the basal node under N limitation if SLs are not necessary for tiller inhibition.

3.3.2 *TB1* Induction by N Limitation in Wheat

TB1/BRC1/FC1 is a transcription factor that plays a central role in tillering/lateral branching. Suppression of tillering has been associated with the high expression of *TB1* in many species. In fact, overexpression of *TB1* from maize in wheat suppressed tillering, confirming that the role of *TB1* is conserved among grasses (Lewis et al., 2008). *TB1* expression has been found to be regulated by many signals; therefore, *TB1* has been suggested to act as a hub integrating hormonal and environmental cues (Wang et al., 2019c). Based on the results presented in this chapter, *TB1* mRNA levels were upregulated in the low N-treated plants. The induced expression of *TB1* in N-limited wheat plants correlated well with the observed tiller suppression, suggesting that *TB1* is also regulated by nutritional signals, such as N, to control tillering. In rice tiller buds, N supply has also been shown to lead to downregulation of *TB1* within 12 h, further supporting that *TB1* facilitates the bud outgrowth control in response to N availability (Xu et al., 2015b). Nevertheless, there is no clear evidence that N itself affects *TB1* expression directly; hence the effect of N supply on *TB1* expression might be controlled by other signals. Several studies have shown that *TB1* expression is regulated by SLs, CKs, sugar availability and other stimuli. *TB1* is considered a downstream target of the SL signalling pathway controlled by the D53 transcriptional repressor. In wheat, it has been shown that *TB1* transcription is controlled by IPA1 and D53 (Liu et al., 2017). In the present study, N limitation induced the expression of SL biosynthesis in nodes. As a result, the induction of *TB1* under the same conditions can be assumed that is controlled by the elevated levels of SLs. Other studies have shown that *TB1* is also negatively regulated by CKs. It is known that CK levels in plants are strongly correlated with N supply. This might be another way in which N limitation regulates *TB1* expression leading to tiller suppression.

The exact mechanism by which *TB1* controls tiller bud outgrowth remains elusive. *GT1* is a homeodomain leucine zipper (HD-ZIP) transcription factor, which modulates shoot branching. In maize, *GT1* has been found to act downstream of *TB1*, controlling

tillering under low-light conditions (Whipple et al., 2011). In Arabidopsis, it was shown that under low light conditions, BRC1/TB1 directly regulates the expression of three HD-ZIP TFs, orthologues of *GT1* (González-Grandío et al., 2017). These factors are responsible for locally regulating ABA biosynthesis leading to bud dormancy. Based on the expression analysis, *TaGT1* expression is strongly induced in basal nodes by N limitation. *GT1* and *TB1* showed a similar expression pattern indicating that the association between *TB1* and *GT1* may also be the case in wheat. This mechanism of tiller suppression has been demonstrated under low light conditions; however, the expression data suggest that a similar mechanism might be involved in tiller suppression under N-limiting conditions.

3.3.3 Distinct Expression Profiles of Wheat *MAX1* genes

In Arabidopsis, there is only one *MAX1* gene that catalyses the conversion of CL to CLA, which is subsequently used as a substrate by a recently identified SABATH-methyltransferase, and which produces Me-CLA (Wakabayashi et al., 2021). Me-CLA is further metabolised by LBO for the synthesis of 1'-OH-MeCLA (Brewer et al., 2016, Yoneyama et al., 2020a). Both Me-CLA and 1'-OH-MeCLA have shown activity as branching inhibitors indicating that non-canonical SLs might be responsible for the branching inhibition activity of SLs (Abe et al., 2014, Brewer et al., 2016). However, in monocotyledons, it has been shown that there are multiple *MAX1* homologues that have been suggested to catalyse different steps in the conversion of CL to bioactive SL molecules. Despite the progress in understanding the function of the different *MAX1* genes in rice, their functional role in wheat remains elusive. Based on the phylogenetic analysis, wheat has 13 distinct *MAX1* genes. Phylogenetic analysis also showed that *MAX1*s from grasses form four different clades. The results here are consistent with Marzec et al. (2020), who reported the presence of four distinct clades, but in their study, only eight out of the 13 identified wheat *MAX1* sequences had been included (Marzec et al., 2020). In clade B, only a single *MAX1* wheat gene was found along with three rice orthologues and one representative from all the other monocotyledons included in the study. Interestingly, two different homoeologous subgroups were found in clade A, while only *B. distachyon* was found to have closely related sequences to both subgroups of clade A. No rice orthologue was present in clade A.

Recent studies have shown that both Os900 and Os1400 convert CL to CLA, while each one show an additional specific activity (Yoneyama et al., 2018a). However, Os1500 does not show enzymatic activity, which has been attributed to a premature stop codon. More specifically, Os900 convert CLA to 4DO, and Os1400 convert 4DO to orobanchol (Zhang et al., 2014). Orobanchol is one of the main SLs found in root exudates, indicating that it acts as a rhizosphere signal. Similarly, Yoneyama et al. (2018) also showed that ZmMAX1b, which belongs to the same clade (clade B), also have activity similar to Os1400. According to Umehara et al. (2010), the expression of *Os1400* was only found in rice roots, while mRNA was undetected in lateral buds (Umehara et al., 2010). Based on the current RNA-seq data, *TaMAX1b-3A*, which is closely related to *Os1400*, *Os900* and *Os5100*, was not found to be expressed in any of the examined tissues. In comparison, members of the *TaMAX1a2* subgroup were found to be expressed exclusively in roots, and their expression was strongly induced by N limitation. A similar, root-specific expression of BdCYP711A31, which also belongs to clade A2, has been reported in *B. distachyon* (Changenet et al., 2021). Therefore, based on the expression pattern, it is assumed that members of subgroup A2 have a similar function to *Os1400* and *Os900* and are therefore involved in the biosynthesis of canonical SLs such as orobanchol in roots. In wheat and other species, N limitation stimulates the biosynthesis of orobanchol in roots (Yoneyama et al., 2012). *TaMAX1a2-3B* and *TaMAX1a2-U* showed 48- and 37-fold induction, respectively, after 8 days under N-limiting conditions, while they accounted on average for 96% of the total *MAX1* transcript abundance under N-limiting conditions, indicating that they play a predominant role in SL biosynthesis in roots. In fact, *SbMAX1a*, which is phylogenetically close to *TaMAX1a2*, has been shown to be involved in the production of orobanchol in sorghum, further supporting our hypothesis (Wu and Li, 2021).

Os1900 and Os5100, which belong to clades C and D, respectively, have shown weak conversion of CL to CLA based on yeast microsomal studies (Yoneyama et al., 2018a). In the same study, Yoneyama et al. (2018) also showed that ZmMAX1c and ZmMAX1a, which are phylogenetically close to Os1900 and Os5100, respectively, showed also weak conversion of CL to CLA, indicating that CL is not the preferred substrate of MAX1 enzymes belonging to those clades. The gene expression data in the present study

revealed that *TaMAX1c* homoeologues are orthologues of *Os1900* and are only expressed in nodes. More specifically, *TaMAX1cs* were the predominant *MAX1* genes expressed in basal nodes, while no expression was detected in roots. This observation can explain why *TaMAX1c* mRNA levels were found to be upregulated by N limitation only in basal nodes and not in roots, based on the time-course gene expression analysis. This finding is consistent with expression analysis in *B. distachyon*, in which transcript levels of *BdCYP711A5* were higher in leaves compared to roots. *SbMAX1c*, which is closely related to *TaMAX1c*, apart from the conversion of CL to CLA, also catalyses the production of an unknown peak, indicating the production of an as yet unidentified SL-like compound with a similar molecular weight of 18-hydroxy-CLA. Marzec et al. (2020), based on *in silico* analysis, speculated that *Os1900* might be involved in the biosynthesis of non-canonical rather than in the biosynthesis of canonical SLs. Our expression analysis supports the hypothesis that *TaMAX1c* homoeologues might be involved in the production of a yet unknown SL molecule or SL intermediate, which is produced and act in shoots as tiller inhibitors.

Expression of *TaMAX1d* homoeologues was found in both tissues suggesting that *MAX1d* function is required in both root and shoots. However, the expression levels (TPM) were higher in nodes compared to roots.

In conclusion, the results showed a clear tissue-specific expression and regulation of *MAX1* genes in response to N limitation, suggesting different functionalities and roles of wheat *MAX1* genes. Further studies manipulating specific *MAX1* genes are required in order to better understand the functional diversity and the role of *MAX1* in wheat.

Chapter 4 Transcriptional and Phytohormonal Changes in Basal Nodes of Wheat Grown under Low Nitrogen and Low Phosphorus Conditions

4.1. Introduction

4.1.1 Background

Nitrogen is an essential macronutrient for plants as it is a fundamental component of DNA, amino acids, proteins, chlorophyll, hormones, and cell structural components (Ueda et al., 2017). As a result, N nutrition has a substantial impact on plant metabolism, growth, and productivity. N is predominantly taken up from the soil as inorganic N, mainly in the form of NO_3^- and additionally in the form of NH_4^+ . Nitrate uptake is facilitated by members of the nitrate transporter 1/peptide family (NPF) and high-affinity nitrate transporters (NRT2). Nitrate transporters are not only responsible for N uptake from the soil but are also involved in the internal translocation of N and also as N sensors (Noguero and Lacombe, 2016, Tegeder and Masclaux-Daubresse, 2018). Some members of the NPF family are also involved in the transport of proteins, hormones, and other compounds (Buchner and Hawkesford, 2014). Following uptake, NO_3^- is assimilated into amino acids. N assimilation takes place either in roots or in mature leaves after transport of the absorbed NO_3^- through the xylem. Necessary enzymes for the 2-step reduction of NO_3^- to NH_4^+ are nitrate reductase (NR) and nitrite reductase (NiR). NR catalyses the reduction of NO_3^- to nitrite, which is subsequently reduced to NH_4^+ by NiR. NH_4^+ originated from NO_3^- assimilation or directly absorbed NH_4^+ is then used by glutamine synthetase (GS) and glutamate synthase (GOGAT) to produce glutamine (Gln) and glutamate, respectively. Gln is further converted into asparagine (Asn) by asparagine synthetase (ASN). Gln and Asn are the main long-distance transport forms of N, while ASN has been shown to play an essential role in N assimilation, remobilisation, and recycling (Gaufichon et al., 2015). Those amino acids are further used for the biosynthesis of other amino acids and N-containing compounds. After the assimilation of NO_3^- in source tissue (roots and mature leaves), reduced N is transported to sink tissue, such as developing tissue, where they are used to support growth (Tegeder and Masclaux-Daubresse, 2018). Amino acids are the main

form of N transported within the plants from N source to sink tissues, while ureides contribute to N distribution but to a lesser extent compared to amino acids in non-legume species. The transport of amino acids to the sink organs is facilitated by amino acid transporters (Yao et al., 2020). Some enzymes involved in N assimilation have also been shown to have an essential role in N remobilisation, such as GS1 and glutamate dehydrogenase (Bernard and Habash, 2009).

Due to the importance of N for cell function and plant growth, plant adaptation to N limitation includes a plethora of morphological, physiological, and transcriptional changes. Those changes as a whole are referred to as N-response, and they allow plants to cope with N-limiting conditions. The development of high throughput RNA-sequencing techniques has allowed genome-wide studies of N-response, providing a fundamental understanding of the regulation of N responsive genes by N supply and plant N status. In fact, several studies in wheat have shown that N status strongly affects N uptake and assimilation genes, nutrient remobilisation, and also other pathways such as central metabolism and photosynthesis, highlighting the pleiotropic effect of N limitation on plant metabolism and growth (Meng et al., 2021, Wang et al., 2019a). More recent studies in model plant species *Arabidopsis* and rice using systems biology approaches provided evidence of transcription factors that act as master regulators of N-response upon exposure of plants to NO_3^- or under N limiting conditions (Gaudinier et al., 2018, Ueda et al., 2020). Those studies provided useful information about the regulation of N-responsive genes but also emphasised the complexity of the N-response. However, most of the studies conducted in wheat, but also in model species, have focused on root tissue on how N affects N uptake and assimilation and on changes that govern root architectural adaptation. In addition, a great number of studies in wheat have also focused on leaf tissue, mainly on flag leaves during reproductive development or grain filling, studying the effect of plant N status on photosynthesis and N remobilisation (Curci et al., 2017, Meng et al., 2021, Sultana et al., 2020). Meanwhile, no studies have focused on molecular pathways involved in shoot architectural changes induced by N limitation during vegetative plant growth in wheat.

As shown in Chapter 3, N limitation strongly reduces tiller number. Tiller formation is divided into two steps; the first step is the initiation of the lateral meristems, and the second step is the bud outgrowth (Kebrom et al., 2013). Meristem initiation has been shown not to be affected by N limitation in rice, whereas formed buds remained dormant under N-limiting conditions (Luo et al., 2017). This observation suggests that signals related to N limitation control the fate of the lateral buds, which remain dormant under N limitation. Transcriptomic studies have provided evidence about the molecular mechanism of bud dormancy in response to other signals that lead to dormancy in other species (Kebrom and Mullet, 2016, Tarancón et al., 2017). However, less is known about the underlying molecular mechanism of N limitation mediated bud dormancy. The fate of a developed bud is known to be controlled by plant hormones, while sugars have been shown to play an essential role as a signal controlling bud outgrowth (Barbier et al., 2019). The response to nutrient-limiting conditions requires not only sensing mechanisms but also local and systemic signals in order to coordinate plant growth at a whole plant level. Plant hormones are likely candidates for facilitating the systemic response to N status to modulate tillering. In fact, CK levels are known to be associated with plant N status; therefore, they are considered long-distance signals of N status (Sakakibara et al., 2006). In addition, as shown in Chapter 3, SL biosynthesis is strongly induced under N-limiting conditions in roots and locally in the basal nodes, suggesting that they might be involved in N-mediated tiller suppression.

The role of SLs under N limitation remains not well understood. More specifically, SL production and exudation are mainly associated with P limitation and, to a lesser extent, with N limitation (Yoneyama et al., 2012). Therefore, SL upregulation under N limiting conditions has been attributed to the lower P uptake by N-limited plants rather than directly to plant N status. In addition, less is known about the signals that control the transcriptional regulation of SL biosynthetic genes. In split-root experiments, it has been demonstrated that N or P themselves are not the signals controlling SL biosynthesis in sorghum and rice under N or P limiting conditions, respectively, but possible shoot-derived signals of N and P status are responsible for SL production regulation (Yoneyama et al., 2015, Yoneyama et al., 2020b).

4.1.2 Chapter Objectives

The aim of this chapter was to provide a better understanding of the transcriptional and phytohormonal changes that govern N response in basal nodes and may be associated with tiller suppression under N limitation. This was achieved by performing RNA-sequencing and phytohormonal analysis in basal nodes of wheat grown for 8 days under N-limiting conditions. Finally, the P limitation effect was also included in the study, mainly focusing on the comparative impact of N and P limitations on SL biosynthesis, signalling and perception.

4.2. Results

4.2.1 Effect of N and P Limitations on Tillering

Both N and P limitations are known to negatively affect tillering. The results under N limiting conditions showed that N limitation strongly induces SL biosynthesis in nodes (section 3.2.4). To further explore the transcriptional changes under N limitation that may be associated with tiller suppression, the basal nodes of wheat grown under N limitation for 8 days were harvested for RNA-sequencing. In this trial, samples from P-limited plants were also included. Based on the tillering data, N limitation had a greater and more rapid effect on tiller outgrowth than P limitation (**Figures 4.1A-B**). The P limitation effect was apparent 12 days after the P limitation, whereas 8 days after the N limitation, a strong suppression of the second tiller outgrowth was observed. In addition, 15 days after the nutrient limitation, the number of tillers in low N plants was 4-fold lower compared to the WT, whereas low P plants showed a 2-fold decrease in tiller number.

4.2.2 Effect of N and P Limitations on Plant N and P Concentration

Total N and P analyses were performed to examine the effect of N and P limitation on the macronutrient concentration of root and shoot (**Figure 4.1C**). The analysis was conducted in sample material 8 days after initiation of the macronutrient limitation (from the same plants as used for the RNA-sequencing). N limitation strongly reduced the N concentration of both roots and shoots. The reduction in N concentration was more substantial in roots than in shoots, with N concentration reduced by 60% in roots and by 50% in shoots. A statistically significant decrease in the N concentration was also observed in low P plants, but the reduction was only by 7-8% in both tissues examined.

In relation to P concentration, a significant decrease in P levels was observed in the root and shoot of low P plants. P concentration dropped by approximately 50% in both tissues 8 days after P limitation. However, a decline in the P concentration was also found in low N-treated plants. The effect of N limitation on P concentration was more prominent in roots, where P levels declined by 20%, while in shoots, P concentration was 8% lower in low N plants compared to the control. Although the decrease in P

concentration was observed in low N plants, low N plants still showed 2-times higher P concentration than the low P treated plants. This decrease in P levels in N-limited plants may be associated with reduced P uptake by N-limited plants to maintain the balance between N and P levels within the plant tissue.

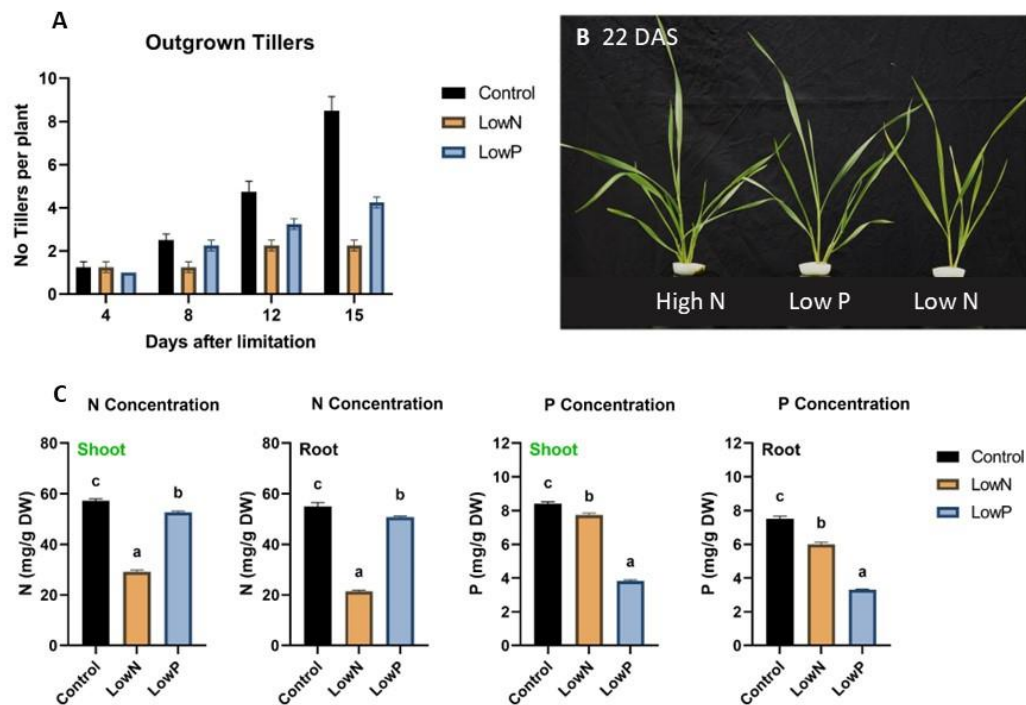


Figure 4.1: Effect of N and P limitation on wheat tillering. (A) The number of outgrown tillers per plant at 4, 8, 12 and 15 days after N or P limitations. Values are means of four biological replicates, and error bars represent SE. Statistical analysis was conducted with repeated measures ANOVA (LSD (5%) = 0.998). **(B)** Representative plants grown under Control (10 mM N and 1 mM P), Low P (10 mM N and 0.01 mM P) and Low N (0.1 mM N and 1 mM P) conditions at 12 days (22 DAS) days after the introduction of the plants to the nutrient limitation. **(C)** N and P concentration in the root and shoot of low N- and low P-treated plants. Values are means of four biological replicates, and error bars represent SE. Statistical analysis was conducted with ANOVA. Different letters denote statistically significant difference between treatment means based on Fisher’s LSD test (N Shoot LSD (5%) = 2.20, N Root LSD (5%) = 2.93, P Shoot LSD (5%) = 0.24, P Root LSD (5%) = 0.43).

4.2.3 RNA-sequencing Results in Basal Nodes

Total RNA was extracted from basal nodes of plants grown under N and P limiting conditions for 8 days and submitted for standard RNA-sequencing. In total, four biological replicates were included per treatment. On average, each sample had 39 M paired-end reads. The number of reads varied between 30 and 56 M for most of the samples, apart from sample “LN4-8”, which yielded only 9 M reads. The low number

of reads of this particular sample could indicate that this sample was problematic. Quality control and downstream analysis were performed on all the raw data as described in section 2.4.4. The quality of the potential problematic sample was assessed at later steps. After the quality control check, raw data were mapped to the *T. aestivum* reference genome IWGSC RefSeq v1.0 using the tool *HISAT2*. On average, 85.6% of the reads were aligned to the reference genome. The alignment rate ranged from 82.7% to 93.6% among the samples. Subsequently, mapped reads were assigned to exons, and the number of reads mapped to annotated genes was counted using the *featureCounts* tool. On average, 52% of the reads were assigned to genes; that is, 23 M assigned reads to genes per sample, which provided adequate coverage of the wheat transcriptome. Count data were then used for differential gene expression analysis performed by the *DESeq2* tool. Transcript abundance was also calculated by utilising the *kallisto* tool and IWGSC RefSeq v1.0 annotation v1.1. Subsequently, the gene abundance was also calculated by summing up the TPM values of the transcripts that correspond to the same gene.

Prior to the differential gene expression analysis, a prefiltering of low expressed genes was applied. Genes which had less than three samples with more than five counts were removed from the analysis. After the prefiltering, in total, 86970 genes were included in the analysis, which corresponds to approximately 32% of the annotated genes. However, the number of genes was not evenly distributed between high confidence (HC) and low confidence (LC) genes. In fact, among the 86970 genes, there were 64401 HC and 22569 LC genes, which accounted for 60% and 14% of the annotated genes of each category, respectively. LC genes are genes with partially supported gene models or gene fragments, while there is evidence of transcription for only 49% of the LC genes. Therefore, the low number of LC in the prefiltered dataset was anticipated. Borill et al. (2019) have reported that around 49% of the HC genes were found to be expressed in wheat leaves.

Table 4.1: RNA-sequencing raw data analysis statistics.

Sample	Block	Treatment	Reads (M)	Alignment Rate (%)	Assignment Rate (%)	Assigned Reads (M)	Pseudo-aligned (%)
C1-1	1	Control	33.1	84.89%	51.1%	19.6	80.8
C2-2	2	Control	42.6	86.10%	51.6%	26.0	81.1
C3-3	3	Control	30.2	84.93%	51.3%	17.8	81.2
C4-4	4	Control	42.7	84.46%	51.7%	25.2	80.5
LN1-5	1	LowN	55.6	85.27%	51.4%	32.8	80
LN2-6	2	LowN	35.1	84.36%	49.9%	20.0	79.5
LN3-7	3	LowN	35.8	82.71%	49.6%	20.3	78.5
LN4-8	4	LowN	88.1	93.14%	64.6%	65.0	79.3
LP1-9	1	LowP	40.9	84.31%	50.7%	23.8	79.6
LP2-10	2	LowP	56.2	87.14%	54.2%	35.3	79.3
LP3-11	3	LowP	44.4	84.85%	50.6%	25.9	80.7
LP4-12	4	LowP	43.1	85.00%	51.6%	25.4	79.9

PCA plot analysis was also performed to assess the quality and the repeatability of the data (**Figure 4.2**). Based on the PCA plot, biological replicates were found clustering into three distinct clusters. Each cluster corresponded to each of the three treatments included in the present study, suggesting good biological and sequencing repeatability. PC1 accounted for 60% of the variance and separated samples based on their N supply, whereas PC2 accounted for 26% of the variance and separated plants based on their P status. In addition, from the PCA plot, it is suggested that the N limitation effect on the transcriptome was stronger than the P limitation effect.

Based on the PCA analysis results (**Figure 4.2**) and the mapping statistics (**Table 4.1**), sample “LN4-8” performed similarly to the other biological replicates; therefore, it was finally included in the differential gene expression analysis despite the low number of reads. Analysis was also carried out without including sample “LN4-8”, and this did not substantially affect the output of the differential gene expression analysis.

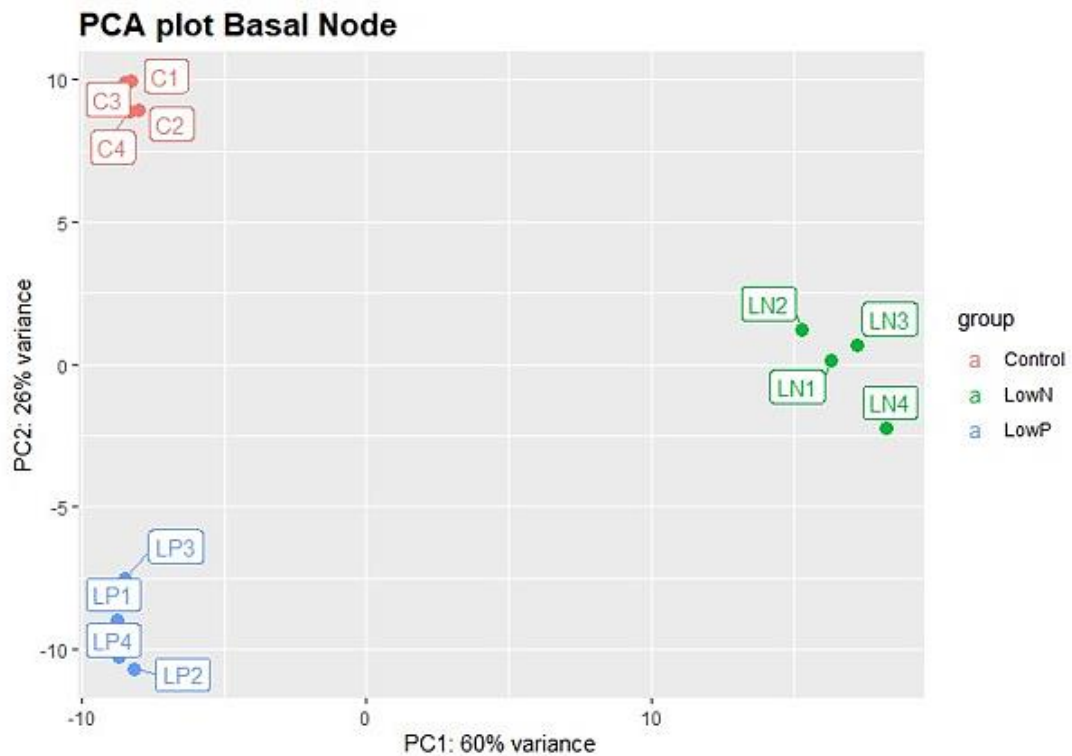


Figure 4.2: Principal component analysis based on the differential gene expression analysis results of N and P limitation effect in the basal node. PCA was based on the 500 most variable genes. Biological replicates of each treatment (n=4) form distinct clusters. PC1 and PC2 account for 60% and 26% of the total variance, respectively.

4.2.4 Transcriptional Changes in Response to N and P Limitations

Genes with p-adjusted value corrected for multiple comparisons (p_{adj}) < 0.01 and fold change difference (FC) > 1.5 ($|\log_2FC| > 0.58$) were considered as significantly differentially expressed (DE) in this experiment. Overall, the N limitation had a stronger effect than the P limitation on the gene expression in the basal node. In total, 5171 genes were found to be DE in nodes under low N compared to high N. N limitation led to the downregulation of 2591 (2335 HC and 256 LC) genes, while 2580 genes (2247 HC and 333 LC) were upregulated (**Figure 4.3A**). On the other hand, P limitation significantly altered the transcript abundance of 674 genes, among which 214 were downregulated and 460 upregulated (**Figure 4.3B**).

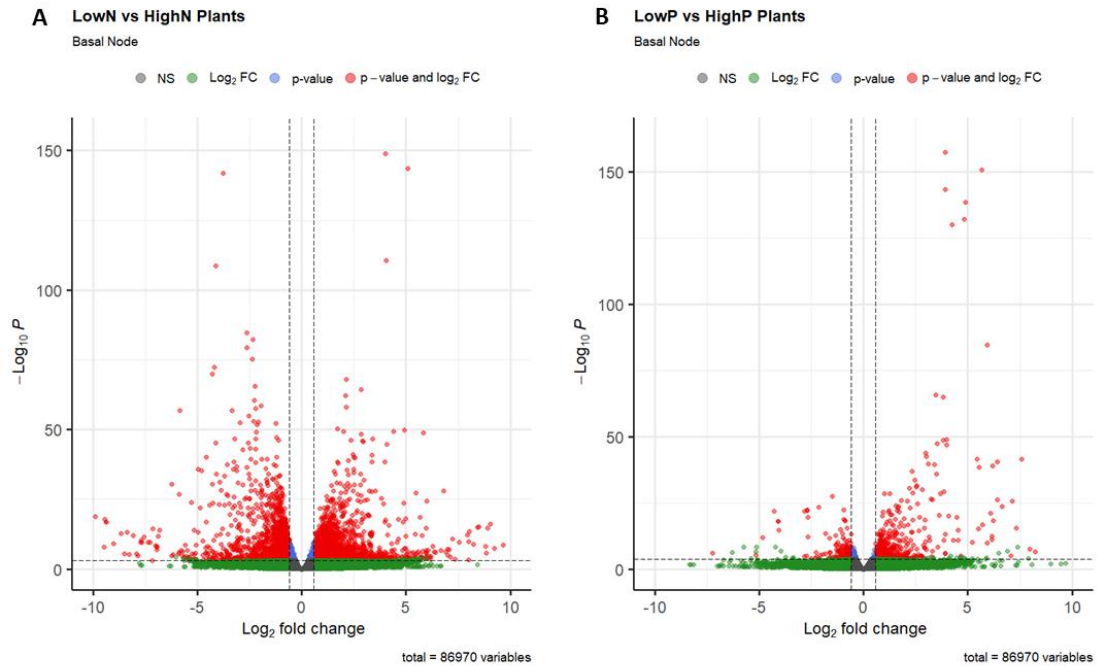


Figure 4.3: Volcano plot of the differential gene expression analysis of the effect of (A) N and (B) P limitations compared to the control. After prefiltering low expressed genes, in total, 86970 genes were included in the analysis. Each dot corresponds to a single gene. Red dots represent significantly DE genes ($p_{adj} < 0.01$ and $|FC| > 1.5$). Overall, 5171 genes were found differentially expressed by N limitation and 674 by P limitation.

4.2.5 Validation of RNA-sequencing Results

RNA-seq results were also confirmed by comparing the gene transcript abundance (TPM) with the relative gene expression value (NRQ) obtained from RT-qPCR. Three different genes were used for the RNA-seq validation, *TaD27*, *TaD17* and *TaCKX3* (TraesCS1A02G159600, TraesCS1B02G176000, TraesCS1D02G157000). For all the three genes, there was a good correlation ($R > 0.9$) between the expression values obtained from the RNA-seq and the RT-qPCR, while the effect of the treatment was also found to be consistent in both methods (**Figure 4.4**). Consequently, it is suggested that the RNA-seq data were reliable.

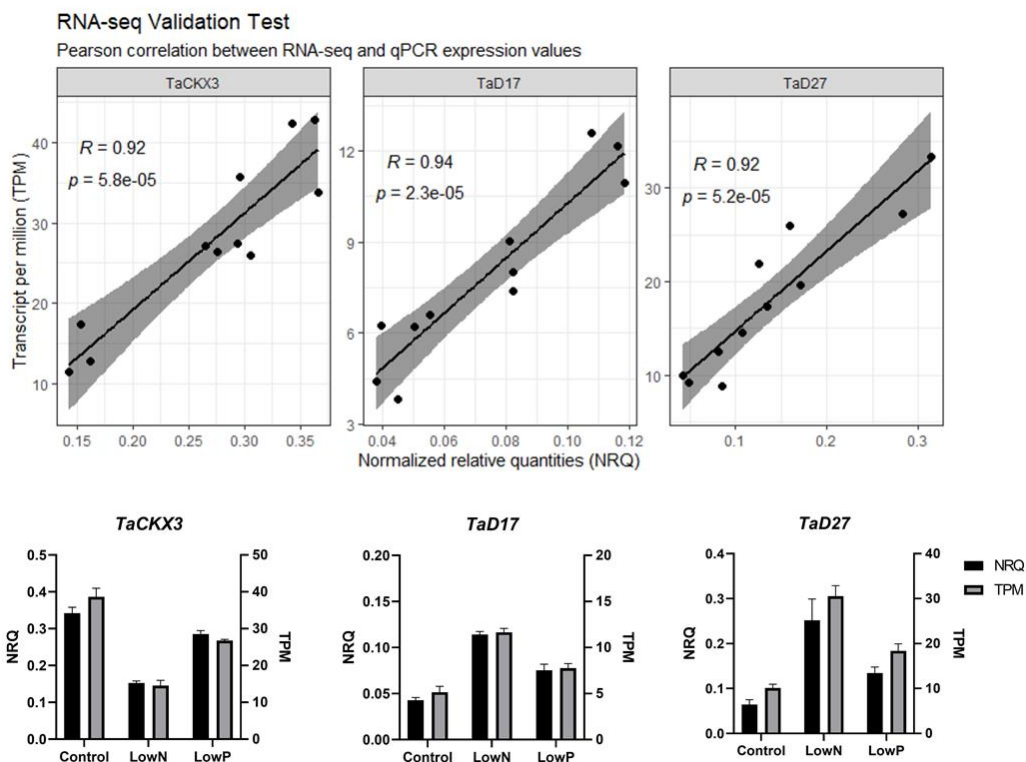


Figure 4.4: RNA-seq validation test results. Three genes were included in the validation test (*TaCKX3*, *TaD17* and *TaD27*). **(Top)** Pearson correlation analysis of TPM values obtained from the RNA-seq and NRQ expression values obtained from RT-qPCR. **(Bottom)** Comparison between average treatment effects (n=4) based on RNA-seq (TPM) and RT-qPCR data (NRQ).

4.2.6 Functional Annotation Enrichment Analysis

For the biological interpretation of the transcriptional changes by N and P limitation in the nodes, GO enrichment analysis was carried out. GO enrichment analysis was performed in GO: profiler separately for the upregulated and downregulated genes, while only HC genes were included in the calculation, as LC genes are not included in the GO wheat reference. Enriched biological process (BP) and molecular function (MF) GO terms with $padj < 0.05$ were retrieved. Subsequently, redundant GO terms were removed using the REVIGO tool.

After removing redundant terms, 51 MF and 46 BP GO terms were found enriched in the list of downregulated genes by N limitation. Genes upregulated under N limiting conditions were enriched in 25 and 21 MF and BP GO terms, respectively. Among the genes downregulated by P limitation, 12 MF and 13 BP GO terms were overrepresented. For P limitation, there were 12 and 10 MF and BP enriched terms,

respectively, in the list of the upregulated genes. The top 10 enriched terms for the upregulated and downregulated BP and MF GO terms are shown in **Figure 4.5** for the N limitation and in **Figure 4.6** for the P limitation.

According to GO enrichment analysis, N limitation downregulated genes enriched for housekeeping functions such as translation (GO:0006412), structural constituent of ribosome (GO:0003735), RNA binding (GO:0003723) and processes related to central metabolism and energy production such as carboxylic acid metabolic process (GO:0019752), carbohydrate catabolic process (GO:0016052), tricarboxylic acid (TCA) cycle (GO:0006099) and generation of precursor metabolites and energy (GO:0006091). Moreover, BP GO term vegetative meristem growth (GO:0010448) was among the enriched terms in the downregulated DE genes. On the other hand, the upregulated genes by N limitation were enriched for terms such as plant cell wall biogenesis (GO:0009834) and terms related to plant responses to biotic stress such as immune system response (GO:0002376), systemic acquired resistance (GO:0009627). In addition, carbohydrate transporters (GO:0008643) and transporter activity (GO:0005215) were among the top GO enriched terms in the upregulated genes indicating changes in resource allocation under N-limiting conditions. Ureide catabolism (GO:0010136) and allantoinase activity (GO:0004038) were also enriched in N-limited nodes. Ureide catabolism is part of the N recycling in plants. The second and third top GO enriched terms for the upregulated genes in response to N limitation were the sesquiterpenoid biosynthetic process (GO:0016106) and strigolactone biosynthetic process (GO:1901336), pointing out that N limitation strongly affected SL biosynthesis. Shoot system development (GO:0048367) was also found to be enriched in the upregulated genes. Finally, the top MF GO term was DNA binding TF activity (GO:0003700), indicating strong changes in the expression of transcription factors (TFs) involved in the modulation of N-response.

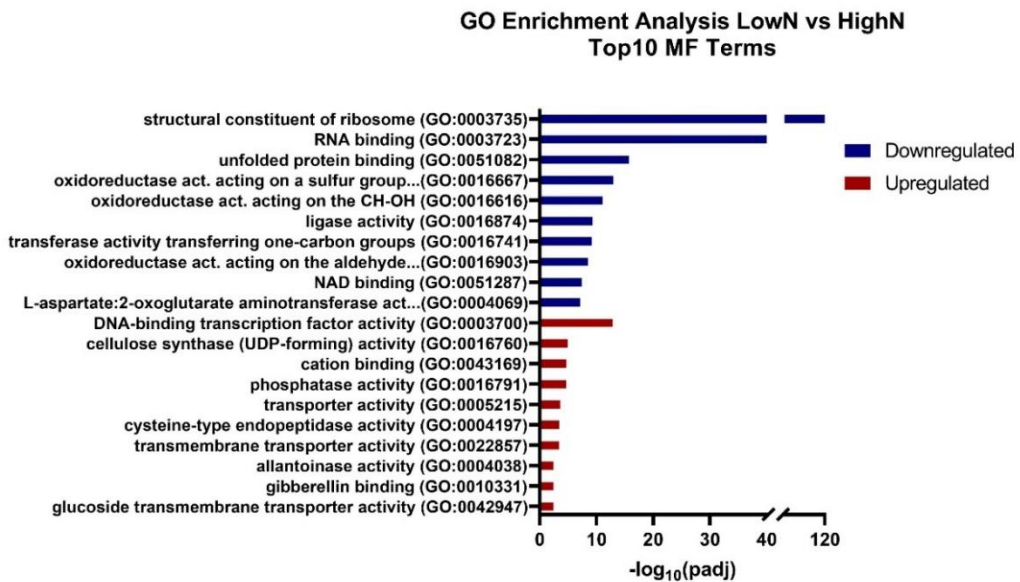
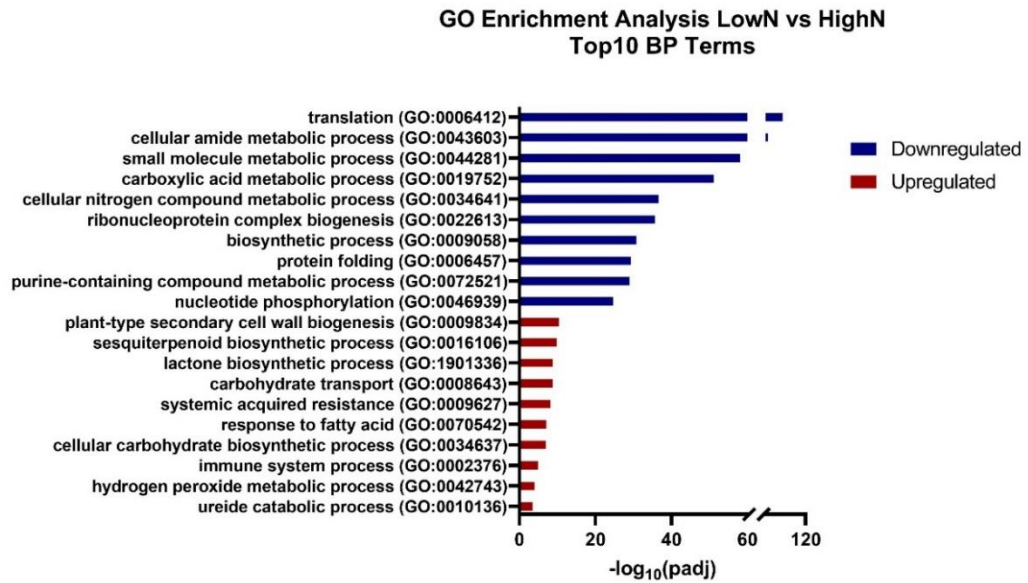


Figure 4.5: GO term enrichment analysis of the differentially expressed genes in the basal node of wheat grown under N limitation for 8 days. (Top) Top 10 enriched GO terms in Biological Process (BP) and (Bottom) Molecular Function (MF) in the upregulated (red) and downregulated (blue) DE genes.

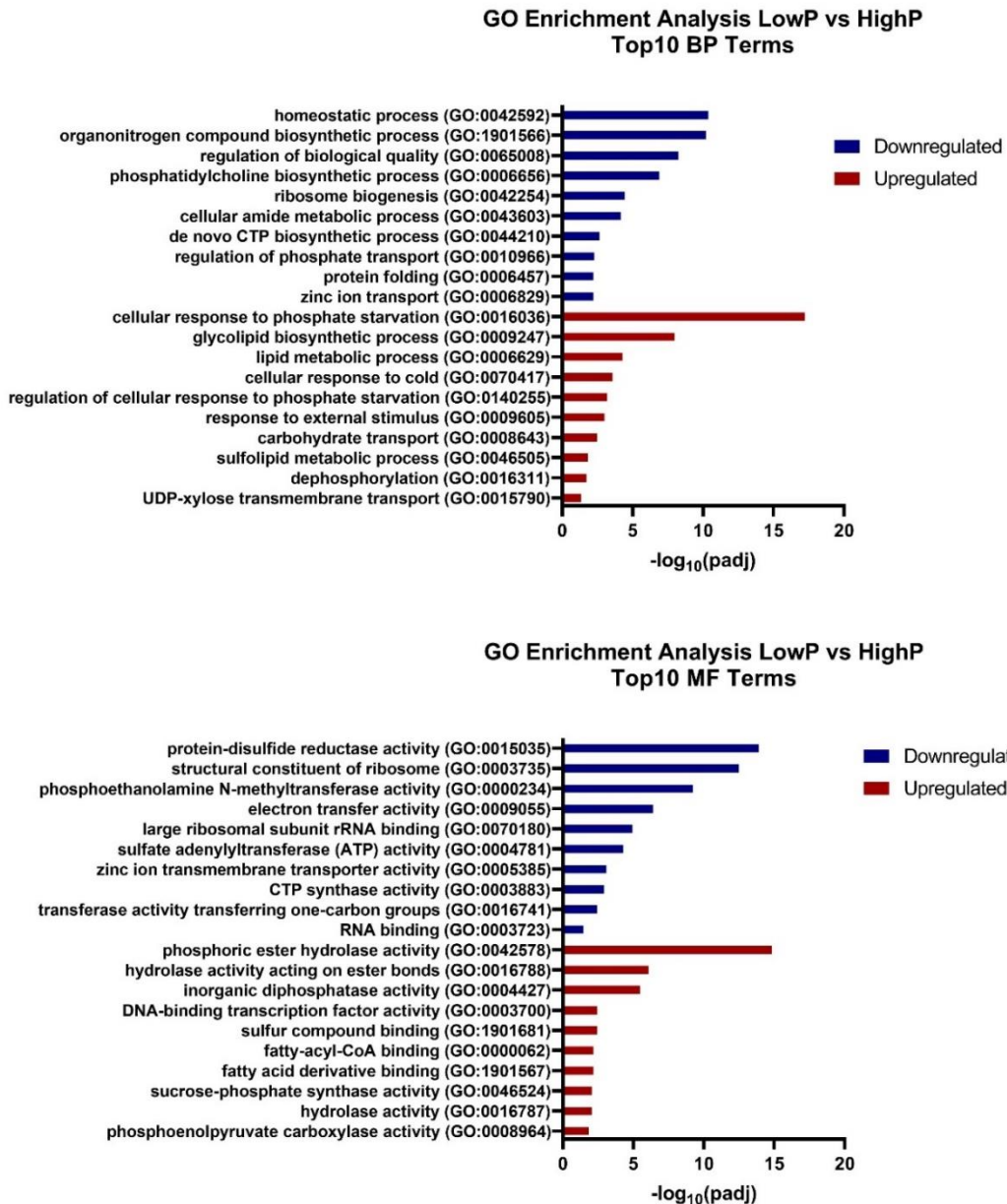


Figure 4.6: GO term enrichment analysis of the differentially expressed genes in the basal node of wheat grown under P limitation for 8 days. (Top) Top 10 enriched GO terms in Biological Process (BP) and (Bottom) Molecular Function (MF) in the upregulated (red) and downregulated (blue) DE genes.

On the other hand, terms related to response to P starvation (GO:0016036), inorganic diphosphate activity (GO:0004427) and dephosphorylation (GO:0016311) were found to be enriched in the list of upregulated genes due to P limitation. In addition, the GO terms lipid metabolic process (GO:0006629) and sulfolipid metabolic process (GO:0046505) were also enriched, indicating induction of cell phosphate recycling mechanisms by retrieving P from phospholipids of the cell membrane (Kobayashi et

al., 2006, Nakamura, 2013). This observation confirmed that P starvation responses had been initiated in low P plants, although the observed response on tillering was not so strong. Carbohydrate transport (GO:0008643) and DNA binding transcription factor activity (GO:0003700) were also found enriched in the upregulated genes under P limitation, but the number of genes contributing to these terms was much lower compared to the low N conditions. Downregulated genes by P limitation were enriched for terms related to phosphate (GO:0010966) and zinc transport (GO:0006829). Finally, protein synthesis and ribosome-related terms (GO:0042254) were also enriched among the upregulated genes by P limitation but to a lesser extent compared to the effect of N limitation on the respective terms.

To further examine which metabolic pathways were mainly affected by N and P limitation, KEGG enrichment analysis was conducted using a custom wheat KEGG reference containing more than 46000 wheat genes annotated to KEGG pathways and BRITE hierarchies. Similarly to GO enrichment analysis, KEGG enrichment analysis was performed separately for downregulated and upregulated genes. The top five enriched terms for each nutrient limitation effect can be found in **Figure 4.7**. For N limitation, 13 and 49 terms were enriched in the upregulated and downregulated genes, respectively. Among the DE by P limitation, nine and 10 pathways were overrepresented in the list of upregulated and downregulated genes, respectively.

Downregulated genes under N limitation were enriched in terms related to translation and central metabolism, consistent with the results from GO enrichment analysis. On the other hand, “transcription factors” was the top KEGG term, while “plant hormone signal transduction” and “carotenoid biosynthesis” were enriched in the list of upregulated genes under N limitation. Finally, upregulated genes were also enriched in the term “transporters”, suggesting that N limitation has a substantial impact on resource allocation. “Translation” and “ribosome” were found to be overrepresented in the list of downregulated genes by P limitation, as also shown under N limiting conditions. Moreover, distinct terms were found enriched among the upregulated genes by P limitation that are mainly related to glycerolipid metabolism. As also mentioned above, dephosphorylation of lipids and replacement of P with S has been

previously reported under P limitation as a way of recycling cell P pools (Nakamura, 2013).

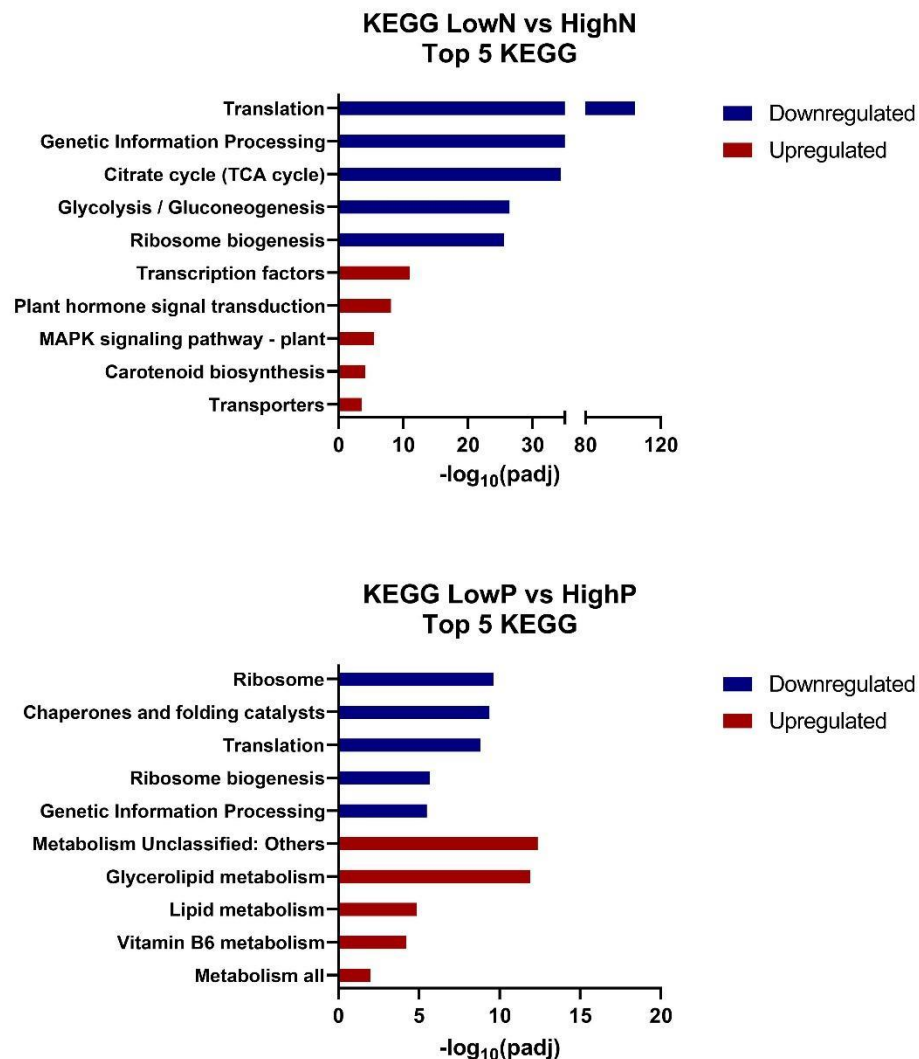


Figure 4.7: KEGG pathway enrichment analysis of the differentially expressed genes (Top) by N limitation and (Bottom) by P limitation in the basal node of wheat grown under the respective nutrient limitation for 8 days. Top five enriched KEGG terms in the upregulated (red) and downregulated (blue) genes.

4.2.7 N Limitation Effect on Genes involved in Dormancy

DORMANCY-ASSOCIATED PROTEIN-LIKE 1 (DRM1) encoding protein has been associated with bud dormancy in many plant species (Finlayson et al., 2010, Kebrom et al., 2012). The exact function of DRMs remains not well understood, but high expression of *DRM1* has been recorded in dormant buds, while its expression is decreased soon after bud outgrowth. As a result, *DRM1* is considered a conserved

molecular marker of bud activity in several plants (Tarancón et al., 2017). Rice presents four *DRM* genes (*DRM1-4*). Based on orthology search, wheat has three homoeologues orthologous to each of the *OsDRM* genes (in total nine genes), apart from *OsDRM2*, for which no wheat orthologues were found. *DRM2* in rice has been found to have very weak expression compared to the rest of the *DRMs* (Luo et al., 2019). In the basal node, *TaDRM4* homoeologues showed the strongest expression (higher TPM) compared to *TaDRM1* and *TaDRM3*. Under N-limiting conditions, the expression of all wheat *DRM* genes was found to be significantly induced in basal nodes (**Appendix D**). This observation was consistent with the observed phenotype and the function of the genes as dormancy markers.

In addition, as suggested by GO enrichment analysis, many genes involved in translation and genes encoding ribosomal proteins were strongly suppressed under low N conditions in the basal nodes. This finding indicates strong suppression of protein synthesis in response to N limitation. Transcriptomic studies in other species, like sorghum and Arabidopsis, have also linked bud dormancy with the suppression of translation-related genes (Kebrom and Mullet, 2016, González-Grandío et al., 2017). Similarly, ribosomal genes are strongly downregulated in dormant buds of rice (Luo et al., 2019).

Apart from a strong downregulation in ribosomal genes, other genes which are required for growth and proliferation were found to be significantly suppressed by N limitation, such as genes involved in DNA replication and cell cycle progression (**Appendix D**). In fact, genes encoding proliferating cell nuclear antigen, essential for DNA replication, were suppressed by N limitation in the basal nodes. Similarly, the wheat orthologues of rice *FLATTENED SHOOT MERISTEM*, which plays an important role in regulating cell cycle progression and vegetative meristem growth, were downregulated by N limitation. Many genes encoding histones (H2A, H2B, H3) and cyclins were also suppressed by N limitation in basal nodes. These results suggested that N limitation strongly suppressed processes related to cell proliferation and DNA replication. Bud outgrowth is a process that requires actively proliferating cells; therefore, suppression of those processes by N limitation contributed to growth suppression. Luo et al. (2017) demonstrated that in actively grown buds after N supply,

the expression of genes involved cell proliferation and DNA replication are induced in buds leading to bud outgrowth (Luo et al., 2017).

4.2.8 N Limitation Effect on Genes involved in N Metabolism and Transport

A large number of genes affected by N limitation in basal nodes were genes involved in N transport, assimilation and recycling. In total, 34 genes encoding nitrate transporters were found to be significantly DE (**Appendix D**). Among them, there was only one high-affinity nitrate transporter, *TaNRT2.16-2D*, which was found to be significantly downregulated by N limitation. In addition, 25 genes encoding NPF transporters were upregulated in nodes by N limitation, whereas eight *NPFs* were strongly downregulated. Apart from nitrate transporters, the transcript abundance of *TaAMT1.2* homoeologues increased in low N plants.

Furthermore, the expression of many genes involved in nitrate assimilation was suppressed under N limitation (**Appendix D**). Those affected genes included *TaNiR1*, *TaNiR2* and *TaNiR* involved in nitrate reduction to ammonium. In fact, *TaNiR* homoeologues showed a 34-fold downregulation, while the expression of *TaNiR2* encoding genes was found 8-fold lower. Strong downregulation was also observed for homoeologous genes encoding GS enzyme (*TaGSr*), which were 4-fold downregulated. Downregulation was also observed in one of the wheat genes encoding NADPH-dependent glutamate synthase (TraesCS3A02G266300) and Fd-GOGAT glutamate synthase (TraesCS2D02G132900). Among the N assimilation genes, only *TaGS1* homoeologues were found to be upregulated by N limitation. It is known that cytosolic GS, apart from the role in N assimilation, also plays an essential role in N recycling and remobilisation (Bernard and Habash, 2009). Previous studies have also reported upregulation of some cytosolic *GS* gene members under N limiting conditions, while others are downregulated (Bernard and Habash, 2009). The significant upregulation of *TaGS1* homoeologues in nodes under N limitation suggests that the encoded GS isoform might be involved in nitrogen remobilization.

Apart from genes involved in primary N metabolism, RNA-seq analysis revealed that N limitation had a strong impact on N recycling by stimulating ureide catabolism. Ureides comprise one of the primary forms of N transported within the plant from source to

sink tissues, along with amino acids (Tegeger and Masclaux-Daubresse, 2018). The main form of ureides found in plants is allantoin. Accumulation of allantoin has been reported under stress conditions suggesting that allantoin might be a regulator of the stress response (Kaur et al., 2021). In addition, under N stress, allantoin degradation contributes to N recycling and reassimilation into amino acids in sink tissue to support critical physiological processes and growth (Lee et al., 2018). Three homoeologues encoding ureide permease (UPS) were induced in basal nodes under N limitation, whereas four orthologous genes of rice *UPS1* were downregulated. *OsUPS1* has been shown to play an important role in rice plant adaptation to N-limiting conditions by affecting ureides partitioning within the plants (Redillas et al., 2019). Consistent with observations in the present study, the expression of *OsUPS1* was downregulated in shoots on rice plants under low N conditions (Lee et al., 2018). N limitation also led to strong induction of genes encoding enzymes involved in allantoin catabolism, allantoinase, and allantoate deiminase. Those changes indicated that under low N conditions, ureide catabolism and utilization as an N source for N reassimilation into amino acids were induced in wheat basal nodes, while ureide catabolism played a less important role under N-sufficient conditions.

4.2.9 N Limitation Effect on Amino Acid Transporters

Amino acid is the predominant form of reduced N transported within the plants (Tegeger and Masclaux-Daubresse, 2018). Under stress conditions, amino acid transport plays an important role in N partitioning and redistribution. Amino acid transport is facilitated by amino acid transporters (AATs). The major subfamily of AATs is the amino acid permease (AAP) family. Wheat amino acid transporters have been shown to play an essential role in N remobilisation during senescence and also during stress conditions. In total, 34 genes annotated as AATs were significantly affected in the basal nodes by N limitation (**Appendix D**). Among the AAP members, six members were downregulated (orthologous genes of *OsAAP7* and *OsAAP5*). On the contrary, orthologues of rice *AAP6* and *AAP8* were significantly upregulated. The expression of *OsAAP6* orthologues was very low (TPM < 0.2), while their expression rose under N limitation, indicating that they are involved in amino acid remobilisation under N limiting conditions. Similarly, all the three homologues of wheat *TaAAP13* were

significantly upregulated in nodes by N limitation. Recently Wan et al. (2021) demonstrated expression of *AAP13* is involved in sink strength for nitrogen transport in wheat (Wan et al., 2021). In addition, N had a negative effect on the mRNA accumulation of genes encoding amino acid transporter-like (ATL) proteins. In addition, eight wheat genes encoding glutamine dumper transporters showed 8-fold downregulation in response to N limitation. GDU transporters have been found to be involved in amino acid export in Arabidopsis cells (Yu et al., 2015). Moreover, five members of proline transporters were strongly upregulated under N-limiting conditions. The effect of N limitation on amino acids transporters locally in the nodes indicated strong changes in N redistribution under N-limiting conditions and diversion of amino acids to growing tissue.

4.2.10 N Limitation Effect on Genes involved in Central Metabolism

As identified by the functional annotation enrichment analysis, several pathways and biological processes related to central metabolism and energy production were overrepresented in the list of DE genes. Further examination showed that N limitation suppressed the expression of several genes involved in glycolysis, TCA cycle and others. More specifically, genes encoding 6-phosphofruktokinase, fructose-bisphosphate aldolase, glyceraldehyde-3-phosphate dehydrogenase, phosphoglycerate kinase and downstream genes of the glycolytic pathway were strongly downregulated. Those enzymes are essential for the maintenance of glycolysis and carbon (C) metabolism. Similar strong downregulation in the basal nodes of N-limited plants was observed in genes encoding enzymes of the TCA cycle such as pyruvate dehydrogenase, malate dehydrogenase, citrate synthase, 2-oxoglutarate dehydrogenase and many others. For the majority of the above-mentioned genes, the negative effect of N limitation on transcript abundance was consistent in all the three homoeologues, indicating a consistent and robust effect of N supply in energy production through glucose utilisation. Tiller bud outgrowth is an energy-consuming process; therefore, the N limitation effect on processes like glycolysis and the TCA cycle could lead to low sugar utilisation in basal nodes, which in turn leads to growth arrest.

4.2.11 N Limitation Effect on Genes involved in Sugar Transport and Signalling

Apart from the observed changes in glucose utilisation, many genes involved in sucrose transport and metabolism were among the DE genes indicating that N limitation did not only affect changes in carbon use but also in the assimilate partitioning (**Appendix D**). Cell wall invertases (cwINV) catalyse the breakdown of sucrose into Glc and Fru in the apoplast; therefore, their function is required for sucrose unloading and partitioning. Many genes annotated as cwINVs and orthologues to *OsCIN1*, *OsCIN2* and *OsCIN7* were found to be significantly downregulated by N limitation in the basal nodes. A similar response was also recorded for the three homoeologues encoding cytosolic INV. Invertase activity is associated with the C sink strength of the tissue since it reflects the ability of the tissue to absorb and utilise sucrose. In sorghum, bud outgrowth is accompanied by upregulation of *cwINVs*, increasing the sugar sink strength of the developing bud (Kebrom and Mullet, 2016). Downregulation was also recorded for three genes encoding proteins with putative fructokinase activity (FPK). According to recent studies, FPKs are also related to the sink strength of the tissue along with sucrose synthetase (SUC) (Stein and Granot, 2018). Wheat orthologues of *OsSUC2* and genes encoding sucrose-phosphate synthase (SPS) were also strongly downregulated in low N nodes. Those changes might reflect the strong impact of N limitation in sugar partitioning to basal nodes and subsequently to developing buds.

In addition to the downregulation of genes involved in sucrose metabolism, the KEGG term “sucrose metabolism” was also enriched in the genes induced by N limitation. Additional examination showed that the majority of those genes encode proteins with hydrolase activity such as cellulase, glycoside hydrolase, and beta-glucosidase activity, suggesting that N deprivation induces break down of polysaccharides and cell wall components to simple sugars to be utilised *in situ* or to be loaded into the phloem and transported in other tissue.

Sugars will eventually be exported transporters (SWEETs) across the plasma membrane. Many orthologous genes of SWEET transporters (23) from other species were found to be differentially expressed by N limitation. In fact, 17 wheat orthologues of *AtSWEET11*, *12*, *13* and *14* were induced by N limitation. On the contrary,

orthologous genes of *AtSWEET6*, *7* and *AtSWEET10*, *15* showed the opposite response (downregulation). The induction of several *SWEET* genes has been previously reported in dormant buds. In *Arabidopsis* and other plant species, *SWEET11*, *12* are induced in dormant buds (Tarancón et al., 2017). *SWEET11*, *12* are involved in phloem loading of sucrose for long-distance transport within the plants (Chen et al., 2012). Higher expression in the nodes of N-limited plants might reflect strong loading of sucrose into phloem and remobilisation into other tissue, like roots, rather than the use of sugars locally in nodes for secondary shoot formation. Similar downregulation was also observed in genes encoding sucrose transporter 1 (*SUT1*), which also facilitates sugar transport across the plasma membrane.

Tre6P is considered an important signalling molecule that coordinates plant growth and development based on the available C resources (Fichtner and Lunn, 2021). More specifically, Tre6P has been found to be positively correlated with sucrose levels. Therefore, it has been suggested that it acts as a signal of sucrose levels and regulates the metabolic status of the tissue (Fichtner and Lunn, 2021). In sink organs such as lateral (tiller) buds, the levels of Tre6P act as a signal affecting developmental decisions, such as the bud outgrowth acting as a signal of the plant capacity to provide the developing tissue with the required sugars. Consistent with that, reduction in Tre6P levels leads to growth suppression. According to the RNA-seq data, N limitation affected the expression of some genes of Tre6P metabolism. All three homoeologues of *TaTPP4*, encoding trehalose-6-phosphate phosphatase (TPP), were found to be significantly upregulated more than 2-fold in the basal nodes of low N plants. The same response was found for *TaTPP8-7D*. On the other hand, N limitation decreased mRNA abundance of *TaTPP1* homoeologues. Opposite regulation of TPP family members in dormant buds has been previously reported in sorghum (Kebrom and Mullet, 2016). Consistent with the observations in this thesis, the orthologues of *TaTPP4* and *TaTPP8* have been found to be upregulated in sorghum dormant buds, while the opposite was true for the orthologues of *TaTPP1*. Moreover, members of the trehalose-6-phosphate synthase family (TPS) were included on the list of the significantly DE genes. Therefore, it is suggested that N limitation affected Tre6P homeostasis, which might be responsible for the observed changes in metabolic reprogramming (C utilization and

sugar transport), leading to growth arrest. Another essential component of the energy signalling pathway is SnRK1. SnRK1 controls the expression of thousands of genes and the function of many enzymes by post-translation modifications (Sakr et al., 2018). SnRK1 suppresses resource partitioning for growth leading to growth arrest. The expression of two wheat genes encoding SnRK1A protein kinase was significantly induced in basal nodes of wheat plants grown under N limitation. Therefore, it is suggested that N status influenced the C signalling mechanisms to control C partitioning and growth.

4.2.12 N Limitation Effect on Transcription Factors

Both GO and KEGG enrichment analyses showed that N limitation had a strong effect on genes which encode proteins with transcription factor activity. TFs are an important component of plant responses since they regulate the expression of several downstream genes to coordinate metabolic and development responses. Therefore, to identify the TFs affected by N limitation in wheat basal nodes, DE transcription factors were identified and classified into different TF families. Initially, wheat TF reference was obtained from Ramirez et al. (2018), which has also been used and utilised more recently by Borrill et al. (2019). This reference contained 4956 genes annotated as TFs and classified into 58 different families (Ramírez-González et al., 2018, Borrill et al., 2019). The list of genes was based on the RefSeq1.0 wheat annotation, so the gene IDs were converted to the RefSeq1.1. Six genes were not present in RefSeq1.1 gene annotation, so they were removed from the list. To identify additional TFs and transcriptional regulators not included in the original list, genes annotated with the GO term “DNA-binding transcription factor activity” (GO:0003700) were retrieved from Biomart. Additionally, 615 genes annotated as TFs were found in RefSeq1.1 wheat annotation with a putative TF activity. Subsequently, the tools iTAK (Zheng et al., 2016), PlantTFDB (Jin et al., 2016) and PlantTFcat (Dai et al., 2013) were used to classify the TFs into different families and to confirm their TF activity. Among the 615 protein sequences, 533 were predicted to be putative TFs or transcriptional regulators based on the results from the above-mentioned tool. After combining both lists, a new wheat TF reference was compiled, including 5483 genes classified into 67 TF families.

After creating the new wheat TF reference, the TFs affected by N limitation were further examined to understand how N limitation coordinated transcriptional changes in nodes. In total, 3063 TFs were found to be expressed in nodes (TPM > 0.5) in at least one of the treatments included in the RNA-seq experiment. N limitation significantly affected the expression of 258 TFs (8.4%) in basal nodes. The majority of the DE TFs, 196 (76%), were upregulated by N limitation, whereas only 62 were found to be suppressed by N limitation. Subsequently, the percentages of the differentially expressed TFs per TF family were calculated and presented in **Figure 4.8**. Thirty-seven TF families were found to have at least one member that was affected by N limitation in the basal nodes. Some TF families like NF-YA, GARP-ARR-B, EIL, C2C2-CO-like, CAMTE and others were exclusively upregulated, while TF families such as whirly, SWI-SNF had only members that were downregulated by N limitation. However, some families, namely bZIP, GARP-G2-like, and others, had members that showed either upregulation or downregulation in response to N limitation (**Figure 4.9**).

**Distribution of Differentially Expressed TF across TF families
in response to N limitation**

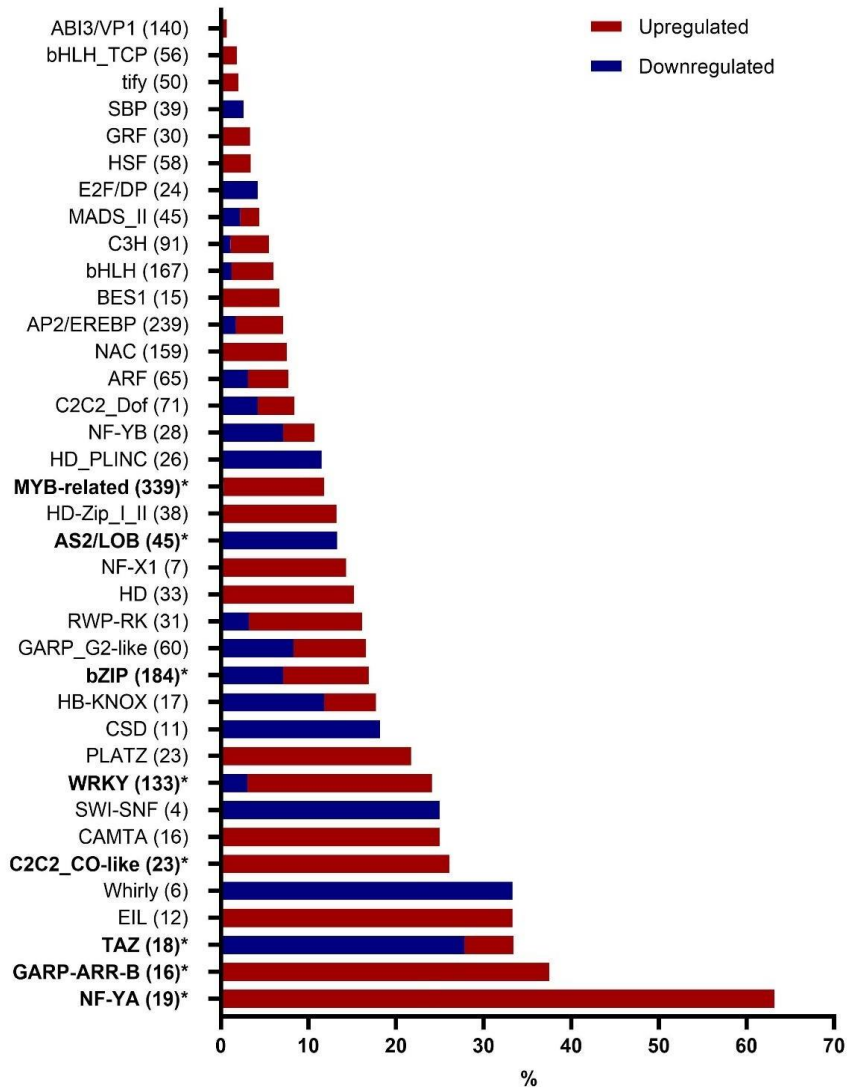


Figure 4.8: Percentage of expressed TFs that were significantly DE in N-deficient basal nodes per TF family. The number of TF expressed (TPM > 0.5) per family is in brackets. Only families with more than two significantly DE members are included. Significantly enriched families are indicated with asterisks.

Among the TF families affected by N limitation, NF-YA showed the most changes proportionally compared to other families. More than 60% of the NF-YA family members expressed in nodes were found to be significantly induced under N-limiting conditions. NF-YA are part of the Nuclear Factor Y (NF-Y) complex, which binds to the CCAAT box in the promoter regions of genes controlling their expression. NF-YAs have been found to be induced by nutrient stress, and their role has been mainly associated with prolonged exposure to stress conditions. NF-YAs suppress genes involved in cell

elongation and C partitioning leading to the suppression of plant growth (Leyva-González et al., 2012). NF-YA encoding genes are induced by N starvation in both above- and below-ground tissues (Zhao et al., 2011). Recent studies in Arabidopsis showed that some members of the NF-YA family, such as *AtNF-YA5*, are essential components of the transcriptional network responding to N status (Gaudinier et al., 2018). Moreover, in Arabidopsis, *NF-YA8* was also found to be affected by sugar levels indicating NF-YAs might also integrate sugar signals (Zhao et al., 2020). Therefore, the observed upregulation of NF-YAs under N limitation in basal nodes might contribute to tiller suppression by repressing genes involved in C utilization for growth.

GARP-ARR-B was the second TF family with the highest proportion of DE members. In total, 16 type-B RRs were found to be expressed in nodes, among which six were found to be significantly upregulated (**Figure 4.9**). Type-B RRs are known to be involved in the CK signalling pathway, being responsible for the transcriptional response to CKs. Arabidopsis loss-of-function mutants of different type-B ARRs are insensitive to CK signals and show an abnormal growth (Argyros et al., 2008, Ishida et al., 2008). The strong effect of N limitation on the expression of type-B RRs indicates the involvement of CK signalling in the N limitation response in nodes.

The C2C2_CO-like family was also found to be enriched in the list of the genes upregulated by N limitation. In total, six members of the CO gene family were found to be upregulated. Two wheat orthologues of *AtBBX16* were significantly induced by N limitation. *AtBBX16* was part of the TF network of N response (Gaudinier et al., 2018). In addition, *AtBBX7* orthologues were among the genes induced by N limitation in nodes.

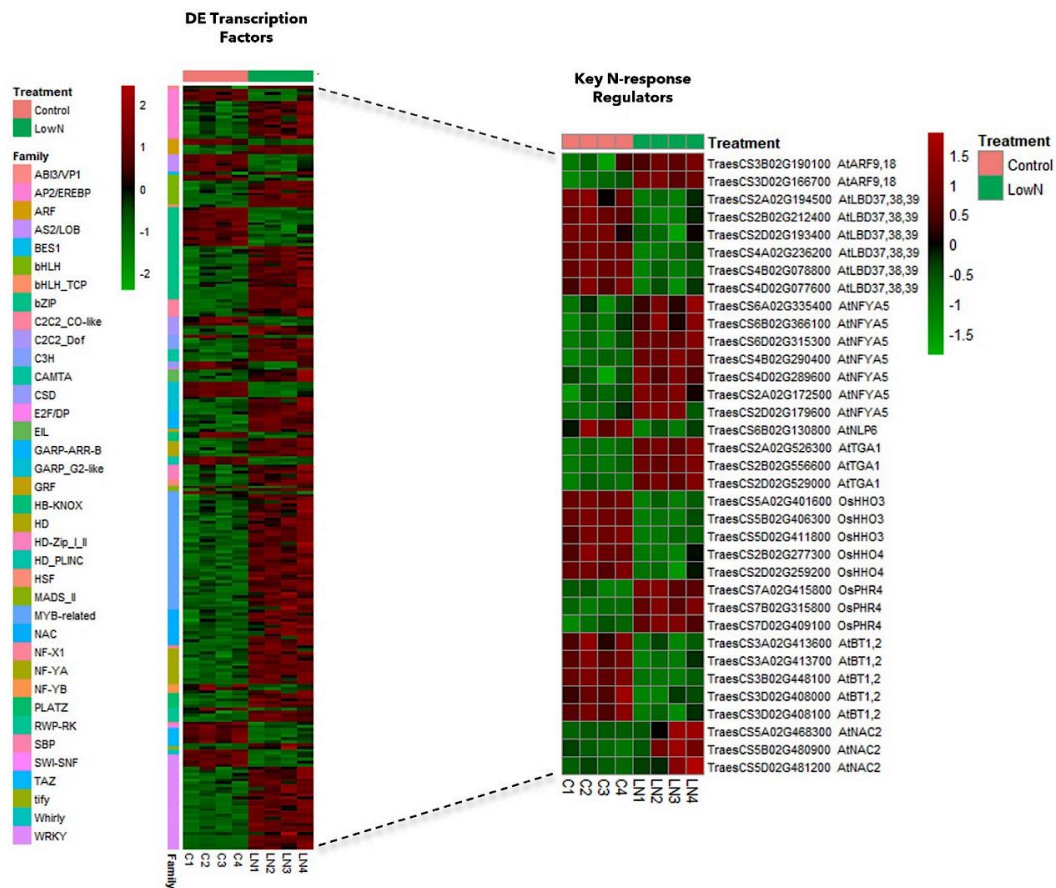


Figure 4.9: Heatmap of differentially expressed transcription factors in the basal node of wheat grown under N limitation for 8 days based on the RNA-seq data. (Left) Heatmap of 258 DE TFs by N limitation. **(Right)** Expression patterns of DE TFs which been identified as key N-response regulators based on previous studies. Each row corresponds to a different gene, while columns correspond to different samples grouped by treatment. Row annotation corresponds to the TF family. Data are Z-scores of regularised log normalised counts (rlog) as generated by DESeq2. Red colour corresponds to higher transcript levels while green to lower. Row names consist of the GeneID and the name of *A. thaliana* or *O. sativa* orthologue.

In nodes, the MYB-related family was the most commonly expressed TF family, with a total of 339 members to be expressed in the basal node. N limitation induced the expression of many MYB family members (39), indicating that MYB transcription factors are an important part of the N response in wheat. MYB family is one of the most widespread families of TFs in plants. Several studies have demonstrated that MYBs are necessary for plant responses to abiotic stress such as drought, salinity, and others, while their functions have been associated with changes in secondary metabolism (Wang et al., 2021). In durum wheat, MYB genes were strongly differentially expressed by N limitation in roots and leaves (Curci et al., 2017). A strong effect of N limitation on MYB TFs has been reported in wheat seedlings growing under

N-limiting conditions (Wang et al., 2019a). Moreover, three orthologues of *OsPHR4* showed a more than 2-fold increase in response to N limitation (**Figure 4.9**). *OsPHR4* in rice is induced by P starvation and governs transcriptional changes of P limitation response along with other PHRs (Ruan et al., 2017). Consistent with the results presented in this thesis, other studies have also shown that *PHRs* are induced under N limitation; thus, PHRs are considered to take part in coordinating N and P homeostasis under nutrient stress (Sun et al., 2018).

Furthermore, N-limiting conditions led to changes in the expression of WRKY TFs. WRKY is one of the most prominent families of TFs in plants. WRKYs have a diverse role in plant response to biotic and abiotic stress, while they interact with many hormonal pathways (Jiang et al., 2017). Plant exposure to stress conditions leads to the induction of many WRKY members. Consistent with that, 28 WRKYs were induced in nodes under N limitation. Wang et al. (2019) reported that N starvation response includes upregulation of many members of WRKY family members in roots. On the contrary, four WRKY TFs were suppressed in N-limited nodes.

Certain TF families were downregulated by N limitation. In fact, the TAZ family of TFs was significantly enriched in the list of downregulated genes. N limitation suppressed the mRNA levels of five members of the TZ family, which accounted for 28% of the expressed TAZ TFs in nodes. The affected genes were orthologues of *AtBT1*, 2 and showed, on average, a 4-fold downregulation in response to N limitation (**Figure 4.9**). BTs are NO_3^- inducible genes controlled directly by the NLP master regulator, suggesting that transcriptional regulation of BTs is a crucial step of the plant nitrate response (Sato et al., 2017). BTP acts as a negative regulator of NO_3^- uptake under sufficient conditions. Moreover, *BT2* expression has been linked to nitrogen use efficiency (NUE) in rice since mutation in *OsBT2* improved NUE (Araus et al., 2016). In addition, in the same study, it was shown that manipulation of *BT* genes also affected tiller number during vegetative stages in rice.

AS2/LOB was another TF family which was found to be enriched in the list of downregulated genes. Further examination revealed that six members of this family were strongly downregulated by N limitation, and they were divided into two homoeologous groups. All the genes were orthologues of Arabidopsis *LATERAL*

ORGAN BOUNDARIES (LBD) 37, 38, 39. AtLBD37, 38, 39 have been identified in many studies as regulators of N response. In rice, a recent coexpression network analysis revealed that OsLBD38 connects major N deficiency modules, playing a pivotal role in maintaining N deficiency response (Ueda et al., 2020). TraesCS4A02G236200, TraesCS4B02G078800, and TraesCS4D02G077600 showed more than 16-fold downregulation, while the transcript abundance of TraesCS2A02G194500, TraesCS2B02G212400, TraesCS2D02G193400 were on average 4-fold lower in the nodes of N-limited plants compared to plant provided with high levels of N (**Figure 4.9**). LBD37, 38, 39 act as a transcriptional repressor of many genes involved in N response, including nitrate transporters and N assimilation enzymes (Rubin et al., 2009). *LBO37, 38, 39* expression is induced by N supply leading to suppression of N limitation response. Rubin et al. (2019) also demonstrated another role of LBOs in growth since manipulation of *LBD37, 38, 39* expression strongly affects N-dependent lateral branching in Arabidopsis.

The bZIP family was significantly enriched in the list of downregulated genes. However, many members of this family were found to be significantly upregulated in N-limited nodes, highlighting the functional diversity of the members of this family. N limitation downregulated the expression of 13 members of bZIP TFs, whereas 18 members of this family were upregulated. Orthology search revealed that eight of the downregulated bZIP TFs encode proteins with high sequence similarity to AtbZIP53, 44 and AtbZIP42. Moreover, two orthologues of *AtbZIP10, 25* were also found to be negatively affected by N limitation. All three homoeologues of *TabZIP9* were also suppressed by N limitation. AtbZIP44, 53 belong to the group of S1-bZIP TFs whose function is linked with the energy status of the cell (Baena-González et al., 2007). S1-bZIP play an important role in transcriptional reprogramming in response to C and N limitation through being targeted by SnRK1, which is a master regulator of C utilization and partitioning. On the other hand, bZIP9, 10 and 25 belong to group C of bZIP and function along with S1-bZIP. The strong downregulation of these bZIP TFs by N limitation in basal nodes suggested that they are also involved in the coordination of C and N metabolism in wheat under N-limiting conditions. On the contrary, the majority of the upregulated bZIP TFs were annotated as involved in ABA response

(Figure 4.11). Wheat orthologues of *AtTGA1* were also induced in nodes **(Figure 4.9)**. *TGA1* has been found to be an essential component of N response in Arabidopsis roots. *TGA1* is downregulated in roots soon after N supply, while it is important for root architectural changes in response to N levels (Alvarez et al., 2014). In addition to that, three genes encoding orthologues of *AtVIP1* were also induced in nodes.

GARR_G2_like was another family which had some members that were upregulated and others that were downregulated, indicating the functional diversity of this family members. In fact, five members of this family were significantly downregulated by N limitation in the basal nodes. Those genes were orthologues of rice *HRS1 HOMOLOG 3 (OsHHO3)* and *OsHHO4*. As suggested by their name *OsHHO3* and *OsHHO4* are homologues of Arabidopsis *HRS1/NIGT1*. *NIGT1* expression is positively regulated by N supply, and it acts as a transcriptional repressor of N-deficiency response genes, such as the transporter *NRT2.1* and other genes of the N metabolism (Maeda et al., 2018). Similarly, the members of the same family, *OsHHO3* and *OsHHO4*, were identified as key regulators of the N-deficiency response in rice (Ueda et al., 2020). In N-limited nodes, wheat orthologous genes to *OsHHO3* showed a more than 10-fold decrease, whereas two orthologues of *OsHHO4* were 3-fold lower **(Figure 4.9)**. The downregulation of *NIGT1/HHO* TFs might contribute to the repression release and the induction of genes involved in N assimilation, recycling, and remobilization under N-limiting conditions (Kiba et al., 2018). On the other hand, other members of the GARP-G2-like family were upregulated by N limitation. These genes included orthologues of rice *OsPCL1*, which is involved in the photoperiodic control of flowering time.

Lastly, wheat *TaGT1* homoeologues and two other orthologous genes of *AtHB21*, *40*, *53* were induced in nodes under N-limiting conditions. Those TFs are members of the HD-ZIP family, and their expression has been associated with tiller suppression (González-Grandío et al., 2017, Whipple et al., 2011). The observed induction is consistent with the data presented in section 3.2.5.

4.2.13 N Limitation Effect on Hormone-Related Genes

Genes affected by N limitation were enriched for KEGG term “plant hormone signal transduction”, indicating a strong effect of N limitation on different hormonal pathways. Consistent with that, GO terms related to various hormones were also enriched among the upregulated and/or downregulated genes. Hormones are known to play an important role in regulating tiller bud outgrowth and in long-distance signalling under nutrient limitations. The GO term “sesquiterpenoid biosynthetic process” (GO:0016106) was among the top 10 BP enriched terms in the upregulated genes. Similarly, the carotenoid biosynthetic pathway was among the top five enriched pathways according to the KEGG enrichment analysis. Both terms include genes involved in the SL biosynthesis, indicating a strong effect of N limitation in SL metabolism locally in the basal nodes. This finding is in accordance with the results presented in Chapter 3. Among the SL-related genes affected were all the three homoeologues of *TaD27* and *TaD10* and two homoeologues of *TaD17*, supporting that there was a strong induction of the genes involved in the core SL biosynthetic pathway (**Figure 4.10**). *TaMAX1d-7B* was the only member of the MAX1 family which was found to be significantly differentially expressed. Other MAX1 genes, such as *MAX1cs*, showed an increased transcript abundance in N-limited nodes, however, the effect was not found to be significant. The RNA-seq allowed the examination of the expression of other genes not included in the expression analysis by RT-qPCR. The wheat orthologues of *OsLBO* and *AtLBO* were also among the genes upregulated in response to N limitation. *LBO* catalyses the biosynthesis of bioactive SL molecules downstream of *MAX1s*. In addition, one homoeologue of *TaD14* (*TaD14-4D*) was found to be downregulated in nodes. In addition, three genes encoding the D53 transcriptional repressor of the SL signalling pathway were found to be upregulated in N-limited nodes. mRNA accumulation of *D53* is positively correlated with the levels of SL; thus, the recorded upregulation supported that the SL signalling pathway was activated under N-limiting conditions. Therefore, the consistent effect of N limitation on the regulation of most of the genes in the SL pathway supported the idea that SLs may be part of plant N response to regulate lateral branching.

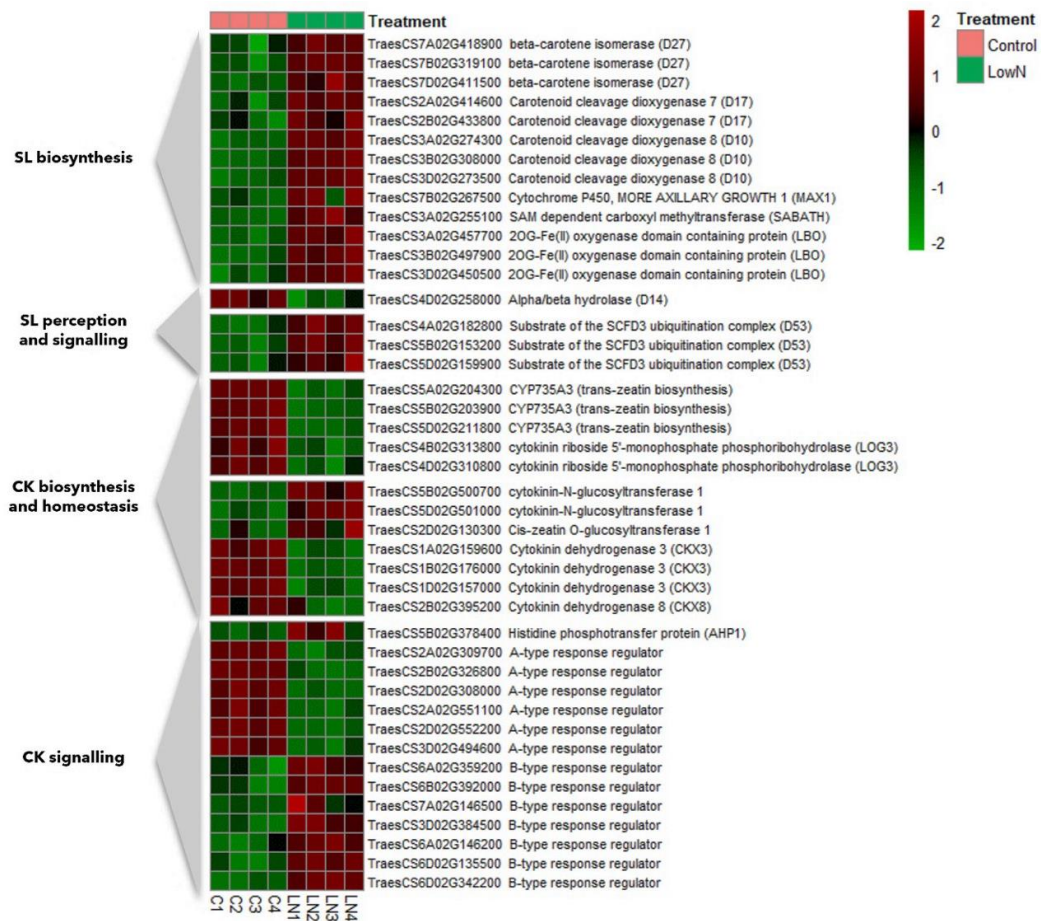


Figure 4.10: Heatmap of differentially expressed SL- and CK-related genes in the basal node of wheat grown under N limitation for 8 days based on the RNA-seq data. Each row corresponds to a different gene, while columns correspond to different samples grouped by treatment. Data are Z-scores of regularised log normalised counts (rlog) as generated by DESeq2. Red colour corresponds to higher transcript levels while green to lower. Row names consist of the GeneID and the gene annotation.

Apart from the SL pathway, other hormonal pathways were found to be affected by N limitation. It is well-known that plant N status is strongly associated with CKs, which have been suggested to play an important role in coordinating plant response to N limitation. Among the hormone-related genes found enriched in N-limited nodes, there were many genes involved in CK biosynthesis and signalling (**Figure 4.10**). N limitation led to strong downregulation of genes encoding CK biosynthetic genes in basal nodes. In fact, the expression of orthologue genes of rice *CYP735A3* involved in tZ biosynthesis was downregulated by N limitation. Wheat genes encoding LOG3 were also found to be suppressed, indicating that N limitation suppressed the expression of CK biosynthetic genes locally in nodes. Apart from CK biosynthesis, genes involved in CK homeostasis were differentially expressed. In fact, cytokinin-N-glucosyltransferase

one homoeologues involved in CK deactivation were induced by N limitation. On the other hand, wheat orthologues of *OsCKX3* were downregulated in nodes. A strong down-regulation of type-A RRs was also found locally in N-limited nodes. Type-A RRs are CK-inducible genes and are important for the negative feedback regulation of the CK response (Müller and Sheen, 2007). Six genes encoding type-A RRs were found to be at least 2-fold lower in N-limited plants. In contrast, type-B RRs are TFs involved in the regulation of genes downstream of the CK. As also shown in section 4.2.12 (**Figure 4.8**), the GARP-ARR-B TF family was among the enriched upregulated TF families, with seven members of this family being significantly upregulated by N limitation.

ABA has also been reported to act as a negative regulator of tillering, and there are indications that ABA might act downstream of the SL and TB1/BRC1 pathways (Luo et al., 2019, González-Grandío et al., 2017). ABA is known to be involved in abiotic stress responses such as drought and physiological processes like senescence. However, there are only a few studies reporting involvement in N limitation responses. Analysis of the differentially expressed genes in the basal nodes revealed that several genes involved in ABA biosynthesis and signalling were affected by N limitation. Two orthologues of a rice gene encoding 9-cis-epoxycarotenoid dioxygenase (NCED2) were found to be 16-fold higher expressed under N limitation. Similarly, the expression of two genes encoding putative abscisic-aldehyde oxidase (AAO), which catalyses the last step of ABA biosynthesis, was induced by N limitation. A strong effect on N limitation was observed in ABA signalling genes. Protein phosphatases 2C (PP2Cs) are important components of the ABA signalling pathway, acting as negative regulators. Twelve genes encoding putative PPC2s were found to be upregulated in response to N limitation. PPC2 expression is positively regulated by ABA. Moreover, eight bZIP TFs encoding orthologues of Arabidopsis abscisic acid-responsive element binding factors (ABFs) were also induced in basal nodes under N-limiting conditions. Those TFs mediate transcriptional responses to ABA controlling the expression of downstream genes and acting as positive regulators of abiotic stress responses. The ABA-inducible wheat orthologues of *OsZIP77* were significantly upregulated under low N. In rice, bZIP77 has been found to promote flowering time in rice by affecting the floral transition (Brambilla et al., 2017).

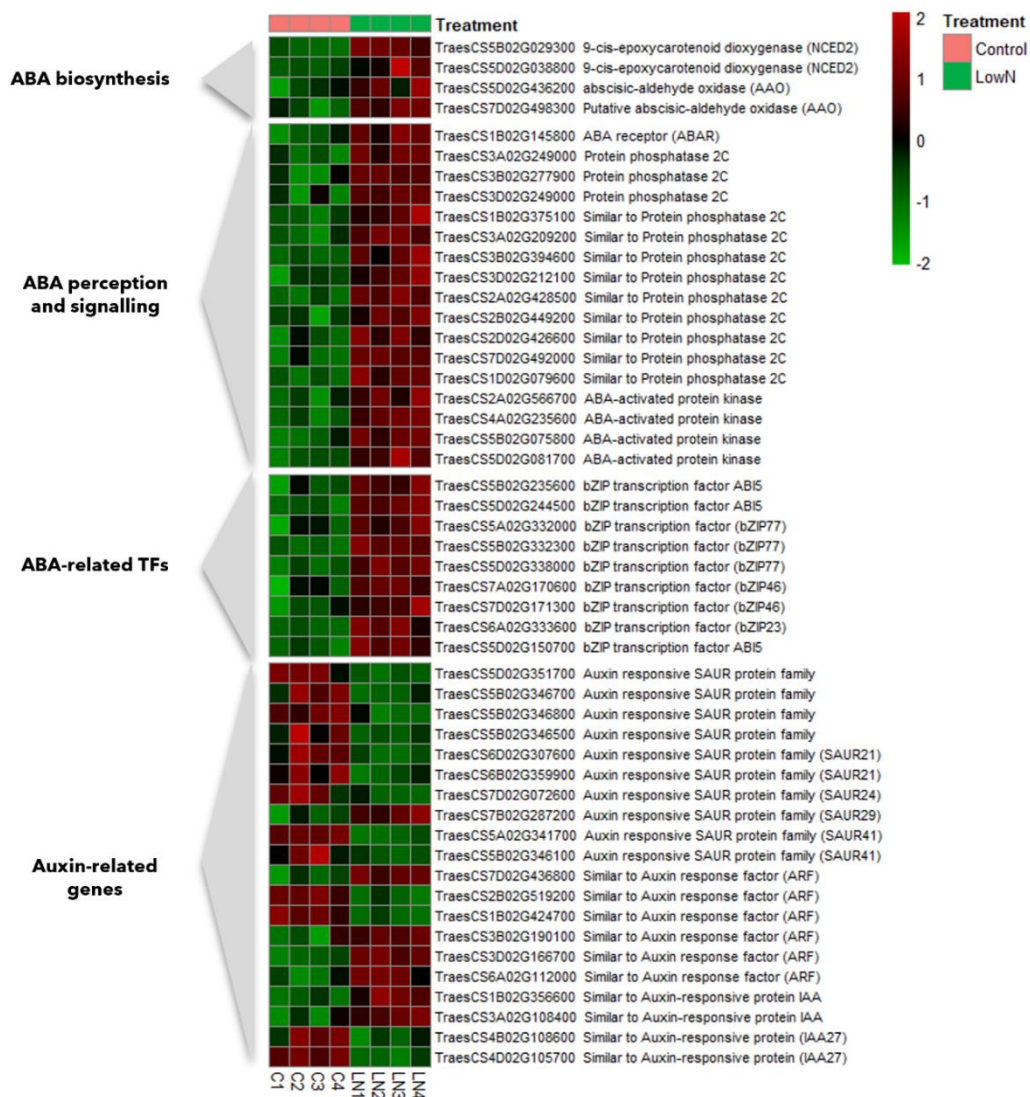


Figure 4.11: Heatmap of differentially expressed ABA- and auxin-related genes in the basal node of wheat grown under N limitation for 8 days based on the RNA-seq data. Each row corresponds to a different gene, while columns correspond to different samples grouped by treatment. Data are Z-scores of regularised log normalised counts (rlog) as generated by DESeq2. Red colour corresponds to higher transcript levels while green to lower. Row names consist of the GeneID and the gene annotation.

Moreover, some genes involved in auxin responses, such as SMALL AUXIN UPREGULATED RNAs (SAURs) and ARF TFs, were differentially expressed in N-limited nodes (**Figure 4.11**). Most of the SAURs are auxin-inducible genes which are involved in cell elongation. Studies in Arabidopsis have demonstrated that SAURs are required for normal plant growth but also in other processes like senescence and response to environmental stimuli (Stortenbeker and Bemer, 2018). In N-limited basal nodes, the

expression of 9 SAUR genes was suppressed, indicating suppression of cell elongation. Among the DE genes, only one member of the SAUR family was upregulated, which was an orthologue of *AtSAUR30* and *OsSAUR29*. *AtSAUR30* has been shown to be involved in senescence (Wen et al., 2019). Moreover, the expression of two wheat ARF encoding genes orthologous to *AtARF18* and *AtARF9* were found to be 2-fold higher under N limitation. Recent studies have shown that ARF18 and ARF9 9 have a central role in the regulation of plant N-response in Arabidopsis, indicating a conserved response of those genes in both Arabidopsis and wheat (Gaudinier et al., 2018). Some members of Aux/IAA family, another component of the auxin response, were also found to be affected by N limitation.

Other hormonal pathways were also found to be affected but to a lesser extent (**Figure 4.12**). Some of the jasmonic acid (JA) biosynthetic and signalling genes, including allene oxide synthase and the JA receptor protein, coronatine-insensitive protein homolog 1a, were upregulated by N limitation. JA acts as a signalling molecule for plant responses by activating defence mechanisms. GO enrichment analysis showed that N limitation triggered plant responses to biotic stress and plant immunity, possibly through the JA signalling pathway. In addition to JA, some genes related to brassinosteroid (BR) metabolism were differentially expressed. GAs are known to play an important role in stem elongation but have also shown an inhibition effect on tillering. GA biosynthetic genes *TaGA3ox2* and *TaGA20ox2* were found to be significantly downregulated in N-limited plants. GAs control tillering by promoting the degradation of TF monoculm 1 (MOC1), which controls tiller number in rice (Liao et al., 2019). N-mediated tiller growth response (NGR5) is an APETALA2 (AP2) TF, which was recently suggested to control tillering in response to N supply in a GA-dependent manner (Wu et al., 2020). NGR5 is negatively affected by GA levels, while under high N supply, NGR5 is suggested to suppress the expression of tiller inhibitory genes *D14* and *SPL14* leading to higher tillering. Wheat orthologues to *OsNGR5* (TraesCS1A02G242800, TraesCS1B02G254300, TraesCS1D02G242800) showed no response to N supply at the transcriptional level, and neither did the mRNA abundance of *TaSPL17* (TraesCS7A02G246500, TraesCS7B02G144900, TraesCS7D02G245200), therefore not supporting the presence of the same mechanism in wheat. Finally,

ethylene-related genes were also found to be affected by N limitation, such as ACC oxidase and genes involved in ethylene signalling.

The RNA-seq data provided insights into the transcriptional regulation of hormone biosynthesis and signalling as part of the N limitation response. The observed effect of N limitation on various hormonal pathways highlighted the complexity of plant responses to N supply.

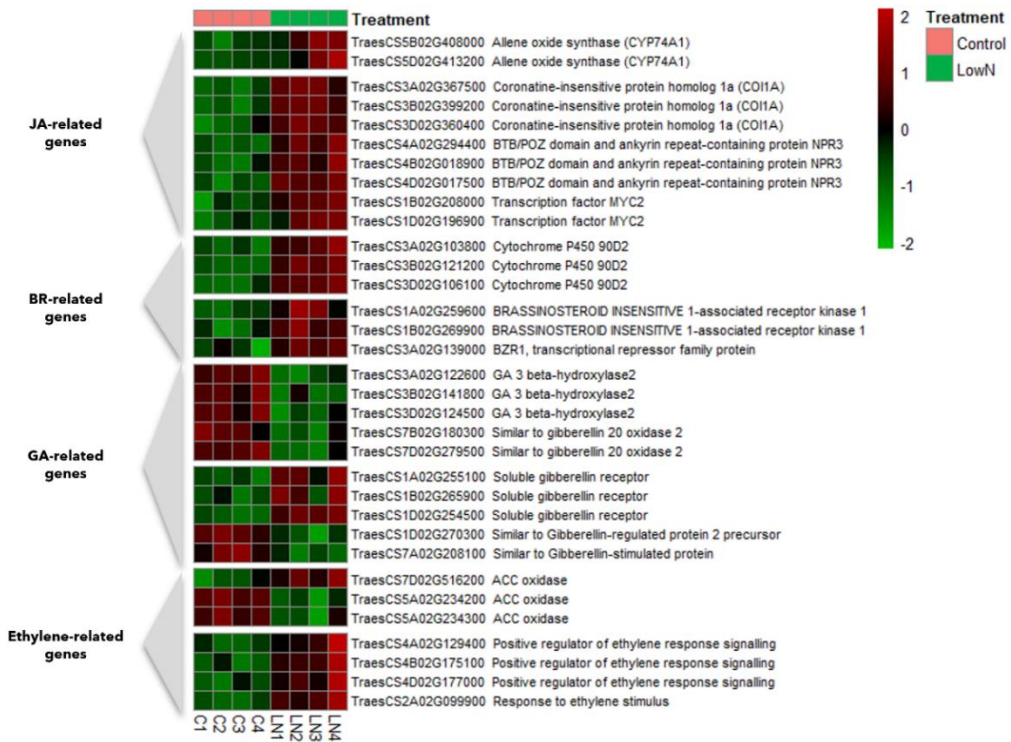


Figure 4.12: Heatmap of differentially expressed other hormone-related genes in the basal node of wheat plants grown under N limitation for 8 days based on the RNA-seq data. Each row corresponds to a different gene, while column corresponds to different samples grouped by treatment. Data are Z-scores of regularised log normalised counts (rlog) as generated by DESeq2. Red colour corresponds to higher transcript levels while green to lower. Row names consist of the GeneID and the gene annotation.

4.2.14 Comparative Analysis of N and P Limitation Effects on SL Biosynthetic, Perception and Signalling Gene Expression in Basal Nodes

The phenotypic results presented in section 4.2.1 demonstrated that both N and P limitations negatively affect tillering. However, the results suggested that N limitation had a more prominent effect on suppressing tillering than P limitation. Both the gene expression data (section 3.2.4) and the analysis of the DE genes from the RNA-seq (section 4.2.13) revealed that N limitation strongly induced SL biosynthetic genes in

the basal node of wheat plants, indicating that SLs might play an important role in plant adaptation to N-limiting conditions. In rice, it has been demonstrated that tiller suppression by P limitation is mediated by SLs (Umehara et al., 2010). SL biosynthesis is strongly induced in rice roots and shoot bases of plants grown under P limitation leading to tiller suppression. In contrast, SL induction by N limitation has been speculated to be due to the reduced P uptake by N-deprived plants rather than the direct effect of N limitation (Yoneyama et al., 2012). However, those studies have mainly referred to SL levels in root exudates or in root tissue where P limitation has a predominant impact on SL production. Less is known about the transcriptional regulation of SL-related genes in the upper part of the plants.

Therefore, the RNA-seq data were utilised for the comparative analysis of the effect of N and P limitation on SL induction (**Figure 4.13**). As described in section 4.2.13, N limitation strongly induced the expression of *TaD27*, *TaD17* and *TaD10* homoeologues. *TaD10* showed the highest fold-change increase, more than 4-fold in N-limited nodes. Similarly, significant overexpression was observed for *MAX1d-7B*, while other *MAX1d* and *MAX1c* homoeologues showed higher transcript accumulation; however, the fold change difference or padj values failed to meet the applied thresholds. Finally, mRNA accumulation of *TaD53a-4A*, *TaD53b-5B* and *-5D* rose under N limitation in the basal nodes. Analysis of the differentially expressed genes in P-limited plants showed that only *TaD27-7B* and two homoeologues of *TaD10* were upregulated in nodes. In addition, the recorded upregulation of *TaD10*s by P limitation was just 2.3-fold higher, while the same genes were 5-fold higher in N-limited nodes. As a result, it is suggested that N limitation had a more substantial effect on SL biosynthesis and signalling genes compared to P limitation in the nodes. To further confirm this observation, differential gene expression analysis was performed between Low N and Low P plants using the DESeq2 tool to identify genes with significant differences between the two treatments. The differential gene expression analysis results confirmed that the mRNA abundance of some SL biosynthetic genes was significantly higher (padj < 0.01 and |FC| > 1.5) in low N nodes compared to low P, such as *TaD10*. Significant differences were observed in the case of *TaD53a-4A* and *TaD53b-5B* between low N and low P

nodes, indicating that under N limitation, the levels of SLs were indeed higher in this tissue, given that *TaD53* expression is regulated by the levels of SLs.

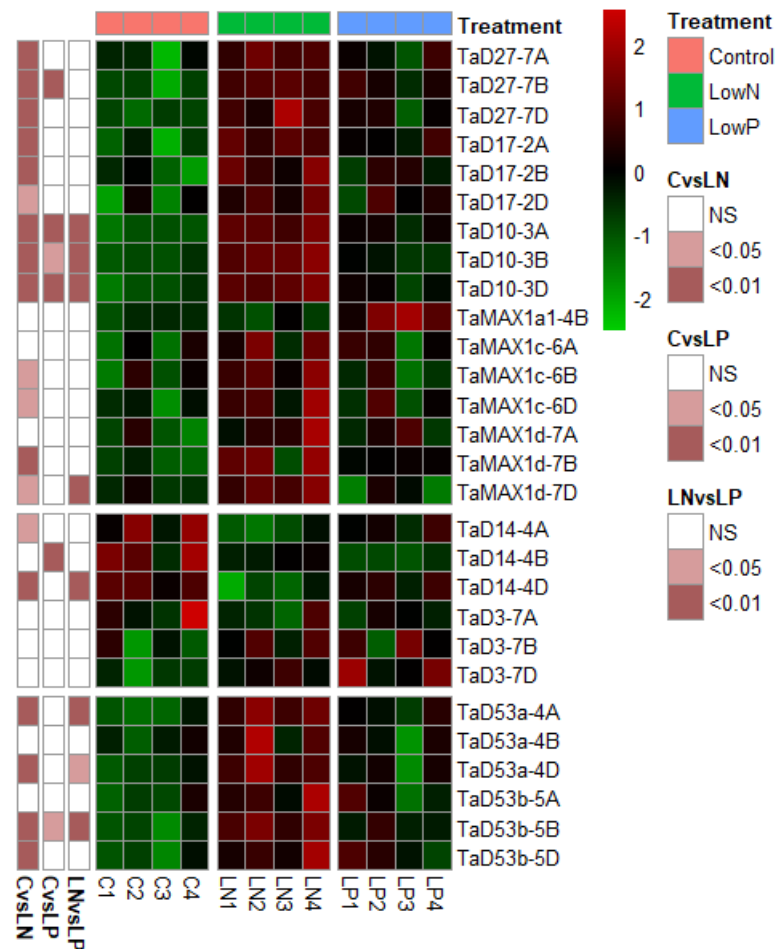


Figure 4.13: Heatmap comparison of SL biosynthetic and signalling gene transcript levels in the basal node of wheat grown under N and P limitation for 8 days based on the RNA-seq data. Each row corresponds to a different gene, while column corresponds to different samples grouped by treatment. SL-related genes that were found to be expressed (TPM > 0.5) in the basal node were only included in the heatmap. Data are Z-scores of regularised log normalised counts (rlog) as generated by the DESeq2 tool. Red colour corresponds to higher transcript levels while green to lower. Row annotations represent the padj values of each comparison according to the differential gene expression analysis.

4.2.15 Comparative Analysis of N and P Limitation Effects on SL Biosynthetic, Perception and Signalling Gene Expression in Root

The findings in basal nodes showed that N limitation led to stronger induction of SL biosynthesis compared to P limitation. To examine the same response in roots, the gene expression of SL biosynthesis and signalling genes was performed in roots samples from the same trial (plants grown under N- and P-limiting conditions for 8 days). The analysis was conducted with RT-qPCR. Overall, the results demonstrated

that SL biosynthetic genes were strongly induced by both nutrient limitations in roots, while the examined SL signalling genes showed a significant downregulation, confirming the negative feedback regulation of *TaD3* and *TaD14*, as also observed in section 3.2.3. Among the SL biosynthetic genes, only *TaMAX1c* did not show any response. As shown in section 3.2.6, *MAX1c* homoeologues have shown low expression in roots compared to the other *MAX1* homoeologues, which may explain the difference in the regulation of *MAX1c* compared to the other *MAX1* homologues.

Subsequently, the expression levels of SL-related genes were compared between N- and P-limited plants in roots (**Figure 4.14**). Although in basal nodes, N limitation led to stronger induction of SL biosynthesis compared to P limitation, the mRNA accumulation of SL biosynthetic genes in roots was as high or even higher in low P roots compared to low N. In fact, no significant difference was observed between the mRNA accumulation of *TaD27* and *TaD17* between low N and low P treatments. A stronger expression of *TaD10* was recorded under low P conditions. However, no significant difference was observed between the two nutrient limitations. The main differences in the effect of N and P limitation on the SL biosynthesis were observed in *MAX1* gene expression. P-limited plants showed higher mRNA levels of *TaMAX1a1* and *TaMAX1d* in roots compared to low N plants. A similar trend was also observed for the predominant *MAX1* homologue, *TaMAX1a2*, whose NRQ value was higher in low P. In terms of SL biosynthesis, both conditions strongly downregulated the expression of *TaD3* and *TaD14* in roots. *TaD3* and *TaD14* were found to be significantly lower in low N roots compared to low P.

Therefore, the results presented suggested that P limitation triggered a stronger induction of SL biosynthesis compared to N limitation in roots, especially in the case of *MAX1* genes. Yoneyama et al. (2012) reported that SL exudation is stronger in wheat plants growing under P-limiting conditions compared to low N, which is also supported by the transcriptomic data.

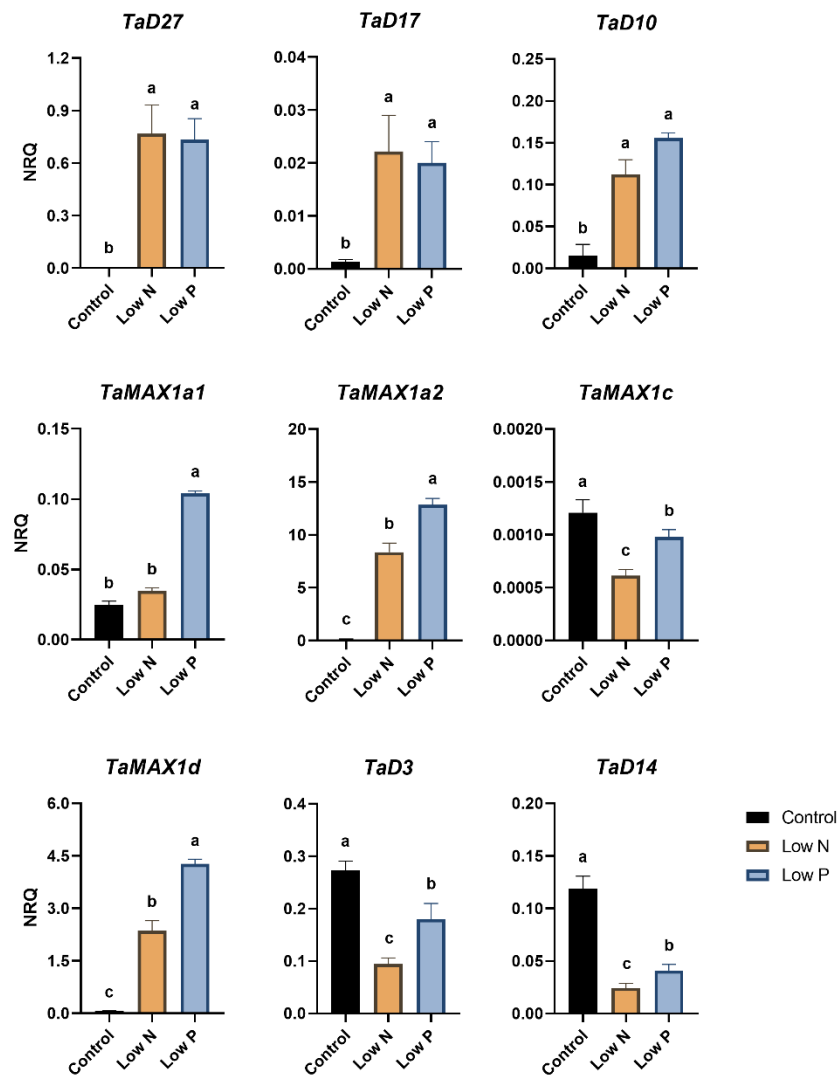


Figure 4.14: Gene expression levels of SL biosynthetic (*TaD27*, *TaD17*, *TaD10*, *TaMAX1a1*, *TaMAX1a2*, *TaMAX1c* and *TaMAX1d*) and signalling genes (*TaD3* and *TaD14*) in the root of wheat grown under N and P limitation for 8 days based on RT-qPCR data. Values are means of four biological replicates and error bars represent SE. Statistical analysis was conducted with ANOVA in $\log_2(1/\text{NRQ})$ transformed values. Different letters denote statistically significant difference between treatment mean based on Fisher's LSD test ($p < 0.05$, *TaD27* LSD (5%) = 0.56, *TaD17* LSD (5%) = 0.44, *TaD10* LSD (5%) = 0.68, *TaMAX1a1* LSD (5%) = 1.79, *TaMAX1a2* LSD (5%) = 1.25, *TaMAX1c* LSD (5%) = 0.33, *TaMAX1d* LSD (5%) = 0.49, *TaD3* LSD (5%) = 0.15, *TaD14* LSD (5%) = 0.49).

4.2.16 Phytohormonal Changes in Basal Nodes in Response to N and P Limiting Conditions

RNA-seq experiment in basal nodes showed that tiller suppression by N limitation is accompanied by extensive transcriptional changes in genes involved in different hormone biosynthesis and signalling (section 4.2.13). Plant hormones are known to

serve the role of long-distance signals coordinating plant response to growing conditions at a whole plant level, while they play an essential role in modulating plant architecture. To examine the effect of N and P limitation on the phytohormonal profile, the levels of major phytohormones were determined using UHPLC-MS/MS. The phytohormone analysis was performed in the pooled root, shoot and basal node samples from plants growing hydroponically under N or P limiting conditions for 8 days in a similar experiment to the one used for the RNA-sequencing.

The targeted phytohormones included in this study can be classified into three main categories: CKs, auxin and ABA. Among the natural cytokinins, the levels of isopentenyl adenine (iP), isopentenyl adenosine (iPA), trans-zeatin (tZ), cis-zeatin (cZ), dihydrozeatin (DHZ) and their riboside (-R) were determined in all the tissues. The concentration of DHZ was below the limit of quantification in all the tissues examined, so it was considered to be not detected (ND). DHZR was only detected in node samples and not in roots and shoots, and the level was lower than the rest of the CKs. The amount of IAA was determined as the primary type of auxin found in plants. Apart from ABA, ABA catabolism products were also determined, namely phaseic acid (PA) and dihydrophaseic acid (DPA). The SL orobanchol and strigol were attempted to be quantified in wheat root samples by UHPLC-MS/MS and by trying different extraction techniques, however, this was not successful.

Phytohormone data were analysed with one-way ANOVA to test if nutrient limitation significantly affected phytohormone levels in each of the examined tissues (**Tables 4.2 and 4.3**). Overall, nutrient limitation had a strong impact on many phytohormones, and the majority of the changes were observed in basal nodes. Out of the 11 phytohormones quantified in nodes, eight showed a statistically significant effect of the treatment, indicating that nutrient limitation strongly affected hormonal balance in basal nodes. Those changes are most likely to be essential for the regulation of developmental processes in basal nodes, including tillering. To identify which nutrient limitation had a significant effect compared to the control, pair-wise comparisons were conducted between low N and control plants and low P and control plants (**Tables 4.2 and 4.3**).

Overall, the N limitation had a significant effect on the majority of the phytohormone tested in the different tissues, while the P limitation was found to affect only the concentration of DPA in the basal nodes. This result suggested that low P conditions for 8 days did not trigger changes in the phytohormonal profile of the analysed phytohormones, which was also consistent with the observed phenotype and the RNA-seq results, given that differentially expressed genes under P limitation were not enriched for hormone-related pathways.

To depict the phytohormonal changes under nutrient-limiting conditions, heatmaps were generated for all the phytohormones analysed in the three different tissues. The data presented are standardised (z-scores) per row per tissue (**Figure 4.15**). The absolute concentration of the phytohormones in the different tissue is shown (**Tables 4.2 and 4.3**).

N limitation strongly reduced the levels of iP, tZ and tZR in roots, basal nodes, and the main shoot. In roots, tZ and tZR showed the highest fold change, with a decrease of more than 5-fold. tZ is considered the most active type of CK in many species. In basal nodes, tZR showed the highest concentration among the other CKs, followed by tZ. This observation indicates that the tZ-type of CKs are the predominant type of CKs in wheat basal nodes. In nodes, N limitation decreased the concentration of tZ-type of CK by more than 10-fold. The concentration of CKs was also reduced by N limitation. tZR was found to be below the limit of quantification in shoots of N-limited plants, indicating that it was downregulated. In addition, tZR concentration in nodes was 16-fold higher than in shoots, demonstrating that the tZ-type of CKs are accumulated in basal nodes. As a result, it is suggested that the N limitation caused a systemic downregulation of iP and tZ-type of CK in wheat. CK act as a positive regulator of tillering; thus, the lower levels of CK locally in nodes might contribute to tiller suppression under N-limiting conditions. The results support the hypothesis that CK can act as a signal of N status. The effect of N limitation on CK levels was also consistent with the RNA-seq data as described in section 4.2.13, which also suggested strong suppression of CK biosynthesis and signalling.

Table 4.2: Concentration of different CKs (pg/mg) in the root, basal node and shoot of wheat grown under Control (10 mM N and 1 mM P), Low N (0.1 mM N) and Low P (0.01 mM P) conditions. Data are means \pm SE (n=4). Statistical analysis was conducted with ANOVA followed by t-tests between the treatments.

	iPA (pg/mg)	iP (pg/mg)	tZR (pg/mg)	tZ (pg/mg)	cZR (pg/mg)	cZ (pg/mg)
Root						
Control	0.40 \pm 0.045	0.09 \pm 0.016	0.35 \pm 0.040	0.10 \pm 0.011	0.45 \pm 0.021	0.10 \pm 0.013
LowN	0.16 \pm 0.034	0.04 \pm 0.003	0.07 \pm 0.034	0.01 \pm 0.006	0.40 \pm 0.022	0.18 \pm 0.022
LowP	0.42 \pm 0.035	0.10 \pm 0.021	0.29 \pm 0.045	0.07 \pm 0.020	0.50 \pm 0.036	0.12 \pm 0.032
p-value	0.002	0.052	0.002	0.003	0.086	0.118
LowN vs Control	0.002	0.078	< 0.001	0.001	0.185	0.052
LowP vs Control	0.642	0.431	0.296	0.124	0.294	0.613
LSD (5%)	0.123	0.049	0.128	0.043	0.088	0.076
Basal Node						
Control	0.66 \pm 0.034	0.16 \pm 0.016	5.24 \pm 0.397	1.28 \pm 0.074	0.49 \pm 0.049	0.19 \pm 0.037
LowN	0.22 \pm 0.044	0.09 \pm 0.006	0.41 \pm 0.092	0.11 \pm 0.020	0.64 \pm 0.070	0.31 \pm 0.069
LowP	0.63 \pm 0.014	0.15 \pm 0.021	5.45 \pm 0.384	1.35 \pm 0.186	0.49 \pm 0.092	0.21 \pm 0.077
p-value	< 0.001	0.018	< 0.001	< 0.001	n.s	n.s
LowN vs Control	< 0.001	0.0114	< 0.001	< 0.001	-	-
LowP vs Control	0.671	0.905	0.662	0.672	-	-
LSD (5%)	0.112	0.050	1.034	0.371	0.230	0.203
Shoot						
Control	0.12 \pm 0.019	0.06 \pm 0.006	0.31 \pm 0.113	0.74 \pm 0.099	0.20 \pm 0.038	0.17 \pm 0.030
LowN	0.04 \pm 0.003	0.04 \pm 0.003	ND	0.06 \pm 0.012	0.39 \pm 0.013	0.15 \pm 0.015
LowP	0.12 \pm 0.008	0.07 \pm 0.003	0.15 \pm 0.010	0.60 \pm 0.074	0.16 \pm 0.020	0.12 \pm 0.026
p-value	< 0.001	0.001	-	< 0.001	< 0.001	n.s
LowN vs Control	< 0.001	0.008	-	< 0.001	< 0.001	-
LowP vs Control	0.713	0.052	0.228	0.191	0.356	-
LSD (5%)	0.038	0.014	0.278	0.230	0.083	0.079

However, among the CKs analysed, the cZ-type of CKs did not show the same response to the N limitation. N-limited plants tended to accumulate cZR and cZ in nodes, although no statistically significant difference was observed. In shoots, cZR concentration was found to be 2-fold higher than in high N treated plants, while the cZ concentration was also higher in roots under N limitation. The role of the cZ-type of CKs is not very well understood. In the past, cZ was considered to be biologically inactive since its activity has been found to be much weaker compared to tZ. However, accumulations of cZ in plant tissues under stress conditions have been previously reported for many species (Schäfer et al., 2015). Given that cZ is the stereoisomer of tZ, it has been proposed that cZ(R) plays the role of the tZ(R) replacement under growth-limiting conditions, and in this way, plants keep CKs in a less active form. After

the introduction of plants to stress conditions, tZ levels declined and were followed by an increase in cZ. A similar pattern was also observed in N-limited nodes.

Table 4.3: ABA, PA, DPA and IAA concentration (pg/mg) in the root, basal node and shoot of wheat grown under Control (10 mM N and 1 mM P), Low N (0.1 mM N) and Low P (0.01 mM P) conditions. Data are means \pm SE (n=4). Statistical analysis was conducted with ANOVA followed by t-tests between the treatments.

	ABA (pg/mg)	PA (pg/mg)	DPA (pg/mg)	IAA (pg/mg)
Basal Node				
Control	2.43 \pm 0.101	1.31 \pm 0.209	3.74 \pm 0.254	2.94 \pm 0.240
LowN	5.10 \pm 0.071	2.81 \pm 0.286	2.45 \pm 0.545	1.47 \pm 0.100
LowP	2.36 \pm 0.160	1.94 \pm 0.218	1.46 \pm 0.261	3.10 \pm 0.128
p-value	< 0.001	0.005	0.004	< 0.001
LowN vs Control	< 0.001	0.00163	0.0318	< 0.001
LowP vs Control	0.689	0.0973	0.00109	0.523
LSD (5%)	0.334	0.769	1.059	0.535
Shoot				
Control	3.44 \pm 0.033	2.95 \pm 0.252	2.79 \pm 0.489	6.04 \pm 0.767
LowN	5.57 \pm 0.342	9.12 \pm 0.400	4.08 \pm 0.461	5.62 \pm 0.111
LowP	4.00 \pm 0.276	3.52 \pm 0.474	3.38 \pm 0.722	4.67 \pm 0.499
p-value	< 0.001	< 0.001	n.s	n.s
LowN vs Control	< 0.001	< 0.001	-	-
LowP vs Control	0.159	0.333	-	-
LSD (5%)	0.814	1.235	1.821	1.702

IAA concentrations were determined in basal nodes and shoots of wheat plants. The results showed that N limitation had a significant effect on the IAA concentration of basal nodes. More specifically, N-limited nodes had 2-fold lower levels of IAA. However, the concentration of IAA in shoots remained unaffected by the N limitation. In addition, the concentration of IAA in shoots was higher compared to that in nodes.

A strong negative correlation between ABA and N supply was observed in basal nodes and shoot tissue. In fact, ABA concentration was 2-fold higher in nodes and 1.6-fold higher in shoots of N-limited plants. Similarly, a 2-fold and 3-fold increase in PA levels was recorded in nodes and shoots, respectively. These results clearly demonstrated that ABA biosynthesis is strongly induced by N limitation. ABA also acts as a negative regulator of tillering. Therefore, the ABA accumulation under N-limiting conditions might contribute to tiller suppression. ABA is also associated with stress responses and senescence. Although some studies have reported a link between N limitation and ABA

biosynthesis, the correlation is not universal. N-limited wheat plants have been shown to accumulate ABA (Teplova et al., 1998); however, the opposite pattern has been reported in other species (Kiba et al., 2010). In this study, N limitation was found to strongly induce ABA accumulation in the above-ground plant tissue, which was further supported by the RNA-seq data based on which there was strong upregulation of genes involved in ABA biosynthesis, signal transduction and ABA-responsive TFs.

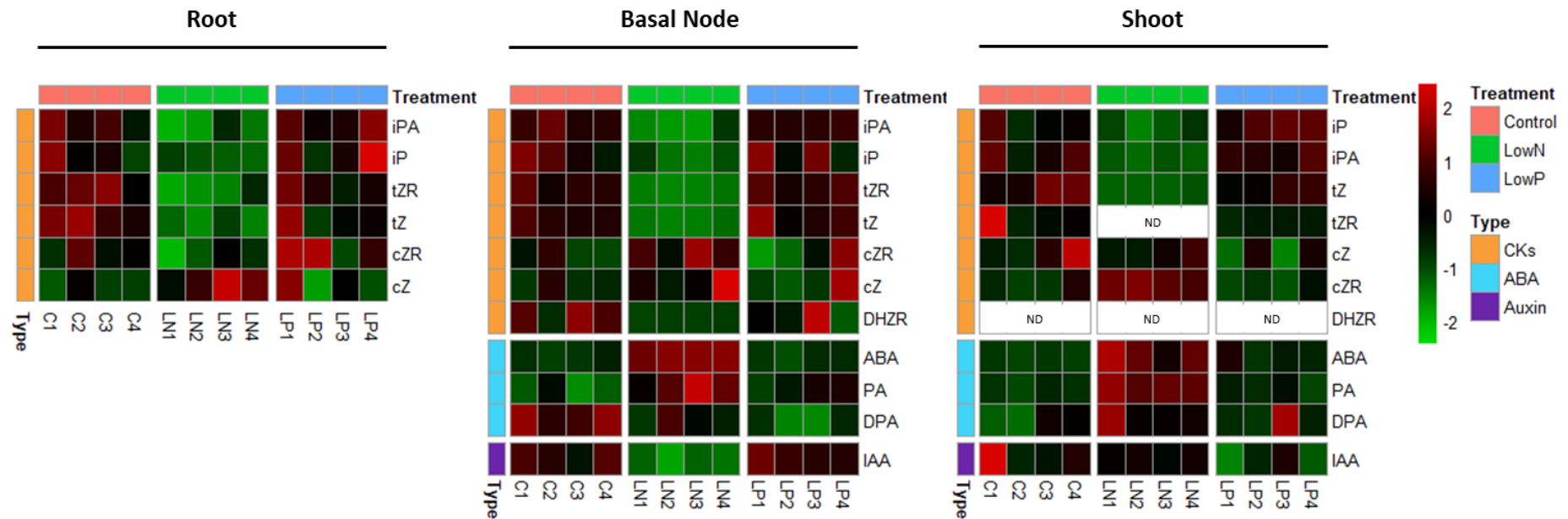


Figure 4.15: Heatmap comparison of analysed phytohormones in roots, basal node and shoot of wheat grown under N and P limitation for 8 days. Each row corresponds to a different phytohormone grouped based on their type (CKs, ABA, and auxin) in three different plant tissue. Each column represents a different sample grouped by treatment (C: Control, LN: Low N (0.1 mM N), LP: Low P (0.01 mM P)). Data were standardised per row by subtracting the population mean from each value and dividing the difference by the standard deviation. The standardisation was performed in each tissue separately. The green colour corresponds to lower phytohormone levels, whereas the red colour to higher. In root tissue, only CKs were analysed. tZR concentration in the shoot of LowN plants was below the detection limit. DHZR was only detected in basal node samples. Abbreviations: isopentenyl adenine (iP), isopentenyl adenosine (iPA), trans-zeatin (tZ), cis-zeatin (cZ), dihydro-zeatin (DHZ) and their riboside (-R), abscisic acid (ABA), phaseic acid (PA), dihydrophaseic acid (DPA), indole-3-acetic acid (IAA) and non-detected (ND).

4.3. Discussion

4.3.1 Wheat Plant Adaptation to N-limiting Conditions Through Transcriptional Changes

N is an important macronutrient for wheat growth and productivity. As presented in section 3.2.2, N limitation has a strong impact on wheat seedling growth. Suppression of tillering is part of plant adaptation to low N availability along with other morphological, physiological and molecular changes. N limitation responses are regulated by a complex network of transcriptional responses leading to physiological and architectural changes allowing the plant to adapt to the N-limiting conditions (Ueda et al., 2020, Gaudinier et al., 2018). Although many studies have focused on the molecular changes underlying the N limitation response, they have mainly focused on roots or leaves. As a result, the transcriptional changes that lead to tiller suppression have not been extensively studied, especially in wheat. To address this question, an RNA-seq experiment was conducted in the basal nodes of wheat grown under N-limiting conditions for 8 days. N limitation for 8 days led to a strong reduction in tiller number, suggesting a strong effect of N limitation on tiller bud outgrowth. The observed tiller suppression by N limitation was accompanied by dramatic changes in the expression of genes from various pathways. In fact, 2591 and 2580 genes were found to be significantly down- and upregulated, respectively, by N limitation in the basal nodes. GO enrichment analysis showed that N limitation regulated pathways related to central metabolism, mRNA translation and protein synthesis, N metabolism and resulted in differential expression of genes involved in hormonal pathways and genes encoding TFs. Those changes set the foundation for understanding how N limitation affects other metabolic and hormonal pathways related to tiller suppression (Figure 4.16).

Transcriptional changes in dormant buds have been characterized in response to other signals that lead to bud dormancy in other species, providing marker genes for bud dormancy (Tarancón et al., 2017). *DRM* is a well-known marker associated with bud dormancy in many species. All homoeologues of *TaDRM1*, 3, 4 were found to be significantly upregulated under N-limiting conditions suggesting that N limitation led to tiller bud dormancy. Further examination of the DE genes revealed that many genes

involved in protein synthesis and genes encoding ribosomal proteins were strongly downregulated, suggesting that the rate of protein synthesis was strongly suppressed in nodes under low N. Moreover, N limitation had a negative effect on genes involved in the cell cycle progression and DNA replication, indicating a negative impact of N limitation on cell growth and proliferation. Similar changes have been reported before in dormant buds (Tarancón et al., 2017, Kebrom et al., 2006, Luo et al., 2019). The transcriptomic analysis showed that N limitation had a strong impact on glucose utilization for energy production. This was reflected by the strong downregulation of genes encoding enzymes necessary for glycolysis and the TCA cycle. Bud outgrowth is an energy-consuming process that requires energy for protein synthesis, cell wall biogenesis and cell proliferation. Therefore, changes in these pathways suggest a strong growth arrest under N limitation leading to bud dormancy.

Many sugar-related genes were found to be affected in the basal nodes under N-limiting conditions. N limitation regulated the expression of genes involved in sugar transport and sucrose metabolism, such as sugar transporters, cwINV and FPK. The function of cwINV has been linked to the sugar sink strength of the tissue, while the same is true for FPKs. In addition, N limitation led to changes in the expression of many SWEET transporters indicating that N limitation had a strong effect on both C partitioning and utilization. As a result, N limitation reduces the sugar sink strength of the bud by altering the expression of genes involved in sucrose metabolism and transport, leading to less sugar transport into the developing buds resulting in bud outgrowth suppression. Tarancón et al. (2017) reported similar changes in dormant buds of *Arabidopsis* and other woody plant species, which were attributed to low C availability in the buds, known as C-starvation response. N and C metabolisms are known to be tightly regulated based on many studies. From the results reported here, the N limitation effect on tiller bud outgrowth is at least partly regulated through modulation of C partitioning and utilization.

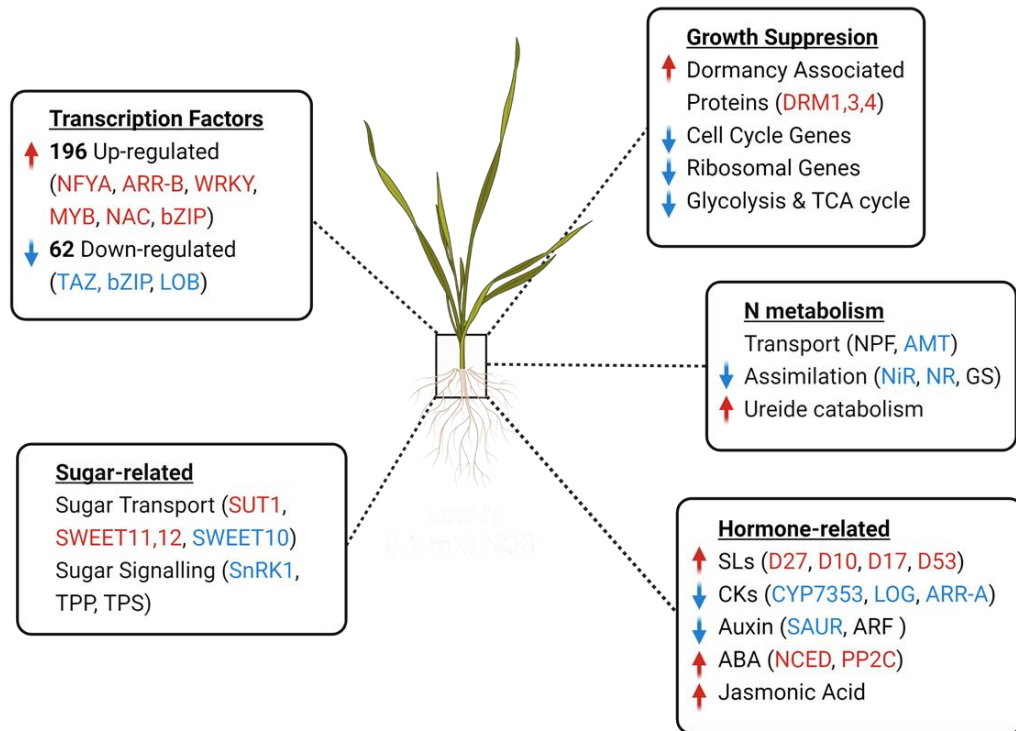


Figure 4.16: Summary of changes observed in the basal nodes of N-limited plants, which might be associated with tiller suppression and the general plant adaptation to N-limiting conditions.

Many genes involved in sugar signalling were found to be affected by N limitation, which provided evidence on how N limitation might control C metabolism. Recent studies have shown that sugar signalling involves Tre6P, which has also been shown to play a central role in controlling bud outgrowth by acting as a metabolic marker of C status. Many genes involved in Tre6P metabolism were differentially expressed by N limitation, strongly supporting the hypothesis that N limitation causes changes in C status signals or at least in cell sensitivity to C signals. It is known that under N limitation, more sugars are diverted into roots where they sustain root growth, while fewer sugars are used in the upper part of the plant for shoot growth. Many genes related to C utilization have been found to be induced in roots of wheat grown under N starvation (Curci et al., 2017). The opposite was observed in nodes suggesting that indeed under N limitation, fewer sugars might be delivered in nodes for bud outgrowth. Consistent with that hypothesis, some genes encoding SnRK1, which is a master regulator of C availability, were also downregulated by N limitation. Some bZIP TFs have been identified as important components of the metabolic reprogramming

downstream of Tre6P and SnRK1 (Wang et al., 2022a, Pedrotti et al., 2018). In fact, many members of the S1-bZIP group are targeted by SnRK1 to control C and N metabolism (Pedrotti et al., 2018). S1-bZIPs have also been found to interact with C-bZIP TFs to control the expression of downstream genes. Wheat genes showing high protein similarities with S1-bZIP and C-bZIP TFs were found to be significantly downregulated under N-limiting conditions, suggesting that they are also involved in the metabolic reprogramming under N limitation. Therefore, it is apparent that the N starvation response shares a similar gene regulatory network as the C-starvation response leading to bud dormancy.

Bud outgrowth is known to be controlled by the hormonal balance between different hormones. The transcriptomic and phytohormonal analysis highlighted that N limitation regulates many different hormonal pathways providing useful information about hormonal changes under N limitation, which might be associated with tillering control. As also shown in section 3.2.4, the N limitation strongly induced SL production in the basal nodes, which was also confirmed by the RNA-seq data. The SL biosynthetic pathway was a highly enriched GO and KEGG term in the upregulated gene set, indicating a strong involvement of SL in plant adaptation to N-limiting conditions. RNA-seq allowed the exploration of more genes in the pathway and each one of the homoeologues separately. For most of the genes in the biosynthetic pathway, the effect was consistent in all the three homoeologues. In addition, some of the *TaD53* genes were found to be significantly upregulated. It has been shown that *D53* expression is induced by SLs forming a negative feedback loop. Therefore, it is suggested that not only the expression of SL biosynthetic genes is induced, but also N limitation leads to transcriptional activation of downstream genes, presumably due to the accumulation of SLs locally in the basal nodes. SLs have been suggested to control tillering either by the D53-mediated control of *TB1* expression or/and by affecting auxin transport.

Based on the RNA-seq data, *TaTB1* homoeologues were not differentially expressed. However, this was mainly due to the fact that *TB1* expression was below the applied threshold; therefore, *TB1* genes were filtered out during the prefiltering of low expressed genes. Exploration of the transcript abundance of *TB1* homoeologues (TPM

values) showed that *TB1* expression was 1.5-fold higher in nodes in the low N treatment. The same increase was also found by RT-qPCR, although the results were not statistically significant. Kebrom and Mullet (2016) have reported that *SbTB1* transcripts were not detected by RNA-seq in sorghum buds. This was mainly attributed by the authors to the lack of a long poly-A tail in the *TB1* transcripts, which might lead to unsuccessful cDNA synthesis of *TB1* transcripts when oligo-dt primers were used (Kebrom and Mullet, 2016). This observation has also been reported for the transcript of *ZmTB1* (Vega-Arreguín et al., 2009). *TB1* has been found to regulate the expression of HD-ZIP TFs, the expression of which has been associated with tiller suppression. The expression of wheat orthologous genes to the identified HD-ZIP targets of *TB1* (among which is *TaGT1*) was significantly induced in wheat nodes under N limitation, suggesting that the same pathway is also involved in tiller suppression under N-limiting conditions. Those HD-ZIP TFs have been proposed to control the expression of ABA biosynthetic genes leading to local accumulation of ABA (González-Grandío et al., 2017). ABA plays an important role in abiotic stress responses, and it additionally promotes bud dormancy (Felemban et al., 2019). In the present study, N supply was found to have an effect on ABA content. A significant increase in the levels of ABA was found in basal nodes and shoots of N-limited plants. This increase in ABA levels was accompanied by changes in ABA biosynthetic genes and ABA signalling genes such as *PP2C* involved in ABA signal transduction. Recently ABA was identified as an important hormone for the negative regulation of tillering by acting downstream of the SL signalling pathway (Luo et al., 2019). However, ABA was found to be induced not only in basal nodes, but also in shoots indicating that it might play a broader role in plant response to N-limiting conditions. ABA is known to control processes such as senescence and autophagy. N and C recycling are both known to be an important part of the N-response; thus, the induction in ABA biosynthesis might control catabolic processes related to N and C remobilization.

The second proposed model for the action of SLs is by affecting auxin transport (Bennett et al., 2006). Phytohormonal analysis revealed that IAA content was reduced in nodes under N limitation. Moreover, SAURs, which play an essential role in IAA response, were downregulated in N-limited nodes. N limitation also regulated the

expression of some ARFs, suggesting that N limitation causes changes in auxin signalling to control N deficiency responses. The amount of IAA was 2-fold lower in N-limited nodes compared to the control plants. The role of auxin in the regulation of tillering is known due to its involvement in apical dominance. However, as has been suggested in other monocotyledonous plants, apical dominance might not be apparent during the vegetative stage, as the apical meristem is located at the base of the shoot; thereby, the effect of the growing shoot apex might not be so strong. Consistent with the present data, Xu et al. (2015) reported that N limitation decreased the amount of IAA in nodes. Similar results have been reported in rice (Sun et al., 2014). This observation is in contradiction with the results from dicotyledonous species such as *Arabidopsis*, where IAA concentration increases in response to N limitation, contributing to the suppression of lateral bud outgrowth (de Jong et al., 2014). With regards to the present data, the higher amount of IAA in the shoot base under N-sufficient conditions might reflect the higher export of auxin from the actively growing emerging tiller, in contrast to N-limiting conditions where due to the tiller suppression, less auxin is exported to the PATS. Thereby, IAA might not play a significant role in N-mediated tiller suppression in monocotyledonous as in dicotyledonous species because we would expect a higher concentration in shoot base to suppress bud outgrowth.

The N limitation response included downregulation in nodes of CK biosynthetic genes such as CYP735A3 and LOG3. Similarly, type-A RRs, which are an essential part of the CK signalling pathway, were suppressed by N limitation (Müller and Sheen, 2007). In contrast, type-B RRs were upregulated, possibly as a feedback regulation to the low levels of CKs. Indeed, the levels of the most abundant type of CKs, tZ and tZR, were strongly reduced under N limitation. tZ is known to be the most active form of CK in plants. N limitation led to a systemic downregulation of CK content in all the tissues examined, confirming the strong link between N and CK levels, which act as a signal of N-status. Other studies have also shown that N limitation leads to a reduction in the levels of CKs (Xu et al., 2015b). CKs act as positive regulators of tillering. As a result, the decline in the levels of CK under N limitation might contribute to the observed tiller suppression.

Under N-limiting conditions, many genes involved in N assimilation, transport and remobilization were found to be affected. Under N-limiting conditions, there was a strong downregulation of N assimilation enzymes such as NR and NiR. Among the N assimilation enzymes, *TaGS1* homoeologues were found to be induced by N limitation. GS1, apart from its role in N assimilation, also plays an important role in the reassimilation of NH_4^+ regenerated by amino acid recycling (Bernard and Habash, 2009). In addition, the expression of many oligo-peptide transporters (NPF) was regulated by N limitation. Similarly, many genes encoding amino acid transporters showed a strong response to N supply, indicating significant changes in N remobilization from N source to N sink tissues. In addition, N limitation was found to promote ureide metabolism. Ureide is one of the main forms of nitrogen transported within the plants, which has a low C/N ratio compared to amino acids from which it is derived. N limitation strongly induces allantoin catabolism which further supports strong upregulation of the N recycling mechanism as part of plant adaptation to growing conditions. Those changes indicate the strong reduction of nitrate assimilation, whereas there is a strong reassimilation of N.

Finally, N limitation, apart from controlling tillering by suppressing bud outgrowth, may influence the final number of formed tillers by affecting developmental tiller cessation. Although no phenotypic data were recorded to support this hypothesis, based on the gene expression data, N limitation has an effect on genes involved in flowering. In fact, N limitation induced the expression of three homoeologous genes encoding GARP G2-like TFs, which are orthologues of *OsPCL1*. In addition, *bZIP77* orthologous genes were induced in wheat nodes under N limitation. Both PCL1 and bZIP77 have been found in rice to promote flowering and heading time. The orthologues of *AtWRKY12*, which is also involved in flowering regulation in Arabidopsis, were regulated by N limitation. Similarly, five genes encoding flower promoting factors (FPF) were strongly induced by N limitation. In contrast, the orthologue of rice terminal flower 1 (*TFL1*) and other genes associated with repression of flowering were downregulated. These results suggest that N limitation promotes flowering and the transition from the vegetative to the reproductive phase, which in turn leads to early cessation of tillering. In rice, early flowering has been associated

with a lower number of tillers. It is known that N limitation stimulates flowering; however, this depends on the severity of N limitation.

Finally, 258 TFs classified into 36 different families were found to be differentially expressed. Among the TF families which were identified responding to N limitation, MYB, WRKY and bZIP were the most abundant, with more than 30 members differentially expressed. The majority of WRKY and MYB members were upregulated by N limitation. Previous transcriptomic studies reported a strong impact of N limitation on MYB and WRKY TFs in roots and leaves of wheat plants, suggesting that members of this family play important roles in plant adaptation to N-limiting conditions. The expression of many MYB TFs is linked with plant resilience to abiotic stress (Roy, 2016). Other studies on wheat and rice have reported a strong influence of N availability on MYB expression (Curci et al., 2017, Wang et al., 2019a). The bZIP family had members which were upregulated or downregulated by N limitation. Most of the upregulated bZIP TFs were ABA-inducible TFs associated with ABA signalling, such as orthologues of *OsbZIP72* and *OsbZIP46*. Downregulated bZIP TFs had protein similarity with AtbZIPs associated with sugars utilization, such as members of the S1- and C-bZIP subfamily. Among the DE TFs families, NF-YA showed proportionally the most striking response to N-limiting conditions. In fact, more than 60% of the expressed NF-YA TFs in nodes were found to be upregulated. In durum wheat, NF-Y TFs are regulated in roots (Curci et al., 2017). Induced expression of NF-Y genes has been associated with increased prolonged exposure to stress conditions, including N stress (Zhao et al., 2011, Leyva-González et al., 2012). In addition, induced expression of NF-Y genes increases N uptake and grain yield in wheat (Qu et al., 2015). Other families which were regulated by N supply were LOB, TAZ and GARP-ARR-B. Type-B RRs are involved in the CK signalling pathway, which, as discussed above, may have a role in plant response to N limitation, as CK levels and metabolism were negatively affected by N limitation. Members of the AS2/LOB family, also known as LOB-domain TFs (LBD), had been initially identified to control plant organ development but are also involved in plant responses to different cues (Zhang et al., 2020). Similarly, the TAZ family was the family with the highest percentage of downregulated TFs. Some

members of the TAZ family, such as BT2 and BT1, were recently found to act as repressors of the nitrate response in *Arabidopsis* (Sato et al., 2017).

The plant N-response is known to involve complex transcriptional networks. Recent studies utilizing system biology analyses have identified important TFs controlling the expression of downstream genes acting as master regulators of the N response (Ueda et al., 2020, Gaudinier et al., 2018). Those TFs control different modules of genes leading to morphological and physiological changes as part of plant adaptation to N-limiting conditions. Many of the previously identified TFs related to plant response to N availability were found to be differentially expressed in basal nodes in this study. *LBD37, 38, 39* homoeologues were strongly downregulated by N limitation. *LBD37, 38, 39* have been previously established as N status regulators acting as repressors of genes involved in N uptake (Gaudinier et al., 2018, Rubin et al., 2009). In rice, *LBD38* was found to connect different N-deficiency response modules, highlighting the importance of *LBD38* in regulating the N response (Ueda et al., 2020). *NIGT1* TFs are N-inducible and act as negative feedback regulators suppressing the expression of nitrate-inducible genes (Maeda et al., 2018). Furthermore, Ueda et al. (2020) showed that *OsHHO3* and *OsHHO4*, which are functional orthologues of *AtNIGT1*, are important components of the N response in rice. The expression of *OsHHO3* and *OsHHO4* orthologues was strongly downregulated in nodes. The expression of BTs has also been linked with NUE and N response in rice and *Arabidopsis* (Araus et al., 2016, Sato et al., 2017). The expression of genes encoding proteins orthologous to *AtBT1, 2* were suppressed by N limitation. In contrast, orthologous genes of previously identified N-inducible TFs, which play central roles in maintaining the coexpression network of the N response, such as *TGA1, NFYA5* and *BBX16*, were found to be strongly upregulated in N-limited nodes (Gaudinier et al., 2018, Alvarez et al., 2014). Finally, the *TaNAC2* homoeologues were also found to be significantly induced by N limitation. In wheat, *NAC2* is involved in the N response by binding to the promoter region of genes for N transporters and N assimilation enzymes. Furthermore, overexpression of *TaNAC2-5A* has been associated with higher N uptake and grain yield (He et al., 2015). The observed effect of N limitation on previously identified key transcriptional regulation of the N response in other species showed that there is a conserved

mechanism of N response among species, while it also provided a good reference for their regulation under low N conditions in wheat nodes (as presented in Figure 4.9).

4.3.2 Tissue-specific Regulation of SL Biosynthetic and Signalling Genes by Nutritional Signals

Results from Chapter 3 showed that N limitation strongly induced SL biosynthesis in basal nodes and roots of wheat plants grown under N limitation. P supply is considered the primary signal controlling SL biosynthesis, and furthermore, SLs are responsible for tillering regulation by P availability (Umehara et al., 2010, Yoneyama et al., 2012). Therefore, a comparative analysis of the transcriptional effect of N and P limitation on SL biosynthetic and signalling genes was carried out. Based on the RNA-seq data in the basal nodes, the N limitation led to a more substantial upregulation of many SL biosynthetic genes compared to the P limitation. P limitation was found to have a significant effect on the mRNA abundance of *TaD10* homoeologues, but the induction was weaker compared to the N limitation response. Differential gene expression analysis between low N and low P plants showed that the transcript levels of many SL biosynthetic and signalling genes were significantly different between the two treatments. Assuming that shoot P status is the primary signal controlling SL biosynthesis in nodes, one explanation could be that the internal concentration of P was not low enough to trigger a low P response. However, the elemental analysis showed that low P plants had a 2-fold lower concentration of P in shoots. N-limited plants also showed reduced P concentration in shoots, but the concentration was much higher than in low P plants. As a result, the P concentration in the shoot cannot explain the strong upregulation of SL biosynthesis in nodes. However, gene expression analysis in roots by RT-qPCR revealed that P limitation had a more substantial effect on SL biosynthesis genes than N limitation. More specifically, the low P effect on most of the *MAX1* genes in roots was stronger compared to the low N effect. Combining these results, it is suggested that SL biosynthesis is regulated by different signals between roots and shoots in response to plant nutritional status. SLs are known to have a dual role as a rhizosphere signal and as plant hormones. In roots, SL production and exudation have been associated with AMF colonization. AMFs are known to facilitate P uptake under P deficiency. In contrast, in nodes, SL act as a negative

regulator of bud outgrowth. Therefore, the distinct role of SL biosynthesis might also explain the presence of distinct mechanisms that control SL biosynthesis in different tissues. Consequently, it may be hypothesised that in roots, P limitation strongly induced SL biosynthesis to increase SL exudation to facilitate AMF colonisation and increase P uptake, while in nodes, SLs act mainly as phytohormone coordinating bud suppression and possible N limitation signalling.

In many species, the recorded increase in SL production and exudation is much stronger under P-limiting conditions compared to N limitation (Yoneyama et al., 2012). However, no previous study has compared the effect of the two nutrient limitations on basal nodes or buds, where SLs act as repressors of tillering. Yoneyama et al. (2012) hypothesised that the N limitation effect on SL biosynthesis is attributed to the lower P uptake observed in N-limited plants. Based on the P analysis performed in this study, N limitation negatively impacted P concentration in both roots and shoots, but the concentration found in N-limited plants was significantly higher compared to the one observed in P-limited plants. Combining those two observations, the P content appears not to be the signal controlling SL biosynthesis in nodes because if this were the case, the induction of SL biosynthesis would be stronger under P limitation. Therefore, there must be other factors, such as N content or other hormones, which regulate SL biosynthesis, at least locally in the nodes. In split root experiments in sorghum, it was shown that N or P were not the signals directly controlling the expression of SL biosynthetic genes in roots (Yoneyama et al., 2015, Yoneyama et al., 2020b). In addition, in the same studies, it was suggested that neither IAA nor CKs are responsible for controlling SL biosynthesis in response to nutritional signals, although both hormones affect the expression of SL biosynthetic genes when applied externally. In fact, the levels of most of the CKs were strongly downregulated in N-limited roots, while no effect was observed under the P limitation. Therefore, CKs cannot be the signal leading to strong upregulation of SL biosynthetic genes under P-limiting conditions.

Chapter 5 Generation and Functional Characterisation of a Strigolactone-deficient Mutant

5.1 Introduction

5.1.1 Background

Strigolactones play an important role in regulating shoot branching in many species. Most of our knowledge about the involvement of SLs in tillering regulation comes from studies in rice. However, there is limited information about the role of SLs in other grasses, such as wheat. Only recently, Zhao et al. (2020) showed that *TaD27*-RNAi lines and *TaD27* overexpressing lines showed higher and lower numbers of tillers, respectively, confirming that SLs play a major role in tillering regulation in wheat. In the same study, the transcriptomic analysis showed that *TaD27* silencing triggers changes in axillary buds, affecting bud development (Zhao et al., 2020). Based on the results presented in Chapters 3 and 4, SL biosynthetic genes are strongly induced by N limitation locally in the basal nodes. Therefore, SLs might play an important role in regulating tiller formation by N limitation and generally in plant adaptation to N-limiting conditions. In addition, fewer studies have focused on the potential role of SLs as signals affecting plant N limitation responses.

5.1.2 Carotenoid Cleavage Oxygenase/Dioxygenase

SLs, based on their nature, belong to the group of apocarotenoids - carotenoid cleavage products. The class of apocarotenoids includes not only SLs but also ABA. Both are biologically important compounds – phytohormones – controlling ubiquitous developmental processes and regulating plant stress responses. As a result, apocarotenoid biosynthesis is considered an essential biosynthetic pathway in plants (Felemban et al., 2019). Apocarotenoid biosynthesis is mainly catalysed by members of the carotenoid cleavage oxygenase (CCO) family, which are commonly referred to as carotenoid cleavage dioxygenases (CCDs). Whether the members of this family have monooxygenase or dioxygenase activity remains elusive. For this reason, both terms, CCOs or CCDs, are used in the literature to describe this protein family. The members of this family are non-haem iron enzymes, in which catalytic iron (Fe^{2+}) is chelated by four histidine residues, a characteristic only found in a handful of enzymes.

Phylogenetic studies have shown that the presence of these four histidines is conserved among CCOs from different species, indicating that they are essential for Fe^{2+} coordination (Harrison and Bugg, 2014). Most of the CCOs show high substrate specificity, catalysing the oxidative cleavage of specific double bonds of their substrates. CCOs in plants are divided into two main types, namely, 9-cis epoxy carotenoid dioxygenases (NCEDs) and CCDs (Harrison and Bugg, 2014). The former class is involved in ABA biosynthesis, whereas the main representatives of CCDs, CCD7 and CCD8, are involved in SL biosynthetic pathway (**Figure 5.1**).

In *Arabidopsis*, the CCO family consists of nine enzymes, five NCEDs (NCED2, 3, 5 and 6) and four CCDs (CCD1, 4, 7 and 8). The number of CCOs in other plant species varies mainly due to the different number of NCED encoding genes present in their genome. NCED enzymes cleave neoxanthin into xanthonin, which is the precursor of ABA. On the other hand, CCDs catalyse the oxidative cleavage of double bonds in various positions in different carotenoids. For instance, CCD1 is responsible for the biosynthesis of volatile compounds responsible for the scent and aroma of certain plant species. CCD4 function has been linked with carotenoid homeostasis in different tissues or biosynthesis of volatile compounds and pigments (Bruno et al., 2016). Finally, CCD7 and CCD8 are part of the core SL biosynthetic pathway working in concert to produce CL, the precursor of bioactive SLs. Phylogenetic and evolutionary studies have revealed that plant CCDs share high amino acid and nucleotide sequence similarity allowing the identification of important domains and amino acid residues (Harrison and Bugg, 2014). Among the plant CCOs, only Viviparous14 (VP14/NCED1) from maize has been crystallised and structurally characterised, providing important information about the active site and substrate specificity of CCOs (Messing et al., 2010).

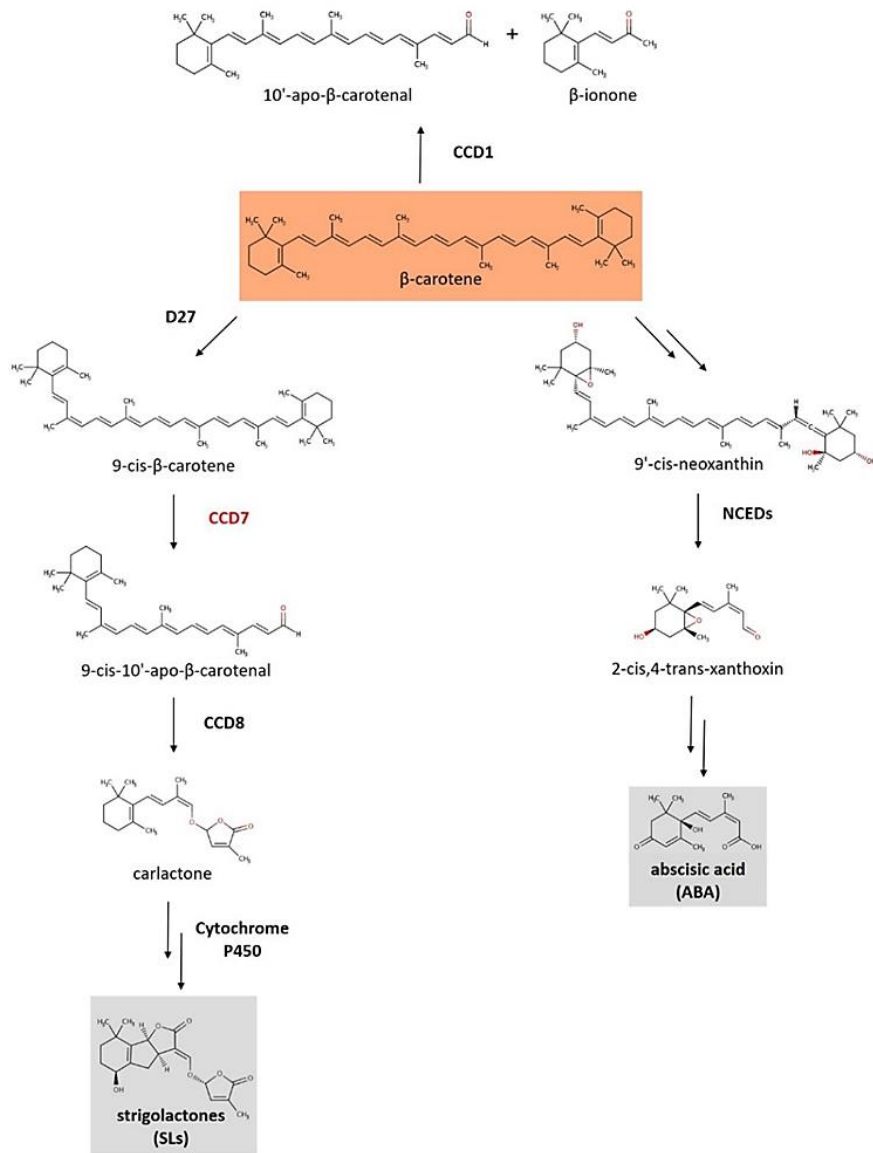


Figure 5.1: Simplified biosynthetic pathway of the main apocarotenoid signalling molecules, SLs and ABA. Carotenoid cleavage dioxygenases (CCDs) catalyse the cleavage of β-carotene, the precursor of SLs and ABA. 9-cis-epoxycarotenoid cleavage dioxygenases (NCEDs) initiate the formation of ABA, whereas CCD7 and CCD8 are key enzymes of SL biosynthesis. The formation of 9-cis-β-carotene, which is the substrate of CCD7, from β-carotene is catalysed by the isomerase DWARF27.

5.1.3 Expression Pattern of *TaD17* in Wheat

SL biosynthesis was initially thought to predominately occur in the root based on the initial discovery of SLs acting as rhizosphere signals. Several studies have shown that SLs are transported from root to shoot to control lateral branching (Mashiguchi et al., 2021). However, the expression of SL biosynthetic genes has also been detected by gene expression studies in basal nodes and axillary buds in different species, such as in rice (Xu et al., 2015b, Umehara et al., 2010). Similarly, grafting experiments in dicotyledonous species have demonstrated that locally synthesized SLs in the shoot are sufficient to regulate branching, further suggesting that apart from the root, SLs are also biosynthesized in above-ground tissue. As presented in sections 3.2.4 and 4.2.13, mRNA of the main biosynthetic genes was detected in basal nodes of wheat plants based on both RT-qPCR and RNA-seq experiments. Zhao et al. (2020) showed that *TaD27-2B* is expressed in axillary meristems of wheat using *in situ* hybridization (Zhao et al., 2020). Similarly, expression of *TaD17* was also detected in dormant lateral buds and the surrounding leaf primordia in wheat, as shown in **Figure 5.2E-F** (unpublished data). These observations indicate that *TaD27* and *TaD17* expression in lateral buds might play a role in tiller bud inhibition in response to different signals. The expression of *TaD17* overlaps with the expression of dormancy-associated genes and cell-cycle genes found to be affected by the SL-mediated bud dormancy (Luo et al., 2019), indicating that SLs, apart from acting as mobile signals, are also biosynthesized *in situ* to control bud dormancy. *In situ* hybridization in wheat roots also showed that *TaD17* expression is localized in the endodermis and the pericycle cells (**Figure 5.2A**).

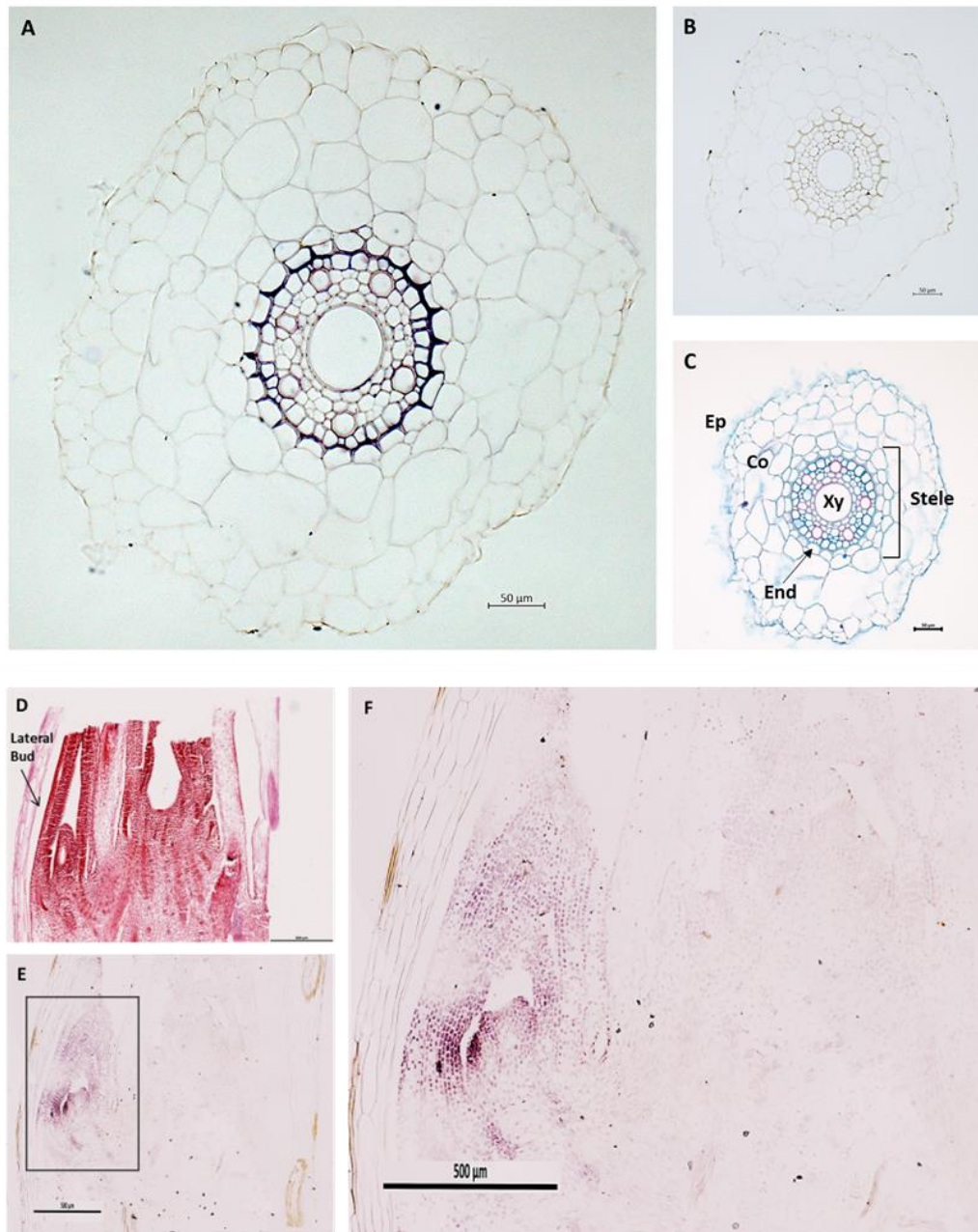


Figure 5.2: *In situ* hybridization analysis of *TaD17* in root and the basal node of wheat. (A) Cross-section of root (anti-sense probe), (B) cross-section of root (sense probe – control), (C) cross-section of root stained with Safranin and fast Green staining. (D) Longitudinal section of basal node at tillering stage stained with Safranin. The arrow indicates the dormant lateral bud. (E-F) Longitudinal section of basal node at tillering stage (antisense probe). Scale bars: A-C, 50 µm; D-E, 500 µm. Abbreviations: epidermis (Ep), cortex (Co), endodermis (End), xylem (Xy). This work is part of unpublished data⁵.

⁵ Petros Sigalas would like to thank Dr Yongfang Wan for kindly performing the *in situ* hybridization, sectioning and microscopy.

5.1.4 Targeting Induced Local Lesions in Genomes (TILLING)

The generation of an SL-deficient plant is a promising way of investigating the role of SLs on wheat architecture and particularly on tillering. This can be achieved by generating a loss-of-function mutant for genes involved in SL biosynthesis. TILLING is an ideal non-transgenic method for this purpose in wheat because different mutant lines with missense mutations in different homoeologues can be identified and stacked for the generation of a triple knock-out (null) plant.

TILLING is a reverse genetic approach for inducing and identifying mutations in specific genes. In principle, TILLING combines chemical mutagenesis, such as the use of the chemical mutagen ethyl methanesulfonate (EMS), with sensitive mutation detection techniques. EMS induces random point mutations in the genome resulting in G/C to A/T substitutions. Those changes provide a great source of genetic variation as they can lead to loss of encoding protein function due to a premature stop codon or an abnormal splicing site. Nucleotide substitutions could also alter protein function due to missense mutations on important amino acid residues in the active site of the encoded protein (Uauy et al., 2017). Several different methods have been historically used for detecting the introduced mutations in genes. Most of the techniques were based on PCR screening of the candidate gene region. However, those methods were expensive and labour-consuming, making TILLING less exploited. The recent development of sequencing technologies along with bioinformatic tools paved the way for utilising TILLING for functional genomic studies.

In plants, the first TILLING population was described in *Arabidopsis* (McCallum et al., 2000), while since then, TILLING populations have been developed in many species, including crop plants such as rice, maize and wheat (Chen et al., 2014). TILLING provides an excellent source for functional studies but also for crop breeding programs as the mutations are non-transgenic and are inherited from one generation to the other. In addition, TILLING is especially suited for polyploid species, such as wheat, since the latter show a higher mutation tolerance rate compared to diploid species (Uauy et al., 2017). The higher tolerance of polyploid species to higher mutation load is attributed to the presence of multiple homoeologues, which compensate for the effect of a truncation mutation in a gene. However, for the same reason, the

generation of knock-out mutant in wheat is a time-consuming process since it requires knocking out all the three homoeologues of the gene of interest.

Wheat TILLING populations have been developed in tetraploid durum wheat cv 'Kronos' and in hexaploid bread wheat cv 'Cadenza' as part of a joint project between the University of California Davis, Rothamsted Research, The Earlham Institute, and the John Innes Centre (Krasileva et al., 2017). The EMS TILLING population of wheat includes more than 2700 mutant lines, 1535 and 1200 in tetraploid and hexaploid wheat, respectively. All the mutant lines have been sequenced by exome capture and initially aligned to the reference genome, IWGSC CSS assembly. All the data became publicly available through www.wheat-tilling.com. In total, more than 10 million mutations have been identified in protein-coding regions. This corresponds to an average of 23-24 mutant alleles per gene. Based on the predicted mutational effect, knock-out mutations have been identified in around 90% of the captured genes (Krasileva et al., 2017). The identification of the mutation sites and the prediction of their effect was also performed based on the RefSeq1.1 gene annotation after alignment to the IWGSC RefSeq v1.0 genome assembly. The updated data have been deposited on Ensembl Plants and are publicly accessible.

5.1.5 Chapter Objectives

The aim of this chapter was first to generate an SL-deficient mutant in hexaploid wheat and, secondly, to understand the role of SLs as a signal under N-limiting conditions. To address the second objective of this chapter, the generated triple knock-out mutant *Tad17* (aabbdd) was used for a transcriptomic study in nodes under two different N regimes.

5.2 Results

5.2.1 Identification of Wheat Candidate Genes for the Generation of an SL-deficient Mutant

The first step for the generation of an SL-deficient mutant was the *in silico* analysis of all the SL biosynthetic genes and the identification of the targeted gene. For the generation of a triple knock-out mutant, mutant lines from the TILLING population of the hexaploid wheat, *T. aestivum* cv. Cadenza, were used (Krasileva et al., 2017). The orthologues of wheat genes involved in the SL biosynthesis and signalling have been identified as described in the previous section 3.2.1. Among the SL biosynthetic genes, *D27*, *D17/CCD7* and *D10/CCD8* were putative genes for the generation of a triple knock-out mutant based on our approach. As there are multiple *MAX1* genes in wheat, the generation of a mutant line for all the copies would be complicated and time-consuming. Therefore, *MAX1s* were excluded as candidate genes for the generation of SL-deficient mutants. All the available mutant lines in the TILLING population of *TaD27*, *TaD17* and *TaD10a* homoeologues were retrieved from the EnsemblPlants database (**Table 5.1**). No available mutations in the protein-coding region (CDS) of any of *TaD27* homoeologues were found, so *TaD27* was also excluded as a candidate gene. In contrast, for the homoeologues encoding *D17/CCD7*, 53 mutations were identified in the coding region of *TaD17-2A*, while there were 96 and 57 in *TaD17-2B* and *TaD17-2D* CDSs, respectively. Among the available mutation types, for the purpose of this study and for functional studies, predicted loss-of-function mutations were required. Loss-of-function mutations are the mutations that lead to a premature stop codon in the open reading frame, also known as nonsense mutations. In fact, three, four and one mutant lines were identified with a stop gained mutation in the A-, B- and D-genome copies of *TaD17*, respectively. Finally, two nonsense mutations were found in the CDS of both *TaD10a-2A* and *TaD10a-2B*, whereas none were found in *TaD10a-2D*. The absence of available premature stop codon mutation was also confirmed by accessing wheat.tilling.com, the legacy database for wheat TILLING population mutants. Another type of mutation that might result in abnormal protein is mutation resulting in different splicing of the exons. However, neither *TaD27* homoeologues nor *TaD10-3D* were found to have any mutant line annotated into this category. Another

important consideration was the presence of three wheat homoeologues (*TaD10b*) with high sequence similarity with *TaD10a* genes (section 3.2.1). Those genes potentially have a similar function to *TaD10a* and might mask the effect of *TaD10a* knock-out.

Hence, due to the presence of available TILLING mutant lines with stop codon gained mutations in all three copies of *TaD17*, this gene was selected for the generation of a *Tad17* triple knock-out mutant.

Table 5.1: Summary of the available hexaploid wheat TILLING mutants in the protein-coding region of SL core biosynthetic genes, *TaD27*, *TaD17* and *TaD10a*. For the generation of a triple knock-out mutant, mutant lines with stop gained mutation in the protein-coding region of all three homoeologues are required.

Gene	Encoded Protein	Gene ID	CDS mutations	Stop codon gained
<i>TaD27-7A</i>	Beta-carotene isomerase D27	TraesCS7A02G418900	0	0
<i>TaD27-7B</i>	Beta-carotene isomerase D27	TraesCS7B02G319100	0	0
<i>TaD27-7D</i>	Beta-carotene isomerase D27	TraesCS7D02G411500	0	0
<i>TaD17-2A</i>	Carotenoid cleavage dioxygenase 7 (CCD7)	TraesCS2A02G414600	53	3
<i>TaD17-2B</i>	Carotenoid cleavage dioxygenase 7 (CCD7)	TraesCS2B02G433800	96	4
<i>TaD17-2D</i>	Carotenoid cleavage dioxygenase 7 (CCD7)	TraesCS2D02G411900	57	1
<i>TaD10a-3A</i>	Carotenoid cleavage dioxygenase 8 (CCD8)	TraesCS3A02G274300	73	2
<i>TaD10a-3B</i>	Carotenoid cleavage dioxygenase 8 (CCD8)	TraesCS3B02G308000	92	2
<i>TaD10a-3D</i>	Carotenoid cleavage dioxygenase 8 (CCD8)	TraesCS3D02G273500	76	0

5.2.2 Identification of Mutations within *TaD17* Homoeologous Sequences

Among the available mutants with a loss-of-function mutation, one mutant line for each of the *TaD17* homoeologues was selected for the generation of the triple knock-out mutant (**Table 5.2**). Mutant lines with predicted larger deletions were preferable because it is more likely to result in non-functional proteins. More specifically, Cad1738, Cad1271 and Cad0880 lines were selected for crossings. Although Cad1247 carries longer deletion compared to Cad1217, Cad1271 was finally selected based on the initial zygosity of the TILLING mutants in the population. More specifically, the Cad1271 line was listed as homozygous in the M2 population; therefore, it was

preferred compared to the heterozygous Cad1247. However, finally, it was proven that even Cad1271 was also heterozygous in the M4 population.

Table 5.2: Mutant line IDs with a stop-gained mutation in the protein-coding region of *TaD17* homoeologues. For each mutant line, the respective mutation site is also reported, along with the position of the premature codon in the protein-coding region (CDS) and in the protein.

Variant ID	Chr	Mutation	Type	AA	Position in transcript	Position in CDS	Position in protein
Cadenza1738	2A	C/T	Stop-gain	Gln/*	539/2058	469/1836	157/ 611
Cadenza1271	2B	G/A	Stop-gain	Trp/*	1275/1848	1275/1848	425/615
Cadenza0880	2D	G/A	Stop-gain	Trp/*	1448/1950	1448/1845	483/614
Cadenza0676	2A	G/A	Stop-gain	Trp/*	1243/2058	1173/1836	391/ 611
Cadenza2070	2A	G/A	Stop-gain	Trp/*	1243/2058	1173/1836	391/611
Cadenza1247	2B	G/A	Stop-gain	Trp/*	1185/1848	1185/1848	395/615
Cadenza0596	2B	G/A	Stop-gain	Trp/*	1274/1848	1274/1848	425/615
Cadenza0908	2B	G/A	Stop-gain	Trp/*	1614/1848	1614/848	538/615

Line Cad1738 carries a C to T change at nucleotide 539 in the *TaD17-2A* transcript (TraesCS2A02G414600). This mutation results in a change of Glu157 to stop codon, hence in deletion of 455 amino acids. Similarly, mutant line Cad1271 carries a G to A substitution at nucleotide 1275 of *TaD17-2B* (TraesCS2B02G433800), leading to a premature stop codon at position 425 out of 615 in D17-2B. Finally, line Cad0880 shows a deletion of 132 amino acids from the C-terminus end of D17-2D due to a G to A substitution at position 1448 of the protein-coding region. The mutation sites in the genomic sequences are shown in **Figure 5.3**, whereas the nucleotide sequences compared to the wild-type sequence are shown in **Figure 5.4**. Based on the above-mentioned deletions, it is likely that the encoded proteins are non-functional. Hence, homozygous plants carrying all three mutations are not expected to produce SLs. The functionality of the mutated proteins is also discussed in section 5.3.1.

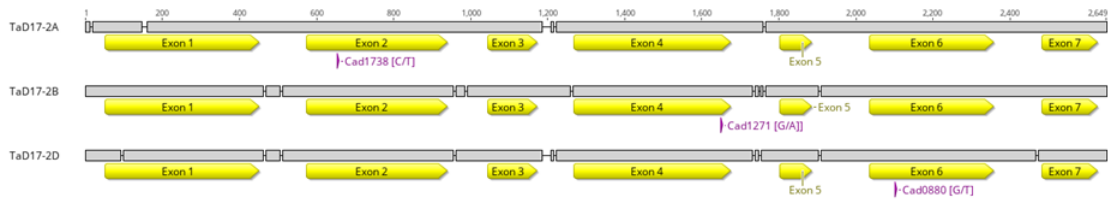


Figure 5.3: Position of the selected mutations within the genomic sequence of *TaD17* homoeologues. Yellow arrows correspond to the exon sequences. The selected mutations that introduce a premature stop codon are indicated by a purple arrow below the exon annotations, along with the name of the corresponding TILLING mutant line.

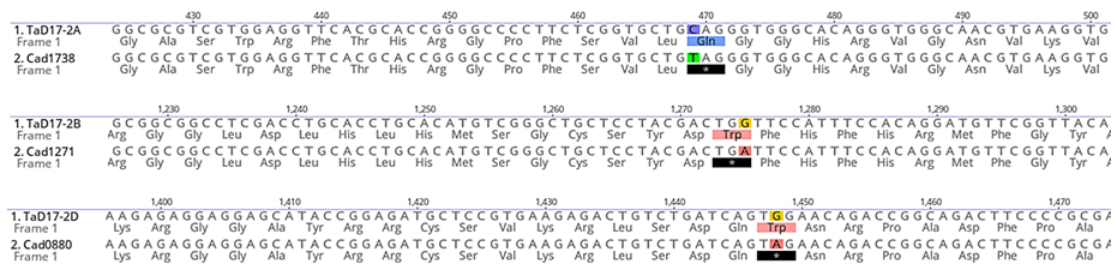


Figure 5.4: Nucleotide and amino acid sequence alignment of the WT *TaD17* homoeologues with the corresponding selected loss-of-function mutant lines. The highlighted nucleotides correspond to the C/T or G/A substitution sites. The premature stop codons are indicated by the black highlight.

5.2.3 Identification of Conserved Amino Acid Residues in Wheat D17/CCD7

After selecting the mutant lines carrying a nonsense mutation in *TaD17* homoeologues, the predicted functionality of the mutated proteins was examined *in silico*. D17/CCD7 belongs to the family of CCOs. The members of this protein family are involved in the specific cleavage of terpenoids having a central role in apocarotenoid biosynthetic pathways, such as in ABA and SL biosynthesis. To identify highly conserved motifs and amino acid residues, a protein alignment of various CCOs from many plant species was conducted. The conservation of regions or specific amino acid residues throughout evolution among different organisms usually indicates the importance of those conserved regions in the structure and functionality of the proteins. Such conserved motifs may act as active sites or binding sites of the protein receptors etc. The amino acid sequence of D17/CCD7, D10/CCD8, and CCD1 from *O. sativa* var Japonica, *Z. mays*, *H. vulgare*, *B. distachyon* and *A. thaliana* were included in the analysis along with all known AtNCEDs (**Figure 5.5**). ZmVP14 (NCD1) is the only member of this protein family in plants that has been previously crystallised and

structurally characterised (Messing et al., 2010); therefore, ZmVP14 was used as a prototype for the identification of important conserved amino acid residues in CCDs.

Based on previous studies and the sequence alignment of CCOs, four histidine residues (His) are conserved across all the examined plant species (**Figure 5.5**). Previous functional studies have shown that those four His are binding sites for the catalytic Fe^{2+} (Messing et al., 2010). Similarly, Harrison and Bugg (2014) also reported that the presence of His is conserved across taxa suggesting that coordination of Fe^{2+} by His residues is essential for the functionality of the CCOs (Harrison and Bugg, 2014). Therefore, the lack of the His residues involving the chelation of catalytic Fe^{2+} could negatively affect the functionality of the enzyme. In addition, previous studies have shown that three glutamic acid (Glu) residues are important for the stereochemistry of ZmVP14. More specifically, Glu264, Glu477 and Glu530 have been suggested to be essential for the positioning of the above-mentioned His residues. According to the protein alignment, Glu264 and Glu530 are conserved across all the examined CCOs. On the other hand, Glu477 was found to be conserved in all NCEDs, while it has been replaced by aspartic acid (Asp) in the CCDs (CCD1, CCD8 and CCD7). The presence of the Asp residue in this position was conserved in all the examined CCDs.

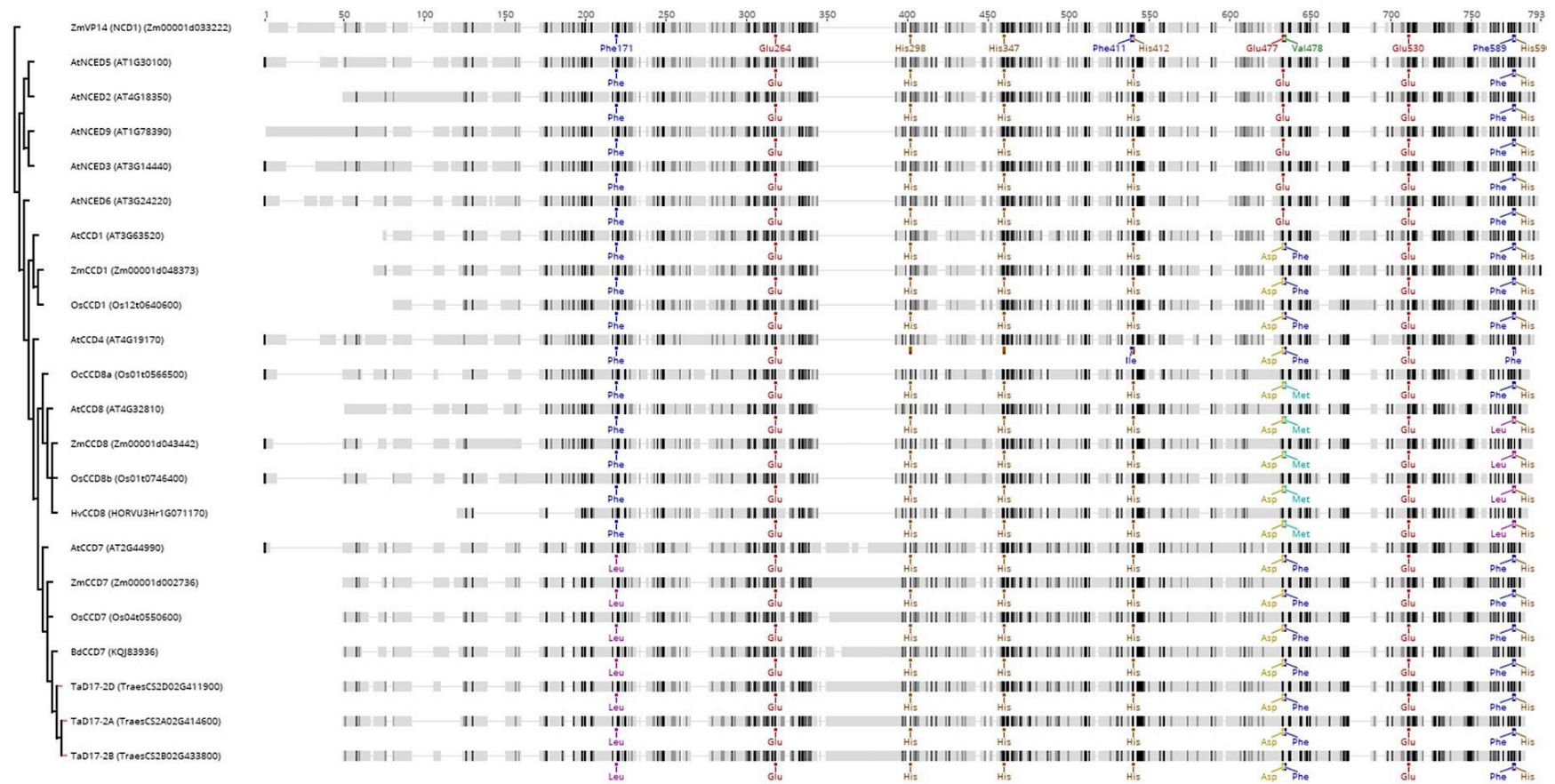


Figure 5.5: Protein alignment of members of the CCD/CO family from various plant species, including TaD17-2A, -2B and -2D. The protein sequence of ZmVP14 (NCD1), which has been previously crystallised, was used for the identification of conserved amino acid residues. The annotated amino acid residues correspond to conserved amino acids involved in Fe²⁺ position (His), substrate positioning (Phe, Leu, Met) and the protein structure (Glu, Asp) according to previous studies.

Substrate positioning in ZmVP14 is coordinated in the active site by three phenylalanine (Phe) residues, Phe171, Phe411 and Ph589. Those Phe residues are generally conserved in plant CCOs; however, some substitutions have been found in different locations among plant CCO enzymes, which presumably alter the stereospecificity of the enzyme (**Figure 5.5**). More specifically, in CCD7, Phe171 has been substituted by leucine (Leu). Substitution of the Phe has also been reported in AtCCD4, in which Phe411 is replaced by isoleucine (Ile, Ile411) (Bruno et al., 2016). Finally, the substrate specificity of CCOs has been attributed to amino acid residue at position 478. In NCEDs, valine (Val), alanine (Ala) or Ile is found in this location, while CCDs were found to carry Phe or methionine (Met). Consistent with that, TaD17/CCD7 was found to have Phe in this position based on the protein alignment, while Met was found in CCD8s.

In addition to the protein alignment, the SWISS-MODEL tool (<https://swissmodel.expasy.org/>) was also used for the prediction of the overall structure and the important amino acid residues of wheat D17/CCD7 encoded by *TaD17-2A* based on homology modelling (Waterhouse et al., 2018). The results highlighted four His residues in the protein sequence of TaD17-2A (His226, His316, His394 and His605), which were predicted to be involved in the tetradentate coordination of the catalytic Fe²⁺. This is consistent with the position of the four His residues identified by the protein alignment. Finally, the Phe486 was also identified as a putative substrate-binding site (**Figure 5.6**).

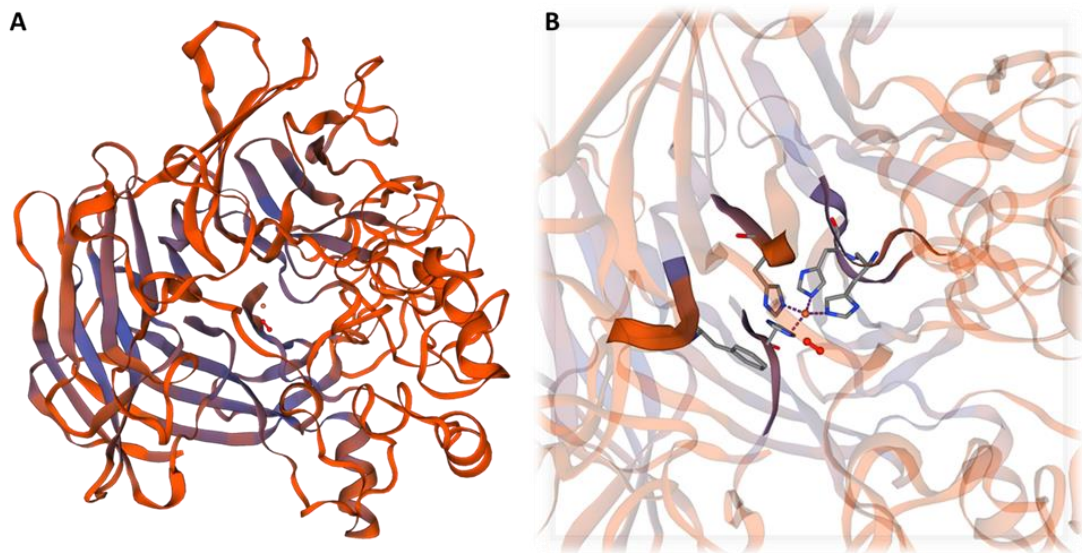


Figure 5.6: (A) Predicted overall structure and (B) active site of TaD17-2A (D17/CCD7) enzyme. The highlighted amino acid residues correspond to the four His residues [His226, His316, His394 and His605] predicted to be involved in the coordination of the catalytic iron (Fe^{2+}) and the Phe486 as substrate binding site. The 3D model was generated using the SWISS-MODEL tool based on homology modelling.

5.2.4 Genotyping of the M4 Generation

After the *in silico* analysis and the selection of mutant lines, Cad1738, Cad1271 and Cad0880, seeds for each line were obtained from Rothamsted's TILLING population seed bank. All the selected mutants were listed as homozygous for the mutations of interest in the M2 generation. Therefore, only four seeds were screened per line. The presence of the mutation and the zygosity state of the lines was confirmed prior to crossings. This was achieved by performing genotyping by sequencing. For this purpose, homoeologue-specific primers were designed for the amplification of the region containing the mutation of interest.

On the grounds that high specificity in terms of amplification was needed for genotyping purposes, gradient PCR was conducted to determine the optimum annealing temperature for each set of primers (**Figure 5.7**). Based on the gel electrophoresis results, primers TaD17_For2A1 and TaD17_RevA1 successfully amplified the 156 bp fragment of *TaD17-2A*. According to the quality of the bands, the best annealing temperature was at 64.6 °C, while it is important to note that successful amplification was achieved without the use of Q5 GC enhancer. For TaD17_ForB1 and TaD17-RevB1, the best band was found at 63.8 °C, which corresponded to a fragment

of 471 bp, as anticipated. TaD17_ForD1 and TaD17_RevD1 showed better amplification of the 447 bp fragment at 66 °C. Q5 GC enhancer significantly improved the amplification of the two latter sets of primers.

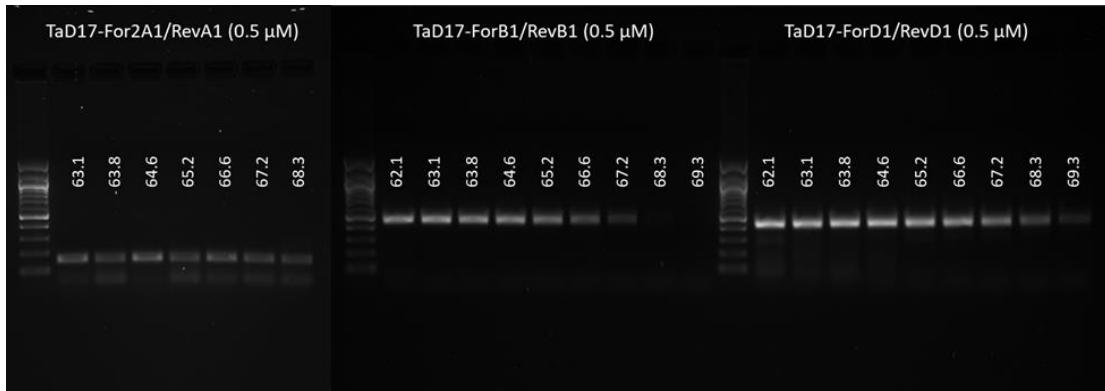


Figure 5.7: Gel electrophoresis of gradient PCR products for the identification of the best annealing temperature for each pair of primers.

Genomic DNA was first extracted from the TILLING mutant plants and was used for PCR amplification of the respective region of interest. PCR products were then purified and sequenced. The sequencing results were then aligned against the WT Cadenza sequence to confirm the presence of the mutation and identify the genotype of the mutant plants. Sequencing results were in accordance with the *in silico* analysis and confirmed the presence of the mutation in *TaD17* homoeologues. All the screened plants of Cad1738 and Cad0880 were found to be homozygous for the targeted SNPs, which was quite convenient for the downstream step of mutant generation (**Figures 5.8A and C**). Although Cad1271 was listed as homozygous in the TILLING population database, all the three mutant plants, which were screened, were found to be heterozygous for the targeted SNP, as is suggested by the double peak on the sequencing chromatograph (**Figure 5.8B**).

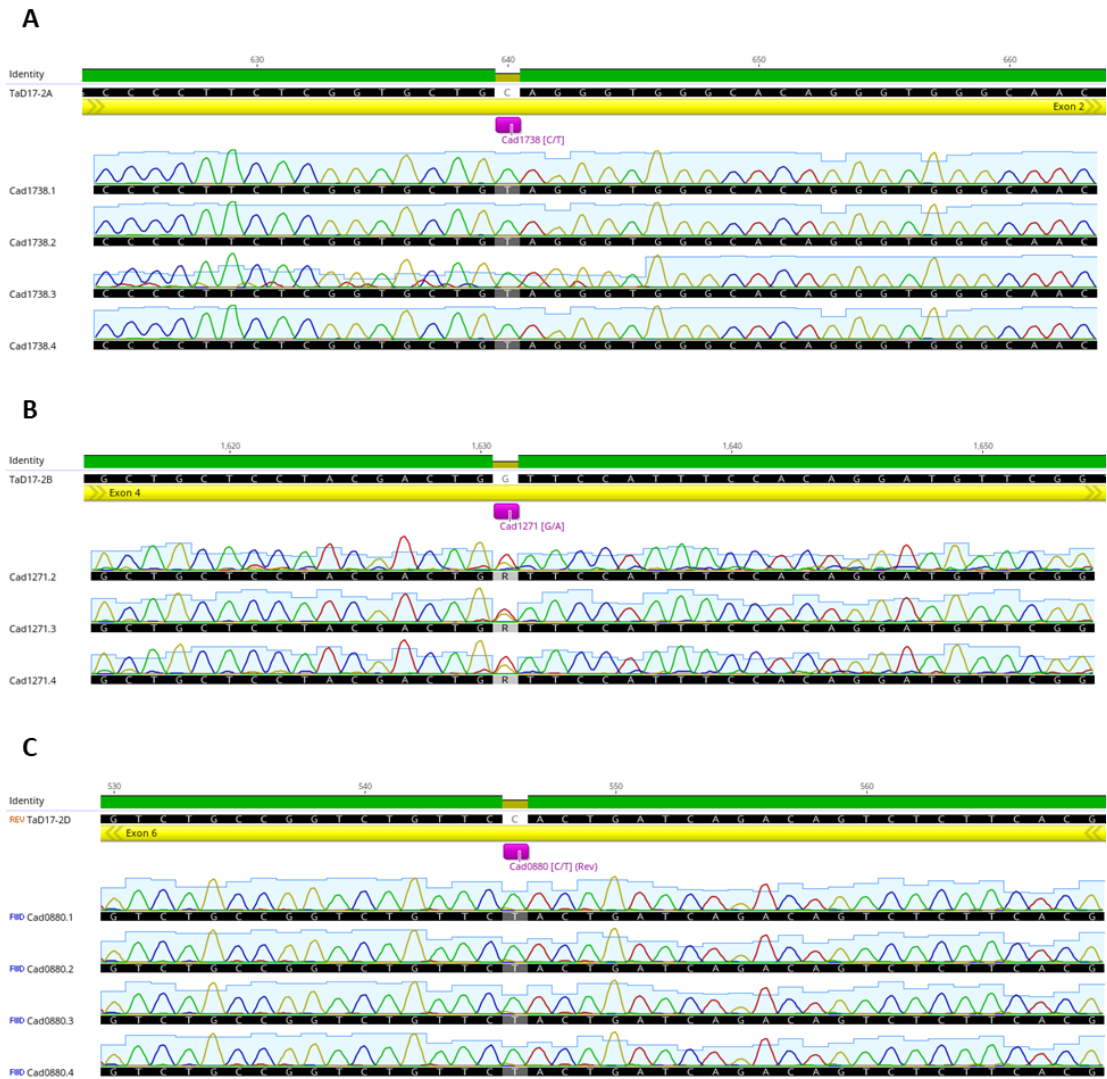


Figure 5.8: (A) Cad1738, (B) Cad1271 and (C) Cad0880 genotyping by sequencing results. Genomic DNA was extracted from M4 mutant plants for each selected line and used for the homoeologue-specific amplification of the region that contains the mutation of interest. The fragment was then sequenced to identify the presence of the SNP based on nucleotide sequence alignment against the WT sequence. The zygosity of the plants was determined based on the SNP base calls in the sequencing chromatograph. The purple annotation corresponds to the mutation of interest.

5.2.5 Design and Optimisation of KASP Assays for the Targeted Mutation Sites

The generation of a triple knock-out mutant in hexaploid wheat required the segregation of three mutations in the same plant, which is achieved by many rounds of crossing. For the high-throughput screening of the plants during the crossing process, a KASP genotyping assay needed to be designed for each of the three selected mutant alleles. KASP is a gel-free fluorescence-based PCR assay for genotyping of SNPs. KASP is preferable compared to other genotyping methods because it is an affordable method which delivers high throughput, highly accurate and effective genotyping of DNA samples (Semagn et al., 2014). The main component of a KASP assay is the assay-specific primers appropriate to distinguish the two alleles (WT, mutant). In total, three primer sequences are required for each studied SNP, one common reverse (forward) homoeologue-specific primer and two SNP-specific forward (reverse) primers. The targeted SNP (mutation site) should be located at the 3' end of the SNP-specific primer sequence allowing specific amplification of the targeted sequence over the non-targeted. At the 5' end, each SNP-specific primer contains a unique tail sequence that corresponds to a universal fluorescence resonant energy transfer (FRET) cassette, one labelled with FAM and the other with VIC fluorescent dyes. At the end of the PCR reaction, the bi-allelic discrimination was achieved based on the generated fluorescent signals due to the competitive binding of the two allele-specific forward primers.

Therefore, the first step in designing the assay-specific primers was to retrieve the genomic sequence of all three genes encoding TaD17/CCD7 of the WT and of the selected mutant lines. Next, the sequences were aligned, and the targeted SNP and the intergenomic SNPs downstream or upstream of the mutation sites were located. Inter-genomic SNPs are single nucleotide variations that exist between genomes (A, B and D). The latter SNP was used for designing primers that amplify specifically the respective genome (A, B or D), whereas two primers that contained the mutation site on their 3' end were designed (**Figure 5.9**). In total, three different KASP assays were developed, one for each of the SNP of the selected mutant lines (**Table 2.3**).

To test the efficiency and the specificity of the designed KASP primers, different DNA samples from already known genotypes (genotyped by sequencing) were used as

positive controls. At least 10 different samples for each genotype (homozygous/heterozygous/WT) were used for testing purposes, including two negative controls. Based on the allelic discrimination plots, all the designed KASP assays showed good clustering and clear separation between the clusters (**Figure 5.10**). Moreover, the genotyping results were consistent with the known genotypes without any mismatch. Those two observations suggest that Cad1738-KASP, Cad1271-KASP, and Cad0880-KASP primers were reliable for genotyping of the targeted SNPs.

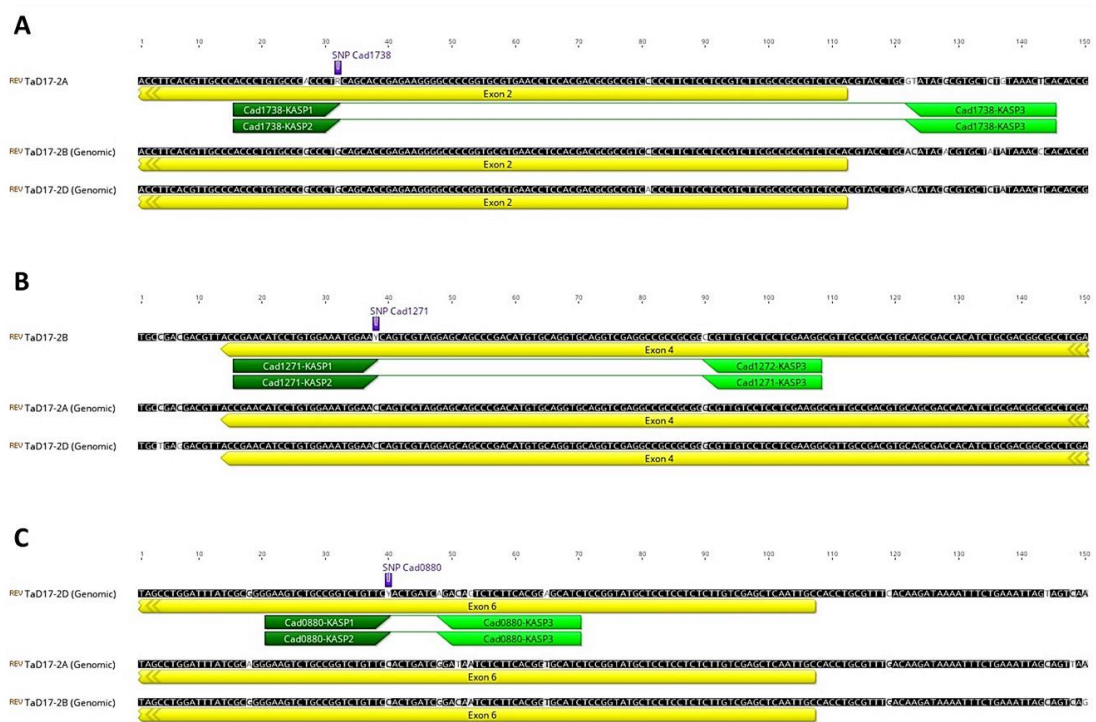


Figure 5.9: Designed KASP assays for genotyping of the selected mutant alleles. (A) *TaD17-2A* Cad1738 mutant allele (B) *TaD17-2B* Cad1271 mutant allele (C) *TaD17-2D* Cad0880 mutant allele. Three primer sequences were designed for each of the targeted SNP, two SNP-specific forward primers with the SNP at the 3' end and a common intragenomic reverse primer. The allele-specific 5' extension (VIC or FAM) was also added to each of the SNP-specific primers for the purpose of KASP assay.

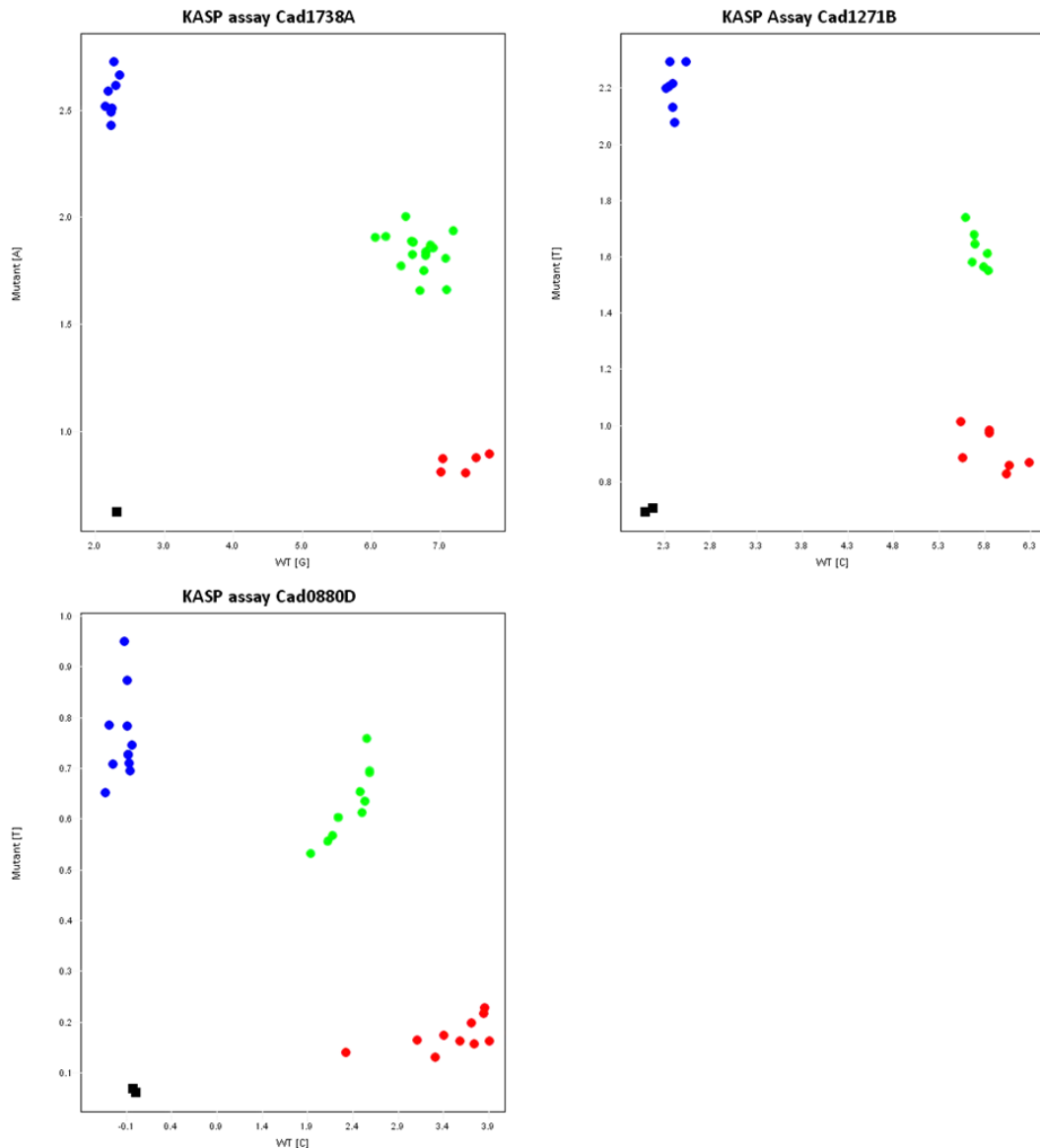


Figure 5.10: Allelic discrimination plots for the designed KASP assays using samples with known genotypes (positive controls) for testing the efficiency and specificity of the KASP assay. KASP assay for Cad1738, Cad1271 and Cad0880 alleles showed good clustering of the samples with the same genotype and clear separation between the clusters.

5.2.6 Stacking of *TaD17* Mutant Alleles

The generation of a triple knock-out mutant starting from TILLING mutant lines required several rounds of crossing in order to stack all the mutant alleles in one individual plant. The followed crossing scheme is illustrated in **Figure 5.11**.

The first round of crossing aimed to combine nonsense mutations in two different homoeologues by crossing the mutant plants identified in the M4 population. More specifically, homozygous plants with stop gain mutation in the *TaD17-2A* (Cad1738)

were crossed with homozygous plants with stop gained mutation in the 2D homoeologue (Cad0880) to produce an F1 progeny containing both A and D *TaD17* mutant alleles. Similarly, Cad1738 was also crossed with heterozygous plants with mutations in the *TaD17-2B* (Cad1271).

The F1 progeny of both combinations was then grown and genotyped by sequencing in order to identify plants that contain the two mutant alleles. For AxB F1, a higher number of plants was screened since the probabilities for a double heterozygous plant were lower than in the AxD F1 (**Figure 5.11**). At least four heterozygous plants, AaBbDD and AaBBDD, were identified and selected in the resulted F1 progenies.

The double heterozygous plants were grown and then crossed to segregate all the *TaD17* mutant alleles in one plant (**Figure 5.11**). More than 30 plants of the resulting progeny were screened for the identification of triple heterozygous plants. Based on the Mendelian inheritance, the probability of a triple heterozygous was one out of 16, while the identification of aaBdDd shared the same likelihood. In total, three triple heterozygous plants (AaBbDd) along with two aaBbDd plants were identified using the designed KASP assays. After confirming the genotypes by sequencing, plants were allowed to self-pollinate to produce an F2 population. Subsequently, around 300 F2 seeds from two triple heterozygous individuals (plant3 and plant4) were grown and screened by KASP assay. Seven triple homozygous individuals for the mutant alleles (aabbdd) were identified in the progeny of plant3, whereas six aabbdd plants were identified in the progeny of plant4. Apart from aabbdd plants, different combinations of homozygous plants were selected along with WT-segregant plants (AABBDD) in both F2 populations.

Crossing scheme - Hexaploid wheat *Tad17* knock-out mutant generation

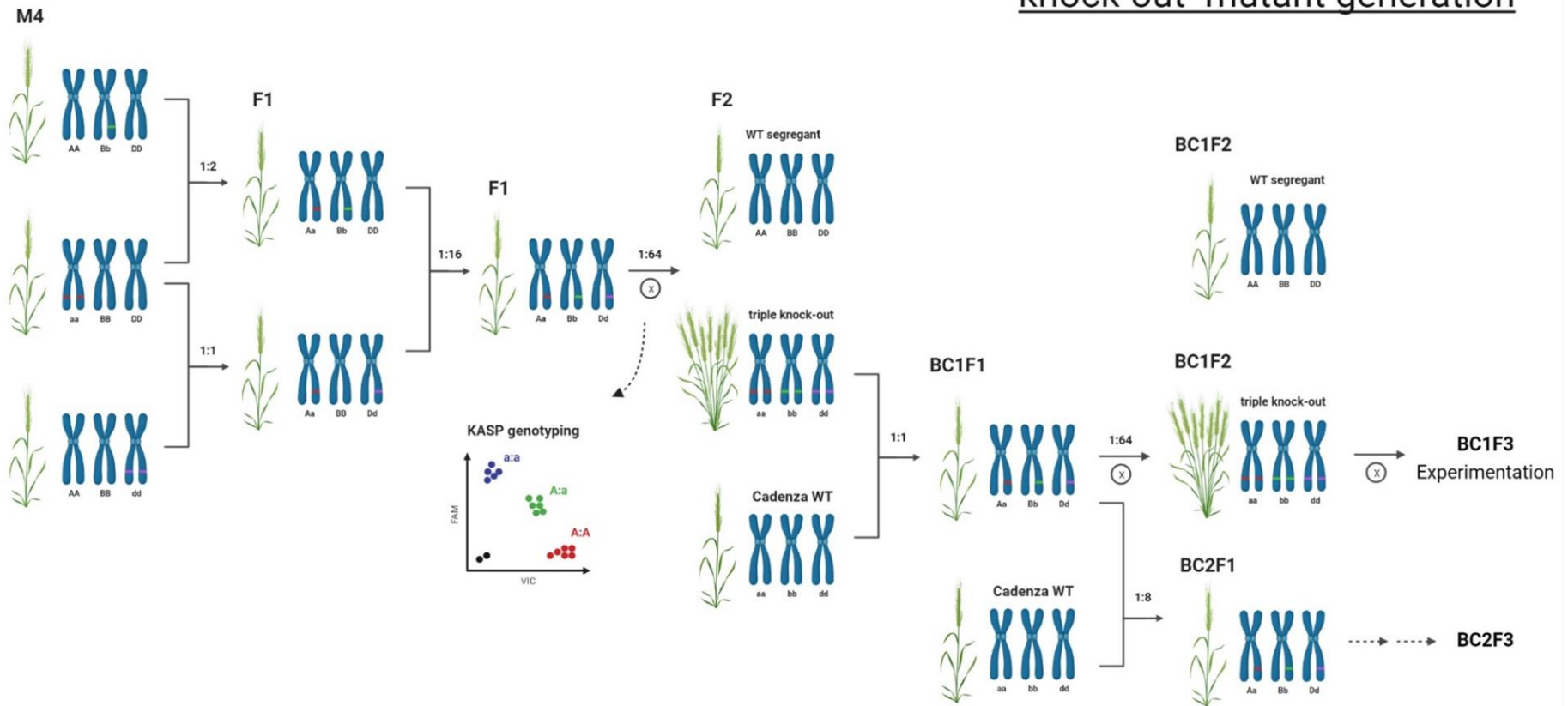


Figure 5.11: Followed crossing scheme to stack the selected *Tad17* mutant alleles in one individual plant. Illustration created with BioRender.

Subsequently, triple homozygous plants for the mutant alleles (aabbdd) were backcrossed with WT Cadenza plants to generate BC1F1 populations. The purpose of the backcrossing was to reduce the background mutation load of the TILLING lines. The produced BC1F1 populations from two individuals (plant3A3 and plant4E1 - one from each F2 population screened in the previous step) were screened for the identification of AaBbDd plants. More than five AaBbDd plants were identified in each of the BC1F1 populations. Selected plants were allowed to self-pollinate to produce BC1F2 populations. Some of the heterozygous plants were backcrossed to WT Cadenza to develop BC2F1 populations to further reduced the mutation load.

The progeny of two self-pollinated BC1F1 AaBbDd plants, plantA4 and plantC6, were grown and screened to identify aabbdd and WT-segregant plants. In fact, at least 200 seedlings per BC1F2 population were screened by KASP assay. Four aabbdd and two AABBDD were identified in the progeny of plantA4, whereas only two aabbdd and two AABBDD were found in the progeny of plantC6. Selected plants were grown in a standard glasshouse in a randomized design to collect some preliminary phenotypic data (section 5.2.7). Plants were allowed to self-pollinate. Seeds from the resulted BC1F3 population of sidling lines (same parental line, plantC6) were used for further experimentation, as explained in section 2.1.5.

Finally, 20 plants from two different BC2F1 populations were screened for the identification of AaBbDd plants. One AaBbDd individual was identified in each of the two different BC2F1 populations screened (plantB6, plantD3). The identified plants were grown and allowed to self-pollinate to produce a BC2F2 population. Around 300 seeds of the resulted progeny of plantD3 were screened by KASP assay. In total, four aabbdd and two AABBDD plants were identified in the BC2F2 and allowed to self-pollinate. Finally, BC2F3 seeds were collected and stored for future experimentation.

5.2.7 BC1F2 *Tad17* Mutants Showed Increased Tillering Phenotype

In total, six triple homozygous plants for the mutant alleles (aabbdd) and four WT segregants (AABBDD) were identified in the BC1F2 populations. One of the identified triple mutants showed many developmental defects potentially related to background mutation. Therefore, five *Tad17* mutants were grown along with the four WT

segregants. The number of shoots per plant was recorded at ear emergence, along with the number of ears at the final harvest (**Figure 5.12**). The mean number of shoots of *Tad17* (aabbdd) was 13 (SE=1.14, n=5), whereas the mean of WT segregants was 7.75 (SE=1.49, n=4). Although the different genotypes were not adequately replicated, the number of shoots and the number of ears per genotype were compared by a two-sample t-test. T-test showed that the difference between the two genotypes was statistically significantly different, $t(7)=2.85$, $p=0.025$. In addition, a significant increase in the final number of ears was recorded between the two genotypes, $t(7)=2.69$, $p=0.031$. In fact, *Tad17* mutants formed 4.3 ± 1.60 more ears than WT segregant plants. The phenotype of those lines close to ear emergence is shown in **Figure 5.13**. Triple knock-out mutant (*Tad17* – aabbdd) showed a higher number of shoots suggesting that SLs are involved in the regulation of tillering in wheat. In addition to that, *Tad17* showed an overall reduced height compared to WT segregant plants, suggesting an effect of SLs on stem elongation. In addition, triple *Tad17* plants from different BC1F2 populations but also plants within each population showed a similar highly branched phenotype indicating the effect is less likely to be related to background mutations given that those lines are segregating background mutations quite independently.

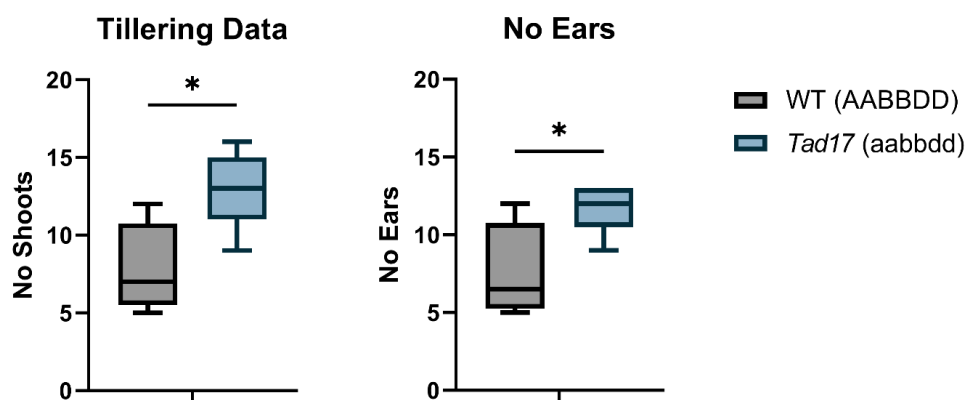


Figure 5.12: Number of shoots at ear emergence and number of ears at final harvest per plant in triple *Tad17* mutants (aabbdd) and WT segregant lines (AABBDD). * denotes significant different between the two genotypes based on two-sample t-test (No Tillers: $t(7) = 2.85$, $p = 0.025$; No Ears: $t(7) = 2.69$, $p = 0.031$).

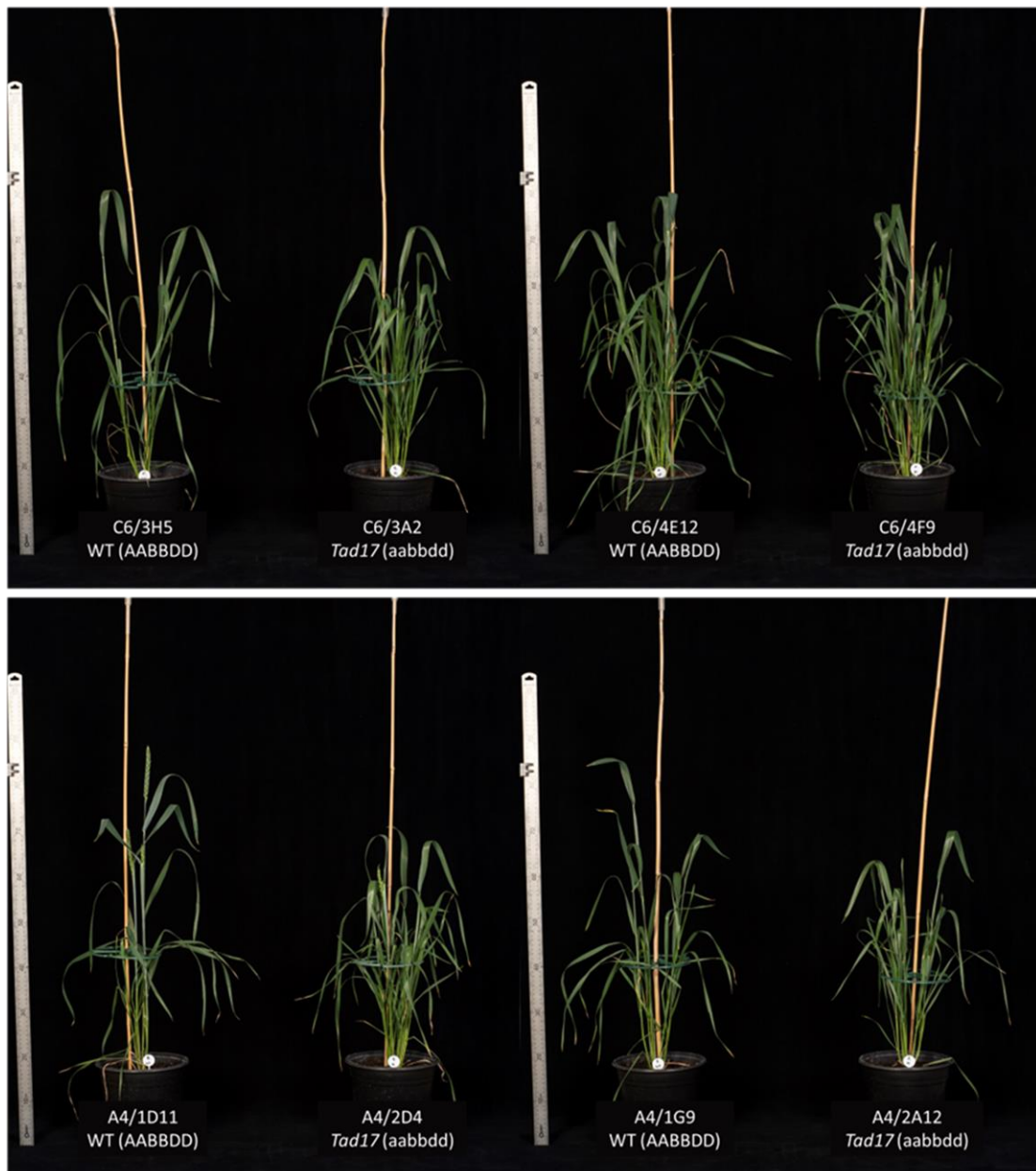


Figure 5.13: Phenotype of *Tad17* TILLING mutant lines from two different BC1F2 populations. Images were taken close to ear emergence. In all the pictures, a metre ruler is shown on the left. **(Top)** Triple *Tad17* mutants (*aabbdd*) along with WT-segregant plants (*AABBDD*) from plantC6 BC1F2 population. **(Bottom)** Triple *Tad17* mutants (*aabbdd*) along with WT-segregant plants (*AABBDD*) from plantA4 BC1F2 population.

5.2.8 Phenotyping of *Tad17* Mutant under High and Low N Conditions

After the initial phenotyping of the BC1F2 mutant lines, it was apparent that the triple *Tad17* mutant formed more tillers than the WT plants. In previous sections (3.2.3, 4.2.13), it was shown that SL biosynthesis was induced by N limitation locally in the nodes indicating that SLs might play a role in controlling tillering in response to N status. Therefore, the response of *Tad17* mutant to N limitation was examined. WT

plants and *Tad17* mutants were hydroponically grown under high N (10 mM) and low N (0.1 mM) conditions. The number of outgrown tillers, along with other phenotypic traits, were recorded in 3-week-old plants, which corresponded to 12 days after the introduction of the plants to N limitation (**Figures 5.14 and 5.15**).



Figure 5.14: Images of 3-week-old representative plants of triple *Tad17* mutants (aabbdd) in comparison to WT segregant (AABBDD) grown under high N (10 mM) or low N (0.1 mM) conditions for 12 days.

A 2-way ANOVA was conducted to examine the effect of genotype and N level on tiller formation. The analysis showed that there was no significant 2-way interaction, $F(1,14)=0.31$, $p=0.588$, $LSD(5\%) = 0.91$. *Tad17* mutant formed more tillers than the WT plants under both N regimes. N limitation had a negative impact on the number of formed tillers in both WT and *Tad17* mutant. Therefore, based on the results, the *Tad17* mutant still responded to N-related signals suggesting that although SL biosynthesis affected tillering, there were other factors contributing to tillering regulation by N status in wheat. Similar results have also been reported by de Jong et al. (2014) in *Arabidopsis* and by Sun et al. (2014) in rice.

In relation to biomass accumulation, ANOVA showed a significant 2-way interaction between genotype and N level, $F(1,13)=6.64$, $p=0.023$, $LSD(5\%)= 0.024$. This finding indicates that the response of root biomass to N limitation was dependent on the genotype. In fact, N limitation had no effect on the root biomass of WT plants, whereas root dry weight (DW) was significantly reduced by N limitation in *Tad17* mutant. In addition, under both N conditions, the root biomass of the *Tad17* mutant was found to be significantly lower compared to the WT. Under high N conditions, the *Tad17* mutant had 15% lower root DW compared to the WT, while under N-limiting

conditions, root biomass was 25% lower in low N plants. This observation indicated that SLs might play a role in root biomass accumulation and resource allocation for root growth, especially under N-limiting conditions.

N limitation significantly reduced the shoot biomass of both genotypes indicating that under N limitation, shoot growth was restricted in both genotypes. No significant difference was found between shoot DW of *Tad17* mutant and WT segregant under high N conditions. However, under N-limiting conditions, the shoot DW of *Tad17* mutant was significantly lower by more than 17% compared to WT control (2-way ANOVA, $F(1,13)=14.08$, $p<0.01$, $LSD(5\%)=0.016$).

Overall, N limitation resulted in a significant increase in root/shoot ratio (N-level effect, $F(1,13)=261.57$, $p<0.001$), showing a redirection of growth toward the root, as has been previously reported in many species (Oldroyd and Leyser, 2020). Despite the observed increase in root fraction in *Tad17* mutant by N limitation, the root/shoot ratio of *Tad17* mutant was significantly lower by 11% compared to the low N WT segregant. Root fraction was also lower in *Tad17* mutant under high N conditions but without a statistically significant difference. This was mainly attributed to the lower root biomass accumulation under low N conditions in the *Tad17* mutant, as described above. Taken together, the effect of genotype on the shoot and root biomass indicated that the *Tad17* mutant showed altered resource allocation, which was mainly apparent under N-limiting conditions.

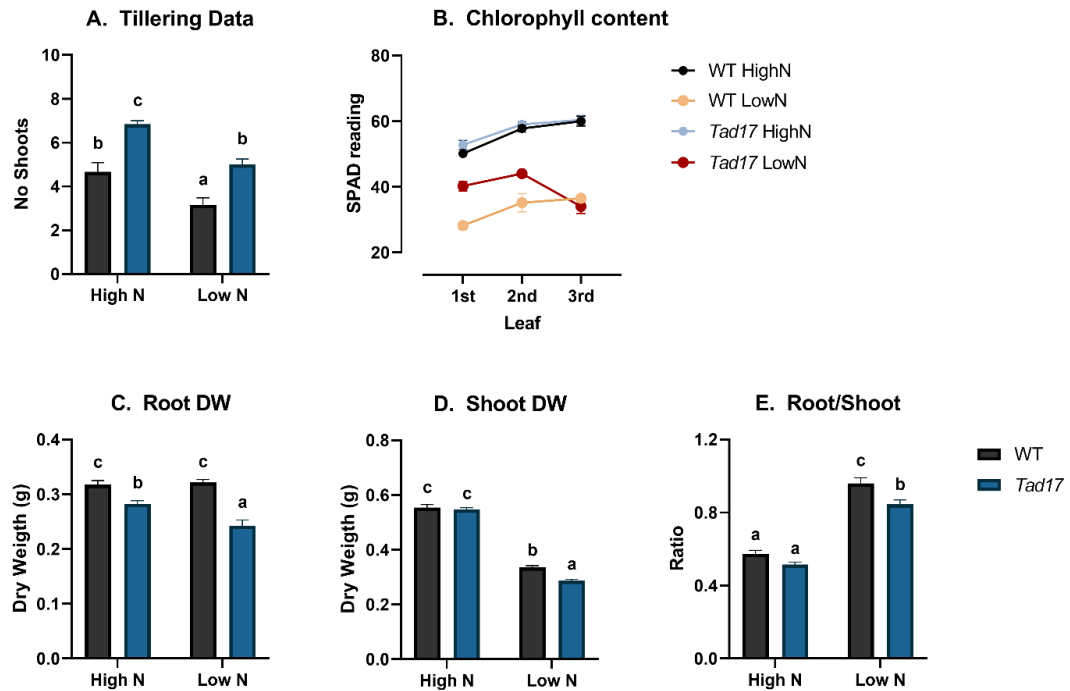


Figure 5.15: Phenotypic responses of triple *Tad17* mutants (aabbdd) to N supply compared to WT segregant plants (AABBDD). (A) Number of shoots per plant, (C) root DW, (D) shoot DW and (E) root/shoot ratio of 3-week-old *Tad17* and WT plants grown on high N (10 mM) or low N (0.1 mM) conditions for 12 days. Values are means of six biological replicates, and error bars represent SE. Statistical analysis was conducted with 2-way ANOVA. Different letters denote statistically significant differences between the group means based on Fisher's LSD test (NoShoots LSD (5%) = 0.91, RootDW LSD (5%) = 0.024, ShootDW LSD (5%) = 0.018, Root/Shoot LSD (5%) = 0.068). (B) Average chlorophyll content across the first, second and third leaf of each genotype under high N and low N conditions. Statistical analysis was conducted with repeated measured ANOVA.

SPAD values were used as a proxy for leaf chlorophyll content of WT and *Tad17* mutant plants. SPAD readings were taken from the three fully expanded leaves of the main stem of 3-week-old plants. The results were analysed with 3-way ANOVA, which showed a significant 3-way interaction between the leaf, genotype and N level (3-way ANOVA, $F(2,32)=6.90$, $p=0.003$). This indicated the genotype effect on chlorophyll content dynamics varies depending on the N levels, as can be shown in **Figure 5.15B**. More specifically, under high N conditions, no effect in the SPAD values was found between *Tad17* mutant and WT plants. In addition, under high N conditions, the chlorophyll content tended to increase from older to younger leaves, with a consistent significant increase in SPAD values between the first and second leaf. Overall, the N limitation had a negative impact on the chlorophyll content of all the examined leaves. However, significant differences in the chlorophyll dynamics were found between

Tad17 mutant and WT segregant under N-limiting conditions. Although the *Tad17* mutant showed a reduction in leaf SPAD values by N limitation, *Tad17* had significantly higher SPAD values in the first and second leaf compared to the low N WT. In fact, SPAD values of the first and the second leaf of the low N *Tad17* mutant were 42% and 25% higher, respectively, compared to the WT plant. The SPAD value of the third leaf was found unaffected. Moreover, under low N conditions, the chlorophyll content of WT plant leaves gradually increased from old to young leaves. The SPAD value of the third leaf was significantly higher than the first leaf by 29%, indicating the reallocation of N from older to younger leaves. On the contrary, a significant decrease in the SPAD value from the second to the third leaf was observed only in *Tad17* mutant under low N (-22%), suggesting that SLs play a role in N translocation from old to young leaves, while this effect is only apparent under N-limiting conditions.

5.2.9 RNA-sequencing in Basal Nodes of the *Tad17* Mutant under High and Low N Conditions

As shown in the previous section (5.2.8), the *Tad17* mutant showed an increased tillering phenotype along with other phenotypic differences compared to WT, suggesting that SLs are involved in tillering regulation in wheat. To understand better how SLs regulate tillering, an RNA-seq experiment was performed in the basal nodes of *Tad17* and WT segregant lines. WT segregant lines are sibling lines with *Tad17*, but they are homozygous for *TaD17* WT alleles. Therefore, *Tad17* and WT segregants show a similar rate of background mutations. In this experiment, BC1F3 lines were used due to time restraints. In order to account for the effect of any background mutation in BC1 lines, the use of progenies from two different BC1F2 plants for each genotype was adopted. Background mutations segregate quite independently in the different BC1F2 lines; therefore, by using different BC1F2, any effect of unwanted background mutation was more likely to be ruled out. Hence, three biological replicates were included per BC1F2 line, which made six biological replicates per genotype (nested experimental design). As the main focus of this work was the involvement of SLs on N response, *Tad17* and WT plants were grown under two different N levels.

Total RNA was extracted from basal nodes of 18-day-old plants grown under high and low N supply for 8 days and submitted for RNA-seq. The number of reads was, on

average, 39.5 M paired-end reads, while that number varied between 27.1 and 49.7 M. On average, 85% of the reads were mapped to the wheat reference genome, while the uniquely mapped reads corresponded to 72%. On average, 57% (53.9-61.8%) of the reads were finally assigned to genes; that is, on average, 26.3 M reads were assigned to genes per sample. The minimum number of reads assigned to genes was 17.6 M. For the transcript abundance calculation, the kallisto tool was used, based on which 76% of the reads were pseudo-aligned to the wheat reference genome. RNA-seq statistics can be found in **Appendix E**.

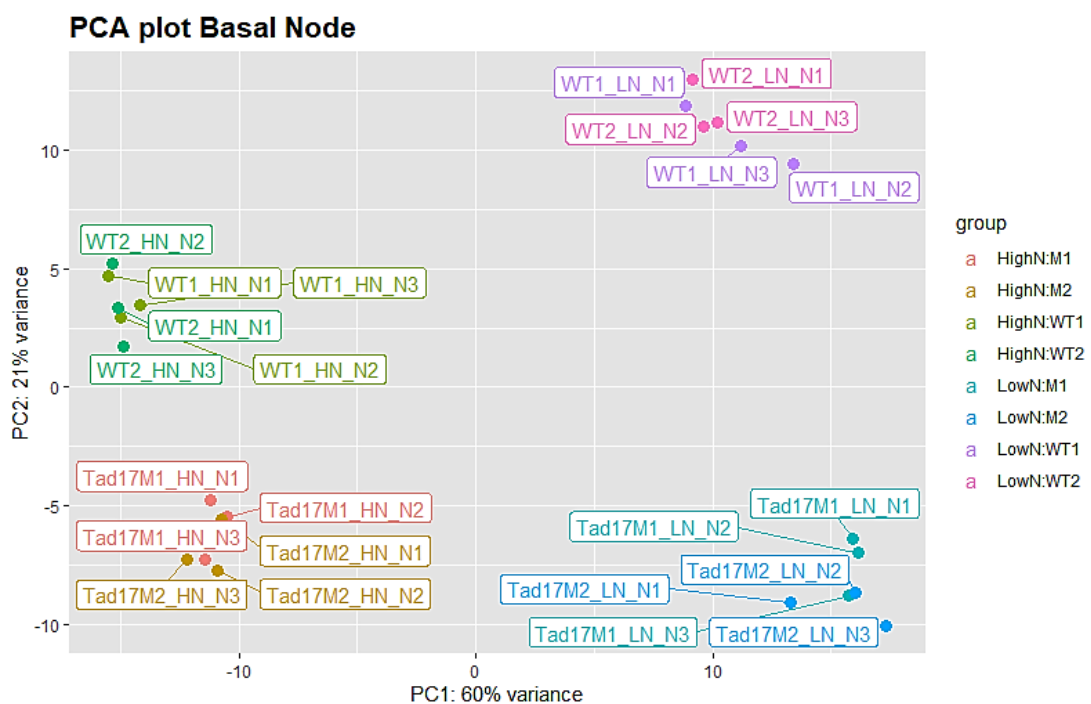


Figure 5.16: Principal component analysis based on the differential gene expression analysis results of genotype (*Tad17*, WT) and N treatment (High N, Low N) effects. PCA was based on the 500 most variable genes. Biological replicates of genotype and N treatment (n=6) form distinct clusters. *Tad17* (M1, M2) and WT (WT1, WT2) sibling lines are also clustering together. PC1 and PC2 account for 60% and 21% of the total variance, respectively.

After prefiltering of low expressed genes, count data generated by the featureCounts tool were used for the differential gene expression analysis. After prefiltering, 91351 genes were included in the analysis. More specifically, 62% of the HC genes (67255 HC) and 15% of the LC genes (24096 LC) passed the prefiltering and were included in the analysis. These results were similar to the result from the RNA-seq experiment conducted in nodes and presented in section 4.2.3.

Prior to the differential gene expression analysis, the quality and the repeatability of the data were assessed by performing a PCA analysis (**Figure 5.16**). Based on the PCA plot, there were four main clusters corresponding to the different genotype and N treatment combinations, suggesting good biological and sequencing repeatability. In addition, the PCA analysis showed that the different lines within the same genotype (*Tad17*: M1 and M2; WT: WT1 and WT2) were also clustering together, suggesting that the observed transcriptomic changes were less likely to be related to the background variability between the lines. PC1 accounted for the majority of the total variance (60%) and separated plants based on the N treatment, indicating that N limitation was the predominant factor affecting the transcriptome in the basal nodes. On the other hand, PC2 accounted for 21% of the variance and corresponded to the genotypic effect. Based on the PCA plot, the distance between WT and *Tad17* clusters in the PC2 was wider in low N treated plants compared to high N conditions, suggesting that genotype had a stronger effect on gene expression under N-limiting conditions. The good biological repeatability and the stronger effect of genotype under N-limiting conditions were also supported by the sample distance matrix, which can be found in **Appendix E**.

5.2.10 Transcriptional Changes in Basal Nodes of *Tad17* Compared to WT Revealed Greater Changes under N Limiting Conditions

For the identification of differentially expressed genes, the DESeq2 tool was used by fitting the appropriate statistical model, Block + Genotype * N level (the script can be found in **Appendix B**). Genes with $\text{padj} < 0.01$ and $\log_2|\text{FC}| > 0.58$ were considered as significantly differentially expressed and retrieved for each comparison of interest. Under high N conditions, 1320 genes were found to be significantly DE in basal nodes of *Tad17* compared to the WT (**Figure 5.17A**). More specifically, 768 genes were downregulated (653 HC and 115 LC), while 552 genes were upregulated (467 HC and 85 LC) in *Tad17*. As suggested by the PCA plot (section 5.2.9), *Tad17* showed more substantial differences compared to WT under N-limiting conditions. Under N-limiting conditions, the number of DE genes in the basal nodes of *Tad17* was four times higher than under high N conditions. In total, 5835 genes were significantly DE under N-limiting conditions in *Tad17* (**Figure 5.17B**). Knock-out of *TaD17* led to significant

downregulation of 3389 genes (2870 HC and 519 LC) and to upregulation of 2446 genes (2061 HC and 385 LC) in N-limited basal nodes.

The genes affected by N limitation were also retrieved. In WT plants, N limitation led to suppression of 6832 genes and induction of 7909 in the basal nodes. In total, 13013 genes were differentially expressed in nodes of *Tad17* mutant in response to N limitation. Apparently, the number of DE genes in response to N limitation was higher than the one presented in section 4.2.4. This might be related to the higher number of biological replicates included in this study (n=6) compared to the RNA-seq experiment presented in Chapter 4 (n=4), which increased the statistical power to identify DE genes.

The main focus of the downstream analysis was the differences between *Tad17* and WT plants and how this effect interacted with plant N status. Therefore, the genes found to be affected by N limitation in this trial were not further explored as the effect of N limitation on the transcriptome in the basal nodes was extensively covered in Chapter 4.

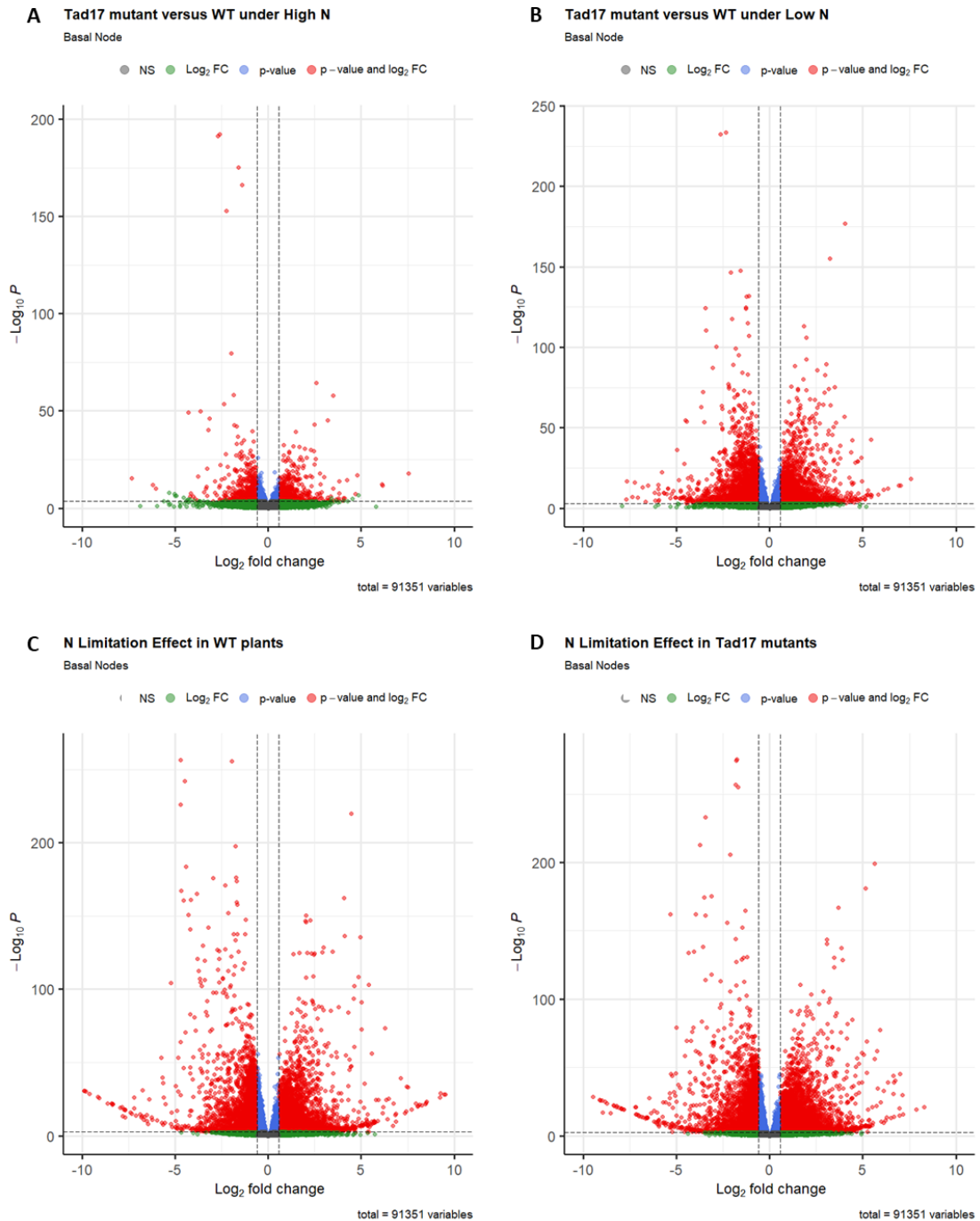


Figure 5.17: Volcano plot of the differential gene expression analysis of the effect of *Tad17* knock-out (A) under high N and (B) under low N conditions and N limitation effect in (C) WT segregant and (D) *Tad17* mutant. After prefiltering low expressed genes, in total, 91351 genes were included in the analysis. Each dot corresponds to a single gene. Red dots represent significantly DE genes ($p_{adj} < 0.01$ and $|FC| > 1.5$). One thousand three hundred twenty genes were found to be differentially expressed in *Tad17* mutant under high N conditions, while 5835 under low N conditions. N limitation significantly affected the expression of 14741 and 13013 genes in the WT and *Tad17* mutant, respectively.

5.2.11 Validation of RNA-seq Results

To validate the RNA-seq results, the gene expression levels of six genes were measured by RT-qPCR. The six genes included in the validation test were *TaCKX3*, *TaD10*, *TaD14*, *TaGS1* (TraesCS6A02G298100, TraesCS6B02G327500, TraesCS6D02G383600LC), *TaNr1* (TraesCS6A02G017500, TraesCS6B02G024900, TraesCS6D02G020700) and *TaSUS2* (TraesCS7A02G158900, TraesCS7B02G063400, TraesCS7D02G159800). Subsequently, a correlation analysis was conducted between the TPM and the NRQ expression values obtained by the RNA-seq and the RT-qPCR, respectively. A high Pearson correlation coefficient ($R > 0.93$) was found for all six genes, suggesting that RNA-seq data were trustworthy.

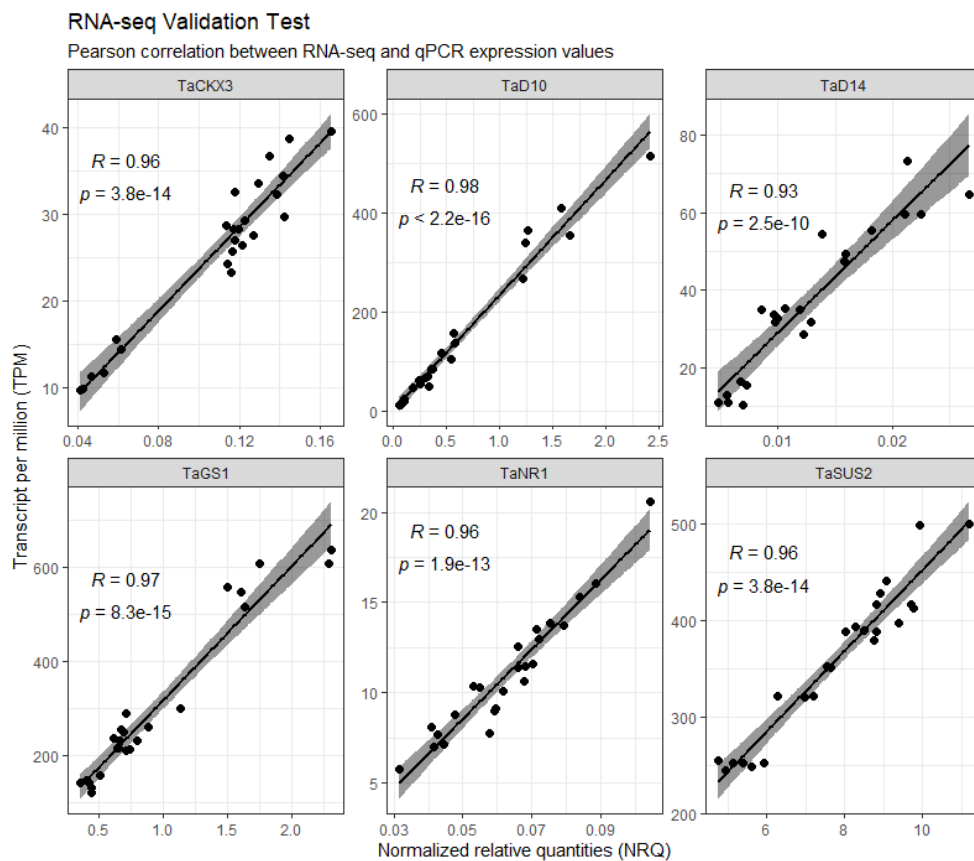


Figure 5.18: RNA-seq validation test results. Pearson correlation analysis of TPM values obtained from the RNA-seq and NRQ expression values obtained from RT-qPCR. Six genes were included in the validation test, namely *TaCKX3*, *TaD10*, *TaD14*, *TaGS1*, *TaNr1* and *TaSUS2*. The comparison between average treatment effects (n=6) based on RNA-seq (TPM) and RT-qPCR data (NRQ) can be found in **Appendix F**.

5.2.12 Functional Annotation Enrichment Analysis of the Transcriptional Changes in *Tad17* Basal Nodes

After identifying the significantly DE genes in *Tad17* under high N or low N conditions, GO term enrichment analysis was performed in GO: profiler in order to identify terms which are enriched in the list of the DE genes. Significant MF and BP enriched terms for each comparison were retrieved. After removing redundant terms with the REVIGO tool, 14 MF and 18 BP GO terms were found to be enriched among the DE genes in *Tad17* under high N conditions. In contrast, under low N conditions, 52 MF and 45 BP terms were overrepresented in the list of DE genes. Among the enriched terms under low N conditions, only the top 32 are presented in **Figures 5.19-20**.

From the GO enrichment analysis, it was found that a greater number of GO terms were enriched in the list of DE genes between *Tad17* and WT under low N supply compared to high N supply. This was anticipated as the effect of *TaD17* knock-out led to more substantial transcriptional changes in the basal nodes under N-limiting conditions, which suggests that the lack of SL biosynthesis affected more biological processes under N-limiting conditions. Nevertheless, many of the enriched GO terms were common in both comparisons, indicating that there are some common processes and pathways controlled by SLs regardless of the plant N status.

According to the GO enrichment analysis, terms related to photosynthesis such as photosynthesis light-harvesting (GO:0009765), photosynthesis (GO:0015979), chlorophyll-binding (GO:0016168) and others were among the top GO terms enriched under both N conditions. Further examination revealed that the same terms were enriched exclusively in the list of downregulated genes suggesting a systematic suppression of genes related to photosynthesis in the basal nodes of *Tad17* mutant. Moreover, BP terms strigolactone metabolic process (GO:1901600) and strigolactone biosynthetic process (GO:1901601) were also among the top enriched terms in both N conditions indicating changes in gene expression levels of SL metabolic genes in *Tad17*. In addition, secondary shoot formation (GO:0010223) was also enriched, indicating changes in genes related to tillering regulation which was consistent with the observed phenotypic differences in tiller number in *Tad17*. However, further examination of the genes annotated with the term secondary shoot formation

(GO:0010223) showed that those genes were also genes involved in SL biosynthesis and signalling. GO enrichment analysis suggested a link between SLs and carbohydrate metabolism as many terms related to carbohydrate metabolism such as disaccharide biosynthetic process (GO:0046351), carbohydrate biosynthetic process (GO:0016051), carbohydrate metabolic process (GO:0005975) were enriched in the list of DE between *Tad17* and WT in both N regimes. In addition to that, carbohydrate transport (GO:0008643) was also enriched, suggesting changes in sugar transporters and altered distribution of sugars in *Tad17*, which might be related to tillering regulation as sugar availability is among the main internal signals controlling bud outgrowth. More generic terms such as transporter activity (GO:0005215) were also enriched, suggesting changes to a wide range of transporters, indicating that not only sugar partitioning but generally resource allocation was altered in *Tad17* compared to WT plants. Trehalose metabolic processes (GO:0005991) were also found enriched in the list of DE genes between *Tad17* and WT independent of the N supply. Tre6P is known to act as a signal of the sugar status affecting developmental decision-making, including bud outgrowth. As a result, this observation provided some indications that SLs might interact with sugar availability signals and the Tre6P metabolic pathway to control bud outgrowth.

Tad17 showed changes in genes related to ureide catabolism, as terms ureide metabolic process (GO:0010135) and allantoinase activity (GO:0004038) were enriched in both lists of DE genes in *Tad17*. More specifically, terms related to allantoin catabolism were enriched in the list of upregulated genes, suggesting that the allantoin catabolic pathway was induced in *Tad17* basal nodes. Allantoin catabolism is part of the plant N recycling mechanism (Lee et al., 2018).

Nevertheless, there were many GO terms enriched in *Tad17* exclusively under N-limiting conditions. Regulation of hormone levels (GO:0010817) was found to be enriched only among the DE genes in N-limited basal nodes on *Tad17* compared to WT, indicating that SL interacts with other hormonal pathways predominately when N is a limiting factor. In fact, the cytokinin metabolic process (GO:0009690), gibberellin metabolic process (GO:0009685) and indole-containing compound metabolic process (GO:0042430) were enriched only under N-limiting conditions. This observation

indicates a direct or indirect effect of SL on CK, GA and IAA metabolisms which was mainly apparent under N-limiting conditions. In addition, the MF term cytokinin dehydrogenase activity (GO:0019139) was also found to be overrepresented, further supporting a link between CK and SLs.

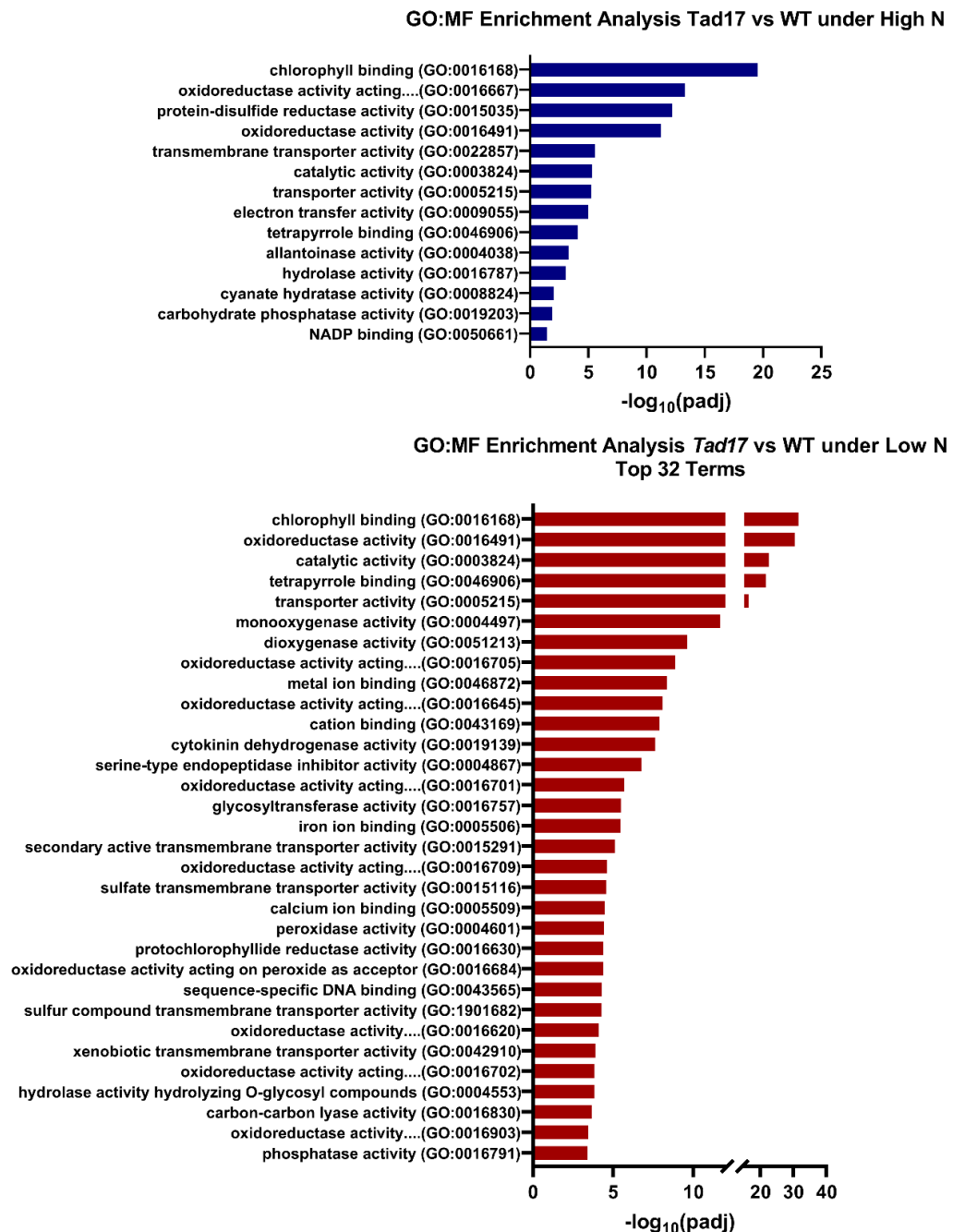


Figure 5.19: Molecular Function (MF) GO term enrichment analysis of the differentially expressed genes in the basal node of *Tad17* mutant (*aabdd*) compared to WT segregant (*AABBDD*). Enriched GO: MF terms in the differentially expressed genes in *Tad17* under (Top) high N and (Bottom) low N conditions.

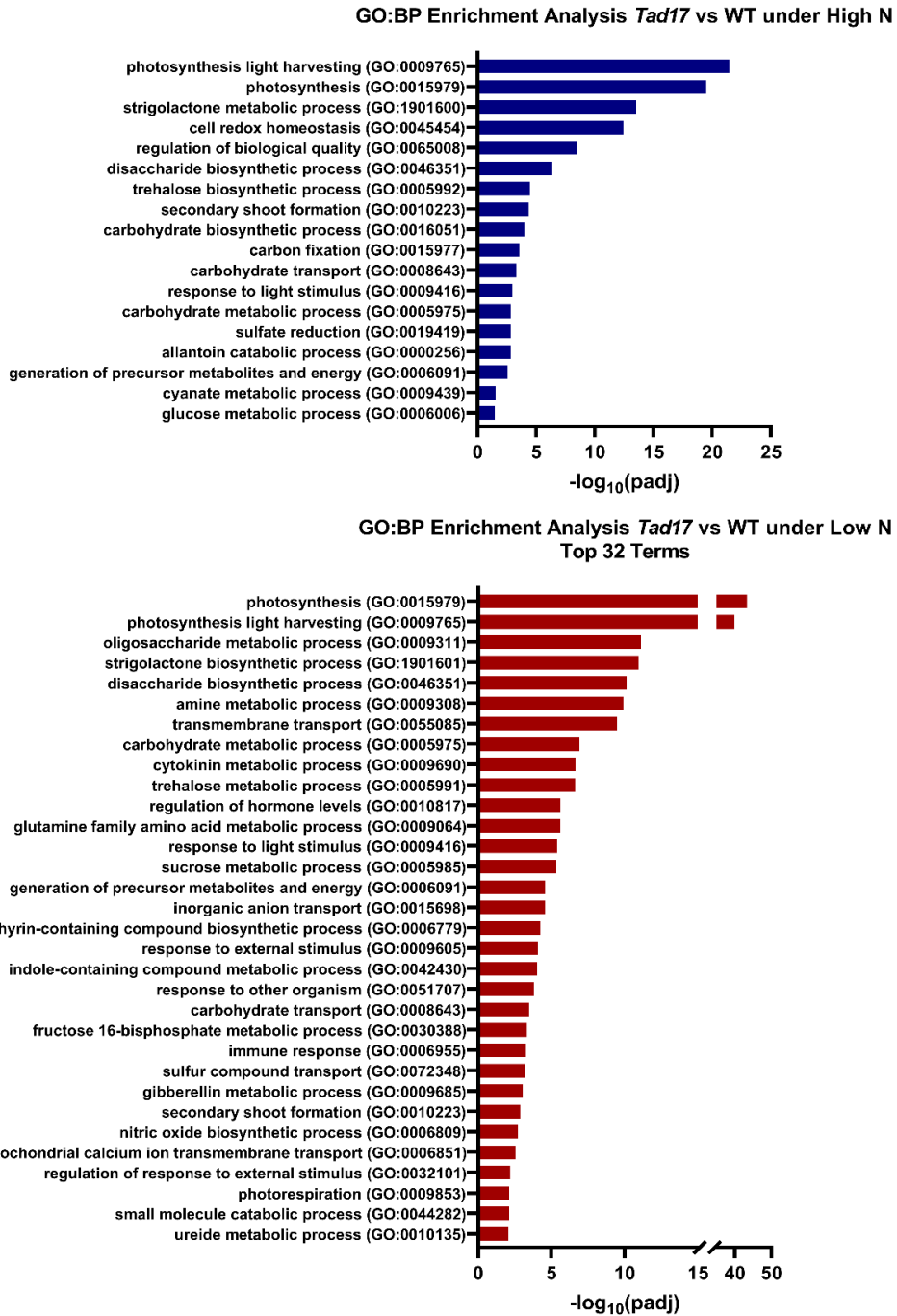


Figure 5.20: Biological Process (BP) GO term enrichment analysis of the differentially expressed genes in the basal node of *Tad17* mutant (aabbdd) compared to WT segregant (AABBDD). Enriched GO: BP terms in the differentially expressed genes in *Tad17* under (Top) high N and (Bottom) low N conditions.

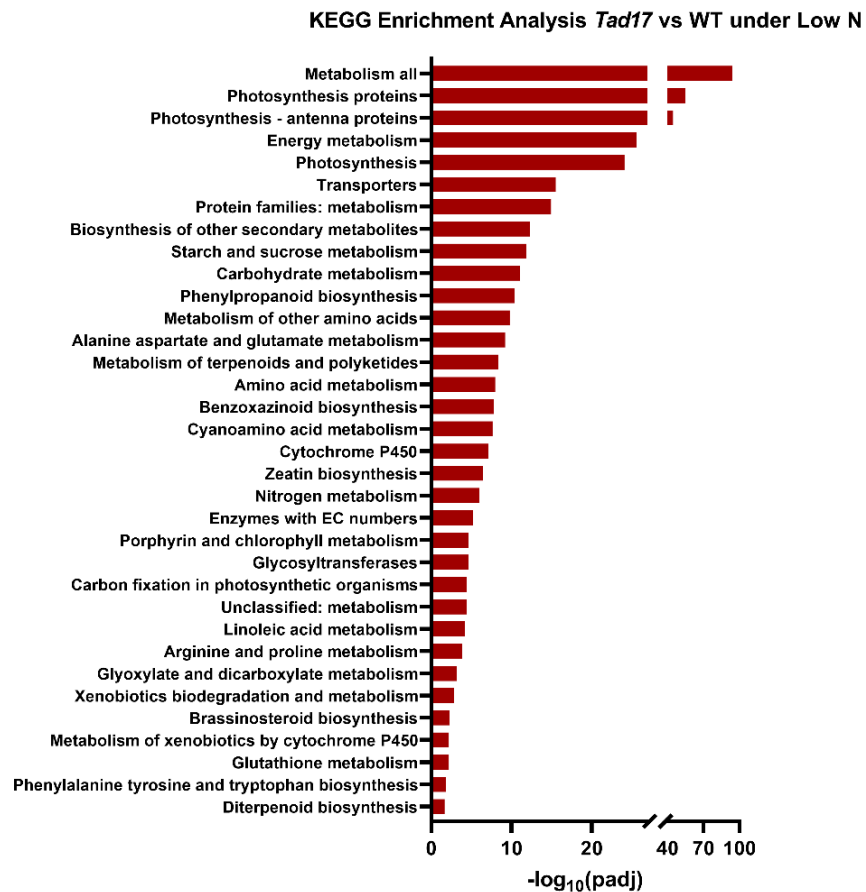
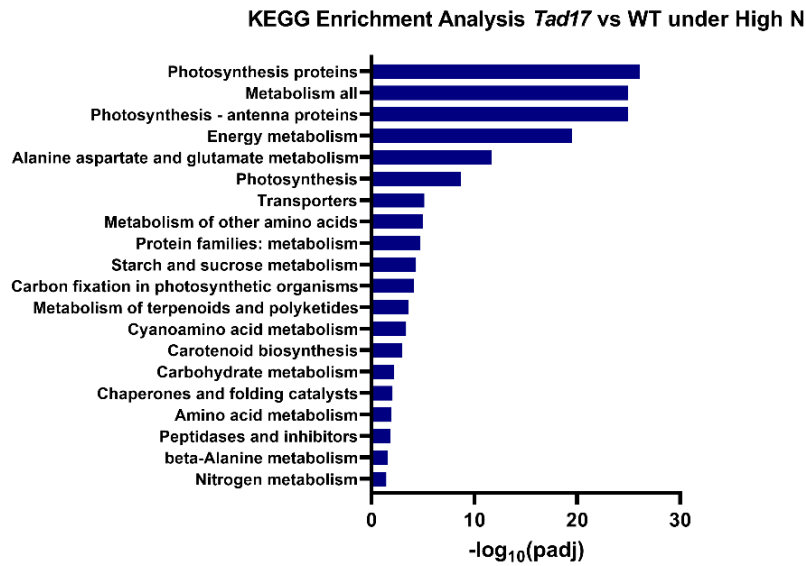


Figure 5.21: KEGG pathway enrichment analysis of the differentially expressed genes in the basal node of *Tad17* mutant (aabbdd) compared to WT segregant (AABBDD). Enriched KEGG terms in the differentially expressed genes in *Tad17* under (Top) high N and (Bottom) low N conditions.

To explore further the affected pathways in *Tad17* mutants, KEGG enrichment analysis was performed for the effect of *Tad17* knock-out mutant in both high and low N conditions (**Figure 5.21**). Consistently with the GO enrichment analysis, KEGG terms related to photosynthesis were significantly enriched under both N regimes. KEGG terms “starch and sucrose metabolism” and “carbohydrate metabolism” were also enriched independently of the N supply. KEGG enrichment analysis also revealed that amino acid metabolism was affected in *Tad17*. More specifically, “alanine aspartate and glutamate metabolism”, “metabolism of other amino acids”, and “cyanoamino acid metabolism” were significantly enriched in both high N and low N *Tad17* compared to the respective WT control. In addition, under low N conditions, terms such as “arginine and proline metabolism” and “phenylalanine tyrosine and tryptophan biosynthesis” were also found to be enriched, suggesting that *Tad17* showed altered expression of genes involved in a wider range of amino acid metabolism under N-limiting conditions. Tryptophan (Trp) biosynthesis is also known to be linked to auxin biosynthesis as Trp is the precursor of IAA biosynthesis. KEGG analysis confirmed a link between CK and SLs, as zeatin biosynthesis was significantly enriched in the list of DE in *Tad17* under N limitation. Recently other studies have also shown a connection between CK and SL metabolism (Zha et al., 2022). Other hormonal pathways were also found to be enriched among the DE genes in *Tad17* under N limitation but to a lesser extent, such as “brassinosteroid biosynthesis” and “diterpenoid biosynthesis”. The latter pathway is related to GA biosynthetic pathway.

5.2.13 *Tad17* Mutants Showed Suppression of Genes Involved in Photosynthesis

As highlighted by GO and KEGG enrichment analysis, the *Tad17* mutant showed a systematic downregulation of genes involved in photosynthesis and carbon fixation. More specifically, genes encoding ribulose biphosphate carboxylase small subunit (TraesCS5A02G165700, TraesCS5B02G162800, TraesCS5B02G162600, TraesCS5D02G169600), different structural components of photosystem I and II, chlorophyll a-b binding protein and many others were suppressed in basal nodes of *Tad17* compared to WT segregant. Although the response was more profound in N-limited basal nodes of *Tad17*, the suppression was consistent in both N regimes included in the study. Basal nodes are not actively photosynthetic tissue, but the

consistency of the response suggests that it might be related to a direct or indirect effect of the lack of SLs in photosynthesis regulation, probably due to changes in carbohydrate metabolism as both photosynthesis and rubisco are known to be influenced by carbohydrate accumulation or by changes in source to sink balance (Paul and Foyer, 2001).

5.2.14 Transcriptional Response of SL Metabolic Genes in Basal Nodes of *Tad17*

SL metabolic pathway was among the top enriched GO terms in basal nodes of *Tad17* under both high N and low N conditions. As a result, it is suggested that the *Tad17* triple knock-out mutant showed altered expression of SL biosynthesis and signalling gene. The responses of all the expressed SL-related genes (TPM>0.5) are presented as a heatmap in **Figure 5.22**. *Tad17* showed a significant upregulation of *TaD27* and *TaD10* homoeologues compared to the respective WT. The expression of both *TaD27* and *TaD10* was 1.8 and 3.6 times higher than the WT under high N conditions. Although the expression of *TaD27* and *TaD10* was induced in nodes under N-limiting conditions, the transcript abundance was 2.2- and 3.6-fold higher in N-limited *Tad17* compared to N-limited WT plants. Analysis of *TaMAX1* homoeologues showed that some of *MAX1* were also induced in the *Tad17* mutant. In addition, the transcript abundances based on this RNA-seq experiment also confirmed that *TaMAX1c* and *TaMAX1d* homoeologues were the predominant *MAX1* genes expressed in basal nodes, as previously discussed in section 3.3.3. The strong upregulation of SL biosynthesis suggests the presence of feedback regulation of SL biosynthetic genes by SL levels, as the absence of SLs in the *Tad17* mutant led to systematically higher expression of the other biosynthetic genes. The presence of negative feedback regulation of SL biosynthetic genes has also been previously reported in other species, such as rice and Arabidopsis, as the expression of the biosynthetic genes has been found to be induced in SL-deficient or -insensitive mutants (Umehara et al., 2008, Mashiguchi et al., 2009, Waters et al., 2012). On the other hand, *TaD14* homoeologues were downregulated in *Tad17* compared to the respective WT. The expression of *TaD3* was not found to be affected, suggesting the presence of a different mechanism that controls the expression of genes involved in SL perception in response to internal SL

levels. Similar downregulation of *TaD14* genes had also been reported in TaD27-RNAi lines in tiller buds (Zhao et al., 2020).

TaD53 is the main repressor of the SL signalling pathway, which is responsible for the transcriptional control of downstream genes (Jiang et al., 2013). *D53* transcription has been demonstrated to be regulated by SLs by a feedback loop (Wang et al., 2015b, Zhou et al., 2013, Song et al., 2017). The transcript abundance of *TaD53* homoeologues was significantly downregulated in nodes of *Tad17* mutant compared to the WT under both the N regimes. This observation suggests that in *Tad17*, the SL signalling pathway is significantly suppressed. The strong suppression of *TaD53* homoeologues also supported that SL biosynthesis was impaired in *Tad17*, providing some evidence that *Tad17* have low levels of SLs. This is supported by the fact that in the absence of SLs, D53 protein is not targeted by the D14-SCF^{D3} complex leading to higher levels of D53 protein, which in turn suppresses the transcription of *D53*, as has been shown for rice and Arabidopsis (**Figure 1.9**) (Zhou et al., 2013, Soundappan et al., 2015).

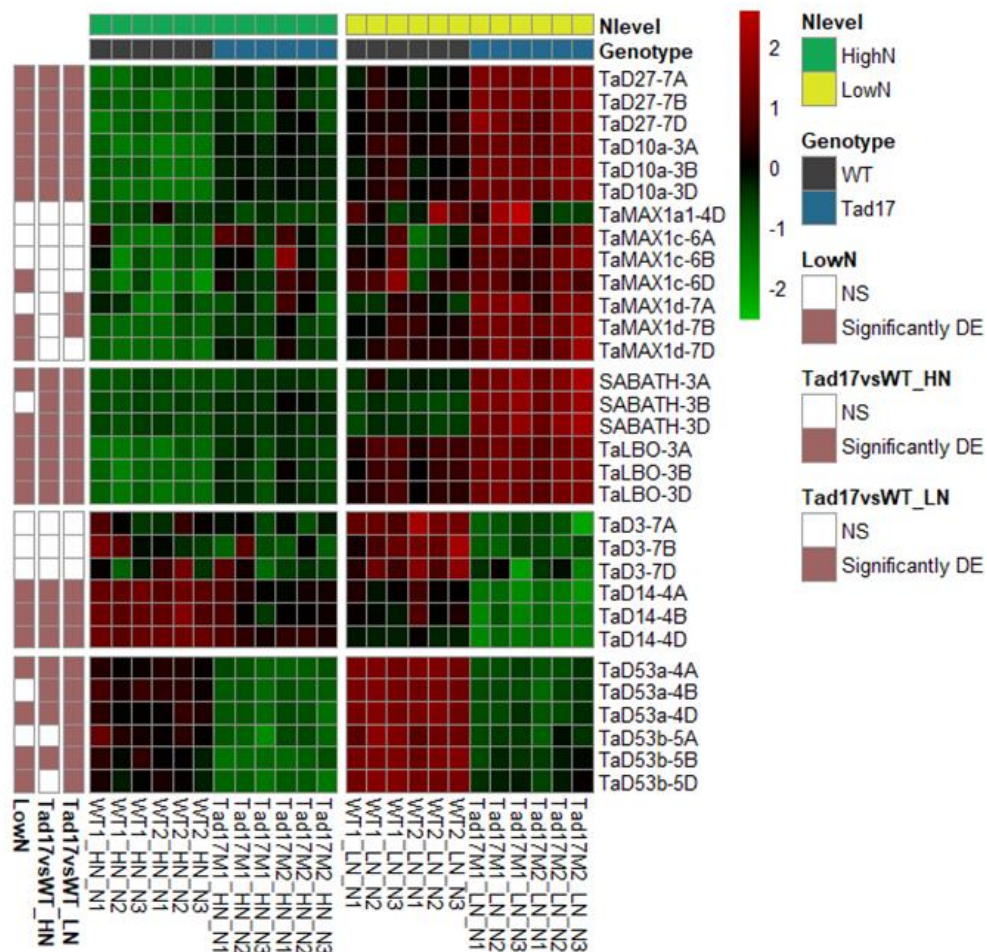


Figure 5.22: Transcriptional regulation of SL-related genes in the basal node of *Tad17* mutant (aabbdd) and WT segregant (AABBDD) grown under high N (10 mM) or low N (0.1 mM) conditions for 8 days based on the RNA-seq data. Each row corresponds to a different gene, while columns correspond to different samples grouped by treatment. Data are Z-scores of regularised log normalised counts (rlog) as generated by DESeq2. Red colour corresponds to higher transcript levels while green to lower. Row names correspond to the gene name. Row annotations indicate significant differential gene expression in N-limited nodes, in *Tad17* mutant under high N and in *Tad17* under low N conditions (from left to right).

Apart from the previously identified SL biosynthetic genes, the expression of three wheat homoeologues encoding putative SABATH methyltransferases and three homoeologues encoding Fe2OG dioxygenase domain-containing proteins were found to be strongly induced in basal nodes of *Tad17*. The transcriptional response of those genes was similar to the other SL biosynthetic genes. Orthology search showed that TraesCS3A02G255100, TraesCS3B02G287100 and TraesCS3D02G256000 are orthologous to SABATH methyltransferase (AT4G36470) recently identified in

Arabidopsis to be involved in Me-CLA biosynthesis downstream of MAX1 (Wakabayashi et al., 2021). On the other hand, TraesCS3A02G457700, TraesCS3B02G497900 and TraesCS3D02G450500 were found to be orthologues of *AtLBO1* (AT3G21420) which catalyses the conversion of Me-CLA to 1'-OH-MeCLA, which is a biologically active non-canonical SL (Brewer et al., 2016). Therefore, based on the orthology of the identified genes and their strong transcriptional response in *Tad17*, similar to the rest of SL biosynthetic genes, it was suggested that those genes might also be involved in SL biosynthesis in wheat nodes.

5.2.15 Response of *DRM* Genes and *TB1* in Basal Nodes of *Tad17* Mutant

Tad17 mutants showed an increased tillering phenotype compared to WT plants under both N levels included in this study. Recent studies have shown that SLs control branching/tillering by regulating bud dormancy (Luo et al., 2019). As mentioned in section 4.2.7, *DRM* genes are molecular markers of bud dormancy in several species (Tarancón et al., 2017). RNA-seq results in basal nodes showed that all the three homoeologues of *DRM1*, 3, 4 were significantly included by N limitation, which is consistent with the results presented in section 4.2.7, suggesting that N limitation controls tillering by affecting bud dormancy (**Figure 5.23E**). Among the nine different *DRM* genes identified in wheat, the three homoeologues of *TaDRM4* showed the highest transcript abundance compared to the other wheat *DRM* genes. In addition, the expression of *DRM4* homoeologues was found to be downregulated on average by 2-fold in basal nodes of *Tad17* compared to WT (**Figure 5.23E**). This observation suggests that SLs are involved in the regulation of bud dormancy by inducing the expression of *DRM* genes. Under N-limiting conditions, the transcript abundance of *TaDRM4s* was found to be 3.5-fold lower compared to the respective WT plant, indicating a stronger effect of SLs on bud dormancy status. Moreover, under N-limiting conditions, two homoeologues of *TaDRM3* and *TaDRM1-4A* were downregulated in the *Tad17* (**Figure 5.23E**). Those results suggested that SLs are involved in the regulation of bud dormancy status by promoting bud dormancy.

However, N limitation resulted in the induction of *DRM* genes even in the *Tad17* mutant, although the expression was much lower compared to WT. As a result, SLs are

not the only signal controlling bud dormancy in response to N limitation. The presence of another mechanism controlling bud dormancy in response to nutritional signals was also in line with the observed phenotype, given that *Tad17* still responded to N limitation by reducing the number of tillers formed.

The expression of *TB1* is known to be associated with branching/tillering control in many species. *TB1* is considered a downstream target of the SL biosynthetic pathway; however, this remains an open topic. Based on the RNA-seq data, the expression of *TaTB1-4A* and *-4D* was significantly lower in the basal nodes of N-limited *Tad17* compared to N-limited WT (**Figure 5.23A-C**). No significant difference was found between *Tad17* and WT under high N conditions, although the TPM values of *TaTB1* homoeologues were lower in *Tad17*. However, *TaTB1* showed a low number of counts in most of the samples (low expressed genes); therefore, *TaTB1* homoeologues were filtered out as low expressed genes in many comparisons. Thus, the expression of *TaTB1* was also measured by RT-qPCR (**Figure 5.23D**). Statistical analysis revealed that there is a strong effect of N limitation on the expression levels of *TaTB1* ($F(1,13)=33.96$, $p<0.01$), while genotype was also found to have a significant effect on *TaTB1* mRNA levels ($F(1,13)=51.51$, $p<0.01$). In fact, the expression of *TaTB1* was significantly lower in the *Tad17* mutant, while the difference between the two genotypes was more substantial under N-limiting conditions. Statistical analysis showed that there were not enough arguments supporting a significant 2-way interaction between the two factors ($F(1,13)=2.08$, $p=0.173$). However, based on the expression pattern, there are indications that the observed induction of *TaTB1* by N limitation is mediated by SLs as the expression of *TaTB1* was not significantly induced in *Tad17* mutants.

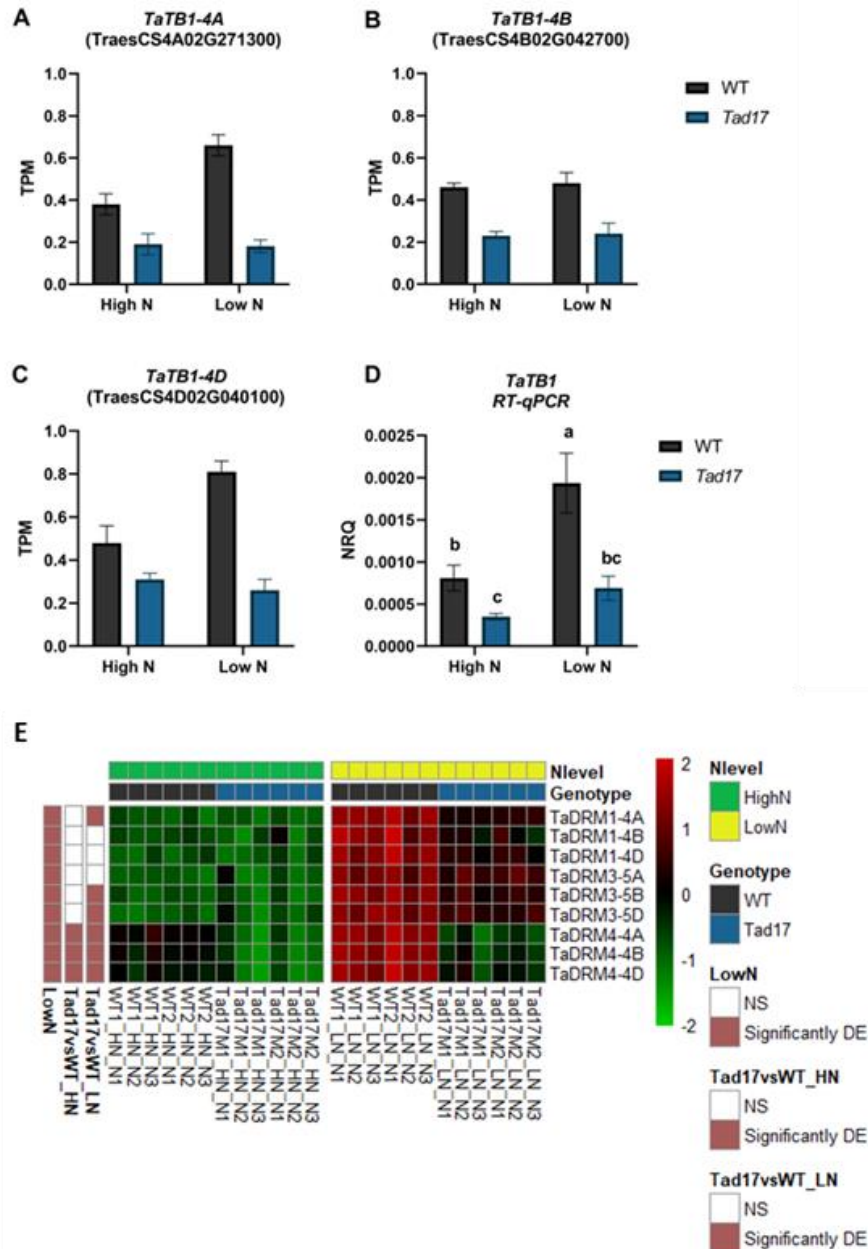


Figure 5.23: Expression of *TB1* and *DRM* genes in the basal node of *Tad17* mutant (aabdd) and WT segregant grown under high N (10 mM) or low N (0.1 mM) conditions for 8 days. (A-C) Transcript abundance (TPM) of *TaTB1* homoeologues in the basal node based on RNA-seq data and (D) based on RT-qPCR (NRQ). Values are means of six biological replicates, and error bars represent SE. Statistical analysis was conducted with 2-way ANOVA in $\log_2(1/\text{NRQ})$ transformed values. Different letters denote statistically significant differences in the gene expression levels between the means based on Fisher's LSD test. (E) Heatmap of *DRM* genes in the basal node based on the RNA-seq data. Each row corresponds to a different gene, while columns correspond to different samples grouped by treatment. Data are Z-scores of regularised log normalised counts (rlog) as generated by DESeq2. Red colour corresponds to higher transcript levels while green to lower. Row names correspond to the gene name. Row annotations indicate significant differential gene expression in N-limited nodes, in *Tad17* mutant under high N and in *Tad17* under low N conditions (from left to right).

5.2.16 SLs Affect Tre6P and Sugar Signalling Genes in Basal Nodes

GO and KEGG enrichment analysis showed that carbohydrate metabolism was among the pathways that were found to be affected in *Tad17* nodes. Tre6P-related terms were also among the enriched terms under both high and low N conditions indicating a link between SL levels and Tre6P metabolism. Tre6P has been found to be an important endogenous signalling metabolite which is involved in regulating carbon assimilation and sugar status signalling in plants (Figueroa et al., 2016). Elevated levels of Tre6P have been found to stimulate branching/tillering, indicating that Tre6P plays a pivotal role in bud outgrowth (Fichtner et al., 2017). In total, nine genes annotated with terms related to trehalose metabolism were differentially expressed in basal nodes of *Tad17* under high N conditions compared to the respective WT segregant. On the other hand, in N-limited plants, 19 genes involved in trehalose metabolism were affected in *Tad17* mutants (**Figure 5.24**).

The expression of two genes encoding TPSs, orthologous to class I OsTPS1, involved in Tre6P biosynthesis from glucose-6P, was found to be significantly induced in the N-limited *Tad17* mutant compared to the respective WT. On the other hand, the transcript abundances of many genes encoding class II TPS were lower in basal nodes of *Tad17*. For instance, all three homoeologues of *TaTPS11* were strongly downregulated in *Tad17* under both N conditions. In addition, *TaTTP6* homoeologues were more than 2-fold lower under N-limiting conditions in the *Tad17* mutant. In sorghum, class II TPS encoding genes have been found to be induced in dormant buds (Kebrom and Mullet, 2016). Therefore, the downregulation of class II TPS encoding genes in *Tad17* might be linked with changes in Tre6P homeostasis leading to bud outgrowth. TPP enzymes are involved in the conversion of Tre6P to trehalose. Many members of the TTP gene family were among the DE genes. This observation suggests that SL interact with Tre6p metabolism to control tillering in wheat.

Tre6P has been suggested to control growth and developmental decision by inhibiting SnRK1 (Fichtner and Lunn, 2021). SnRK1 suppresses biosynthetic processes and growth. As a result, Tre6P and SnRK1 have opposite roles in controlling growth, as SnRK1 suppresses growth, whereas elevated levels of Tre6P stimulate growth. Recent studies have suggested that Tre6P inhibits SnRK1 leading to growth release. Under N-

limiting conditions, the expression of the SnRK1A-subunit encoding genes was significantly downregulated in *Tad17* compared to WT (**Figure 5.24**). Downregulation in transcript abundance of *SnRK1A* was also observed in *Tad17* compared to WT under high N but without statistical significance. In addition, the N-mediated induction of *SnRK1A* homoeologues was affected in the *Tad17* mutant, as the expression of SnRK1 genes was not significantly altered by N limitation in the *Tad17* basal nodes as it was in WT plants. Thus, it is suggested that SLs affect sugar signalling under N-limiting conditions by inducing sugar status signalling genes.

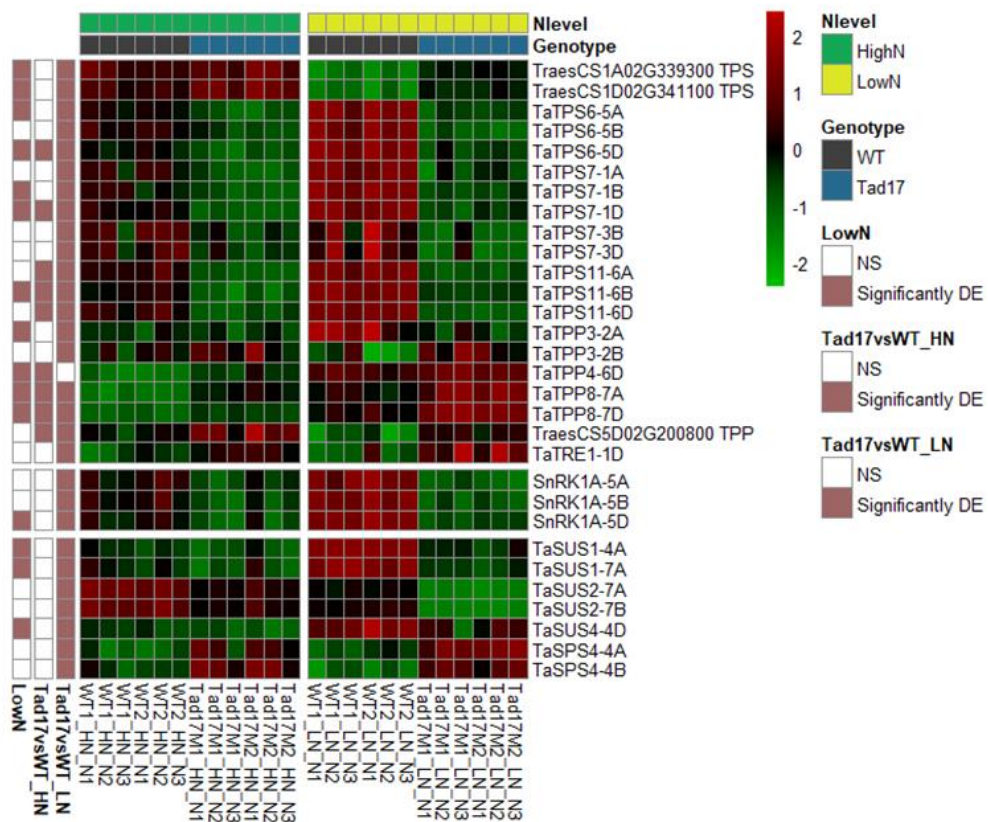


Figure 5.24: Heatmap of selected differentially expressed genes involved in Tre6P and carbohydrate metabolism and sugar signalling in the basal node of *Tad17* mutant (aabbdd) and WT segregant grown under high N (10 mM) or low N (0.1 mM) conditions for 8 days. Each row corresponds to a different gene, while columns correspond to different samples grouped by treatment. Data are Z-scores of regularised log normalised counts (rlog) as generated by DESeq2. Red colour corresponds to higher transcript levels while green to lower. Row names correspond to gene names. Row annotations indicate significant differential gene expression in N-limited nodes, in *Tad17* mutant under high N and in *Tad17* under low N conditions (from left to right).

The interaction between SL and sugar availability signals was further supported by the altered expression of genes involved in sugar and carbohydrate metabolic processes in *Tad17* basal nodes. Vacuolar invertase encoding genes responsible for sucrose utilization were induced in *Tad17*. In addition, under N-limiting conditions, genes encoding sucrose synthase (SuSy) were strongly downregulated in *Tad17*. Moreover, the mRNA levels of genes encoding SPS4 were induced in *Tad17* compared to WT (**Figure 5.24**). In Arabidopsis, overexpression of SPS genes promoted growth and triggered changes in carbon partitioning and carbohydrate levels (Maloney et al., 2015). Thereby, based on the RNA-seq results, it was apparent that sugar signalling and carbohydrate metabolism were strongly affected in the *Tad17* mutant predominately under low N conditions.

5.2.17 *Tad17* Showed Altered Expression of Amino Acid Metabolism Genes, Predominately of Gln and Asn

Many studies have shown that amino acids play an important role in the regulation of tillering as signals apart from their role as N-source. Manipulation of Gln and Asn metabolism and homeostasis has been found to control tillering in monocotyledonous species, while both amino acids are the main form of nitrogen translocated from source to sink tissue and found in the xylem. Gln is synthesised by glutamate by GS enzyme. *TaGS1* encoded by TraesCS6A02G298100, TraesCS6B02G327500 and TraesCS6D02G383600LC are involved in N remobilization and reassimilation under low N conditions. The expression of *TaGS1-6A*, *-6B* was found to be significantly induced in basal nodes of *Tad17* independent of N supply (**Figure 5.25**). *Tad17* mutants also showed higher expression of genes encoding other GS isoforms such as *TaGSr* and *TaGSs*, but the effect was mainly found under N-limiting conditions. Low levels of Gln result in suppression of tillering; therefore, the observed induction in GS encoding genes might indicate higher rates of N reassimilation and higher levels of Gln locally in nodes, which subsequently contribute to the stimulated bud outgrowth observed in *Tad17* mutants.

In addition to changes in genes involved in Gln biosynthesis, the expression of genes encoding Asn synthetase (ASN) was suppressed in the basal nodes of *Tad17* compared to the control (**Figure 5.25**). Homoeologues of *TaASN1* (TraesCS5A02G153900 and

TraesCS5D02G159100) and *TaASN4* (TraesCS4A02G109900, TraesCS4B02G194400, TraesCS4D02G195100) were found to be significantly downregulated in nodes of *Tad17* independently of the N supply. *ASN* gene expression has been associated with the sugar status of the tissue. More specifically, *TaASN1* has been shown to be a sugar starvation inducible gene, as its expression is induced under low sugar availability (Kebrom et al., 2012). The altered expression of *ASN* encoding genes presumably indicated an effect of SLs on the sugar status of the nodes and the amino acid homeostasis, which might contribute to the stimulated tillering phenotype. In low tillering *tin* mutants, induced expression of the *TaASN1* gene has been reported, which has been associated with suppressed bud outgrowth (Kebrom et al., 2012). In addition, genes encoding asparaginase (ASPGB1), responsible for the degradation of Asn, showed significantly higher transcript abundance in *Tad17* mutant compared to WT regardless of plant N status (**Figure 5.25**). Asparaginase encoding genes were strongly downregulated by N limitation in WT plants, while the regulation was not observed in the *Tad17* mutant. Overexpression of *ASN1* genes has been previously reported in dormant sorghum buds, while the opposite has been reported for asparaginase encoding genes (Kebrom and Mullet, 2016).

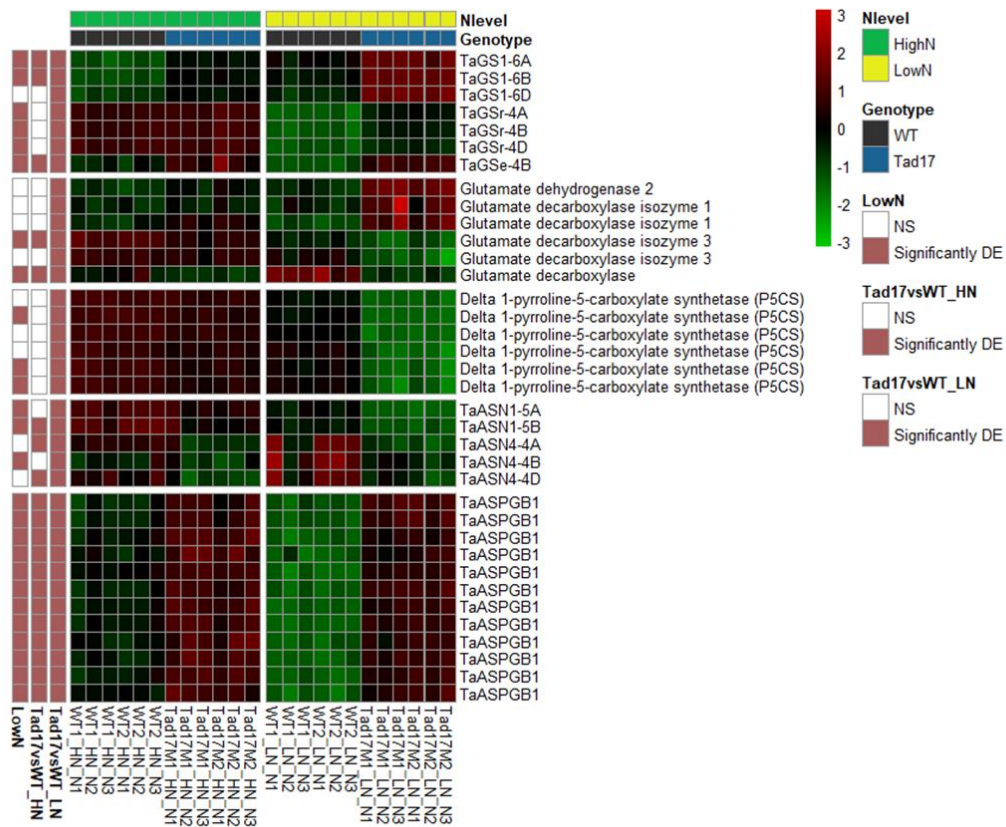


Figure 5.25: Heatmap of differentially expressed genes involved in Gln and Asn metabolism in the basal node of *Tad17* mutant (aabbdd) and WT segregant grown under high N (10 mM) or low N (0.1 mM) conditions for 8 days. Each row corresponds to a different gene, while columns correspond to different samples grouped by treatment. Data are Z-scores of regularised log normalised counts (rlog) as generated by DESeq2. Red colour corresponds to higher transcript levels while green to lower. Row names correspond to the gene name or the encoded enzyme. Row annotations indicate significant differential gene expression in N-limited nodes, in *Tad17* mutant under high N and in *Tad17* under low N conditions (from left to right).

5.2.18 N-limited *Tad17* Showed Significant Changes in N-responsive Genes

As shown in the previous sections, SL biosynthesis is strongly induced under N-limiting conditions; therefore, SLs may act as a signal of N status controlling the N limitation response. In fact, the RNA-seq analysis revealed that the *Tad17* mutant showed more substantial transcriptional changes in basal nodes compared to WT plants under N limitation than the same comparison under high N conditions. This observation suggests that lack of SLs and imbalance in tillering regulation have a much stronger effect on different pathways when N is a limiting factor. In previous sections (5.2.13-17), SLs were found to affect several pathways under both N conditions. However, SLs

were required for the transcriptional regulation of some genes in response to N limitation, as shown, for instance, in the case of genes encoding asparaginase (section 5.2.17). In order to find how N limitation response was altered in *Tad17* mutants, two approaches were followed.

Initially, the list of the significantly DE genes that responded to N limitation (called N-responsive genes thereafter) was compared with the genes that were found to be DE in the basal nodes of N-limited *Tad17* compared to WT. The analysis showed that in N-limited basal nodes of *Tad17* mutant, the expression of 2577 N-responsive genes was significantly affected. Further analysis showed that those genes were divided into four clusters based on the response to N limitation and the response in *Tad17* plants (**Figure 5.26A**). More specifically, cluster1 included 1098 N-inducible genes whose transcript abundance was significantly lower in nodes of *Tad17* compared to WT under N-limiting conditions. This suggests that SLs were required for the transcriptional response of those genes to N limitation, or at least the lack of SLs decreased the rate of induction by N limitation. On the other hand, 610 genes were found to be suppressed by N limitation, whereas their transcript abundance was higher in N-limited nodes of *Tad17* (cluster 2). Cluster 3 contained 484 genes whose expression was induced by N limitation, but the induction was much stronger in *Tad17* mutants. Finally, 385 genes repressed by N limitation were significantly lower in the *Tad17* mutant and grouped in cluster 4. The identified genes were further clustered into subclusters based on their overall response to N limitation and their expression under high N conditions in *Tad17* mutants, as shown in **Figure 5.26B**. For simplicity, only cluster (and not subcluster) information was used in the following sections.

The second way to study how the N limitation response differed in the *Tad17* mutant compared to the N limitation response of WT. This was achieved by studying the genes that showed a significant 2-way interaction between factors genotype and N level. This was achieved by extracting the significantly differentially expressed genes from the interaction term in the linear model fitted in DESeq2. In total, 1398 genes showed a significantly different response to N limitation between *Tad17* and WT plants. However, the genes extracted from the interaction term included not only genes whose expression showed a different response to N limitation but also genes that

showed a different response to the mutation under only one condition, making the interpretation of the data more complicated whilst it was not the main focus of this study.

Although the second method was a more statistically robust method for comparing the N response, it is more conservative; therefore, the list of genes obtained from the first method was utilized to identify N-responsive pathways and biological processes that were affected by the lack of SL biosynthesis in *Tad17* mutants.

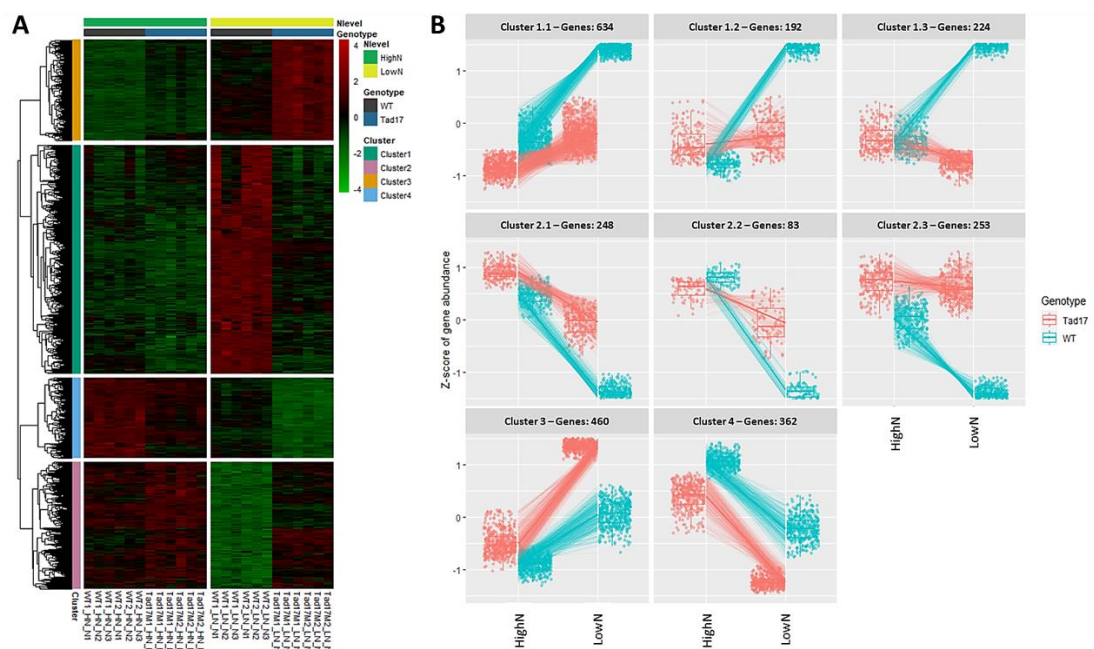


Figure 5.26: Effect of SLs on the transcriptional regulation of N-responsive genes. (A) Heatmap of N-responsive genes that were significantly differentially expressed in *Tad17* (aabbdd) under low N conditions compared to WT-segregant (AABBDD). Each row corresponds to a different gene, while columns correspond to different samples grouped by treatment. Data are Z-scores of regularised log normalised counts (rlog) as generated by DESeq2. Red colour corresponds to higher transcript levels while green to lower. Row annotation corresponds to the four clusters based on the transcriptional response. **(B)** Different graphical representations of the transcriptional regulation of the identified N-responsive genes affected in *Tad17*. Further subclustering was performed using the DEGpattern tool. Genes belonging to clusters 1 and 2 were subcluster into three subclusters based on the response of *Tad17* to N limitation.

5.2.19 Functional Annotation Enrichment Analysis of N-responsive Genes Affected in *Tad17*

Functional annotation enrichment analysis was performed in the list of N-responsive genes affected in *Tad17* mutants under N-limiting conditions as described in section 5.2.18 (Figure 5.27, Appendix G). The analysis showed that the response of many

hormonal pathways to N limitation was altered in *Tad17*, suggesting that SLs interact with other hormones to control tillering in response to N status signals. Among the identified pathways was the strigolactone metabolic process (GO:1901600), which was mainly enriched among genes included in cluster 3 (**Figure S4**). This indicates the presence of negative feedback regulation by the SL levels, as also reported in section 5.2.14. Other hormonal pathways were cytokinin metabolic process (GO:0009690), gibberellin metabolic process (GO:0009685), response to jasmonic acid (GO:0009753) and others. Cytokinin metabolic process is among the pathways that are strongly suppressed by N limitation, while CK levels are linked with plant N status acting as systemic signals (Sakakibara et al., 2006, Sakakibara, 2021). Therefore, the observed changes in CK metabolism indicated the involvement of SLs in the N-mediated regulation of CK biosynthesis and signalling.

As shown in section 4.2.11, biological processes related to carbohydrate transport and metabolism were significantly affected by N limitation. Those changes may reflect changes in the sugar strength status of the tissue and thereby contribute to bud dormancy. GO terms related to carbohydrate metabolism and signalling, such as disaccharide metabolic process (GO:0005984), carbohydrate transport (GO:0008643) and trehalose biosynthetic process (GO:0005992), were significantly enriched GO: BP terms in the list of N-responsive genes affected in *Tad17*. Similarly, KEGG terms “starch and sucrose metabolism” and “carbohydrate metabolism” were among the top enriched KEGG terms, suggesting that SL-deficient mutant showed altered regulation of carbon use and partitioning in response to nutritional signals.

Changes in N metabolic genes, nitrate transporters and amino acid metabolism comprise the main responses of the plant to cope with N deficiency. Changes in amino acid metabolism contribute to N re-assimilation, while changes in amino acid and nitrate transport contribute to N remobilization and partitioning between different tissues as part of plant adaptation to N-limiting conditions. KEGG terms “nitrogen metabolism”, “amino acid metabolism”, and GO: BP terms glutamine family amino acid metabolic process (GO:0009064), inorganic anion transport (GO:0015698), amino acid transport (GO:0006865) and nitrate assimilation (GO:0042128) were enriched among the N-responsive genes affected in *Tad17*. This observation denoted that SLs

were required for the coordination of N metabolism and remobilization under N-limiting conditions. More specifically, terms related to nitrate metabolism were enriched among the genes included in cluster 2, meaning that SL-deficient mutant showed alleviated downregulation of nitrogen metabolism in response to N deficiency. On the other hand, the ureide catabolic process (GO:0010136) was overrepresented among genes in cluster 3. Ureide (allantoin) breakdown contributes to N recycling, which is induced under N-limiting conditions. *Tad17* mutants showed stronger expression of ureide catabolism, indicating that under N-limiting conditions, *Tad17* basal nodes were stronger N sinks compared to WT plants and showed higher levels of N recycling and reassimilation.

Therefore, GO and KEGG enrichment analysis showed that *Tad17* – presumably SL-deficient – showed altered expression of metabolic and signalling pathways important for the metabolic and physiological adaptation of plants to N-limiting conditions.

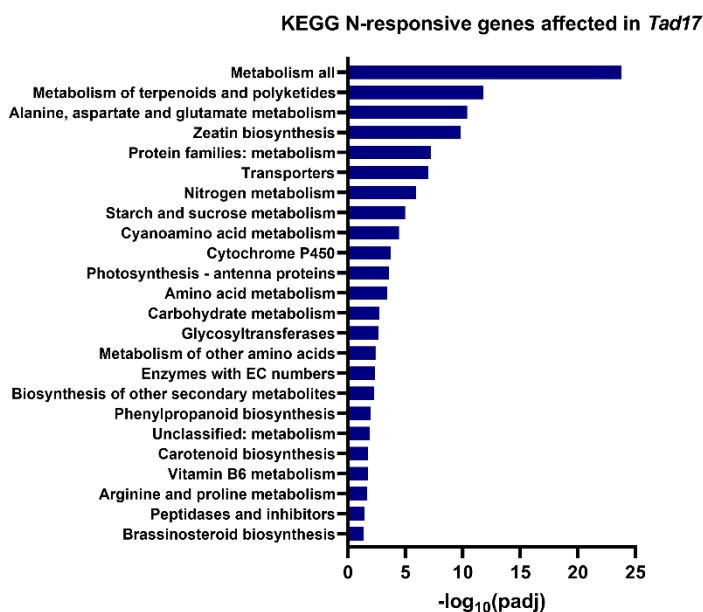
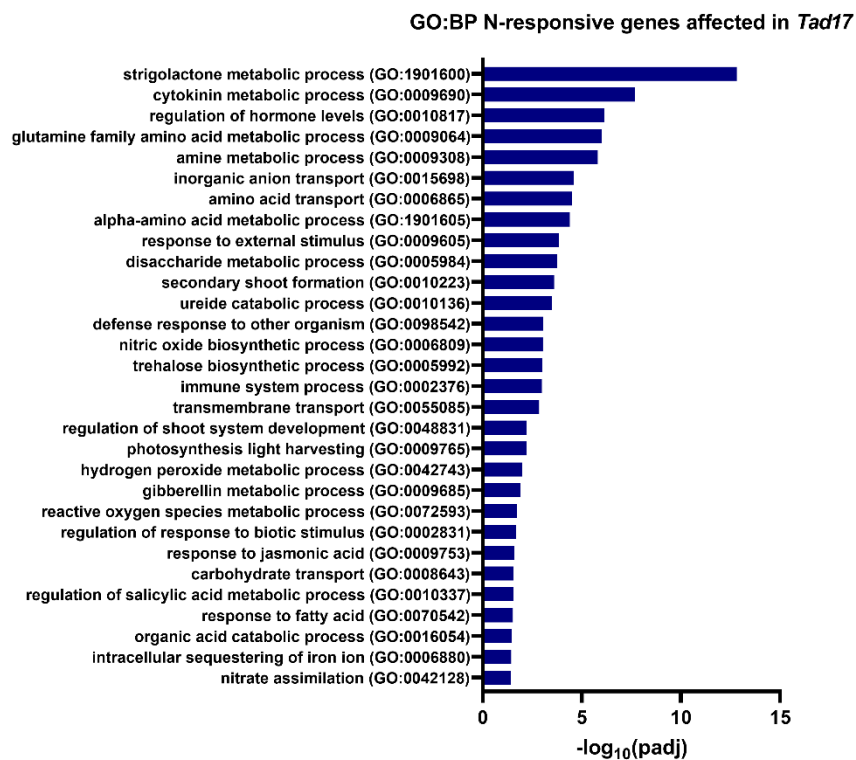


Figure 5.27: (A) Biological Process (BP) GO term and (B) KEGG enrichment analysis of the differentially expressed N-responsive genes in the basal node of *Tad17* mutant under low N conditions.

5.2.20 SLs Affected the Transcriptional Regulation of CK Metabolic and Signalling Genes to N Limitation

GO and KEGG enrichment analysis showed that many biological processes and pathways related to hormone metabolism were enriched in the list of N-responsive genes, which were DE in the N-limited *Tad17* compared to WT. Among the top GO terms was the cytokinin metabolic process, while “zeatin biosynthesis” was among the top 5 KEGG terms. More specifically, the cytokinin metabolic process was the top term among genes included in cluster 2. Cluster 2, as mentioned in section 5.2.18, included genes suppressed by N limitation but found to be upregulated in *Tad17*, suggesting that SLs may act via controlling CK-homeostasis.

In the previous section (4.2.16), it was demonstrated that CK levels were systematically downregulated by N limitation. In addition, N limitation strongly affected the expression of many genes involved in CK metabolism and signalling (**Figure 4.10**), suggesting that N limitation suppresses tillering by affecting the expression of genes involved in CK homeostasis leading to decreased CK content in basal nodes. Consistent with the previous finding, the expression of CK biosynthetic genes was suppressed in the basal nodes of WT segregant plants in response to N limitation, while changes were also found in genes involved in CK homeostasis and signalling. (**Figure 5.28**). However, as shown in the heatmap (**Figure 5.28**), the transcript abundance of CK biosynthetic genes was significantly higher in nodes of *Tad17* compared to WT under N-limiting conditions. The DE biosynthetic genes included genes encoding IPT enzymes. Moreover, wheat homoeologues encoding CYP735A and LOG enzymes were upregulated in *Tad17* basal nodes under N-limiting conditions. CYP735A catalyses the formation of tZR from iPA, whereas LOG catalyses the conversion of tZR to tZ (Takei et al., 2004b, Kurakawa et al., 2007). Both tZR and tZ have been shown to be important for the regulation of shoot architecture (Kiba et al., 2013). The expression of those genes was strongly suppressed by N limitation in WT plants, but the same was not true in N-limited basal nodes of *Tad17*. Most of the biosynthetic genes were also included in the list of genes that showed a significant interaction between genotype and N level. Therefore, it is suggested that SLs are required for the suppression of CK biosynthetic genes in nodes in response to N

limitation. Similarly, the expression of many CKX genes involved in CK degradation remained at high levels in *Tad17*, despite the fact that they were strongly suppressed by N limitation in WT plants. The expression of genes encoding CK glycosyltransferase involved in CK deactivation was also upregulated in *Tad17* compared to WT under N-limiting conditions.

In addition, wheat homoeologues encoding AHK4 CK receptor protein were not among the N-responsive genes. However, their mRNA levels were significantly induced in *Tad17* mutant under N-limiting conditions compared to WT, while an upregulation was also recorded in *Tad17* grown under high N compared to WT but without a statistically significant difference. Finally, type-A RRs, which are CK-inducible genes, were strongly downregulated under N limiting conditions due to the lower levels of CKs. Type-A RRs are used as molecular markers of CK levels, while in *Arabidopsis*, it has been demonstrated that type-A RRs are required for branching control by CKs (Müller et al., 2015). The mRNA levels of 12 wheat genes encoding type-A RRs remained at high levels in the *Tad17* mutant, indicating that CK signalling was not suppressed in *Tad17* by N limitation. Thereby, SLs are required for the transcriptional regulation of CK metabolism and signalling in response to N limitation. Although some genes were also found to be affected in the high N treated *Tad17* compared to WT, the effect was not as strong and consistent as that observed in N-limited plants.

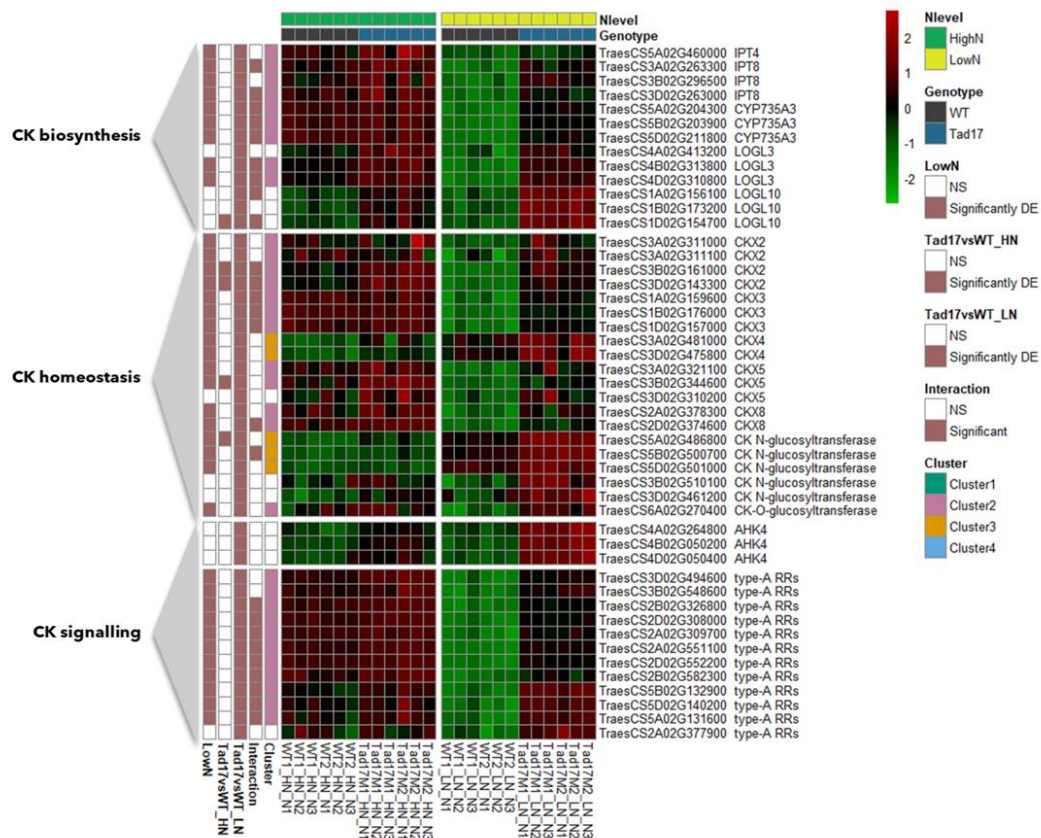


Figure 5.28: Heatmap of differentially expressed genes involved in CK biosynthesis, homeostasis and signalling in the basal node of *Tad17* mutant (aabbdd) grown under low N (0.1 mM) conditions for 8 days. Each row corresponds to a different gene, while columns correspond to different samples grouped by treatment. Data are Z-scores of regularised log normalised counts (rlog) as generated by DESeq2. Red colour corresponds to higher transcript levels while green to lower. Row names consist of the GeneID and the encoded enzyme. Row annotations indicate significant differential gene expression in N-limited nodes, *Tad17* mutant under high N and *Tad17* under low N conditions, significant 2-way interaction and cluster information (from left to right).

5.2.21 SLs are Required for Nutrient and Carbohydrate Remobilization under N-limiting Conditions

The RNA-seq analysis in N-limited nodes revealed that N limitation led to strong changes in the gene expression of various transporters. This was consistent with the results presented in sections 4.2.8-9 and 4.2.11, suggesting that changes in amino acid and sugar transport are part of the N limitation response. Those changes might reflect strong remobilization of organic compounds and inorganic elements as part of plant adaptation to N limitation. *Tad17* showed altered expression of many N-responsive

genes encoding various transporters under N-limiting conditions. As suggested by GO and KEGG enrichment analysis, most of the responses were focused on amino acid, carbohydrate and inorganic anion transport.

In fact, the expression of many N-responsive amino acid transporters was found to be affected in N-limited *Tad17* compared to the WT, likely leading to changes in amino acid transport and remobilization (**Figure 5.29**). Amino acids are the main form of N remobilized within the plant, but they also play an important role as signalling molecules. Among the amino acid transporters, wheat orthologues of *OsAAP7*, which were highly expressed in nodes, showed significant downregulation to N limitation, whilst their mRNA levels were not affected by N limitation in *Tad17* (cluster 2). This indicates that SLs are required for the transcriptional regulation of *AAP7* in response to N supply. On the other hand, wheat homoeologues of *TaAAP13* were found to be included in cluster 3. *TaAAP13* showed high expression in basal nodes compared to other AAP encoding genes. N limitation induced the expression of *TaAAP13*, however, the induction was much stronger in *Tad17* mutants. The mRNA abundance of *TaAAP13* homoeologues was also found to be higher in high N treated *Tad17*, suggesting that the effect of SLs on *TaAAP13* expression is independent of N supply. The opposite response was observed in orthologues genes of *OsATL11* and *OsATL14*, which belonged to cluster 4. Apart from the N-responsive amino acid transporters, a few other amino acid transporters were found to be upregulated in *Tad17* only under low N conditions. Wheat orthologues of *OsAAP1* were not induced by N limitation, however, the expression was 2-fold higher in *Tad17* compared to WT under N-limiting conditions. *OsAAP1* is highly expressed in axillary buds and is involved in neutral amino acid uptake and reallocation to buds (Ji et al., 2020). Therefore, the upregulation of *TaAAP1* might reflect stronger amino acid transport to buds under N-limiting conditions leading to tillering induction. Similar upregulation under N-limiting conditions was found for orthologues of *OsAAP8* in *Tad17* basal nodes.

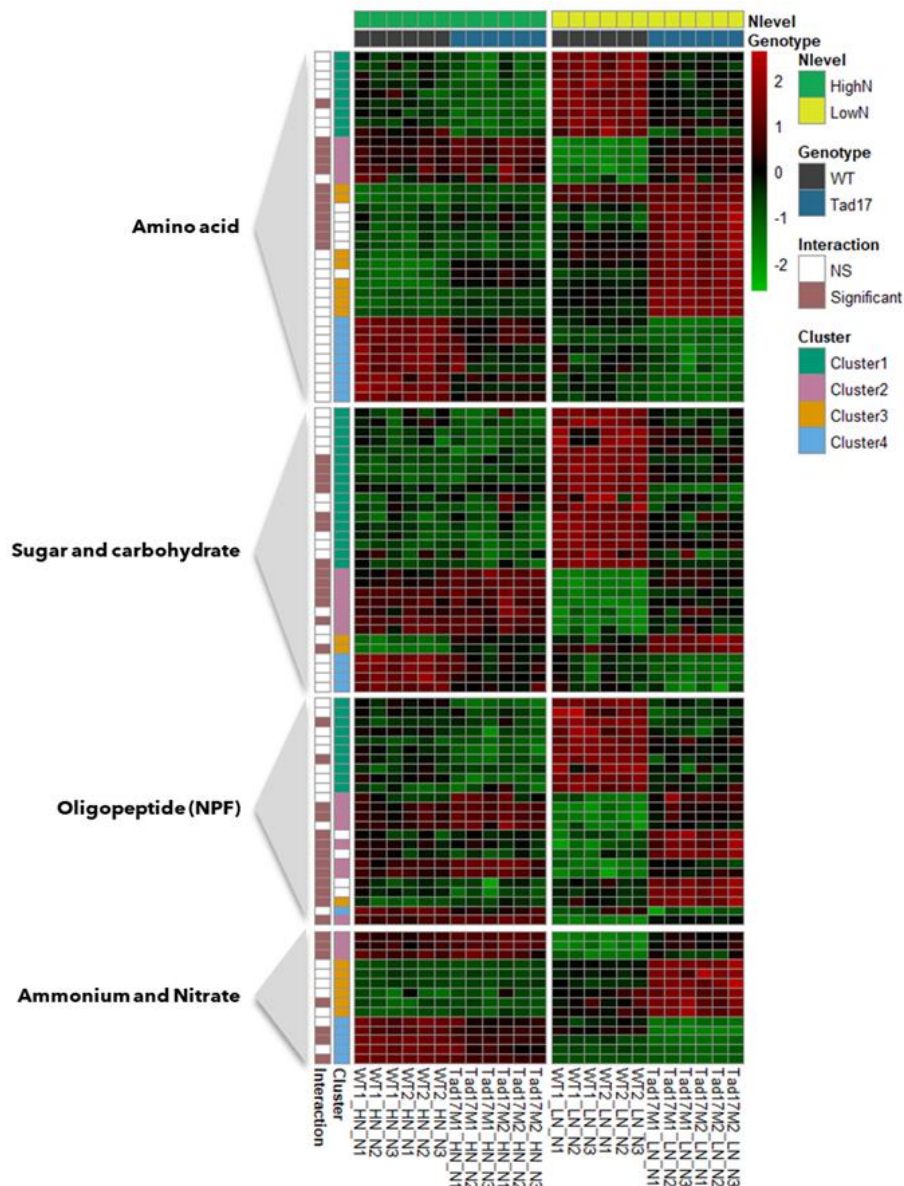


Figure 5.29: Heatmap of various N-responsive transporters significantly differentially expressed in the basal node of *Tad17* mutant (aabbdd) grown under low N (0.1 mM) conditions for 8 days. Each row corresponds to a different gene, while columns correspond to different samples grouped by treatment. Data are Z-scores of regularised log normalised counts (rlog) as generated by DESeq2. Red colour corresponds to higher transcript levels while green to lower. Row names consist of the GeneID and the encoded enzyme. Row annotations indicate significant 2-way interaction and cluster information (from left to right).

Analysis of the DE transporters showed that more than 30 N-responsive genes annotated as carbohydrate transporters showed altered expression in *Tad17* under N limiting conditions (**Figure 5.29**). Among them, 15 genes were included in cluster 1, showing a strong induction by N limitation, but they were downregulated in *Tad17* mutants. Wheat homoeologues encoding SUT1 also belonged to cluster 1. Sucrose transporters play an important role in carbohydrate partitioning between different

tissues (Xu et al., 2018). SUT1 is mainly involved in sucrose loading into the phloem. Thereby, the downregulation of SUT1 in basal nodes of *Tad17* might indicate less loading of sucrose into the phloem and subsequently less transport of sucrose into the root, whereas more sucrose was utilized into the nodes for bud outgrowth. Cluster 1 also included SWEET transporters, which are involved in sugar remobilization between tissues. On the contrary, wheat orthologues to *AtSWEET10*, *15*, which were strongly suppressed by N limitation, remained at high levels in *Tad17* mutants under low N conditions. The RNA-seq also showed induced expression of N limitation repressed genes encoding glucose-6-phosphate transporter in basal nodes of *Tad17*. Glucose-6-phosphate is important for carbon utilization, while it is also required for the biosynthesis of Tre6P as it is used as a substrate from TPS.

The SL-deficient mutant showed altered expression in many transporters involved in inorganic nutrient transport, such as NPF transporters. NPFs are involved but not limited to N transport (Buchner and Hawkesford, 2014, Wang et al., 2020a). In addition, N-responsive ammonium and high-affinity nitrate transporters were also found in the DE genes in *Tad17* under N-limiting conditions, suggesting that N remobilization was altered in SL-deficient mutants. Among the affected NPF transporters, *TaNPF7.1* homoeologues showed a significant interaction between N and genotype, denoting that the response to N limitation was dependent on the genotype. More specifically, the N limitation led to substantial overexpression of *TaNPF7.1* in *Tad17*, while the expression was either unaffected or suppressed in WT plants. *TaNPF7.1* are orthologues of *AtNPF7.2*, which is induced by NO_3^- and is involved in NO_3^- retrieval from the xylem (Li et al., 2010). As a result, the induced expression of *TaNPF7.1* in basal nodes presumably reflected stronger N sink strength of *Tad17* buds. *Tad17* also showed lower mRNA levels of *TaNPF6.1-7A* and *-7D* compared to WT under N limiting conditions. *TaNPF6.1* are orthologues of *OsNPF6.3 (NRT1.1A)* and *AtNPF6.3 (NRT1.1)* involved in root-to-shoot N transport and NO_3^- signalling (Léran et al., 2013, Bouguyon et al., 2015). *OsNPF6.3* is related to NO_3^- and ammonium utilization, as overexpression of *NPF6.3* in rice led to increased NUE (Wang et al., 2018d). Therefore, it is suggested that *Tad17* showed altered N utilization under N-limiting conditions. In addition, the N limitation suppressed the expression of all *TaAMT1.2* homoeologues,

as also found in section 4.2.8. The expression of *TaAMT1.2* was significantly higher in *Tad17*, suggesting that SL control the transcriptional response to N limitation.

5.2.22 SLs affect the Transcriptional Response of GA Biosynthetic Genes to N Limitation

Functional annotation enrichment analysis showed that among the N-responsive genes affected in *Tad17*, there were genes involved in GA metabolism. The majority of those genes were included in cluster 2, while many of those genes also showed a genotype-dependent response to N limitation, as shown in **Figure 5.30**, suggesting that SLs are required for the transcriptional regulation of GA homeostasis under N limitation. *TaGA3ox2* homoeologues involved in the biosynthesis of bioactive GAs were strongly downregulated under N-limiting conditions in WT plants. This finding was consistent with the data presented in section 4.2.13. However, in *Tad17*, their expression remained at higher levels. Similar results were obtained for *TaGA20ox7* homoeologues, which belonged to cluster 2. In contrast, *GA2ox3-1B* and *GA2ox3-1D* showed a strong induction by N limitation, while their expression was unaffected by N limitation in the basal nodes of *Tad17*. As a result, in N-limited *Tad17*, *GA2ox3* expression was significantly lower compared to WT plants. This was consistent with the previously reported downregulation of *GA2ox3* homoeologues in *d27* wheat mutants (Zhao et al., 2020). Changes in the expression of other GA metabolic genes were also recorded, as shown in **Figure 5.30**, demonstrating that SLs controlled N-mediated changes in GA metabolism.

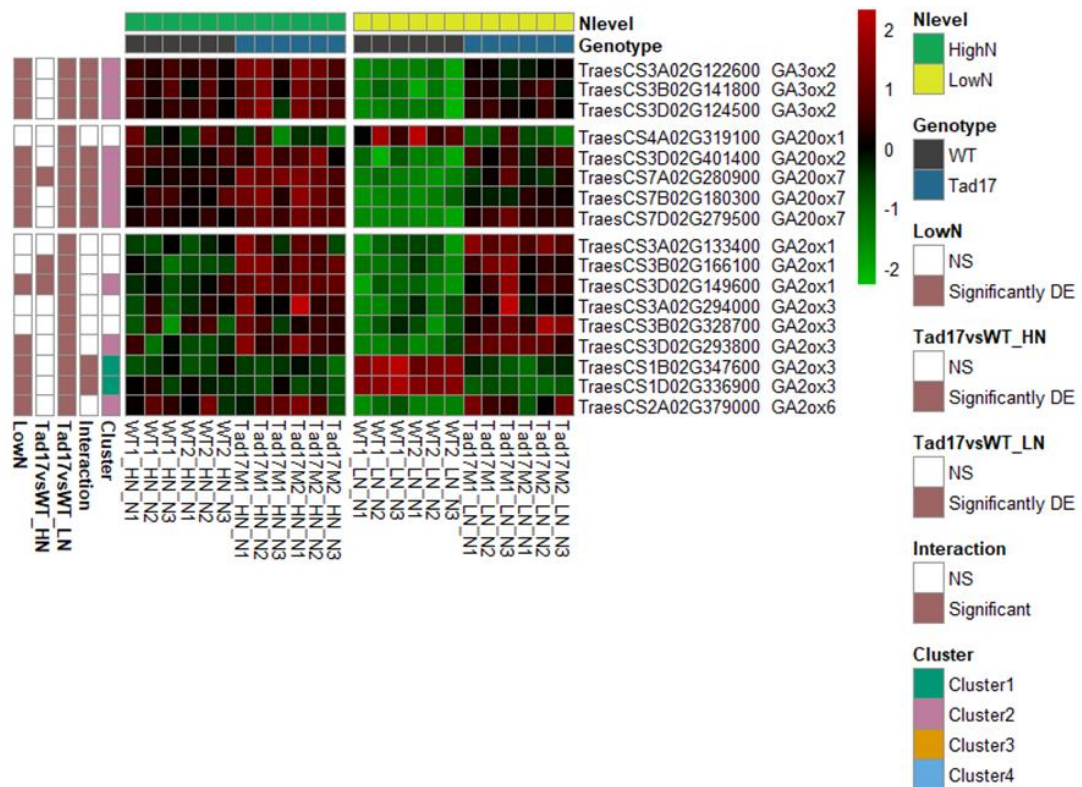


Figure 5.30: Heatmap of significantly differentially expressed genes involved in GA metabolism in the basal node of *Tad17* mutant (aabbdd) grown under low N (0.1 mM) conditions for 8 days. Each row corresponds to a different gene, while columns correspond to different samples grouped by treatment. Data are Z-scores of regularised log normalised counts (rlog) as generated by DESeq2. Red colour corresponds to higher transcript levels while green to lower. Row names consist of the GeneID and the encoded enzyme. Row annotations indicate significant differential gene expression in N-limited nodes, *Tad17* mutant under high N and *Tad17* under low N conditions, significant 2-way interaction and cluster information (from left to right).

5.2.23 Interaction Between SL and IAA under N-limiting Conditions

As shown in sections 5.2.17, *Tad17* mutants showed altered expression of genes involved in amino acid metabolism. Among the affected genes were many genes involved in Trp biosynthesis, as highlighted by GO enrichment analysis (**Figure 5.19**). More specifically, *Tad17* showed lower expression of genes encoding indole-3-glycerol phosphate synthase (IGPS), tryptophan synthase (TSA) and tryptophan synthase-related protein (TS) encoding genes (**Figure 5.31**). On the other hand, indole-3-glycerol phosphate lyase (IGL) encoding genes were upregulated in *Tad17* mutant under low N conditions. N limitation-induced Trp catabolic genes, indoleamine 2,3-dioxygenase, were found to be downregulated in N-limited *Tad17*. Consequently, SLs controlled Trp

metabolism, especially under N-limiting conditions. Trp is known to be the precursor of IAA biosynthesis, suggesting that SL might interact with IAA biosynthesis to control tillering. In fact, YUCCA7 homoeologues catalysing auxin biosynthesis were included in *Tad17* in both N conditions compared to the respective WT control. In addition, YUCCA3 genes were included in *Tad17* mutants but only under N-limiting conditions. Induction was also observed in IAA homeostasis genes, indole-3-acetic acid-amido synthetase, demonstrating the lack of SL biosynthesis affected IAA biosynthesis and homeostasis. IAA biosynthesis was also among the top KEGG pathways affected in TaD27-RNAi wheat plants (Zhao et al., 2020). Apart from IAA biosynthesis, many IAA transporters, such as PIN and LAX, showed significant differential expression in *Tad17* (**Figure 5.31**). PINs are auxin efflux carriers, whilst LAXs are auxin influx carriers. LAX3 homoeologues were strongly downregulated in *Tad17* basal nodes under both N conditions.

Changes in IAA biosynthesis and transporters were accompanied by strong transcriptional changes in Aux/IAA and SAUR genes (**Figure 5.31**). Aux/IAA are transcription factors that function as repressors of early auxin response genes. The majority of them were significantly induced in *Tad17* mutant, predominately under N-limiting conditions. In contrast, wheat orthologues of *OsIAA25* showed consistent downregulation in *Tad17* mutants independent of plant N status, suggesting that they might play a role in the induced tillering phenotype of *Tad17* mutants. Furthermore, SAURs play an important role in auxin-induced growth. Overexpression of SAUR genes has been linked with induced growth, while resend studies have shown that SAURs are also regulated by other hormones (Stortenbeker and Bemer, 2018). In total, 18 genes encoding SAUR were DE in *Tad17* under N-limiting conditions. The majority of the SAUR encoding genes were upregulated in *Tad17* mutants. Wheat orthologues of *OsSAUR41* showed a strong downregulation in response to N limitation, while in *Tad17* mutant, the expression did not significantly change. Wheat orthologues of *OsSAUR56* were the most highly expressed SAUR genes in nodes among the DE SAUR genes suggesting that they may play an important role in auxin-induced growth locally in nodes and showed induced expression in *Tad17* under N-limiting conditions.

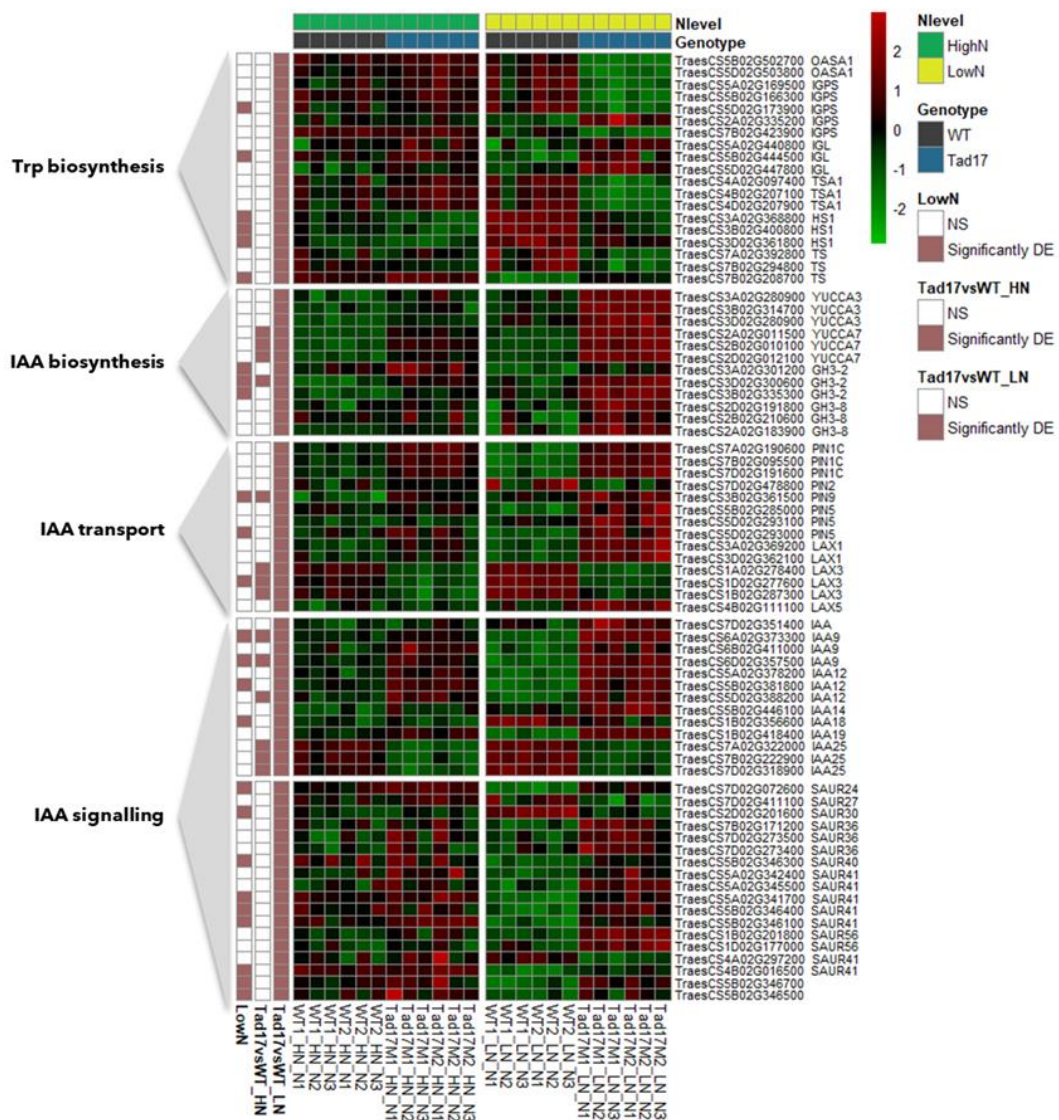


Figure 5.31: Heatmap of differentially expressed genes involved in Trp and IAA biosynthesis, IAA homeostasis, transport and signalling in the basal node of *Tad17* mutant (*aabdd*) grown under low N (0.1 mM) conditions for 8 days. Each row corresponds to a different gene, while columns correspond to different samples grouped by treatment. Data are Z-scores of regularised log normalised counts (rlog) as generated by DESeq2. Red colour corresponds to higher transcript levels while green to lower. Row names consist of the GeneID and the encoded enzyme. Row annotations indicate significant differential gene expression in N-limited nodes, *Tad17* mutant under high N and *Tad17* under low N conditions (from left to right).

5.2.24 SLs Control the Expression of Different N-response Master Regulators

Transcription factors are known to play an important role in regulating plant response to environmental stress through controlling the expression of many downstream

genes. Plant response to N limitation involved the regulation of thousands of genes. Several studies have identified important TFs controlling the expression of N-responsive genes acting as master regulators (Ueda et al., 2020, Gaudinier et al., 2018, Kiba et al., 2018). The RNA-seq in basal nodes of WT and *Tad17* mutants under different N levels showed that many TFs were DE in *Tad17* nodes (**Figure 5.32**). Further analysis revealed that many of the identified DE TFs were involved in N-response and also showed a genotype-dependent response to N limitation (significant interaction between factors genotype and N level) (**Figure 5.32**).

Five members of the TAZ family of TFs, orthologues of *AtBT1, 2* were significantly downregulated by N limitation consistently with the results presented in section 4.2.12. *AtBT1, 2* suppress the expression of N uptake and assimilation genes under N-sufficient conditions. The downregulation under N-limiting conditions plays an important role as it releases the expression of those genes leading to the N limitation response (Araus et al., 2016). The expression of all the genes was found to be significantly higher in *Tad17* mutants, suggesting that SLs might control the suppression of *BT1, 2* under N limitation. Several studies have shown that *LBD37, 38, 39* in Arabidopsis act as master regulators of N response, maintaining N deficiency response (Rubin et al., 2009). The expression of *LBD37, 38, 39* was downregulated by N limitation in the basal nodes. Wheat orthologues of *LBD37, 38, 39* showed a significantly lower transcript abundance in N-limited *Tad17* compared to WT.

AtBBX16 was identified by Gaudinier et al. (2018) as another TF important for the regulation of N response. N limitation suppressed the expression of *BBX16* wheat orthologues; however, the expression was, on average, 5-fold lower in *Tad17* mutant than in WT segregant. Different members of the GARP-like family of TFs have been found to be an important component of N responses (Kiba et al., 2018, Ueda et al., 2020). Wheat orthologues of *OsHHO3* and *OsHHO4* were strongly downregulated by N limitation. This observation was consistent with the results presented in section 4.2.12. However, N-limited basal nodes of *Tad17* showed significantly lower expression of *HHO3* and *HHO4* orthologues, indicating that SLs are required for the modulation of N-response. In contrast, *NIGT1/HHO1* wheat orthologues, also members of the GARP-G2-like family, showed a significant upregulation in response to

N limitation in basal nodes. Members of the NIGT1 subfamily are downregulated in roots of Arabidopsis by N limitation leading to the transcriptional release of nitrogen starvation responsive genes (Kiba et al., 2018, Maeda et al., 2018). Based on the transcriptomic analysis in roots, *TaNIGT1* homoeologues were downregulated in roots in response to the N limitation, indicating a tissue-specific regulation of *TaNIGT1* in response to the N limitation in wheat (**Appendix H**). All three homoeologues of *TaNIGT1* also showed a significant 2-way interaction, as the *Tad17* mutant showed significantly lower levels of *NIGT1* transcripts in the basal nodes. As a result, it is suggested that SLs might control N response by controlling the transcriptional regulation of *NIGT1*. The opposite effect was found in the roots of the *Tad17* mutant, clearly demonstrating an interaction between SL and the regulation of NIGT1 subfamily members in response to N limitation.

PHR4 is an MYB-related TF involved in the regulation of P starvation response, but it is also involved in the coordination of N and P homeostasis. N limitation induced the expression of *TaPHR4* homoeologues in the basal nodes; however, in *Tad17* N-limited plants, the expression levels were significantly lower, suggesting that SLs control the induction of *PHR4* in response to N limitation.

In section 4.2.12, it was shown that the NF-YA family was the TF family with the highest proportion of DE members induced by N limitation. Gaudinier et al. (2018) showed that NF-YA5 plays an important role in regulating the transcriptional regulatory network in response to N availability signals in Arabidopsis. *NF-YAs* were strongly upregulated in basal nodes of wheat grown under N-limiting conditions suggesting that they might involve in tiller suppression. Previous studies have also associated NF-YA members with growth suppression and prolonged exposure to nutrient-limiting conditions (Leyva-González et al., 2012). *Tad17* mutants showed significantly attenuated upregulation of *NFYA5* and other members of the NF-YA TF family, suggesting that *Tad17* showed an alleviated response to N limitation.

Therefore, the strong regulation of the N response master regulator in N-limited *Tad17* mutants denoted that SLs are required for the fine-tuning of N limitation responses, presumably acting as a signal.

to be affected in *Tad17* mutant in any of the N levels. Overall, the N limitation led to the downregulation of iPA concentration in both genotypes (N level effect, $F(1,11)=51.11$, $p<0.01$). This observation was consistent with the results presented in section 4.2.16. In contrast, a significant 2-way interaction between the N level and genotype was found for iP concentration ($F(1,10)=5.84$, $p=0.036$). In fact, iP concentration was decreased in nodes of WT plants under N-limiting conditions, consistently with previous results. However, *Tad17* mutant plants showed a 1.7-fold higher concentration of iP in the nodes under N-limiting conditions compared to WT. No difference was observed between the two genotypes under high N conditions. This observation indicated that the effect of *Tad17* knock-out on iP levels was dependent on plant N supply.

N limitation led to a strong downregulation of both tZ and tZR levels in the basal nodes of both genotypes. This observation indicated that the decrease in tZ and tZR content by N limitation is not regulated by SLs. However, under both N regimes, *Tad17* mutants showed a significant accumulation of both tZ-type of CKs in the basal nodes. In fact, under high N supply, tZR concentration was 1.4-fold higher ($t(5)=3.02$, $p=0.029$) and tZ more than 2-fold higher ($t(5)=4.33$, $p<0.01$) than the respective WT control. Similarly, under low N conditions, tZR concentration was found 2-fold higher in nodes of *Tad17* mutants compared to the WT segregant ($t(4)=10.9$, $p<0.01$), while tZ was 1.8-fold higher ($t(4)=3.83$, $p<0.01$). The higher accumulation of tZ and tZR in the basal nodes of the *Tad17* mutant may be related to the higher tillering phenotype, as CKs positively regulate tillering.

Finally, the cZR concentration in the basal nodes was not found to be affected in *Tad17* mutant in any of the two N levels. However, the N limitation induced the accumulation of cZR in the basal nodes regardless of the genotype ($F(1,11)=38.03$, $p<0.01$). A small increase in the cZR concentration in nodes has also been observed in section 4.2.16 but without a statistically significant effect.

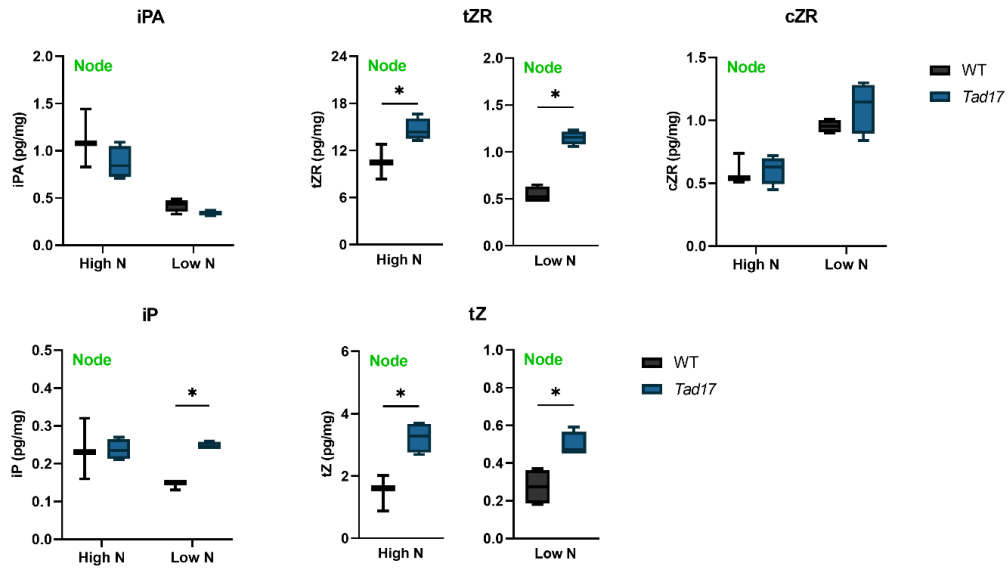


Figure 5.33: CK concentration in the basal node of triple *Tad17* mutant (*aabddd*) and WT segregant grown on high N (10 mM) or low N (0.1 mM) conditions for 8 days (18 DAS). Values are means of four biological replicates, and error bars represent SE. Statistical analysis was conducted with 2-way ANOVA (iPA, iP and cZR) or with independent samples t-test per N level (tZ and tZR). * denotes statistically significant difference between genotypes at the same level of N based on Fisher's LSD test (iPA LSD (5%) = 0.253, iP LSD (5%) = 0.064, cZR LSD (5%) = 0.211) or t-test ($p < 0.05$). Abbreviations: isopentenyl adenine (iP), isopentenyl adenosine (iPA), trans-zeatin (tZ), cis-zeatin (cZ) and their riboside (-R).

5.2.26 Sugar Analysis in Crown of *Tad17* Mutant under High and Low N Conditions

Sugar analysis was performed in the crown of 3-week-old *Tad17* mutant and WT segregant plants for the determination of Glc, Fru, sucrose and starch content (**Figure 5.34**). The effect of N supply and genotype was examined by 2-way ANOVA.

A statistical significant interaction between factors genotype and N levels were found for both Glc ($F(1,14)=23.57$, $p < 0.01$, $LSD(5\%)=1.05$) and Fru ($F(1,14)=42.49$, $p < 0.01$, $LSD(5\%)=0.61$). In fact, both Glc and Fru showed a similar pattern. N limitation did not significantly alter the Glc and Fru concentration in the crown of WT plants. *Tad17* mutants were found to accumulate a higher amount of both Glc and Fru only under high N conditions, whereas no effect between the two genotypes was observed under N-limiting conditions.

The effect of *Tad17* knock-out on sucrose levels was also found to be N-dependent (2-way ANOVA, $F(1,14)=33.16$, $p < 0.01$, $LSD(5\%)=7.75$). Sucrose content rose under N limitation in both genotypes (N effect, $F(1,14)=477.77$, $p < 0.01$), indicating that N

limitation mediated sucrose increase is not controlled by SLs. However, as also observed for Glc and Fru, sucrose concentration was higher in the crown of *Tad17* compared to the WT plants under high N supply.

In the WT segregant, starch concentration was almost 2-fold higher than in low N treated plants. An increase under N limitation was also observed in mutant plants. This observation suggests that N limitation induced starch accumulation in the crown. Genotype was found to have a significant effect on starch content regardless of the N regime. Under both N conditions, the starch concentration in *Tad17* mutants was more than 75% higher. This indicates that *Tad17* mutants accumulated more starch in the crown compared to WT plants indicating an effect of SL on carbon partitioning and utilization.

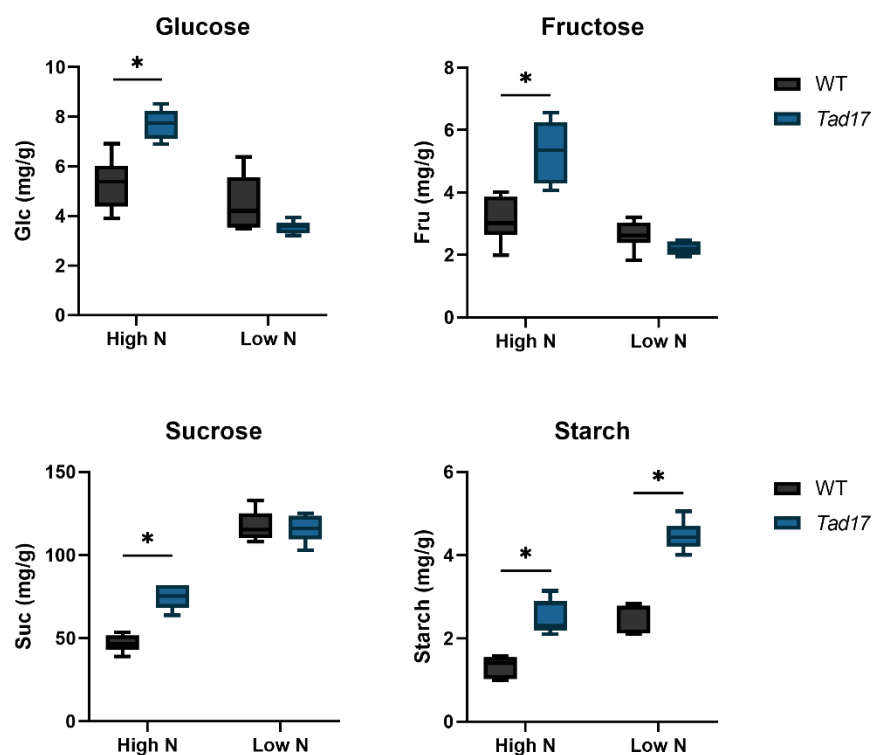


Figure 5.34: Sugar content (Glc, Fru, sucrose and starch) in the crown of 3-week-old triple *Tad17* mutant (aabbdd) and WT segregant grown on high N (10 mM) or low N (0.1 mM) conditions for 12 days. Values are means of six biological replicates, and error bars represent SE. Statistical analysis was conducted with 2-way ANOVA. * denotes statistically significant difference between genotypes at the same level of N based on Fisher's LSD test (Glu LSD (5%) = 1.05, Fru LSD (5%) = 0.61, Suc LSD (5%) = 7.75, Starch LSD (5%) = 0.42). Abbreviations: glucose (Glc), fructose (Fru), sucrose (Suc).

5.2.27 Elemental Analysis in Root and Shoot of *Tad17* Mutant under High and Low N Conditions

Elemental analysis in root and shoot samples of *Tad17* mutants was performed to examine the inorganic mineral concentration compared to the WT segregant under two different N levels. The results of the major macronutrients (N, P, K and S) in root and shoot are presented in **Figure 5.35**. Statistical analysis was conducted by 2-way ANOVA.

Root N concentration showed a significant 2-way interaction between genotype and N level (2-way ANOVA, $F(1,14)=8.41$, $p=0.01$, $LSD(5\%)=1.76$). Root N content was decreased in both genotypes in response to N limitation, as anticipated. However, under N-limiting conditions, the *Tad17* mutant showed significantly higher N concentration in the root. No significant effect was found between the *Tad17* mutant and WT plants when supplied with high N nutrient solution. Therefore, although *Tad17* N root concentration responded to N limitation, *Tad17* showed a higher accumulation of N in roots.

In contrast, shoot N concentration did not significantly differ between the two genotypes under N-limiting conditions, however, the high N treated *Tad17* mutant showed a lower N concentration compared to the respective control (2-way ANOVA, $F(1,14)=22.94$, $p<0.01$, $LSD(5\%)=1.83$).

ANOVA showed a significant 2-way interaction between genotype and N level for root P concentration (2-way ANOVA, $F(1,14)=8.77$, $p=0.01$, $LSD(5\%)=0.31$). N limitation led to a decrease in the P concentration in the root of WT plants, which was consistent with previous results presented in section 4.2.2. Under both N regimes, the *Tad17* mutant showed a significantly higher concentration of P in roots. In fact, *Tad17* supplied with high N had more than 9% higher P concentration, while an increase of 21% was recorded under low N conditions between *Tad17* and WT plants. In addition, the response of N limitation on P concentration was attenuated in *Tad17* mutants. More specifically, N limitation resulted in a 17% decrease in WT root P concentration, whereas in just 8% in *Tad17* mutant. As a result, it is suggested that SLs might be involved in P root concentration but might also affect N-mediated regulation of P

uptake. It is known that P and N assimilation are linked; therefore, SLs might play an important role in the coordination of P and N metabolism.

P concentration in the shoot was also found to be affected in *Tad17* mutants. Under high N supply, P concentration was found significantly lower in *Tad17* mutant, while the opposite effect was found under N-limiting conditions. Furthermore, P concentration in shoots was decreased in response to N limitation in WT plants by around 7%, which was in accordance with the decrease also reported in section 4.2.2. However, no significant impact of N limitation on shoot P content was found in *Tad17* mutants, which was reflected by the significant 2-way interaction of genotype and N level ($F(1,14)=16.3$, $p<0.01$, $LSD(5\%)=0.35$). This observation further supported that N-mediated regulation of P uptake and partitioning is at least partly facilitated by SLs.

No effect of the genotype in K accumulation was found in roots in any of the N treatments. In addition to that, the decrease in K concentration in response to N limitation was not found to be affected in *Tad17* mutant (2-way ANOVA, $F(1,14)=0.21$, $p=0.65$, $LSD(5\%)=2.24$). Even though K concentration was decreased in both genotypes in the shoot in response to N limitation, K concentration was consistently lower in *Tad17* mutant compared to WT plants (Genotype effect, $F(1,14)=75.2$, $p<0.01$).

Finally, S uptake and assimilation are known to be associated with N supply. In both root and shoot, both genotypes responded to N limitation by decreasing the S concentration (N level effect in root, $F(1,14)=183.5$, $p<0.01$; N level effect in shoot, $F(1,14)=665.2$, $p<0.01$). However, a significant increase in the S concentration of *Tad17* mutants was found under N limitation in roots. In contrast, *Tad17* mutant showed lower S accumulation in shoots under high N conditions, while no statistically significant effect was observed under low N in shoots.

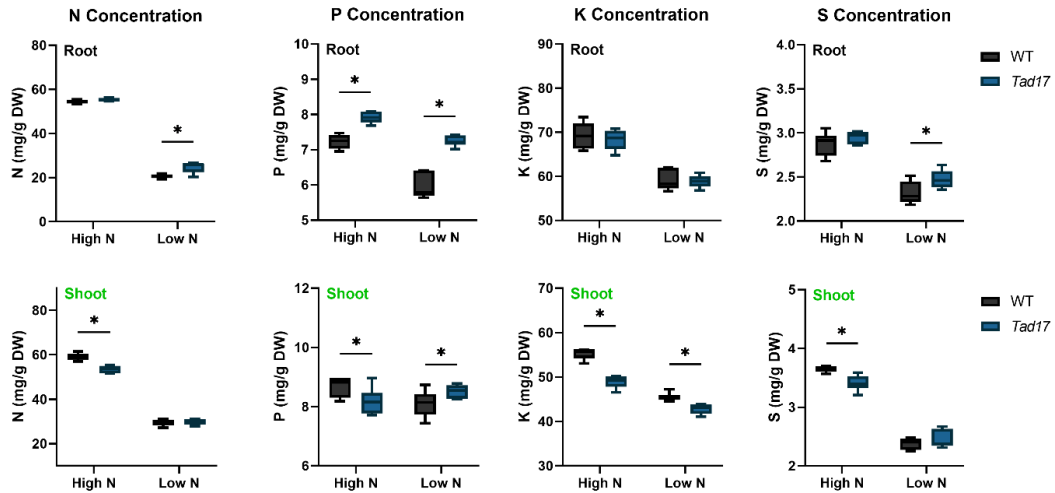


Figure 5.35: Macronutrient concentration (N, P, K and S) in root and shoot of triple *Tad17* mutant (aabbdd) and WT segregant grown on high N (10 mM) or low N (0.1 mM) conditions for 8 days (18 DAS). Values are means of six biological replicates, and error bars represent SE. Statistical analysis was conducted with 2-way ANOVA. * denotes statistically significant difference between genotypes at the same level of N based on Fisher's LSD test (N Root LSD (5%) = 1.76, N Shoot LSD (5%) = 1.83, P Root LSD (5%) = 0.31, P Shoot LSD (5%) = 0.35, K Root LSD (5%) = 2.24, K Shoot LSD (5%) = 1.57, S Root LSD (5%) = 0.12, S Shoot LSD (5%) = 0.13).

5.3 Discussion

5.3.1 Mutant D17/CCD7 Protein Functionality

The selected TILLING mutant lines for the generation of *Tad17* triple knock-out mutant carry mutations that lead to a premature stop codon in the coding sequence of *Tad17* homoeologues. Therefore, it is predicted that the encoded D17/CCD7 proteins will lack several amino acids from the COOH-terminal end, which presumably have a negative impact on D17/CCD7 functionality. The impact of this deletion on D17/CCD7 functionality was examined *in silico*. D17/CCD7 enzyme belongs to the family of CCOs, the members of which are involved in different steps of apocarotenoids biosynthesis, including the biosynthesis of SLs (CCDs) and ABA (NCEDs). Among the identified plant CCOs, only *ZmVP14* (NCED1) has been structurally characterized. CCO protein sequences show significant high protein similarity, which makes the *ZmVP14* structure an ideal prototype for studying CCDs and NCEDs. In *ZmVP14*, the catalytic iron molecule is coordinated by four His residues (Messing et al., 2010). Moreover, three Phe residues have also been shown to involve in the bonding of the oxygen required for the oxidative reaction (Phe411, Phe171 and Phe589). Phylogenetic and evolutionary studies have shown that these amino acid residues are conserved among plant CCDs, suggesting their importance for the functionality of the protein (Priya and Siva, 2014). In *VP14*, Val478 is responsible for the stereospecificity of the enzyme, whereas *AtCCD4* and *AtCCD7* contain Phe or Met in this position (Bruno et al., 2016).

Protein alignment and subsequent phylogenetic analysis revealed that those amino acid residues are also conserved in wheat CCDs. In addition, the results revealed that in all plant D17/CCD7, the Phe171 is replaced by Leu (e.g. Leu106 in *TaD17-2A*), which might attribute to the stereospecificity of D17/CCD7s. More importantly, for the purpose of this study, most of the identified amino acid residues are located close to the COOH-end of the wheat CCD7s, suggesting the deletions in the mutant proteins would lead to nonfunctional enzymes. More specifically, the CCD7 in the *Cad1738* mutant line lacks all the His residues required for Fe²⁺ binding (His263, His316, His394 and His605) and the Phe residues important for the substrate positioning (**Figure 5.36**). Similarly, the mutant line *Cad1271* shows a deletion of 191 amino acids from the COOH-terminus end of *TaD17-2B*, thus lacking His609, Asp489 and Phe610, important

for the stereospecificity. Similar deletions were also found in TaD17-2D in Cad0880. Taking everything into account, it is suggested that the mutant proteins would not be functional due to the lack of important amino acids residues for the functionality of the proteins, thereby, the triple homozygous mutant plants for the mutant alleles (*Tad17*) are not expected to be able to synthesize CL, the precursor of bioactive SLs, and thereby be SL-deficient.

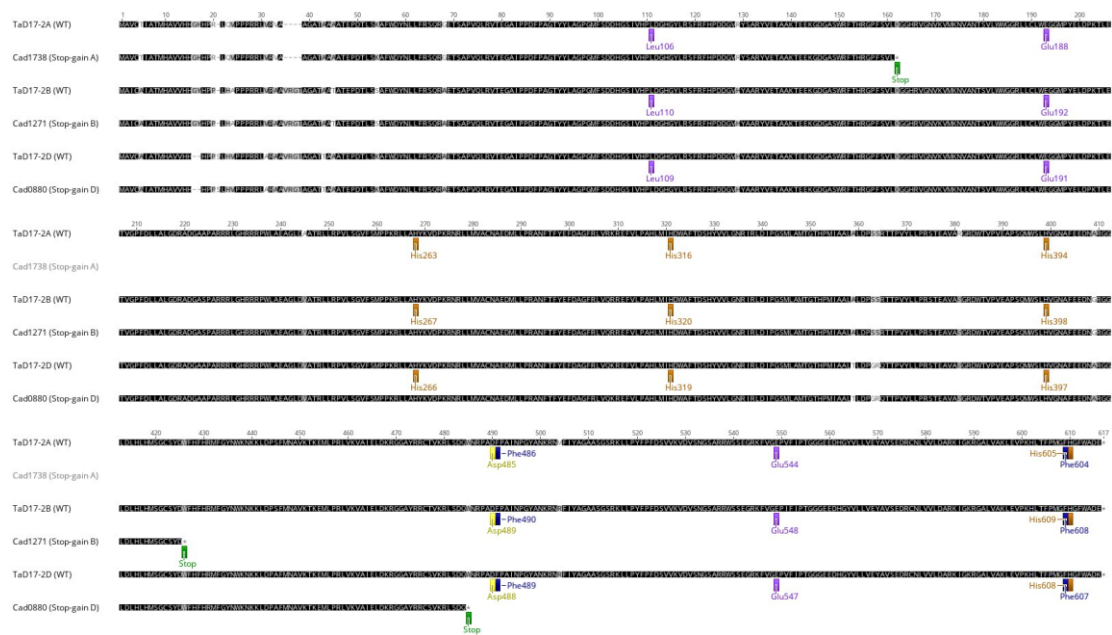


Figure 5.36: Protein alignment of the *T. aestivum* proteins sequences of D17/CCD7-2A, -2B and -2D and the mutant protein of the selected TILLING lines Cad1738, Cad1271 and Cad0880. The highlighted amino acid residues correspond to important amino acids for the functionality of the protein as identified by the phylogenetic analysis of plant CCDs.

5.3.2 Is *Tad17* Mutant SL-deficient?

In different plant species, *d17* mutants have been found to produce lower amounts of SLs in the root exudates, confirming that disruption in the function of D17/CCD7 leads to SL deficiency (Umehara et al., 2008, Butt et al., 2018). Epi-5DS was almost undetectable in the root exudates of *d17* rice mutants, while the endogenous levels of epi-5DS were also decreased, suggesting that lack of D17/CCD7 functionality leads to SL deficiency (Umehara et al., 2008). However, no hormone data were obtained in this study to confirm the lack of SL biosynthesis in the *Tad17* mutant. An alternative to the absolute quantification of SLs in root exudates is the *Striga* or *Orobanch* seed germination bioassay (Matusova et al., 2005, Jamil et al., 2012). Root exudates from SL-deficient mutants fail to promote the germination of *Striga* or *Orobanch* seeds due

to the absence of SLs, forming a widely used method for indirect estimation of SL production (Umehara et al., 2008, Zhao et al., 2020, Gomez-Roldan et al., 2008). Due to time restraints, neither the germination bioassay was used for the indirect estimation of SLs in root exudates of *Tad17* mutants. Therefore, is the generated *Tad17* mutant SL-deficient?

Based on the phenotypic and gene expression data, there are several lines of evidence supporting that SL biosynthesis was impaired in the triple knock-out *Tad17* mutant. *Tad17* showed a high tillering phenotype similar to previously characterised SL-deficient mutants, such as *d* (*d27*, *d17*, *d10*) mutants in rice or *max* mutants in Arabidopsis (Umehara et al., 2008, Gomez-Roldan et al., 2008, Alder et al., 2012). Thereby, the bushy phenotype of *Tad17* suggests that *Tad17* presumably produces significantly lower levels of SLs. In addition, the *Tad17* mutant showed a similar phenotype to the *Tad14* SL-insensitive mutant (**Appendix I**), in which SL signalling is constantly suppressed due to a non-sense mutation in the D14 receptor protein of SLs. This observation further supported the proposition that SLs levels in *Tad17* were significantly lower than wildtype.

In addition, the transcriptomic analysis in the basal nodes of *Tad17* mutants showed that SL biosynthetic genes were strongly induced. More specifically, the expression of *TaD27* and *TaD10* homoeologues were significantly induced in *Tad17* mutants. The transcription of SL biosynthetic genes is controlled by negative feedback regulation (Mashiguchi et al., 2021, Mashiguchi et al., 2009). In several studies, SL-deficient or SL-insensitive mutants have shown a strong upregulation of SL biosynthesis genes in Arabidopsis and rice (Umehara et al., 2008, Mashiguchi et al., 2009, Arite et al., 2007, Waters et al., 2012). Application of GR24, synthetic SL analogue, leads to downregulation of SL biosynthetic genes in SL-deficient mutant but not in SL signalling mutant, implying that SL biosynthesis is controlled by the SL signalling pathway. Recently, similar to the results presented in this work, Zhao et al. (2020) also reported a strong upregulation of SL biosynthetic genes in the confirmed SL-deficient TaD27-RNAi wheat plants (Zhao et al., 2020). RNA-seq in basal nodes also showed significant downregulation of *TaD53* encoding genes. D53 is the transcriptional repressor of the SL signalling pathway, which is controlled by a positive feedback loop by SL levels (Song

et al., 2017). More specifically, in the presence of SLs, D53 is ubiquitinated and degraded by D14- SCF^{D3} complex (Zhou et al., 2013, Wang et al., 2015b, Soundappan et al., 2015), leading to the transcriptional realize of downstream genes, including D53 encoding genes (**Figure 1.9**). This means that there is a positive correlation between the expression of D53 encoding genes and the SL levels. As a result, the strong downregulation of *TaD53* homoeologues suggested that the SL signalling pathway was constantly suppressed in *Tad17* mutants. These observations signified that in *Tad17*, SL biosynthesis is significantly impaired, as also suggested by the *in silico* analysis of the mutant TaD17 proteins. Similar downregulation of *TaD53s* in both N levels compared to the respective WT was also observed in roots, further confirming the systemic suppression of SL signalling in *Tad17* mutants (data not shown).

5.3.3 *TaD17* Is Involved in Tillering Regulation in Wheat

Although SL-deficient mutants have been extensively studied in several species showing that SLs are involved in tillering regulation and in other aspects of plant growth and development, the involvement of SLs in wheat growth had not been comprehensively studied before. *Tad17* mutant lines from different populations and under different experimental conditions showed a highly branched phenotype, suggesting that TaD17 and SLs are involved in tillering regulation in wheat. SL-deficient mutants in other species also form more tiller/branches (Umehara et al., 2008, Gomez-Roldan et al., 2008, Brewer et al., 2016). In addition, just recently, Zhao et al. (2020) showed that TaD27-RNAi lines, which catalyze the formation of 9-cis- β -carotene, the substrate of D17, also formed more tillers than WT plants (Zhao et al., 2020). TaD27-RNAi lines and the *Tad17* mutant lines generated as part of this work were the first wheat SL-deficient mutants, providing a great tool for studying the role of SLs in wheat.

The phenotype *Tad17* mutant also indicated that the *Tad17* mutant had a shorter stature compared to WT plants, suggesting that SLs also affect plant height apart from tillering (**Figure 5.13**). Lin et al. (2009) also reported that the rice *d27* mutant showed a severe dwarf phenotype (Lin et al., 2009). Similarly, SL-insensitive mutant *d3* and SL-deficient mutant *d10* also showed a severe dwarf phenotype compared to WT control (Umehara et al., 2008, Umehara et al., 2010). Consistent with the results presented in

this work, in *d17* rice mutants, the increased tillering was accompanied by reduced plant height (Zou et al., 2006, Butt et al., 2018). The dwarf phenotype of the SL-deficient mutants can be rescued by the application of GR24, indicating that stem elongation is affected by the lack of SLs. However, *Arabidopsis max3* and *max4* SL-deficient mutants have not shown such a severe dwarf phenotype as compared to rice (Umehara et al., 2008). However, in other dicotyledonous species, such as in pea and tomato, SL-deficient mutants have also shown a strong reduction in plant height (Kohlen et al., 2011, de Saint Germain et al., 2013). Therefore, it can be hypothesized that the effect of SLs on plant height can be attributed to competition between growing tillers/branches and the growing stem for carbohydrates. Precocious stem elongation in wheat *tin* lines led to reduced tillering mainly due to sugar deprivation of the lateral buds (Kebrom et al., 2012), while a similar response has also been reported in *phyB* mutants in sorghum (Kebrom and Mullet, 2016). Other studies have also shown a negative correlation between plant height and branching (Ishikawa et al., 2005, Kebrom et al., 2006, Finlayson et al., 2010). This hypothesis is in accordance with the diversion theory of apical dominance, according to which the growing stem inhibits bud outgrowth by diverting sugar away from the lateral buds (Kebrom, 2017). In fact, there is increasing evidence supporting the role of sugar availability on bud outgrowth (Mason et al., 2014). Therefore, the reduced height in SL mutants may not be due to a direct effect of SLs on stem elongation but due to the increased tillering. Growing tillers are strong sinks for photoassimilates; therefore, they compete with stems for sugars. SLs have been shown to keep buds in a dormant state, while bud release from dormancy is an irreversible process. Soon after bud outgrowth is released, the actively grown side tillers are strong sinks which deplete sugars at the expense of stem elongation. This hypothesis has been confirmed in rice, as removal of the excess side shoot can partly restore the reduced height of *d17* mutants (Zou et al., 2006).

However, in pea, removal of the side shoot from SL mutants was not sufficient to restore the dwarf phenotype (de Saint Germain et al., 2013). Therefore in pea, the reduced phenotype of the SL-deficient mutant is not just a consequence of the excessive branching and the competition between sink organs for sugars. In the same study, it was shown that SLs stimulate internode elongation by affecting cell division,

yet SLs act independently of GAs, which are known as the main hormones involved in internode length. The exact mechanism of SL control over plant height remains an open question; however, it is not unlikely that there is a differentiation in the effect of SLs on stem elongation between monocotyledonous and dicotyledonous species. In fact, this differentiation may also be attributed to the different growth patterns as, in pea, the internode is elongated during the vegetative growth stage, while internode elongation is suppressed during the tillering phase in grasses and start to elongate after the transition to the reproductive phase (Kebrom, 2017, McMaster, 2005).

Although the effect of SLs on plant height and stem elongation has not been fully elucidated, more studies have focused on the involvement of SLs in bud outgrowth. The data presented in this study showed that SLs might control tillering by controlling bud dormancy. The expression of *DRM4*, which was highly expressed in wheat nodes among other *DRM* genes, showed significant downregulation in the *Tad17* mutant. *DRM* genes are molecular markers for bud dormancy (Tarancón et al., 2017); therefore, this observation indicated that SLs promote bud dormancy of the lateral bud, while in SL-deficient plants, buds are released from dormancy leading to a higher number of tillers. The effect of SLs on DRM was more prominent under N limitation, indicating that SLs required for the N limitation mediated bud dormancy. However, DRM genes showed an upregulation in response to N limitation even in *Tad17* mutant compared to the high N treated *Tad17*, implying that SLs are not the only signals controlling bud dormancy in response to N availability, which is consistent with the observed phenotype. Lun et al. (2009) reported that *d27* SL-deficient mutant showed that the induced tillering is due to the stimulated bud outgrowth, especially of high order tillers, rather than to more tiller bud initiation as found in rice (Lin et al., 2009). In addition, consistently with our results, in rice, SLs suppress tillering by stimulating dormancy of lateral buds and reducing the expression of cell cycle genes (Luo et al., 2019). However, it has been reported that wheat D27-RNAi lines showed more lateral buds compared to WT plants proposing that SLs also affect bud initiation apart from bud dormancy (Zhao et al., 2020). However, Zhao et al. (2020) reported the total number of initiated buds per plant in field-grown wheat. However, tiller buds in wheat are known to be formed at the base of the shoot; therefore, the more formed tillers a

plant has, the more tiller buds will be formed in total per plant. Therefore, this observation does not necessarily prove that SLs are involved in bud initiation directly as for that comparison, the rate of bud initiation and the number of initiated tiller buds per shoot/tiller should be compared.

TB1/BRC1/FC1 is a transcription factor which has been shown by many studies to be involved in the suppression of tillering. Many studies have shown that TB1/BRC1/FC1 is a downstream target of the SL signalling pathway to control tillering based on the observation that *tb1/brc1/fc1* mutants are insensitive to SLs (Minakuchi et al., 2010, Aguilar-Martínez et al., 2007). In fact, the application of GR24 induced the expression of *BRC1* in Arabidopsis. (Aguilar-Martínez et al., 2007). More recent studies have shown that *BRC1* transcription is controlled by SMXL6, 7, 8 in dicotyledonous species, therefore in the presence of SLs D53 is degraded leading to higher levels of BRC1 and shoot branching inhibition (Jiang et al., 2013, Wang et al., 2015b, Soundappan et al., 2015, Seale et al., 2017). In monocotyledonous species, SLs have been suggested to control *TB1* expression through the interaction of D53 with IPA1, which transcriptionally activates *TB1* expression (Lu et al., 2013, Song et al., 2017, Liu et al., 2017). In dicotyledons, this mechanism has been proven as SL-deficient plants show lower levels of *TB1/BRC1*, while *smxl6, 7, 8* mutants showed induced *TB1/BRC1* expression (Seale et al., 2017, Dun et al., 2012). However, this mechanism has not been proven robust in monocotyledons. GR24 application did not affect the mRNA accumulation of *TB1/FC1*, while SL-deficient mutant did not show altered expression of *TB1/FC1* in rice (Arite et al., 2007, Minakuchi et al., 2010). Similarly, *TB1* expression in maize remained at high levels in highly branched SL-deficient plants (Guan et al., 2012), raising evolutionary questions regarding the divergence between monocotyledons and dicotyledons. Yet, more recent studies showed that *FC1* expression was suppressed in SL-deficient and SL-insensitive rice mutants (Fang et al., 2020), whereas two recent studies showed that the application of GR24 induced the expression of TB1/FC1 in rice tiller buds (Xu et al., 2015b, Zha et al., 2022).

Expression analysis of *Tad17* mutant lines showed that *TaD17* is expressed in the leaf primordia around the lateral buds (**Figure 5.2**, unpublished data). *In situ* hybridization has shown a similar expression pattern for *OsFC1* in the same tissue in rice (Minakuchi

et al., 2010). Moreover, the leaf primordia are the same site as the one that has been found to be affected by SL-induced dormancy in rice (Luo et al., 2019). Therefore, Luo et al. (2019) suggested that the site of SL action in controlling bud outgrowth is at the leaf primordia surrounding the lateral bud. The overlap of *TaD17* and other biosynthetic gene expressions with the expression of *TB1/FC1* is in favour of the idea that *TB1* is a downstream target of the SL pathway. The RNA-seq experiment in the *Tad17* mutant failed to identify significant transcriptional changes in *TaTB1* homoeologues under high N conditions, although a suppression was observed in the *Tad17* mutant compared to the WT control. *TB1* is expressed locally in lateral buds, whilst the RNA-seq was conducted in the whole basal nodes, which presumably explains the fact that *TB1* homoeologues were among the low expressed genes, and they were excluded from most of the comparisons as low expressed genes. However, under low N conditions – where *TaTB1* expression was induced in WT plants – the differential gene expression analysis showed significantly lower levels of *TaTB1* in the *Tad17* mutant. The expression pattern of *TaTB1* homoeologues also highlighted that SLs are required for the induction of *TB1* under N limitation. Gene expression analysis in basal nodes by RT-qPCR showed that *TB1* levels were indeed suppressed in *Tad17*, whereas the effect was more noticeable under N-limiting conditions. This observation is in favour of the model that *TB1* is a downstream target of the SLs signalling pathway. Nevertheless, similarly to the contradictory results reported in rice, Zhao et al. (2020) reported that *TB1* expression was not affected in the D27-RNAi wheat mutants according to RNA-seq.

However, as has been shown in *Arabidopsis*, *brc1* mutants were still able to respond to changes in SL levels implying that SLs can also act independently of BRC1 via a parallel mechanism (Seale et al., 2017). The parallel mechanism of SL control on bud dormancy has been suggested to be mediated by affecting auxin transport (Shinohara et al., 2013, Bennett et al., 2016). The SL-deficient mutant in wheat showed changes in IAA metabolism and signalling genes supporting the interaction between SLs and IAA in controlling tillering. However, the IAA pathway was among the pathways affected in *Tad17* mutant under N adequate conditions. Only under N limitation, the

expression of many genes involved in IAA biosynthesis and signalling was DE in *Tad17*, indicating a link between SL and IAA metabolism.

Nevertheless, the results presented in this study clearly demonstrated the downregulation of *TB1* in wheat in *Tad17* mutant, proving a link between SLs and *TB1* in wheat. However, why was this effect more prominent under low N conditions? It is hypothesised that under high N conditions, the effect of SLs on tiller bud outgrowth is not so strong as the plants have adequate resources; therefore, there is no need for strict control of tillering, whereas, under low N conditions, SL role becomes more important in controlling *TB1* expression to suppress tillering based on nutritional signals. In the same manner, Bennett et al. (2016) suggested that *TB1/BRC1* might not be required for bud dormancy per se but may be required for stabilising bud activity. Based on this theory and the results presented in this thesis, it is hypothesised that under adequate N supply, there is no strong need for plants to control bud outgrowth; therefore, *TB1* remains at low levels as it is not critical in controlling bud outgrowth, while other signals such as auxin, sugar availability and other play a role. On the other hand, under N-limiting conditions, due to lack of available resources tillering regulation is more important for plant survival and adaptation; therefore, SL-mediated regulation of *TB1* becomes more prominent.

Sugar availability is another signal controlling bud outgrowth and dormancy in many species (Tarancón et al., 2017). Recent studies have highlighted the importance of Tre6P in the regulation of tillering/branching in relation to the sugar status of the plants (Fichtner et al., 2017). More specifically, high levels of sugars in tissue are accompanied by an increase in Tre6P, leading to bud outgrowth. *Tad17* showed significant changes in genes involved in Tre6P metabolic pathways, such as genes encoding TPS and TPP. Those changes indicated that SLs might interact with sugar availability signals to control bud outgrowth. Apart from the Tre6P pathway, *Tad17* showed changes in carbon partitioning and utilization. Sugar analysis at the base of wheat plants showed that *Tad17* mutant accumulated higher levels of Glc, Fru and sucrose at the base of the plants, implying that locally more sugars were available for bud outgrowth. In addition, the starch content of the base of the plants was found to

be increased in *Tad17* mutants suggesting that SL may be interact with sugar signalling and control sugar utilization and partitioning.

Most of the studies focus on the hormonal effect on bud outgrowth and sugar availability, however, recent studies have shown that amino acid delivery to the growing stem might also play a regulatory role in bud outgrowth. Manipulation of AAPs leads to changes in tillering/branching in rice and other species (Wang et al., 2019b, Lu et al., 2018, Zhang et al., 2010a). In addition, several studies have highlighted the importance of amino acids, especially Gln and Asn, in controlling plant architecture (Luo et al., 2018a, Ohashi et al., 2017, Ohashi et al., 2018, Ohashi et al., 2015b). Moreover, Asn and Gln is the major form of N transported over long distances, participating in N remobilization. *Tad17* showed changes in the expression of GS encoding genes, while the changes were more apparent under N-limiting conditions. GS enzyme is involved in the formation of Gln, and it is an important step for N assimilation but also for N recycling and reassimilation. The expression of GS was induced in basal nodes of *Tad17*. Lack of GS has been shown to result in a reduction in the levels of Gln and Asn in the bases of rice plants leading to tiller suppression (Ohashi et al., 2018). Therefore, SLs may also interact with other signals and regulate amino acid utilization and partitioning. ASN is an important enzyme for Asn biosynthesis but also for plant development, as manipulation in ASN expression leads to different tillering phenotypes in rice (Luo et al., 2018a). Apart from response to N signals, ASN has been reported to act as a marker gene for the C status of the tissue as it is important for keeping the balance between C and N metabolism. In fact, ASN1 is considered a sugar-starvation inducible gene (Kebrom et al., 2012). The expression of three and five genes encoding ASN was suppressed in SL nodes under high and low N conditions, respectively, compared to the WT controls. Lower expression of ASN suggested an effect of SLs on sugar levels, which, as mentioned above, were elevated in the base of *Tad17* mutants. Lower expression of the ASN1 gene has been reported in WT plants compared to the low tillering *tin* mutants in wheat. ASPG catalyse the catabolism of Asn and is important for the utilization of Asn (Gaufichon et al., 2015). High expression of ASPG encoding genes has been reported in sink tissues. Different wheat genes encoding ASPG were found to be significantly induced in *Tad17* mutants,

further supporting changes in amino acid metabolism and levels affected by the lack of SLs which might be another mechanism of SL control over tiller development which has not been studied before.

5.3.4 SLs Are Required But Are Not the Only Signal Controlling Tillering in Response to N Availability

N limitation strongly suppressed bud outgrowth leading to reduce tillering. SL biosynthesis, as shown in Chapters 3 and 4, is strongly induced by N limitation, suggesting that SLs may contribute to tillering regulation by acting as signals of N status. In fact, this mechanism has been proven in the case of P limitation (Kohlen et al., 2011, Umehara et al., 2010). More specifically, SL-deficient and SL-insensitive mutants failed to control tillering in response to P supply. Under both high N and low N conditions, the *Tad17* mutant showed a higher number of tillers compared to WT segregants (**Figure 5.15**). However, *Tad17* still possessed the ability to regulate tillering in response to N-limitation, as the N-limited *Tad17* mutant formed fewer tillers compared to the *Tad17* mutants treated with high N. This was also consistent with the results from a pot experiment using both *Tad17* SL-deficient and *Tad14* SL-insensitive mutant in a range of different N levels (**Appendix I, Figure S6**), suggesting that SLs are required for full suppression of tillering by N limitation, but SLs are not the only signal contributing to tillering inhibition in response to N supply. Similar results have been obtained in *max1* mutant in Arabidopsis (de Jong et al., 2014). In rice, *d3* and *d10*, SL-insensitive and SL-deficient mutants have also been found to be responsive to N limitation signals consistently with our results (Luo et al., 2018b).

Therefore, although elevated levels of SLs are the predominant signals controlling tillering under P limitation, this is not the case for N limitation. This differentiation between the two macronutrient limitations suggests that tiller inhibition under N-limiting conditions also involves other metabolic or hormonal pathways. N is required in larger quantities compared to P and is involved in many metabolic processes important for plant growth and development. As shown in Chapter 4, wheat plants show higher sensitivity to N supply compared to P (sections 4.2.1, 4.2.4). Therefore, due to the importance of N, plants might have developed more than one mechanism to control architectural responses to N limitation to increase N utilization and their

chances of survival. The complexity of tillering regulation by N supply has also been shown by the fact that *brc1 brc2* Arabidopsis mutants still responded to N limitation, suggesting that other factors apart from SLs and TB1 master regulator are responsible for N limitation mediated tillering regulation (Seale et al., 2017). As shown in Chapter 4, N limitation showed a wide range of transcriptional changes, including changes in carbon metabolism and utilization, resource allocation and other hormonal pathways, which may comprise parallel or interconnected mechanisms to the SL-mediated tillering regulation. Among the potential signals controlling tillering under N limitation are CKs. It is well known that CKs act as signals of N availability (Sakakibara et al., 2006, Sakakibara, 2021). CK biosynthesis and CK levels showed a significant downregulation under N limiting conditions (**Figure 5.33**). CKs act as positive regulators of tillering; therefore, the reduced accumulation of CKs, such as tZ and tZR, in the basal nodes contributes to tiller inhibition. Although the *Tad17* mutant showed changes in CK concentration in the basal nodes compared to WT plants (discussed extensively in section 5.3.6), N-limited *Tad17* also showed reduced levels of tZ and tZR in nodes compared to high N-treated *Tad17* mutants. The lower CK accumulation in basal nodes of *Tad17* mutant under low N may explain the reduction of tillering observed in *Tad17* mutants under N limitation despite the lack of SLs biosynthesis. In other words, the N-mediated regulation of CK biosynthesis is not dependent on SLs. CK biosynthesis and signalling have been found to be controlled by NO₃⁻ availability signals governed by NLP and NIGT1 TFs and by glutamine-related signals, which presumably connect assimilated N with de novo CK biosynthesis (Kamada-Nobusada et al., 2013, Sakakibara, 2021, Maeda et al., 2018). Lack of SLs increases the levels of CKs, however, it is not sufficient to suppress the N limitation downregulation of CK content in basal nodes, leading to a reduction in tiller number.

5.3.5 SLs Affect Resource Allocation under N-limiting Conditions

N limitation is known to trigger changes in biomass allocation between roots and shoots. More specifically, the results presented in this study suggested that N limitation led to strong suppression in shoot biomass accumulation, whereas root biomass accumulation did not significantly change within the examined time frame. It is known that under N limitation, this shift in biomass allocation is an important part

of plant adaptation to nutrient-limiting conditions. Under N-limiting conditions, root growth is promoted while shoot growth is suppressed, allowing the plant to explore more soil for available nutrients and increase nutrient capture (Oldroyd and Leyser, 2020). In other words, under nutrient-stress conditions, root growth is prioritized at the expense of shoot growth. This response is usually reflected by an increase in root/shoot ratio, as also observed in WT plants (**Figure 5.15**). However, the *Tad17* mutant showed a significantly lower root/shoot ratio compared to N-limited WT plants, which was mainly attributed to the lower root biomass accumulation of *Tad17* plants, suggesting that biomass allocation to root was attenuated in *Tad17*. A similar observation has also been reported in *max1* in Arabidopsis and in *d3* and *d10* in rice (de Jong et al., 2014, Luo et al., 2018b). However, the root fraction was not affected when N was sufficient in Arabidopsis, which was consistent with our results (**Figure 5.15**). Those observations clearly demonstrated that SLs are required for the regulation of resource allocation between above and below-ground biomass as part of plant adaptation to N-limiting conditions. Apart from changes in root growth, plant response to N limitation also involves changes in root architecture, which includes an increase in lateral and seminal root elongation while lateral root density is reduced. Sun et al. (2014) showed that SL-deficient and SL-insensitive mutants did not show the same sensitivity to N and P limitations with regard to root architectural changes (Sun et al., 2014). Therefore, it is suggested that under N-limiting conditions, SLs are not only involved in biomass allocation towards the roots but also in changes in root architecture.

Based on the above observations and the overall plant response of *Tad17* to N conditions, the SL effect on biomass allocation in response to N supply may be attributed to a direct effect of SLs on root growth or to an indirect effect. The indirect effect is based on the competition of sink tissues for carbohydrates and nutrients. Both roots and basal nodes are not photosynthetic tissues, hence, their growth relies on photoassimilates produced in source leaves. Normally under N-limiting conditions, bud outgrowth is suppressed, and less carbon is utilized for tiller outgrowth, therefore, there are fewer active N and C sinks above ground, leading to more sugars diverted into the roots to support root growth. However, in the lack of SLs in *Tad17* mutants,

tiller buds are released for dormancy; therefore, there are more actively growing sinks in the upper part of the plants and the balance between source and sinks is disrupted. In fact, many genes that reflect the sink strength of the tissue, such as invertases, sugar and carbohydrate transporters, amino acid metabolic genes and others, were found to be significantly DE in *Tad17*, suggesting that SLs may suppress the sink strength of the tissue. The sink strength of a tissue relies on size and activity. Barbier et al. (2019) reported that the sugar sink strength of the lateral buds is especially high upon bud release from dormancy (**Figure 1.2**). Therefore, in SL-deficient plants, more buds are released from dormancy, leading to an increase in the number of sinks but also in the sugar and N sink strength of the tissue leading to an imbalance in carbohydrate transport into the roots, which in turn affects root growth rate, especially under low N conditions where C is a limiting factor along with N. There are few studies showing a promotion or root growth after the application of SLs, supporting a direct effect of SLs on root biomass allocation. As a result, the indirect hypothesis is more likely to be true.

Plant response to N limitation does not only include changes in root and shoot biomass allocation, but also involves strong remobilization of inorganic nutrients, and predominately N. N limitation triggers N remobilization from older to younger leaves (Smart, 1994). In this study, SPAD readings from different leaves were recorded and used as an estimation of leaf N content. SPAD estimates leaf chlorophyll concentration, however, many studies have shown that SPAD readings and leaf chlorophyll concentration positively correlate with leaf N content (Mehrabi and Sepaskhah, 2022). Therefore, the increase in SPAD readings from older (first leaf) to younger leaves (third leaf) in N-limited WT plants might reflect the remobilization of N from older to younger leaves (**Figure 5.15B**). However, this response was affected in *Tad17* mutants as young leaves tend to be more chlorotic compared to older leaves indicating that the lack of SLs interrupted the typical remobilization of N. Zha et al. (2022) also reported that the first leaf in N-limited rice plants remained green in SL-deficient mutants, while in WT plants the first leaf (older) turned yellow, also supporting that N remobilization between the tissue is altered in SL mutants (Zha et al., 2022). N is remobilized mainly in the form of amino acids, which are transported

to N sink tissues, where N is reassimilated. In fact, many amino acid transporters were found to be significantly DE in the basal nodes of *Tad17* mutants compared to WT plants under low N conditions, while others showed genotype-dependent regulation to N limitation, implying that SLs are required for their regulation to N limitation. The same was observed for NRT2 and ammonium transporters, indicating that overall N remobilization and distribution are affected by SLs. In rice leaves, several amino acid and ammonium transporters involved in the remobilization of N were shown to be suppressed in the leaves of *d3* and *d10* mutants (Luo et al., 2018b), further supporting the observation of this work that under N limiting conditions, the increase in SLs content contribute to nutrient remobilization.

5.3.6 SL and CK Interaction

SLs and CKs have a central role in regulating tillering/branching, acting antagonistically in regulating bud outgrowth (Dun et al., 2012). More specifically, SLs suppress, whereas CKs promote bud outgrowth. Phytohormonal analysis in the basal node of plants showed that *Tad17* mutant showed elevated levels of CKs under both high and low N conditions (**Figure 5.33**). However, in pea and Arabidopsis, no differences in CK levels in the shoot tips were found between SL mutants and WT (Foo et al., 2007). Similarly, Arite et al. (2007) reported that *d10* rice mutant showed similar levels of CKs in shoot apices compared to WT (Arite et al., 2007). However, recent studies in rice have reported increased CK levels in the tiller buds or plant bases of *d10* and *d53* mutants (Zhang et al., 2010b, Duan et al., 2019b). Among the examined CKs, only tZR and tZ concentrations were found to be significantly higher in *Tad17* mutants independently from the plant N status. tZR and tZ are considered the most active forms of CKs playing a central role in the regulation of plant architecture. In addition, as mentioned in section 4.2.16, tZ and tZR are the predominant forms of CKs found in basal nodes, indicating their importance in the regulation of growth in this particular tissue. Consistent with the results of this study, elevated levels of tZ and tZR have also been reported in shoot bases of rice *d53* mutants (Duan et al., 2019b). In contrast, the application of GR24 led to the downregulation of all forms of CKs in rice tiller buds (Zha et al., 2022). All these observations indicate a negative effect of SLs on CK levels at

shoot bases. Therefore, the high tillering phenotype of the *Tad17* mutants may be at least partly due to the higher accumulation of CKs in the basal nodes.

However, the transcriptomic analysis performed as part of this study did not show any significant response of CK metabolic genes in *Tad17* mutants under high N conditions, which could explain the observed induction in CK content. Only *TaLOG10-1D* was found to be induced in the basal nodes of high N treated *Tad17* compared to WT. In pea, SL-deficient and SL-insensitive mutants have shown higher expression of the *IPT1* gene compared to WT, indicating the SLs may negatively affect CK biosynthesis (Dun et al., 2012). However, other studies have shown that SLs regulate CK levels by controlling mainly CK degradation rather than by controlling CK biosynthesis (Ha et al., 2014, Duan et al., 2019a). More specifically, Duan et al. (2019) demonstrated external application of GR24 induces the expression of *OsCKX9* in rice, while the *d53* mutant showed lower expression of *CKX9*, concluding that SLs control CK levels by inducing CK degradation. However, other CKX encoding enzymes did not show any response to SL levels, while *OsCKX9* was not highly expressed compared to other CKX encoding genes. Based on the results presented in this thesis, the expression of some CKX encoding genes was found to be higher in *Tad17* mutants (**Figure 5.28**). However, this might be due to a negative feedback loop of CK response that regulates the transcription of most *CKX* genes. More specifically, the external application of CKs triggers rapid induction of different *CKX* genes (Duan et al., 2019b, Tsai et al., 2012). Therefore, the induction of *TaCKX* genes in *Tad17* may be a result of the higher levels of CKs found in *Tad17* basal nodes and not affected by the SLs. A possible explanation for the elevated levels of CKs is that the effect of lack of SLs in *Tad17* mutant on CK biosynthesis or degradation was subtle under high N conditions, therefore, the genes were not identified as DE by the RNA-seq data.

However, the results suggested that SLs had a profound effect on CK-related genes under N-limiting conditions. When N was limiting, the lack of SL biosynthesis in *Tad17* mutant had a drastic effect on many genes involved in CK biosynthesis, catabolism and signalling. It is widely accepted that there is a positive correlation between N and CK levels (Sakakibara et al., 2006, Sakakibara, 2021). N limitation led to strong suppression of CK biosynthetic genes and a systemic decrease in CK levels (**Figures**

5.28, 5.33). Therefore, based on our results, SLs are required for the full suppression of CK biosynthetic genes by N signals, given that under N-limiting conditions, the expression of many biosynthetic genes remained at higher levels compared to WT plants. The effect of SLs on CK biosynthesis was consistent in gene encoding IPT, CYP735 and LOG enzymes. IPTs are involved in de novo CK biosynthesis producing iP-type of CKs, while CYP735 convert iP-ribose to tZ-ribose (**Figure 1.10**) (Kudo et al., 2010). Based on the current understanding of CK biosynthesis, LOG enzymes convert ribotides to the respective free base cytokinin (tZ, iP, etc.). In fact, under low N conditions, not only tZR and tZ levels were upregulated in *Tad17* mutants, but also, iPA concentration was higher in the basal nodes. This observation suggested that SLs may affect *de novo* CK biosynthesis in basal nodes, and they are also involved in the suppression of CK biosynthesis under N-limiting conditions.

A question that arises from the hormonal and transcriptomic data presented in this study is that although the transcript abundance of many SL biosynthetic genes was significantly higher in N-limited *Tad17* mutants compared to WT, why did the *Tad17* mutant still show a significant reduction in CK levels in the basal nodes in response to N limitation? As a result, although SLs are required for the suppression of CK biosynthetic genes in response to N limitation, the lack of SLs is not sufficient to prevent the reduction of CK levels under N limitation. The reduction of tZ and tZR concentration in *Tad17* mutants in response to N limitation can explain why *Tad17* mutants still possess the ability to reduce their tiller number in response to N status. Under both N conditions, the tZ-type of CKs was higher than the WT, while the same rate of increase in tillering was observed in both conditions compared to the respective WT. Therefore, this observation suggests that the main signal for the suppression of tillering by N limitation is the reduction in CK content, while SLs are required for keeping CKs at low levels.

As stated above, although CK biosynthetic genes were strongly induced in the *Tad17* mutant compared to WT, the *Tad17* mutant still showed a strong reduction in CK levels. This may be explained by the presence of post-translational control of CK biosynthetic enzymes, or the reduction may be due to the lack of available substrate. In the case of CK biosynthesis, purine and, more specifically, adenine is the precursor

for iP-ribose biosynthesis. Purine catabolism is known to be induced under N-limiting conditions as part of the N recycling mechanism through the allantoin catabolic pathway (Casartelli et al., 2019). *Tad17* mutant showed induction in allantoin catabolic genes suggesting strong recycling of purine-derived N leading to lower levels of purines. Therefore, the lack of purine, the substrate of CK biosynthesis, might explain the reduction of CK content in *Tad17* despite the higher expression in CK biosynthetic genes. In addition, although the strong induction of SL biosynthesis, genes encoding CK catabolic and inactivation enzymes (CKX, CK glycosyltransferase) showed a systematic induction in *Tad17* mutant under N-limiting conditions. CK catabolic enzymes are regulated by feedback regulation (Duan et al., 2019b). Therefore, the CK degradation might be strongly induced in *Tad17* mutant under low N to keep the CK levels low. Presumably, the feedback mechanism that controls CK levels is stronger under low N conditions to keep CK levels low. The opposite might be true for the biosynthesis genes, which are controlled by negative feedback regulation. Under high N conditions due to the high levels of CK, the effect of SLs on CK biosynthetic genes is masked by the negative feedback regulation, while under low N conditions, due to the overall reduction in CKs levels, the feedback regulation is weaker and the effect of SLs becomes more apparent. This can explain the fact that in previous studies, despite the increase in CK content, no strong effect on CK biosynthetic genes was reported. It is suggested that although the induction of CK biosynthesis due to the lack of SLs in *Tad17*, other mechanisms related to N-status induce CK homeostasis and degradation to keep CKs at low levels resulting eventually in suppression of tillering under N-limiting conditions.

In addition, although the CK levels in *Tad17* N-limited plants were significantly lower compared to the same genotype under high N, there was a strong induction in AHK encoding genes. *TaAHK4* encodes a CK receptor protein. Many type-A RRs showed a significant 2-way interaction meaning that their response to N limitation was dependent on the genotype. CKs are known to induce the expression of type-A RRs, while they are important for the CK-mediated regulation of growth. Application of GR24 reduces the expression of type-A RRs, whereas the expression was higher in different rice SL-deficient mutants (Duan et al., 2019b). Therefore, it is suggested that

SLs reduce sensitivity to CKs. Similarly to this observation, Dun et al. (2012) reported that the SL-deficient mutant is more sensitive to CK than WT plants, whilst the application of GR24 reduces CK-induced growth in SL-deficient mutants but not in SL-insensitive mutants (Dun et al., 2012).

As a result, it is suggested that SLs suppress CK levels by affecting CK biosynthesis and/or CK degradation, while SLs may also have a role in plant sensitivity to CKs. However, other studies have shown that CK levels also affect SL biosynthesis. SL biosynthetic genes have been found to be suppressed after the application of CK, while this effect has been found in both root and basal nodes of rice plants (Xu et al., 2015b). Apart from the effect on SL biosynthesis and signalling genes transcription, CK application reduced the levels of SL in root exudates of sorghum, further confirming that CK has a negative effect on SL production (Yoneyama et al., 2020b). Taken together, it is suggested that CK and SL have an antagonistic action in controlling plant architecture, while both are essential for plant adaptation to different N levels.

Chapter 6 General Discussion

6.1 Introduction

In the first chapter (Chapter 1), our current understanding of tillering regulation, SL biosynthesis and signalling, and the N limitation responses was presented, focusing mainly on findings in monocotyledonous plants. In the following chapters, further insights into SL biosynthesis, perception and signalling genes in wheat and their regulation by nutritional signals (Chapter 3); the transcriptional effect of N limitation on different pathways and their link to tillering regulation (Chapter 4); the role of SLs in modulating plant architecture and nutrient limitation responses (Chapter 5) were covered extensively in the discussion sections of the corresponding chapters. Therefore, this general discussion chapter discusses the future perspective that arises from the key findings and their potential implementation for wheat crop improvement.

6.2 Future Perspective

6.2.1 Shoot Architecture

Tillering is an important component of plant architecture in cereal crops, along with plant height, tiller angle and others. Manipulation of plant architecture has been shown to have the potential to increase crop productivity and grain yield. The most classical example is the introduction of semi-dwarfing alleles in modern rice and wheat varieties during the green revolution leading to high-yielding semi-dwarf elite varieties with almost double grain yield production than taller varieties (Khush, 1999). However, due to the increasing global population and the predicted demand for wheat, global wheat production needs to increase to cover the global demand. On the grounds that the availability of agricultural land is not predicted to increase and the potential negative impacts of global warming on plant productivity in many areas around the globe, there is an urgent need for further increases in wheat grain yield production. As a result, novel alleles are required for crop improvement.

Tillering is an important agronomic trait and an important component of grain yield in cereal crops. Wang et al. (2018) reported that tiller number is a critical target for rice

breeding (Wang et al., 2018a), yet the same can be applied to other cereals as the number of fertile tillers positively correlates with grain yield (Harasim et al., 2016). In fact, manipulation of tiller formation in cereals can potentially increase grain yield (Sakamoto and Matsuoka, 2004). SLs were shown to play an important role in wheat architecture not only by affecting the number of tillers but also by affecting plant height, tiller angle and other aspects of plant architecture important for plant productivity. A similar observation has been found in SL mutants in many species, such as rice, where the role of SLs in plant architecture has been more extensively studied. Therefore, manipulation of SL biosynthesis and signalling may potentially be utilized for improving wheat plant architecture and breeding wheat lines with improved characteristics.

However, the relationship between the number of tillers and grain yield is complex, as grain yield is also affected by tiller abortion and tiller fertility. It is known that late-formed tillers show lower fertility and therefore do not contribute equally to the final grain yield. In addition, some of the late-formed tillers fail to produce an inflorescence and do not contribute to the final yield. In fact, excessive tillering, as observed in SL-deficient mutant lines, can lead to yield reduction, especially under stress conditions due to ineffective use of available resources (Kebrom et al., 2012). What is apparent in rice SL mutants is that an increase in tiller number does not necessarily associate with an increase in grain yield, as the *d17* SL-deficient mutant had a negative impact on seed-setting and produced smaller and thinner panicle/ears leading to yield reduction (Wang et al., 2020c). In addition, based on the multiple actions of SLs, complete loss of SL production to increase tillering would also have a negative impact on root symbiotic associations and nutrient limitation responses which might have a negative impact on nutrient capture under nutrient limiting conditions.

That being the case, the exploration of new beneficial alleles of SL biosynthetic and signalling genes might be utilized to improve tillering without yield reduction and without compromising other functions of SLs. A recent example is the identification of HIGH TILLERING AND DWARF 1 (HTD1^{HZ}), a beneficial allele of *OsD17*, which leads to partly loss-of-function of D17 and defective SL biosynthesis. This allele leads to higher tiller production without a negative effect on other agronomic traits leading to

improved crop performance. Interestingly, it was found that this allele $HTD1^{HZ}$ has been co-selected with *Semidwarf 1 (SD1)* and contributed to the development of semi-dwarf elite rice varieties during the green revolution (Wang et al., 2020c). In addition, an introduced mutation using CRISPR-Cas9 leading to partial loss-of-function mutation led to increased tillering and had a beneficial impact on rice grain yield. Genetic variation in tillering of elite rice cultivars has been associated with variation in SL production (Cardoso et al., 2014). All these observations highlight the potential of manipulation of SL production and signalling in shaping plant architecture and improving grain yield production. However, SL metabolism has not been extensively studied in wheat, and the genetic variation in SL production and signalling remains unexploited. In addition, tillering has been considered as a less important trait for wheat breeding probably due to its plasticity. The identification of SL biosynthetic, perception and signalling genes and their involvement into modulating plant architecture as presented in this thesis can be the foundation for exploring novel alleles in wheat germplasm for improving wheat plant architecture. Apart from the architecture of the individual plant, crop architecture at a population scale is also important in cereal crops as plant architectural traits are affected by plant density, soil volume, light availability etc. Recently, it was shown that SLs are also involved in the regulation of plant architecture in relation to plant density and soil volume by neighbouring plants (Wheeldon et al., 2022, Yoneyama et al., 2022). Therefore, by utilization of this finding, manipulation of SLs might allow adjustment of not only plant architecture at the individual scale, but crop architecture at a population scale for higher productivity.

6.2.2 Plant Response to Nutrient-limiting Conditions

Nutrient availability is among the main signals controlling SL biosynthesis and signalling. N and P limitations strongly induced SL biosynthesis in wheat roots. In the basal nodes, N had a more substantial effect on SL biosynthetic and signalling gene transcription than P limitation, which might be associated with plant sensitivity to nutrient limitation, as wheat plants showed higher sensitivity to N compared to P limitation, at least in relation to tillering control. Numerous studies have shown that SL production and exudation are promoted under nutrient-stress conditions. It is well

established that P and, to a lesser extent, N limitations induce SL production and exudation (Yoneyama et al., 2012), while a more recent study has shown that other nutrient deprivations, such as S, also promote SL biosynthesis (Shindo et al., 2018).

Based on the SL functionality, the induction of SLs under nutrient-limiting conditions has a dual role, acting as plant hormone controlling plant architecture but also as rhizosphere signal promoting AMF association to increase nutrient capture. Both actions contribute to plant responses to nutrient-limiting conditions. The results presented in this thesis showed that SL biosynthesis was among the top enriched pathways under N-limiting conditions in the basal nodes, implying that potentially SLs do not act only as a branching inhibitor but also as a systemic signal coordinating N-limitation responses. *Tad17* mutant showed that although SLs are required for full branch suppression by N limitation, SLs are not essential for shoot architectural changes in response to N limitation. It was also shown that SLs interact with CKs to control plant architecture. However, apart from the regulation of tillering, other changes which contribute to plant adaptation to N-limiting conditions were found to be affected in SL-deficient mutants, such as resource allocation between root and shoot, nutrient remobilization and many others. Other studies have also shown that SLs play an important role in modulating nutrient limitation responses and resource partitioning between tissues. Plants growing under N- or P-limiting conditions also normally show changes in root architecture, such as the promotion of lateral root growth and root angle to improve nutrient capture and increase exploration of soil, respectively (Oldroyd and Leyser, 2020). However, it has been shown that SL mutants in rice displayed a different response to N and P limitation in terms of root architectural changes, and the same was observed in Arabidopsis SL mutants (Ruyter-Spira et al., 2011, Sun et al., 2014).

Apart from the architectural adaptation to nutrient-limiting conditions, SLs are likely involved in controlling transcriptional networks related to nutrient limitations, leading to morphological and physiological changes as part of plant adaptation to nutrient-limiting conditions. In fact, it was shown that tomato SL-deficient mutants failed to activate most of the P-starvation mechanism, suggesting that SLs act as a signal triggering the P-starvation response (Santoro et al., 2021). Similarly, Marro et al. 2021

showed that, in tomato, SLs regulate the expression of important TFs that control the P and N limitation responses, such as the transcription factors *NIGT1* and *PHO2* (Marro et al., 2022). *NIGT1* belongs to the family of GARR_G2_like, which play a central role in N limitation response, while members of this family have also been found to control the balance between N and P metabolism (Kiba et al., 2018, Maeda et al., 2018). The RNA-seq data in wheat *d17* mutant showed changes in many TFs previously identified as master regulators of N-response, such as the genes encoding the TFs *NIGT1*, *HHO3,4*, *LBD37, 38, 39* and *BT1,2* and others when growing under N-limiting conditions. In addition, the SL mutant showed changes in *PHR4* under N-limiting conditions. PHRs are known to govern transcriptional changes of the P limitation response and to take part in coordinating N and P homeostasis under nutrient stress (Sun et al., 2018, Ruan et al., 2017). Hence the changes in *PHR4*, along with the observed changes in *NIGT1*, may suggest that SL play a role in linking N and P metabolism under nutrient-limiting conditions. Changes in that TFs under N-limiting conditions are associated with N limitation responses, such as transcription of N transporters and N assimilation enzymes aiming to increase N uptake and optimize nutrient use. The induction of many members of the NF-YA family of TF by N limitation, whose role has been associated with long-term exposure to nutrient stress (Leyva-González et al., 2012), was found to be attenuated in *Tad17* mutants, indicating that *Tad17* showed changes in N-limitation sensing.

Therefore, manipulation of SL biosynthesis or signalling by the exploration of the genetic variation among wheat germplasm for beneficial alleles might be a useful tool for improving varieties with optimized nutrient use efficiency. In an alternative approach, other studies have shown the potential use of SL analogues as growth regulators to improve plant response to nutrient stress. Soil application of SL analogues to maize and sunflower crops increased N uptake efficiency under low N conditions (Chesterfield et al., 2020). Therefore, SLs have the potential to be utilized in different ways in order to increase plant nutrient use efficiency and reduce fertilizer inputs.

6.2.3 Strigolactone Structural Diversity

As it has been previously discussed, SLs have been shown to have multiple functions acting as plant hormones, as rhizosphere signals involved in plant association with AMFs but also involved in parasitic plant seed germination. All those functions can be utilized to tackle agricultural problems related to plant architecture, nutrient capture or in crops where parasitic weeds are reducing crop productivity (Chesterfield et al., 2020). As plant hormones, SLs have been found to regulate different aspects of plant growth and development. SLs are mainly associated with plant architecture as they are involved in tillering, plant height, and tiller angle, but as shown in this thesis, they play an important part in modulating plant adaptation to nutrient-limiting conditions. As covered in sections 6.2.1 and 6.2.2, manipulation of SL biosynthesis or signalling pathways might be a promising way to improve cereal crops such as rice or wheat. However, severe manipulation of SL biosynthesis, such as in SL-deficient mutants, although able to change plant architecture, does not necessarily lead to yield benefit, while the AMF association would be negatively affected and vice versa. Therefore, strong manipulation of SL biosynthesis and signalling resulted in a compromise in other actions of SLs, which may not be beneficial. As a result, less severe mutants such as signalling mutants or partly loss-of-function mutants might be useful for the purpose of crop improvement.

Another possible approach will be the manipulation of specific functions of SLs. Although this might initially sound very challenging, there is evidence that plants produce different types of SLs, which raises fundamental questions about their activity and functionality *in planta*. To date, there are more than 30 naturally occurring SLs identified in plants, while plants have been found to produce a mixture of different canonical and non-canonical SLs. Most of the structural diversity of naturally occurring SLs is a result of steps downstream of CL, leading to the formation of different bioactive SL molecules. The steps downstream of CL are catalysed mainly by members of cytochrome P450 CYP711 encoding by *MAX1*. Cereals have multiple *MAX1* genes in their genome, which raises more questions about their functionality and their specificity. In rice and other species, it has been demonstrated that some *MAX1* homologues are involved in the biosynthesis of the canonical SL, orobanchol. In

contrast, the function of some rice *MAX1* remains elusive. Less is known about the biosynthetic pathway of strigol, which is another canonical SLs found in plant species. More recently, *SABATH* methyltransferase and *LBO* were found to be involved in the formation of Me-CLA and 1'-OH-MeCLA, which are both non-canonical SLs, providing some insights into the formation of non-canonical SLs (Brewer et al., 2016, Yoneyama et al., 2020a, Wakabayashi et al., 2021). In addition, *Arabidopsis lbo* mutants have an intermediate tillering phenotype as they produce more tillers than the WT plants but fewer tillers than SL-deficient mutants (Brewer et al., 2016). Therefore, it is suggested that plants produce more than one type of SLs with tillering inhibitory activity. In addition, the functionality of canonical and non-canonical SLs also remains an open question. Canonical SLs are mainly found in root exudates, while both non-canonical SLs Me-CLA and 1'-OH-MeCLA have shown tiller inhibitory activity (Abe et al., 2014, Brewer et al., 2016). Consequently, Yoneyama et al. 2018 suggested that non-canonical SLs might act as branching inhibitors, while canonical SLs produced mainly in roots and act as rhizosphere signals (Yoneyama et al., 2018b). The diversity of SLs and especially of the non-canonical SLs and their specific functionality has not been extensively studied due to limitations in their quantification in plant tissue but also due to the lack of understanding of the functionality of the biosynthetic enzymes.

As part of this thesis, wheat *MAX1* genes were identified while their spatial expression pattern was examined. The results showed that the *TaMAX1a2* homoeologous subgroup was predominately expressed in roots and based on an orthology search, predicted to be involved in the biosynthesis of canonical SLs. On the other hand, *TaMAX1c* homoeologues were only found to be expressed in above-ground plant tissue, implying that they may be responsible for the biosynthesis of SLs that act as branching inhibitors. In addition, the wheat orthologues of *AtLBO* and *AtSABATH-methyltransferase* showed the same feedback regulation as the other SL biosynthetic genes in *Tad17* mutants, suggesting that they are functional orthologues also involved in the biosynthesis of non-canonical SLs in wheat. Identification of those genes in the wheat genome and the information generated as part of this thesis can be utilized for the manipulation of different *MAX1* homoeologous subgroups, which may result in changes in SL profile in plants. Cardoso et al. (2014) showed that the observed

variation in SL biosynthesis among rice accession was associated with different copy numbers of *MAX1*, which was associated with variation in tillering in those varieties (Cardoso et al., 2014). Therefore, it is suggested that SL diversity and genetic variation in genes downstream of the core SL biosynthetic pathways need to be further exploited. Finally, as also suggested by Chesterfield et al. (2020), further understanding of the functionality of different enzymes leading to SL diversity and the functionality of different SL molecules should allow targeted manipulation of SL biosynthesis and the SL profile, leading to changes in desired actions of SLs, assuming that different SLs may have distinct functionalities *in planta*.

Appendix A: RT-qPCR Primer Efficiency Test

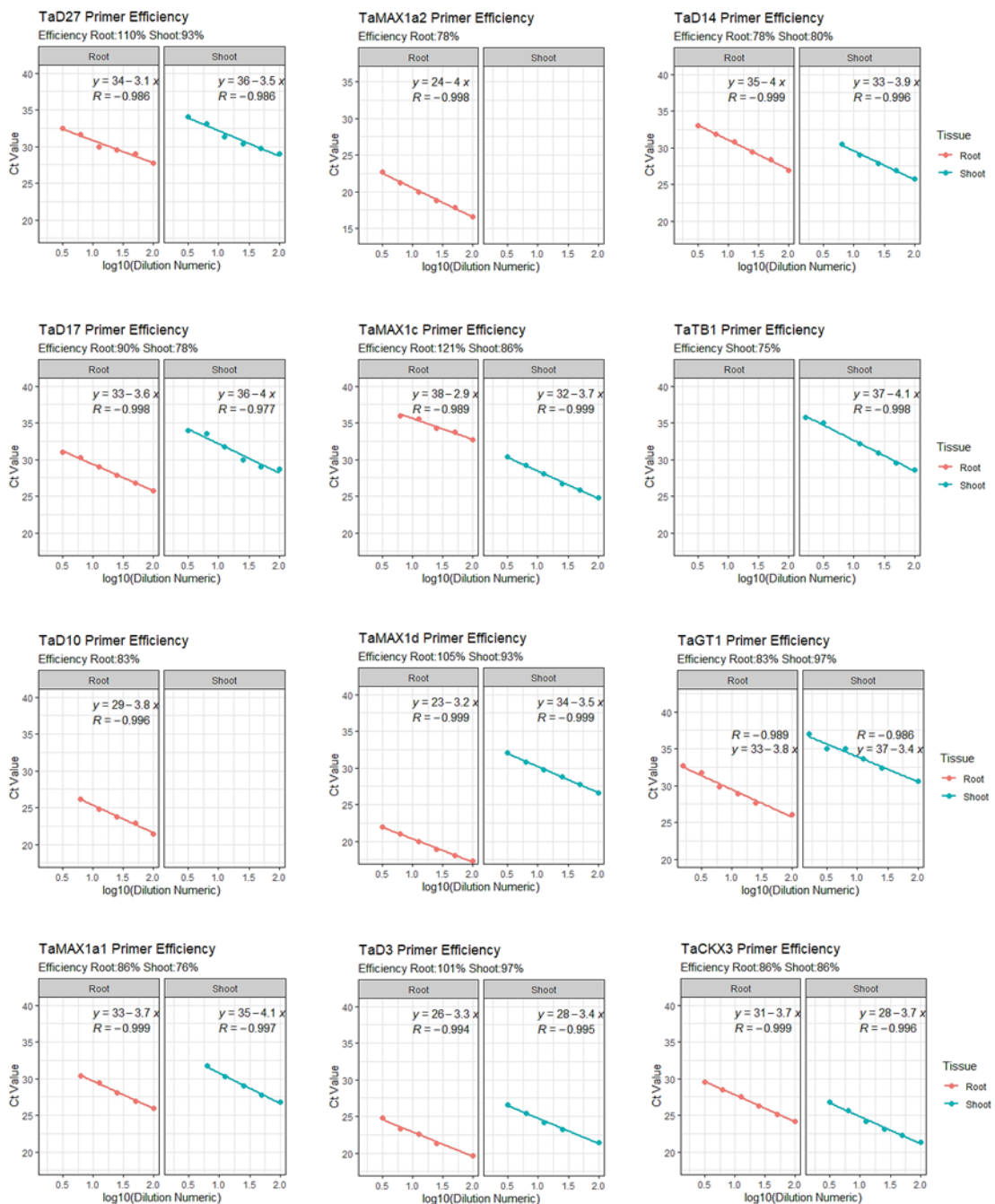


Figure S1: RT-qPCR primer efficiency test by using a dilution series of cDNA from root and shoot total RNA samples. Efficiency was calculated based on the slope of the standard curve.

Appendix B: Differential Gene Expression Analysis R Script (DESeq2)

```
#This is an example of the script used for the differential gene
expression analysis

#This example corresponds to the analysis of the RNA-seq from Tad17
mutants at two different N levels

#Input files required: factor data and count table (generated by
featureCounts tool)

# Load the required packages

library(DESeq2)
library(pheatmap)
library(RColorBrewer)
library(PoiClaClu)
library(dplyr)
library(ggplot2)
library(ggrepel)
library(DEGreport)
library(tidyverse)
library(EnhancedVolcano)

#Set the directory where the required files are stored

setwd("F:/Petros Documents_PhD_revised/d17_LowN_RNA-seq/RNA-seq
Analysis/FeatureCounts_Based/Nodes")

#Input factor data file

factordata <- read.table("expdesign_nodes.txt",header=T,sep="\t")

head(factordata)

factordata$Block<-as.factor(factordata$Block)

factordata$Nlevel<-as.factor(factordata$Nlevel)

factordata$Genotype<-as.factor(factordata$Genotype)

factordata$BC1F2<-as.factor(factordata$BC1F2)

factordata$Line<-as.factor(factordata$Line)

str(factordata)

#Input count data

countdata <-
as.matrix(read.table("d17NodesCountData.txt",sep="\t",header = T,
row.names = 1))

head(countdata)

str(countdata)
```

```

#Define the model with interaction term in the formula (2-way
interaction)

dds <- DESeqDataSetFromMatrix(countdata, factordata, design = ~
Block+Genotype+Nlevel+Nlevel:Genotype)

dds

dds <- estimateSizeFactors(dds)

#Filter out genes where there are less than 3 samples with normalized
counts greater than or equal to 5

idx <- rowSums( counts(dds, normalized=TRUE) >= 5 ) >= 3

dds <- dds[idx,]

dds

design(dds)

dds$Nlevel<-relevel(dds$Nlevel,ref= "HighN")

dds$Nlevel

dds$Genotype<-relevel(dds$Genotype,ref= "d17WT")

dds$Genotype

#Perfomr DESeq2

dds <- DESeq(dds)

resultsNames(dds)

plotDispEsts(dds, main="Dispersion Plot Nodes")

#Perform PCA plot

vsd <- vst(dds, blind = FALSE)

head(assay(vsd), 3)

str(factordata)

str(vsd)

plotPCA(vsd,intgroup = c("Nlevel", "BC1F2")) +
geom_label_repel(aes(label=name)) + ggtitle("PCA plot Basal Node") +
theme(plot.title = element_text(size=16, face="bold"))

#Sample Distances

sampleDists <- dist(t(assay(vsd)))
sampleDistMatrix <- as.matrix( sampleDists )
rownames(sampleDistMatrix) <- paste( vsd$SampleID)
colnames(sampleDistMatrix) <- paste( vsd$SampleID)
colors <- colorRampPalette( rev(brewer.pal(9, "Blues")) )(225)
pheatmap(sampleDistMatrix,

```

```

        clustering_distance_rows = sampleDists,
        clustering_distance_cols = sampleDists, show_colnames = T,
color = colors, main = "Sample Distance Matrix Basal Node")

#Define cut-off for DE genes

padj.cutoff<-0.01

lfc.cutoff<-0.58

#What is the effect of d17 mutation under High N?

d17MresHN <- results(dds,alpha=0.01,name="Genotype_d17M_vs_d17WT")

summary(d17MresHN)

d17MresHN <- d17MresHN[order(d17MresHN$padj),]

head(d17MresHN)

d17MresHN_results <-
as.data.frame(dplyr::mutate(as.data.frame(d17MresHN),
Effect=ifelse(d17MresHN$padj<padj.cutoff &
d17MresHN$log2FoldChange>lfc.cutoff, "d17M:UP",
ifelse(d17MresHN$padj<padj.cutoff & d17MresHN$log2FoldChange< -
lfc.cutoff, "d17M:DOWN", "No Effect"))),
row.names=rownames(d17MresHN))

count(d17MresHN_results, padj<0.01)

d17MresHN_sig<-
filter(as.data.frame(d17MresHN_results), padj<padj.cutoff &
abs(log2FoldChange)>lfc.cutoff)

count(d17MresHN_sig, Effect)

d17MresHN_Plot<-EnhancedVolcano(d17MresHN, lab = NA, x =
'log2FoldChange', y = 'pvalue', pCutoffCol='padj', pCutoff = 0.01,
FCcutoff= 0.58, xlim = c(-10,10), title="Tad17 mutant versus WT under
High N", subtitle= "Basal Node")

d17MresHN_Plot

d17MresHN_MA<-plotMA(d17MresHN, ylim=c(-2,2), main="MA Plot Tad17
versus WT under High N")

#What is the effect of d17 mutation under LowN?

d17MresLN <- results(dds,alpha=0.01,list(c("Genotype_d17M_vs_d17WT",
"Genotyped17M.NlevelLowN")))

summary(d17MresLN)

d17MresLN <- d17MresLN[order(d17MresLN$padj),]

head(d17MresLN)

d17MresLN_results <-
as.data.frame(dplyr::mutate(as.data.frame(d17MresLN),
Effect=ifelse(d17MresLN$padj<padj.cutoff &

```

```

d17MresLN$log2FoldChange>lfc.cutoff, "d17M:UP",
ifelse(d17MresLN$padj<padj.cutoff & d17MresLN$log2FoldChange< -
lfc.cutoff, "d17M:DOWN", "No Effect"))),
row.names=row.names(d17MresLN))

count(d17MresLN_results, padj<0.01)

d17MresLN_sig<-
filter(as.data.frame(d17MresLN_results), padj<padj.cutoff &
abs(log2FoldChange)>lfc.cutoff)

count(d17MresLN_sig, Effect)

d17MresLN_Plot<-EnhancedVolcano(d17MresLN, lab = NA, x =
'log2FoldChange', y = 'pvalue', pCutoffCol='padj', pCutoff = 0.01,
FCcutoff= 0.58, xlim = c(-10,10), title="Tad17 mutant versus WT under
Low N", subtitle= "Basal Node")

d17MresLN_Plot

d17MresLN_MA<-plotMA(d17MresLN, ylim=c(-2,2), main="MA Plot Tad17
versus WT under Low N")

#Is the effect of N limitation different between genotypes
(Interaction Term)?

d17Minter <- results(dds, alpha=0.01, name="Genotyped17M.NlevelLowN")

summary(d17Minter)

d17Minter <- d17Minter[order(d17Minter$padj),]

head(d17Minter)

d17Minter_results<-subset(as.data.frame(d17Minter), padj<0.01)

d17Minter_sig<-
filter(as.data.frame(d17Minter_results), abs(log2FoldChange)>0.58)

count(d17Minter_sig, log2FoldChange>0.58)

d17Minter_Plot<-EnhancedVolcano(d17Minter, lab = NA, x =
'log2FoldChange', y = 'pvalue', pCutoffCol='padj', pCutoff = 0.01,
FCcutoff= 0.58, xlim = c(-10,10), title="Is d17 mutation effect
different across different N levels?", subtitle= "Basal Nodes")

d17Minter_Plot

#N limitation in the WT plants?

LNresWT <- results(dds, alpha=0.01, name="Nlevel_LowN_vs_HighN")

summary(LNresWT)

LNresWT <- LNresWT[order(LNresWT$padj),]

head(LNresWT)

LNresWT_results <-
as.data.frame(dplyr::mutate(as.data.frame(LNresWT),
Effect=ifelse(LNresWT$padj<padj.cutoff &

```

```

LNresWT$log2FoldChange>lfc.cutoff, "LN:UP",
ifelse(LNresWT$padj<padj.cutoff & LNresWT$log2FoldChange< -
lfc.cutoff, "LN:DOWN","No Effect"))), row.names=row.names(LNresWT))

count(LNresWT_results, padj<0.01)

LNresWT_sig<-filter(as.data.frame(LNresWT_results), padj<padj.cutoff &
abs(log2FoldChange)>lfc.cutoff)

count(LNresWT_sig, Effect)

LNresWT_Plot<-EnhancedVolcano(LNresWT, lab = NA, x = 'log2FoldChange',
y = 'pvalue', pCutoffCol='padj', pCutoff = 0.01, FCcutoff= 0.58, xlim =
c(-10,10), title="N Limitation Effect in WT plants", subtitle= "Basal
Nodes")

LNresWT_Plot

LNresWT_MA<-plotMA(LNresWT, ylim=c(-2,2), main="MA Plot LowN versus
HighN in WT plants")

#N limitation in the Tad17 mutant?

LNresd17M <- results(dds, alpha=0.01, list(c("Nlevel_LowN_vs_HighN",
"Genotyped17M.NlevelLowN")))

summary(LNresd17M)

LNresd17M <- LNresd17M[order(LNresd17M$padj),]

head(LNresd17M)

LNresd17M_results <-
as.data.frame(dplyr::mutate(as.data.frame(LNresd17M),
Effect=ifelse(LNresd17M$padj<padj.cutoff &
LNresd17M$log2FoldChange>lfc.cutoff, "LN:UP",
ifelse(LNresd17M$padj<padj.cutoff & LNresd17M$log2FoldChange< -
lfc.cutoff, "LN:DOWN","No Effect"))), row.names=row.names(LNresd17M))

count(LNresd17M_results, padj<0.01)

LNresd17M_sig<-
filter(as.data.frame(LNresd17M_results), padj<padj.cutoff &
abs(log2FoldChange)>lfc.cutoff)

count(LNresd17M_sig, Effect)

LNresd17M_Plot<-EnhancedVolcano(LNresd17M, lab = NA, x =
'log2FoldChange', y = 'pvalue', pCutoffCol='padj', pCutoff = 0.01,
FCcutoff= 0.58, xlim = c(-10,10), title="N Limitation Effect in Tad17
mutants", subtitle= "Basal Nodes")

LNresd17M_Plot

LNresd17M_MA<-plotMA(LNresd17M, ylim=c(-2,2), main="MA Plot LowN
versus HighN in Tad17 plants")

#Generate a heatmap for a list of genes (e.g. SL metabolic genes)

rld <- rlog(dds, blind = FALSE)

```

```

SLs<-read_excel("SL metabolic Gene List.xlsx", sheet = "Sheet1")

SLs_heatmap<-unlist(SLs$GeneID, recursive = TRUE, use.names = TRUE)

col_anno <- as.data.frame(colData(rld)[, c("Nlevel", "Genotype")])

row_anno<-data.frame(SLs, row.names = 1)

anno_colors = list(Nlevel = c(HighN = "#0eb34a", LowN = "#e6ed1c"),
Genotype = c(WT="#323232", Tad17="#1b6393"),
LowN=c("NS"="white", "Significantly
DE"="#a65b5b"), Tad17vsWT_HN=c("NS"="white", "Significantly
DE"="#a65b5b"), Tad17vsWT_LN=c("NS"="white", "Significantly
DE"="#a65b5b"))

pheatmap_order<-
c(13, 14, 15, 19, 20, 21, 1, 2, 3, 7, 8, 9, 16, 17, 18, 22, 23, 24, 4, 5, 6, 10, 11, 12)

pheatmap(assay(rld)[SLs_heatmap, pheatmap_order], color=colorRampPalett
e(c('green3', 'black', 'red3'))(100), scale = "row", annotation_col =
select(col_anno, Genotype, Nlevel), annotation_colors = anno_colors,
cluster_rows = FALSE, annotation_row =
select(row_anno, Tad17vsWT_LN, Tad17vsWT_HN, LowN), labels_row =
row_anno$GeneName, cluster_cols = FALSE, gaps_col = c(12), gaps_row =
c(13, 19, 25), cellwidth=10, cellheight=11, fontsize_col=10)

```

Appendix C: List of Orthologous SL-related Sequences

Table S1: List of gene accession numbers (GeneID) of SL biosynthetic (D27, D17 and D10) orthologous protein sequences used for the phylogenetic analysis.

Gene Name	Species	GeneID
<i>AtD27</i>	<i>A. thaliana</i>	AT1G03055
<i>OsD27</i>	<i>O. sativa</i>	Os11t0587000
<i>HvD27</i>	<i>H. vulgare</i>	HORVU7Hr1G096970
<i>TaD27-7D</i>	<i>T. aestivum</i>	TraesCS7D02G411500
<i>TaD27-7A</i>	<i>T. aestivum</i>	TraesCS7A02G418900
<i>TaD27-7B</i>	<i>T. aestivum</i>	TraesCS7B02G319100
<i>AtMAX3</i>	<i>A. thaliana</i>	AT2G44990
<i>OsD17</i>	<i>O. sativa</i>	Os04g0550600
<i>HvD17</i>	<i>H. vulgare</i>	HORVU2Hr1G097770
<i>TaD17-2B</i>	<i>T. aestivum</i>	TraesCS2B02G433800
<i>TaD17-2A</i>	<i>T. aestivum</i>	TraesCS2A02G414600
<i>TaD17-2D</i>	<i>T. aestivum</i>	TraesCS2D02G411900
<i>AtMAX4</i>	<i>A. thaliana</i>	AT4G32810
<i>OsD10</i>	<i>O. sativa</i>	Os01g0746400
<i>OsD10-like</i>	<i>O. sativa</i>	Os01g0566500
<i>HvD10</i>	<i>H. vulgare</i>	HORVU3Hr1G071170
<i>TaD10a-3A</i>	<i>T. aestivum</i>	TraesCS3A02G274300
<i>TaD10a-3B</i>	<i>T. aestivum</i>	TraesCS3B02G308000
<i>TaD10a-3D</i>	<i>T. aestivum</i>	TraesCS3D02G273500
<i>TaD10b1-3A</i>	<i>T. aestivum</i>	TraesCS3A02G074200
<i>TaD10b2-3A</i>	<i>T. aestivum</i>	TraesCS3A02G074100
<i>TaD10b1-3B</i>	<i>T. aestivum</i>	TraesCS3B02G088400
<i>TaD10-like-2A</i>	<i>T. aestivum</i>	TraesCS2A02G074900
<i>TaD10-like-U</i>	<i>T. aestivum</i>	TraesCSU02G085100

Table S2: List of gene accession numbers (GeneID) of MAX1 orthologous protein sequence used for the phylogenetic analysis.

Gene Name	Species	GeneID
<i>AtMAX1</i>	<i>A. thaliana</i>	AT2G26170
<i>Os1500 (CYP711A4)</i>	<i>O. sativa</i>	Os01g0701500
<i>Os5100 (CYP711A6)</i>	<i>O. sativa</i>	Os06g0565100
<i>Os1900 (CYP711A5)</i>	<i>O. sativa</i>	Os02g0221900
<i>Os900 (CYP711A2)</i>	<i>O. sativa</i>	Os01g0700900
<i>Os1400 (CYP711A3)</i>	<i>O. sativa</i>	Os01g0701400
<i>HvMAX1 (CYP711A29)</i>	<i>H. vulgare</i>	HORVU4Hr1G079620
<i>HvCYP711A5</i>	<i>H. vulgare</i>	HORVU6Hr1G040170
<i>HvCYP711A30</i>	<i>H. vulgare</i>	HORVU3Hr1G013470
<i>HvCYP711A6</i>	<i>H. vulgare</i>	HORVU7Hr1G087750
<i>BdCYP711A31</i>	<i>B. distachyon</i>	XP_010237353
<i>BdCYP711A30</i>	<i>B. distachyon</i>	XP_003575594
<i>BdCYP711A29</i>	<i>B. distachyon</i>	XP_003562092
<i>BdCYP711A6</i>	<i>B. distachyon</i>	XP_003560652
<i>BdCYP711A5</i>	<i>B. distachyon</i>	XP_003571126
<i>TaMAX1a1-4A</i>	<i>T. aestivum</i>	TraesCS4A02G412100
<i>TaMAX1a1-4B</i>	<i>T. aestivum</i>	TraesCS4B02G312300
<i>TaMAX1a1-4D</i>	<i>T. aestivum</i>	TraesCS4D02G309900
<i>TaMAX1a2-U</i>	<i>T. aestivum</i>	TraesCSU02G146300
<i>TaMAX1a2-3B</i>	<i>T. aestivum</i>	TraesCS3B02G088700
<i>100% identical to TaMAX1a2-3B (removed)</i>		TraesCSU02G235400
<i>TaMAX1a2-3D</i>	<i>T. aestivum</i>	TraesCS3D02G073900
<i>TaMAX1b-3A</i>	<i>T. aestivum</i>	TraesCS3A02G466400
<i>TaMAX1c-6B</i>	<i>T. aestivum</i>	TraesCS6B02G217300
<i>TaMAX1c-6D</i>	<i>T. aestivum</i>	TraesCS6D02G174100
<i>TaMAX1c-6A</i>	<i>T. aestivum</i>	TraesCS6A02G187200
<i>TaMAX1d-7A</i>	<i>T. aestivum</i>	TraesCS7A02G360300
<i>TaMAX1d-7D</i>	<i>T. aestivum</i>	TraesCS7D02G362800
<i>TaMAX1d-7B</i>	<i>T. aestivum</i>	TraesCS7B02G267500
<i>SbMAX1a</i>	<i>S. bicolor</i>	XP_002458367
<i>SbMAX1b</i>	<i>S. bicolor</i>	XP_002456213
<i>SbMAX1c</i>	<i>S. bicolor</i>	XP_002453551
<i>SbMAX1d</i>	<i>S. bicolor</i>	XP_002438586
<i>ZmMAX1a (CYP711A13)</i>	<i>Z. mays</i>	Zm00001d046207
<i>ZmMAX1b (CYP711A18)</i>	<i>Z. mays</i>	Zm00001d039697
<i>ZmMAX1c (CYP711A19)</i>	<i>Z. mays</i>	Zm00001d053569

Table S3: List of gene accession numbers (GeneID) of SL perception (D3, D14) and signalling (D53, TB1) orthologous protein sequences used for the phylogenetic analysis.

Gene Name	Species	GeneID
<i>AtMAX2</i>	<i>A. thaliana</i>	AT2G42620
<i>OsD3</i>	<i>O. sativa</i>	Os06t0154200
<i>HvD3</i>	<i>H. vulgare</i>	HORVU7Hr1G023610
<i>TaD3-7A</i>	<i>T. aestivum</i>	TraesCS7A02G110500
<i>TaD3-7B</i>	<i>T. aestivum</i>	TraesCS7B02G008400
<i>TaD3-7D</i>	<i>T. aestivum</i>	TraesCS7D02G106000
<i>AtD14</i>	<i>A. thaliana</i>	AT3G03990
<i>OsD14</i>	<i>O. sativa</i>	Os03t0203200
<i>HvD14</i>	<i>H. vulgare</i>	HORVU4Hr1G070070
<i>HvD14-like</i>	<i>H. vulgare</i>	HORVU5Hr1G089150
<i>TaD14-4A</i>	<i>T. aestivum</i>	TraesCS4A02G046700
<i>TaD14-4B</i>	<i>T. aestivum</i>	TraesCS4B02G258200
<i>TaD14-4D</i>	<i>T. aestivum</i>	TraesCS4D02G258000
<i>AtSMXL6</i>	<i>A. thaliana</i>	AT1G07200
<i>AtSMXL7</i>	<i>A. thaliana</i>	AT2G29970
<i>AtSMXL8</i>	<i>A. thaliana</i>	AT2G40130
<i>OsD53</i>	<i>O. sativa</i>	Os11t0104300
<i>OsD53-like</i>	<i>O. sativa</i>	Os12g0104300
<i>TaD53a-4A</i>	<i>T. aestivum</i>	TraesCS4A02G182800
<i>TaD53a-4B</i>	<i>T. aestivum</i>	TraesCS4B02G135800
<i>TaD53a-4D</i>	<i>T. aestivum</i>	TraesCS4D02G130600
<i>TaD53b-5A</i>	<i>T. aestivum</i>	TraesCS5A02G155000
<i>TaD53b-5B</i>	<i>T. aestivum</i>	TraesCS5B02G153200
<i>TaD53b-5D</i>	<i>T. aestivum</i>	TraesCS5D02G159900
<i>ZmD53b</i>	<i>Z. mays</i>	Zm00001d023208
<i>ZmD53a</i>	<i>Z. mays</i>	Zm00001eb404750
<i>SbD53</i>	<i>S. bicolor</i>	SORBI_3008G002400
<i>AtBRC1</i>	<i>A. thaliana</i>	AT3G18550
<i>AtBRC2</i>	<i>A. thaliana</i>	AT1G68800
<i>OsFC1</i>	<i>O. sativa</i>	Os03t0706500
<i>HvTB1</i>	<i>H. vulgare</i>	HORVU4Hr1G007040
<i>ZmTB1</i>	<i>Z. mays</i>	Zm00001eb054440
<i>TaTB1-4A</i>	<i>T. aestivum</i>	TraesCS4A02G271300
<i>TaTB1-4B</i>	<i>T. aestivum</i>	TraesCS4B02G042700
<i>TaTB1-4D</i>	<i>T. aestivum</i>	TraesCS4D02G040100

Appendix D: Selected Differentially Expressed Genes under Low N

Table S4: Selected differentially expressed genes in the basal node of wheat grown under N limitation for 8 days based on the RNA-seq data.

GeneID	Orthologue	Description	LowN	
			LFC	padj
Dormancy Associated				
TraesCS4A02G158100	Os03g0342900	DRM1	1.19	9.29E-18
TraesCS4B02G155000	Os03g0342900	DRM1	0.98	2.75E-06
TraesCS4D02G169100	Os03g0342900	DRM1	0.96	3.31E-08
TraesCS5A02G211600	Os09g0437500	DRM3	2.32	4.56E-10
TraesCS5B02G212300	Os09g0437500	DRM3	1.60	2.25E-14
TraesCS5D02G222300	Os09g0437500	DRM3	2.32	3.41E-05
TraesCS4A02G245100	Os11g0671000	DRM4	1.01	4.16E-13
TraesCS4B02G070300	Os11g0671000	DRM4	0.95	4.84E-09
TraesCS4D02G069100	Os11g0671000	DRM4	1.40	2.84E-03
Cell Cycle				
TraesCS5A02G336500	Os01g0896300	FLATTENED SHOOT MERISTEM	-0.75	6.55E-11
TraesCS5B02G335500	Os01g0896300	FLATTENED SHOOT MERISTEM	-0.76	7.42E-06
TraesCS5D02G341200	Os01g0896300	FLATTENED SHOOT MERISTEM	-0.79	4.02E-06
TraesCS2A02G364000	Os02g0805200	Proliferating cell nuclear antigen	-0.72	5.79E-07
TraesCS2B02G382000	Os02g0805200	Proliferating cell nuclear antigen	-0.77	1.78E-07
TraesCS2D02G361800	Os02g0805200	Proliferating cell nuclear antigen	-0.70	5.17E-07
TraesCS6D02G357600	Os02g0805200	Proliferating cell nuclear antigen	-0.75	1.06E-04
TraesCS4D02G053100	AT1G08880	Histone H2A	-6.18	1.75E-04
TraesCS5A02G098300	AT1G08880	Histone H2A	-0.59	1.18E-04
TraesCS1A02G190400	AT1G07790	Histone H2B.1	-0.82	1.19E-08
TraesCS1A02G229100	AT1G07790	Histone H2B.1	-0.60	3.90E-03
TraesCS1B02G192500	AT1G07790	Histone H2B.1	-0.73	5.47E-06
TraesCS1B02G244900	AT1G07790	Histone H2B.1	-0.72	7.53E-04
TraesCS3A02G357500	AT1G07790	Histone H2B.1	-0.68	1.04E-03
TraesCS4A02G030500	AT1G07790	Histone H2B.1	-0.62	6.93E-04
TraesCS6A02G040200	AT1G07790	Histone H2B.1	-0.61	1.36E-04
TraesCS2A02G214700	Os03g0721900	Similar to Histone H2A	-0.91	2.12E-08
TraesCS2B02G239700	Os03g0721900	Similar to Histone H2A	-0.95	3.86E-09
TraesCS2D02G220500	Os03g0721900	Similar to Histone H2A	-0.80	7.43E-07
TraesCS5A02G462100	Os01g0502700	Similar to Histone H2A	-0.58	9.41E-04
TraesCS5B02G477300	Os01g0502700	Similar to Histone H2A	-1.24	6.52E-04
TraesCS6D02G062800	Os01g0502700	Similar to Histone H2A	-0.73	1.29E-04
TraesCS6D02G107000	Os01g0502700	Similar to Histone H2A	-0.67	1.76E-03
TraesCS1A02G368000	Os08g0490800	Similar to Histone H2B	-0.61	1.45E-04
TraesCS1A02G388600	Os08g0490800	Similar to Histone H2B	-0.68	9.20E-04
TraesCS1B02G386500	Os08g0490800	Similar to Histone H2B	-0.67	3.01E-05
TraesCS1B02G386600	Os08g0490800	Similar to Histone H2B	-0.64	9.02E-03

TraesCS1B02G386700	Os08g0490800	Similar to Histone H2B	-0.74	2.08E-03
TraesCS1D02G396600	Os08g0490800	Similar to Histone H2B	-0.68	2.94E-04
TraesCS6B02G376900	Os08g0490800	Similar to Histone H2B	-0.59	5.38E-03
TraesCS4B02G275500	Os12g0415800	Similar to Histone H3	-0.61	5.74E-03
TraesCS6A02G099700	Os12g0415800	Similar to Histone H3	-0.65	2.05E-07
TraesCS7B02G341600	Os03g0390600	Similar to Histone H3	-0.62	9.18E-03
TraesCS6A02G401600	AT1G51060	Probable histone H2A.1	-0.61	1.27E-03
TraesCS7D02G488600	AT1G51060	Probable histone H2A.1	-0.71	9.55E-03
N transport				
TraesCS6A02G226800	Os02g0620600	Ammonium Transporter (TaAMT1.2)	-2.09	3.73E-06
TraesCS6B02G254800	Os02g0620600	Ammonium Transporter (TaAMT1.2)	-1.61	1.02E-09
TraesCS6D02G208200	Os02g0620600	Ammonium Transporter (TaAMT1.2)	-1.66	2.62E-10
TraesCS7B02G020500	Os05g0338900	TaNPF2.12	0.91	1.38E-03
TraesCS7D02G120200	Os05g0338900	TaNPF2.12	0.78	3.54E-05
TraesCS7A02G054100	Os01g0960900	TaNPF2.14	0.78	4.84E-04
TraesCS7D02G049400	Os01g0960900	TaNPF2.14	1.23	2.43E-11
TraesCS4A02G440600	Os01g0960900	TaNPF2.15	1.54	1.61E-04
TraesCS1D02G257200	Os05g0410900	TaNPF3.2	1.05	4.42E-09
TraesCS1D02G256700	Os05g0410500	TaNPF3.4	-1.29	8.92E-03
TraesCS7D02G357300		TaNPF4.1	0.88	3.46E-03
TraesCS2A02G309100	Os04g0441800	TaNPF4.2	2.04	1.05E-20
TraesCS2B02G326200	Os04g0441800	TaNPF4.2	1.83	7.14E-21
TraesCS2A02G264500	Os11g0283500	TaNPF4.4	1.48	2.98E-14
TraesCS2B02G277600	Os11g0283500	TaNPF4.4	0.61	3.13E-03
TraesCS2D02G259400	Os11g0283500	TaNPF4.4	0.95	9.94E-05
TraesCS5D02G398000	Os11g0282800	TaNPF4.5	1.06	4.28E-09
TraesCS3A02G383200		TaNPF5.22	1.37	4.11E-03
TraesCS7A02G301700	Os08g0155400	TaNPF6.1	0.64	2.25E-03
TraesCS7B02G201900	Os08g0155400	TaNPF6.1	0.61	4.41E-04
TraesCS1A02G031300	Os01g0556700	TaNPF6.5	-4.61	5.19E-05
TraesCS1B02G038700	Os01g0556700	TaNPF6.5	-1.86	1.28E-08
TraesCS1D02G032700	Os01g0556700	TaNPF6.5	-2.31	1.50E-06
TraesCS6B02G290500	Os02g0689900	TaNPF7.1	-1.42	2.66E-04
TraesCS4A02G075900		TaNPF8.12	1.13	1.28E-03
TraesCS4B02G231500	Os03g0235300	TaNPF8.14	1.51	6.26E-06
TraesCS2A02G007500		TaNPF8.16	0.89	5.74E-03
TraesCS2D02G009200		TaNPF8.16	1.87	2.64E-03
TraesCS2A02G007100		TaNPF8.18	1.04	9.30E-03
TraesCS7A02G381700	Os10g0110800	TaNPF8.22	1.13	9.53E-03
TraesCS7B02G283800	Os10g0110800	TaNPF8.22	0.64	5.78E-03
TraesCS7A02G381500		TaNPF8.23	-2.12	6.89E-07
TraesCS7D02G377800		TaNPF8.23	-3.77	6.42E-03
TraesCS6B02G171000		TaNPF8.25	-1.60	2.31E-06
TraesCS3A02G392900		TaNPF8.6	0.82	3.87E-03
TraesCS4B02G052200		TaNPF8.9	0.91	6.90E-04
TraesCS2D02G073500		TaNRT2.16	-2.61	2.75E-04

N assimilation

TraesCS6A02G333900		Nitrite reductase, chloroplastic	-4.96	1.96E-33
TraesCS6B02G364600		Nitrite reductase, chloroplastic	-5.47	1.08E-05
TraesCS6D02G313100		Nitrite reductase, chloroplastic	-4.95	9.19E-12
TraesCS6A02G017500		Nitrate reductase 1	-1.58	2.35E-05
TraesCS6B02G024900		Nitrate reductase 1	-1.28	2.37E-05
TraesCS6A02G326200		Nitrate reductase 1	-3.69	4.01E-31
TraesCS6B02G356800		Nitrate reductase 2	-3.06	1.66E-18
TraesCS6D02G306000		Nitrate reductase 2	-3.10	6.21E-33
TraesCS4A02G063800		Glutamine synthetase	-2.15	5.27E-49
TraesCS4B02G240900		Glutamine synthetase	-1.94	1.57E-23
TraesCS4D02G240700		Glutamine synthetase	-2.38	5.06E-72
TraesCS6A02G298100		Glutamine synthetase (cytosolic)	0.69	1.11E-07
TraesCS6B02G327500		Glutamine synthetase (cytosolic)	0.77	2.51E-08
TraesCS6D02G383600LC		Glutamine synthetase (cytosolic)	0.70	2.25E-05
TraesCS3A02G266300		NADPH dependent Glutamate Synthase	-0.81	9.57E-05
TraesCS2D02G132900		Fd-GOGAT Glutamate Synthase	-0.60	1.14E-04

Ureide Metabolism

TraesCS7A02G479600	Os12g0503000	OsUPS1	-2.90	5.50E-05
TraesCS7B02G382000	Os12g0503000	OsUPS1	-3.10	2.57E-13
TraesCS7D02G466800	Os12g0503000	OsUPS1	-4.06	2.63E-04
TraesCS7D02G466900	Os12g0503000	OsUPS1	-5.30	4.83E-22
TraesCS5A02G104200	Os12g0502800	Similar to OsUPS2	1.36	1.84E-03
TraesCS5B02G114400	Os12g0502800	Similar to OsUPS2	0.79	6.17E-03
TraesCS5D02G116600	Os12g0502800	Similar to OsUPS2	1.47	2.59E-04
TraesCS2A02G587900	Os04g0680400	Allantoinase	1.15	5.75E-04
TraesCS2B02G595300	Os04g0680400	Allantoinase	1.81	2.02E-04
TraesCS2D02G565300	Os04g0680400	Allantoinase	1.78	5.04E-05
TraesCS7A02G481500	Os06g0665500	Allantoate deiminase	1.14	3.19E-05
TraesCS7B02G383900	Os06g0665500	Allantoate deiminase	1.27	3.66E-05

Amino Acid

TraesCS1A02G264500	Os05g0424000	OsAAP7	-1.17	3.02E-11
TraesCS1B02G275200	Os05g0424000	OsAAP7	-1.40	3.78E-16
TraesCS1D02G264700	Os05g0424000	OsAAP7	-1.60	6.05E-24
TraesCS3A02G388100	Os01g0878400	OsAAP5	-1.76	1.42E-24
TraesCS3B02G420600	Os01g0878400	OsAAP5	-1.43	2.39E-17
TraesCS3D02G381400	Os01g0878400	OsAAP5	-1.61	1.35E-18
TraesCS2A02G3339100	Os04g0460200	OsATL14	-1.88	2.75E-03
TraesCS6A02G002400	Os02g0101000	OsATL11	-1.17	7.53E-03
TraesCS6B02G007400	Os02g0101000	OsATL11	-1.92	1.25E-10
TraesCS7B02G293500	Os06g0633800	OsATL5	-1.41	4.34E-30
TraesCS7A02G392300	Os06g0633100	GLUTAMINE DUMPER 6	-3.25	4.36E-07
TRAESCS7A02G392200	Os06g0633100	GLUTAMINE DUMPER 6	-2.88	3.56E-04
TRAESCS7A02G392400	Os06g0633100	GLUTAMINE DUMPER 6	-5.26	1.02E-04
TraesCS7B02G294400	Os06g0633100	GLUTAMINE DUMPER 6	-3.24	2.19E-06
TRAESCS7B02G294200	Os06g0633100	GLUTAMINE DUMPER 6	-3.08	1.61E-03

TRAESCS7B02G294300	Os06g0633100	GLUTAMINE DUMPER 6	-3.13	2.56E-03
TRAESCS7D02G387700	Os06g0633100	GLUTAMINE DUMPER 6	-3.87	8.50E-05
TRAESCS7D02G387800	Os06g0633100	GLUTAMINE DUMPER 6	-3.06	1.67E-06
TraesCS4A02G215300	AT1G44100	TaAAP13	0.76	5.15E-04
TraesCS4B02G100800	AT1G44100	TaAAP13	0.71	1.85E-03
TraesCS4D02G097400	AT1G44100	TaAAP13	1.21	1.26E-06
TraesCS3A02G388000	Os01g0878700	OsAAP6	7.12	1.04E-03
TraesCS3B02G420700	Os01g0878700	OsAAP6	4.03	8.04E-16
TraesCS3D02G381500	Os01g0878700	OsAAP6	8.41	2.04E-13
TraesCS3A02G407000	Os01g0882800	OsAAP8	0.82	2.76E-06
TraesCS3B02G441200	Os01g0882800	OsAAP8	0.81	2.55E-08
TraesCS3B02G441100	Os01g0882800	OsAAP8	1.29	8.01E-12
TraesCS3D02G402300	Os01g0882800	OsAAP8	0.59	3.05E-03
TraesCS7D02G189100	Os06g0228500	OsATL12	0.79	8.50E-03
TraesCS3B02G449100	Os01g0908600	OsProT1	1.60	2.41E-14
TraesCS3D02G408800	Os01g0908600	OsProT1	3.49	5.24E-03
TraesCS2A02G268400	Os03g0644400	OsProT2	0.99	2.41E-09
TraesCS2B02G287200	Os07g0100800	OsProT3	0.86	1.91E-03
TraesCS2D02G267400	Os07g0100800	OsProT3	1.41	1.73E-07
Sugar Transporters				
TraesCS4A02G016400	Os03g0170900	Sucrose transporter (SUT1)	1.11	8.86E-11
TraesCS4B02G287800	Os03g0170900	Sucrose transporter (SUT1)	1.10	5.30E-11
TraesCS4D02G286500	Os03g0170900	Sucrose transporter (SUT1)	1.38	8.47E-09
TraesCS6A02G382400	Os12g0476200	AtSWEET11,12,13,14	1.32	4.39E-09
TraesCS6A02G382600	Os12g0476200	AtSWEET11,12,13,14	2.21	1.67E-28
TraesCS6B02G421800	Os12g0476200	AtSWEET11,12,13,14	1.96	6.05E-11
TraesCS6D02G367200	Os12g0476200	AtSWEET11,12,13,14	0.73	1.00E-03
TraesCS6D02G367300	Os12g0476200	AtSWEET11,12,13,14	0.65	2.21E-03
TraesCS6D02G367400	Os12g0476200	AtSWEET11,12,13,14	2.31	3.35E-23
TraesCS6A02G009000	Os11g0508600	AtSWEET11,12,13,14	1.78	2.57E-07
TraesCS6A02G009100	Os11g0508600	AtSWEET11,12,13,14	3.60	7.27E-05
TraesCS6B02G015100	Os11g0508600	AtSWEET11,12,13,14	2.28	1.21E-27
TraesCS6B02G015200	Os11g0508600	AtSWEET11,12,13,14	5.34	3.90E-05
TraesCS6B02G015300	Os11g0508600	AtSWEET11,12,13,14	1.82	1.06E-11
TraesCS6D02G009600	Os11g0508600	AtSWEET11,12,13,14	2.51	5.78E-28
TraesCS6D02G009700	Os11g0508600	AtSWEET11,12,13,14	2.51	2.22E-09
TraesCS6D02G012100	Os11g0508600	AtSWEET11,12,13,14	4.09	3.68E-42
TraesCS7A02G147300	Os02g0513100	AtSWEET11,12,13,14	3.35	5.15E-36
TraesCS7B02G050500	Os02g0513100	AtSWEET11,12,13,14	2.02	1.31E-46
TraesCS7D02G149000	Os02g0513100	AtSWEET11,12,13,14	1.43	7.68E-17
TraesCS2A02G204900	Os07g0561800		-2.27	3.03E-05
TraesCS2B02G232400	Os07g0561800		-3.88	3.26E-11
TraesCS2D02G211100	Os07g0561800		-2.77	5.93E-03
TraesCS6A02G218800	Os02g0301100	AtSWEET6,7	-0.66	9.43E-04
TraesCS6D02G201900	Os02g0301100	AtSWEET6,7	-1.12	8.69E-09
TraesCS1B02G147200	Os05g0214300	AtSWEET3	-1.79	1.14E-13

TraesCS7A02G261100	Os08g0535200	AtSWEET10,15	-2.52	2.38E-08
TraesCS7B02G160000	Os08g0535200	AtSWEET10,15	-1.97	4.28E-10
TraesCS7D02G263100	Os08g0535200	AtSWEET10,15	-3.10	1.84E-34
Sugar Signalling				
TraesCS6A02G301800		TaTPP4	1.03	8.02E-05
TraesCS6B02G330900		TaTPP4	1.42	1.01E-08
TraesCS6D02G281100		TaTPP4	1.49	8.97E-06
TraesCS7D02G182600		TaTPP8	3.81	2.65E-03
TraesCS6A02G248400		TaTPP1	-2.27	7.08E-03
TraesCS6B02G276300		TaTPP1	-2.43	3.52E-04
TraesCS6D02G230500		TaTPP1	-2.34	6.14E-05
TraesCS1A02G339300		TPS	-1.05	1.74E-11
TraesCS1B02G351600		TPS	-0.89	3.54E-06
TraesCS1D02G341100		TPS	-1.18	9.87E-14
TraesCS1D02G340400		TaTPS7	0.69	8.66E-03
TraesCS5D02G210000		TaTPS6	0.93	4.81E-04
TraesCS5D02G284800	Os09g0499000	SnRK1A protein kinase	0.80	4.90E-03
TraesCS7B02G150700	Os08g0516900	SnRK1A protein kinase	0.69	9.10E-03

Appendix E: *Tad17* Mutant RNA-sequencing Supplementary Data

Table S5: RNA-sequencing raw data analysis statistics

Sample ID	N Level	Genotype	Reads (M)	Alignment Rate (%)	Assignment Rate (%)	Assigned Reads (M)	Pseudo-aligned (%)
Tad17M1_HN_N1	High N	<i>Tad17 (M1)</i>	47.1	84.7%	58.0%	31.6	75.4%
Tad17M1_HN_N2	High N	<i>Tad17 (M1)</i>	40.3	86.0%	57.9%	27.2	77.2%
Tad17M1_HN_N3	High N	<i>Tad17 (M1)</i>	49.7	81.6%	54.4%	31.6	73.3%
Tad17M1_LN_N1	Low N	<i>Tad17 (M1)</i>	35.1	88.3%	60.2%	24.3	77.6%
Tad17M1_LN_N2	Low N	<i>Tad17 (M1)</i>	43.3	83.1%	55.7%	28.0	73.8%
Tad17M1_LN_N3	Low N	<i>Tad17 (M1)</i>	49.5	84.0%	56.7%	32.5	74.0%
Tad17M2_HN_N1	High N	<i>Tad17 (M2)</i>	29.8	87.2%	56.7%	20.1	79.1%
Tad17M2_HN_N2	High N	<i>Tad17 (M2)</i>	45.4	82.7%	53.9%	28.9	75.0%
Tad17M2_HN_N3	High N	<i>Tad17 (M2)</i>	32.5	82.9%	55.4%	21.1	74.9%
Tad17M2_LN_N1	Low N	<i>Tad17 (M2)</i>	47.8	88.9%	60.6%	33.5	78.3%
Tad17M2_LN_N2	Low N	<i>Tad17 (M2)</i>	42.5	84.7%	56.6%	27.9	74.8%
Tad17M2_LN_N3	Low N	<i>Tad17 (M2)</i>	34.6	81.2%	53.9%	21.7	72.2%
WT1_HN_N1	High N	WT (WT1)	44.1	87.7%	60.1%	30.8	78.9%
WT1_HN_N2	High N	WT (WT1)	44.7	84.6%	57.1%	29.8	76.3%
WT1_HN_N3	High N	WT (WT1)	28.0	82.9%	55.8%	18.2	74.4%
WT1_LN_N1	Low N	WT (WT1)	45.5	88.8%	61.8%	32.2	78.2%
WT1_LN_N2	Low N	WT (WT1)	27.1	83.9%	56.1%	17.6	74.8%
WT1_LN_N3	Low N	WT (WT1)	38.7	83.4%	56.1%	25.2	74.6%
WT2_HN_N1	High N	WT (WT2)	27.6	87.0%	59.3%	18.9	78.1%
WT2_HN_N2	High N	WT (WT2)	35.9	88.3%	59.8%	25.0	80.2%
WT2_HN_N3	High N	WT (WT2)	40.9	83.0%	55.2%	26.5	75.6%
WT2_LN_N1	Low N	WT (WT2)	38.2	88.1%	59.7%	26.4	78.8%
WT2_LN_N2	Low N	WT (WT2)	39.0	85.5%	57.5%	26.0	76.2%
WT2_LN_N3	Low N	WT (WT2)	39.8	84.6%	56.7%	26.2	75.8%

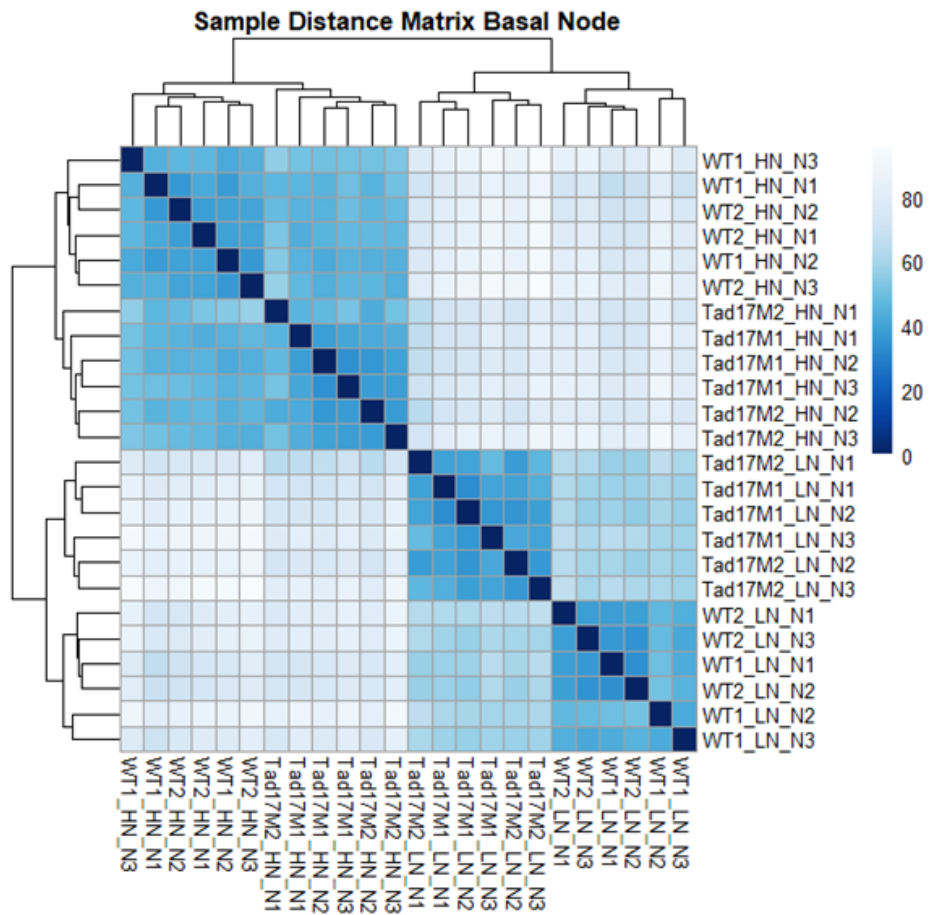


Figure S2: Sample distance matrix based on the differential gene expression analysis performed by DESeq2 (the script can be found in Appendix B).

Appendix F: RNA-seq Validation Test

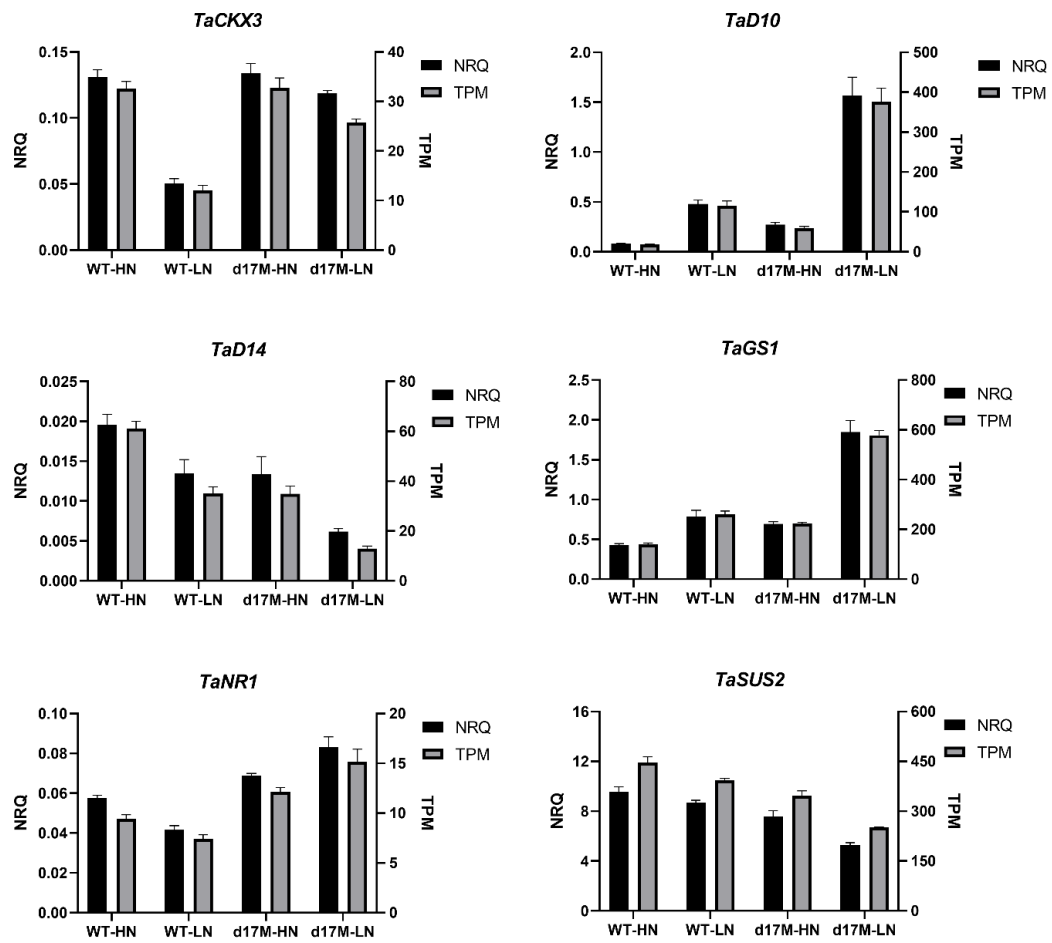


Figure S3: Validation test of RNA-seq results in *Tad17* basal nodes under two different N levels. Comparison between average treatment effects (n=6) based on RNA-seq (TPM) and RT-qPCR data (NRQ).

Appendix G: Additional GO and KEGG Enrichment Analysis

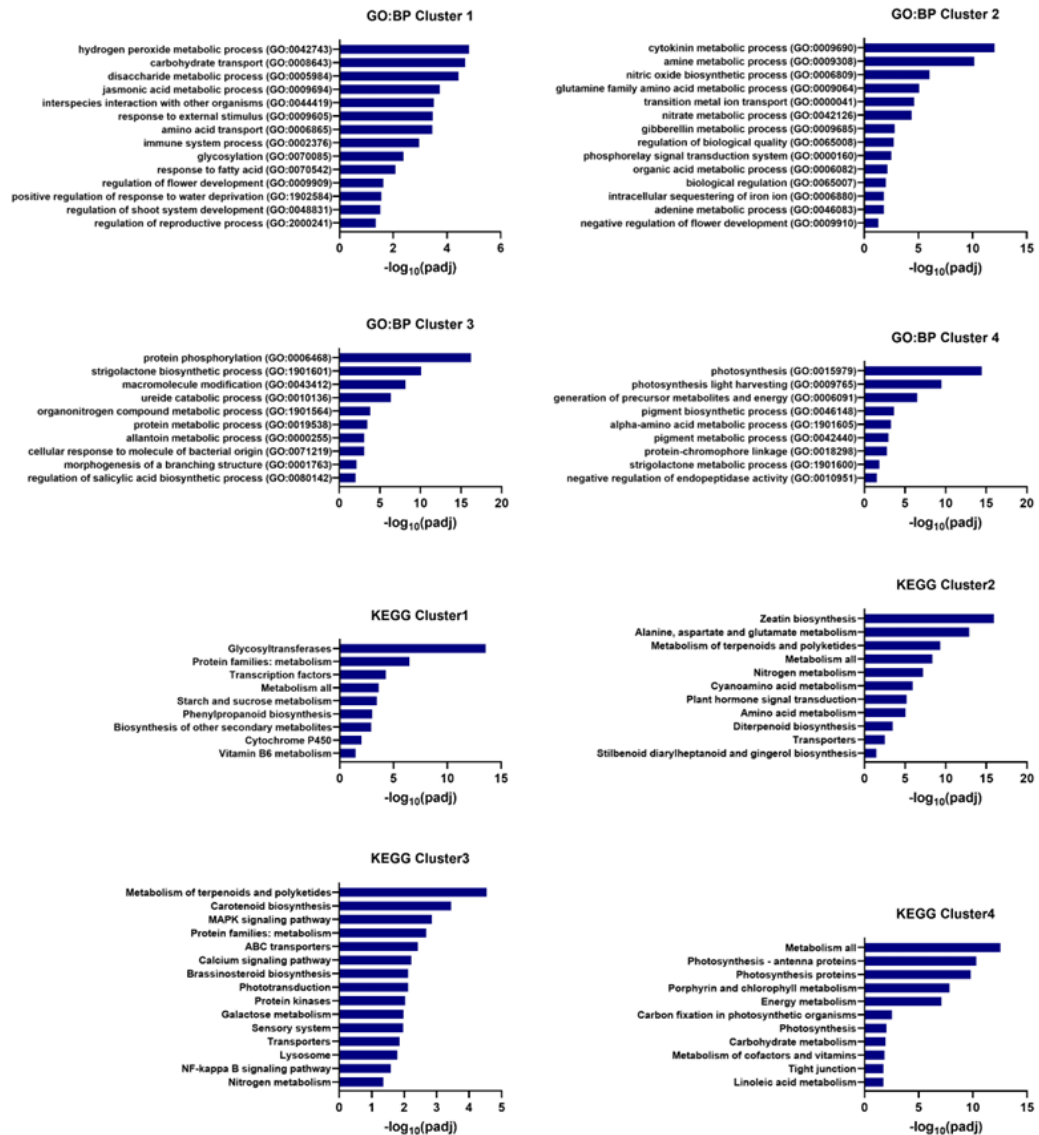


Figure S4: Biological Process (BP) GO term and KEGG enrichment analysis per cluster (1-4) of the differentially expressed N-responsive genes in the basal node of *Tad17* mutant under low N conditions.

Appendix H: Expression of *TaNIGT1* in Basal Nodes and Root of *Tad17*

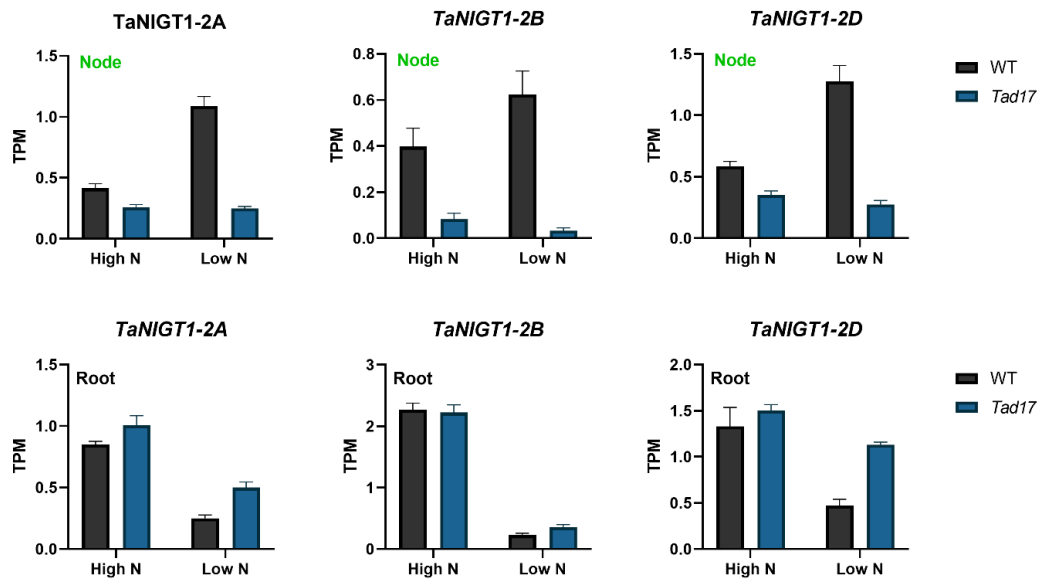


Figure S5: Expression of wheat orthologues of NIGT1 in the basal node and root of *Tad17* mutant (aabbdd) and WT segregant grown under high N (10 mM) or low N (0.1 mM) conditions for 8 days. Transcript abundance (TPM) of *TaNIGT1* homoeologues (TraesCS2A02G116100, TraesCS2B02G135600, TraesCS2D02G119100) based on RNA-seq data. Values are means of six biological replicates, and error bars represent SE.

Appendix I: Phenotype of *Tad17* (BC1F3) and *Tad14* (BC3F3) triple knock-out Mutant in Three Different N Levels

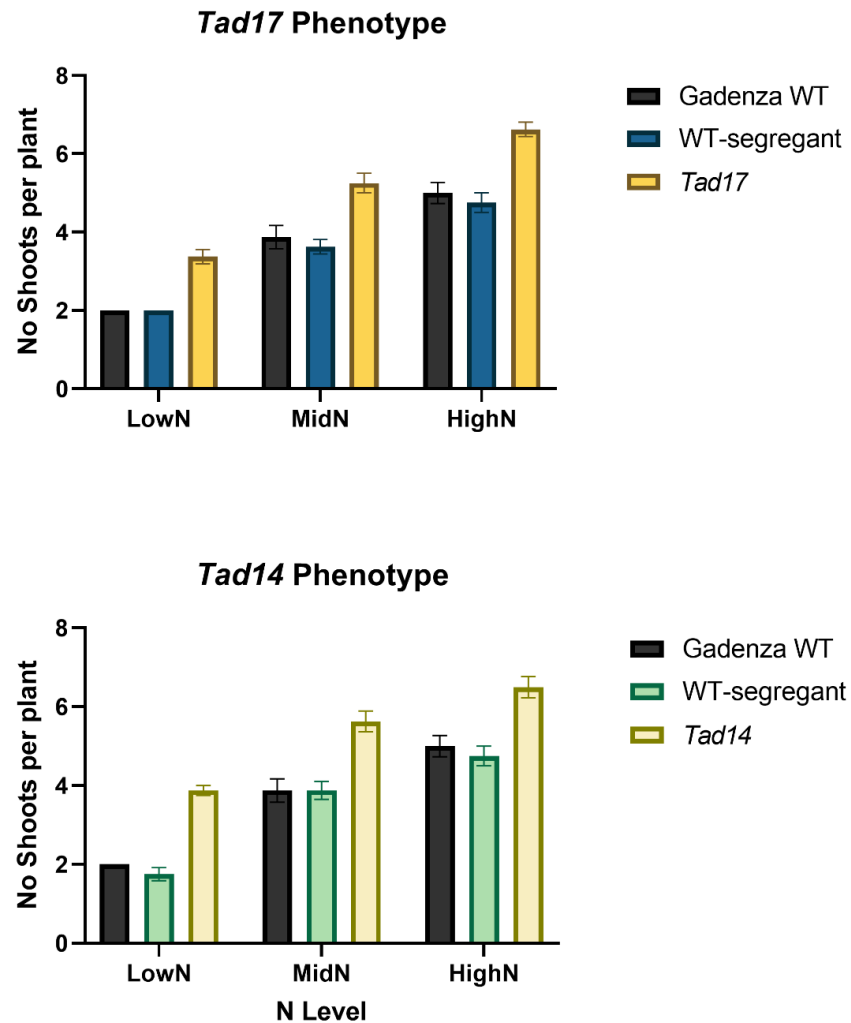


Figure S6: Number of shoots of *Tad17* SL-deficient (BC1F3) and *Tad14* SL-insensitive mutants (BC3F3) grown under three different N regimes (Low, Mid and High N) compared to the respective WT segregant lines. Values are means of eight biological replicates (four biological replicates from two different BC_xF₂ lines), and error bars represent SE. Plants were grown in pots filled with a mixture of vermiculite and perlite for three weeks in a CE room.

References

- ABE, S., SADO, A., TANAKA, K., KISUGI, T., ASAMI, K., OTA, S., KIM, H. I., YONEYAMA, K., XIE, X., OHNISHI, T., SETO, Y., YAMAGUCHI, S., AKIYAMA, K., YONEYAMA, K. & NOMURA, T. 2014. Carlactone is converted to carlactonoic acid by MAX1 in Arabidopsis and its methyl ester can directly interact with AtD14 in vitro. *PNAS*, 111, 18084-18089.
- AGUILAR-MARTÍNEZ, J. A., POZA-CARRIÓN, C. & CUBAS, P. 2007. Arabidopsis BRANCHED1 Acts as an Integrator of Branching Signals within Axillary Buds. *The Plant Cell*, 19, 458-472.
- AKIYAMA, K., MATSUZAKI, K.-I. & HAYASHI, H. 2005. Plant sesquiterpenes induce hyphal branching in arbuscular mycorrhizal fungi. *Nature*, 435, 824-827.
- ALDER, A., JAMIL, M., MARZORATI, M., BRUNO, M., VERMATHEN, M., BIGLER, P., GHISLA, S., BOUWMEESTER, H., BEYER, P. & AL-BABILI, S. 2012. The Path from β -Carotene to Carlactone, a Strigolactone-Like Plant Hormone. *Science*, 335, 1348-1351.
- ALVAREZ, J. M., RIVERAS, E., VIDAL, E. A., GRAS, D. E., CONTRERAS-LÓPEZ, O., TAMAYO, K. P., ACEITUNO, F., GÓMEZ, I., RUFFEL, S., LEJAY, L., JORDANA, X. & GUTIÉRREZ, R. A. 2014. Systems approach identifies TGA1 and TGA4 transcription factors as important regulatory components of the nitrate response of *Arabidopsis thaliana* roots. *The Plant Journal*, 80, 1-13.
- ALZUETA, I., ABELEDO, L. G., MIGNONE, C. M. & MIRALLES, D. J. 2012. Differences between wheat and barley in leaf and tillering coordination under contrasting nitrogen and sulfur conditions. *European Journal of Agronomy*, 41, 92-102.
- ARAUS, V., VIDAL, E. A., PUELMA, T., ALAMOS, S., MIEULET, D., GUIDERDONI, E. & GUTIÉRREZ, R. A. 2016. Members of BTB Gene Family of Scaffold Proteins Suppress Nitrate Uptake and Nitrogen Use Efficiency. *Plant Physiology*, 171, 1523-1532.
- ARGYROS, R. D., MATHEWS, D. E., CHIANG, Y. H., PALMER, C. M., THIBAUT, D. M., ETHERIDGE, N., ARGYROS, D. A., MASON, M. G., KIEBER, J. J. & SCHALLER, G. E. 2008. Type B response regulators of Arabidopsis play key roles in cytokinin signaling and plant development. *The Plant Cell*, 20, 2102-2116.
- ARITE, T., HANADA, A., UMEHARA, M., YAMAGUCHI, S., ISHIKAWA, S., KYOZUKA, J. & MAEKAWA, M. 2009. d14, a Strigolactone-Insensitive Mutant of Rice, Shows an Accelerated Outgrowth of Tillers. *Plant and Cell Physiology*, 50, 1416-1424.
- ARITE, T., IWATA, H., OHSHIMA, K., MAEKAWA, M., NAKAJIMA, M., KOJIMA, M., SAKAKIBARA, H. & KYOZUKA, J. 2007. DWARF10, an RMS1/MAX4/DAD1 ortholog, controls lateral bud outgrowth in rice. *The Plant Journal*, 51, 1019-1029.
- BAENA-GONZÁLEZ, E., ROLLAND, F., THEVELEIN, J. M. & SHEEN, J. 2007. A central integrator of transcription networks in plant stress and energy signalling. *Nature*, 448, 938-942.
- BANASIAK, J., BORGHI, L., STEC, N., MARTINOIA, E. & JASIŃSKI, M. 2020. The Full-Size ABCG Transporter of *Medicago truncatula* Is Involved in Strigolactone Secretion, Affecting Arbuscular Mycorrhiza. *Frontiers in Plant Science*, 11, 18.
- BARBIER, F., PÉRON, T., LECERF, M., PEREZ-GARCIA, M.-D., BARRIÈRE, Q., ROLČÍK, J., BOUTET-MERCEY, S., CITERNE, S., LEMOINE, R., PORCHERON, B., ROMAN, H., LEDUC, N., LE GOURRIEREC, J., BERTHELOOT, J. & SAKR, S. 2015a. Sucrose is an early modulator of the key hormonal mechanisms controlling bud outgrowth in *Rosa hybrida*. *Journal of Experimental Botany*, 66, 2569-2582.

- BARBIER, F. F., DUN, E. A., KERR, S. C., CHABIKWA, T. G. & BEVERIDGE, C. A. 2019. An Update on the Signals Controlling Shoot Branching. *Trends in Plant Science*, 24, 220-236.
- BARBIER, F. F., LUNN, J. E. & BEVERIDGE, C. A. 2015b. Ready, steady, go! A sugar hit starts the race to shoot branching. *Current Opinion in Plant Biology*, 25, 39-45.
- BAUER, B. & VON WIRÉN, N. 2020. Modulating tiller formation in cereal crops by the signalling function of fertilizer nitrogen forms. *Scientific Reports*, 10, 20504.
- BEGUM, N., QIN, C., AHANGER, M. A., RAZA, S., KHAN, M. I., ASHRAF, M., AHMED, N. & ZHANG, L. 2019. Role of Arbuscular Mycorrhizal Fungi in Plant Growth Regulation: Implications in Abiotic Stress Tolerance. *Frontiers in Plant Science*, 10, 1068.
- BENNETT, T., LIANG, Y., SEALE, M., WARD, S., MÜLLER, D. & LEYSER, O. 2016. Strigolactone regulates shoot development through a core signalling pathway. *Biology Open*, 5, 1806-1820.
- BENNETT, T., SIEBERER, T., WILLETT, B., BOOKER, J., LUSCHNIG, C. & LEYSER, O. 2006. The Arabidopsis MAX Pathway Controls Shoot Branching by Regulating Auxin Transport. *Current Biology*, 16, 553-563.
- BERNARD, S. M. & HABASH, D. Z. 2009. The importance of cytosolic glutamine synthetase in nitrogen assimilation and recycling. *New Phytologist*, 182, 608-620.
- BERRY, P. M., SPINK, J. H., FOULKES, M. J. & WADE, A. 2003. Quantifying the contributions and losses of dry matter from non-surviving shoots in four cultivars of winter wheat. *Field Crops Research*, 80, 111-121.
- BOOKER, J., AULDRIDGE, M., WILLS, S., MCCARTY, D., KLEE, H. & LEYSER, O. 2004. MAX3/CCD7 is a carotenoid cleavage dioxygenase required for the synthesis of a novel plant signaling molecule. *Current Biology*, 14, 1232-1238.
- BOOKER, J., SIEBERER, T., WRIGHT, W., WILLIAMSON, L., WILLETT, B., STIRNBERG, P., TURNBULL, C., SRINIVASAN, M., GODDARD, P. & LEYSER, O. 2005. MAX1 Encodes a Cytochrome P450 Family Member that Acts Downstream of MAX3/4 to Produce a Carotenoid-Derived Branch-Inhibiting Hormone. *Developmental Cell*, 8, 443-449.
- BORGHI, L., KANG, J., KO, D., LEE, Y. & MARTINOIA, E. 2015. The role of ABCG-type ABC transporters in phytohormone transport. *Biochemical Society Transactions*, 43, 924-930.
- BORRILL, P., HARRINGTON, S. A., SIMMONDS, J. & UAUY, C. 2019. Identification of Transcription Factors Regulating Senescence in Wheat through Gene Regulatory Network Modelling. *Plant Physiology*, 180, 1740-1755.
- BOUGUYON, E., BRUN, F., MEYNARD, D., KUBEŠ, M., PERVENT, M., LERAN, S., LACOMBE, B., KROUK, G., GUIDERDONI, E., ZAŽÍMALOVÁ, E., HOYEROVÁ, K., NACRY, P. & GOJON, A. 2015. Multiple mechanisms of nitrate sensing by Arabidopsis nitrate transceptor NRT1.1. *Nature Plants*, 1, 15015.
- BRAMBILLA, V., MARTIGNAGO, D., GORETTI, D., CERISE, M., SOMSSICH, M., DE ROSA, M., GALBIATI, F., SHRESTHA, R., LAZZARO, F. & SIMON, R. 2017. Antagonistic transcription factor complexes modulate the floral transition in rice. *The Plant Cell*, 29, 2801-2816.
- BRAY, N. L., PIMENTEL, H., MELSTED, P. & PACTER, L. 2016. Near-optimal probabilistic RNA-seq quantification. *Nature Biotechnology*, 34, 525-527.

- BREWER, P. B., DUN, E. A., GUI, R., MASON, M. G. & BEVERIDGE, C. A. 2015. Strigolactone Inhibition of Branching Independent of Polar Auxin Transport. *Plant Physiology*, 168, 1820–1829.
- BREWER, P. B., YONEYAMA, K., FILARDO, F., MEYERS, E., SCAFFIDI, A., FRICKEY, T., AKIYAMA, K., SETO, Y., DUN, E. A., CREMER, J. E., KERR, S. C., WATERS, M. T., FLEMATTI, G. R., MASON, M. G., WEILLER, G., YAMAGUCHI, S., NOMURA, T., SMITH, S. M., YONEYAMA, K. & BEVERIDGE, C. A. 2016. LATERAL BRANCHING OXIDOREDUCTASE acts in the final stages of strigolactone biosynthesis in Arabidopsis. *PNAS*, 113, 6301-6306.
- BRUNO, M., KOSCHMIEDER, J., WUEST, F., SCHAUB, P., FEHLING-KASCHEK, M., TIMMER, J., BEYER, P. & AL-BABILI, S. 2016. Enzymatic study on AtCCD4 and AtCCD7 and their potential to form acyclic regulatory metabolites. *Journal of Experimental Botany*, 67, 5993-6005.
- BUCHNER, P. & HAWKESFORD, M. J. 2014. Complex phylogeny and gene expression patterns of members of the NITRATE TRANSPORTER 1/PEPTIDE TRANSPORTER family (NPF) in wheat. *Journal of Experimental Botany*, 65, 5697-5710.
- BULMAN, P. & HUNT, L. 1988. Relationships among tillering, spike number and grain yield in winter wheat (*Triticum aestivum* L.) in Ontario. *Canadian Journal of Plant Science*, 68, 583-596.
- BUTT, H., JAMIL, M., WANG, J. Y., AL-BABILI, S. & MAHFOUZ, M. 2018. Engineering plant architecture via CRISPR/Cas9-mediated alteration of strigolactone biosynthesis. *BMC Plant Biology*, 18, 174.
- CARDOSO, C., ZHANG, Y., JAMIL, M., HEPWORTH, J., CHARNIKHOVA, T., DIMKPA, S. O. N., MEHARG, C., WRIGHT, M. H., LIU, J., MENG, X., WANG, Y., LI, J., MCCOUCH, S. R., LEYSER, O., PRICE, A. H., BOUWMEESTER, H. J. & RUYTER-SPIRA, C. 2014. Natural variation of rice strigolactone biosynthesis is associated with the deletion of two *MAX1* orthologs. *PNAS*, 111, 2379-2384.
- CASARTELLI, A., MELINO, V. J., BAUMANN, U., RIBONI, M., SUCHECKI, R., JAYASINGHE, N. S., MENDIS, H., WATANABE, M., ERBAN, A., ZUTHER, E., HOEFGEN, R., ROESSNER, U., OKAMOTO, M. & HEUER, S. 2019. Opposite fates of the purine metabolite allantoin under water and nitrogen limitations in bread wheat. *Plant Molecular Biology*, 99, 477-497.
- CHANGENET, V., MACADRÉ, C., BOUTET-MERCEY, S., MAGNE, K., JANUARIO, M., DALMAIS, M., BENDAHMANE, A., MOUILLE, G. & DUFRESNE, M. 2021. Overexpression of a Cytochrome P450 Monooxygenase Involved in Orobanchol Biosynthesis Increases Susceptibility to Fusarium Head Blight. *Frontiers in Plant Science*, 12, 662025.
- CHEN, J. G., CHENG, S. H., CAO, W. & ZHOU, X. 1998. Involvement of endogenous plant hormones in the effect of mixed nitrogen source on growth and tillering of wheat. *Journal of Plant Nutrition*, 21, 87-97.
- CHEN, L., HAO, L., PARRY, M. A., PHILLIPS, A. L. & HU, Y. G. 2014. Progress in TILLING as a tool for functional genomics and improvement of crops. *Journal of Integrative Plant Biology*, 56, 425-443.
- CHEN, L. Q., QU, X. Q., HOU, B. H., SOSSO, D., OSORIO, S., FERNIE, A. R. & FROMMER, W. B. 2012. Sucrose efflux mediated by SWEET proteins as a key step for phloem transport. *Science*, 335, 207-211.

- CHESTERFIELD, R. J., VICKERS, C. E. & BEVERIDGE, C. A. 2020. Translation of Strigolactones from Plant Hormone to Agriculture: Achievements, Future Perspectives, and Challenges. *Trends in Plant Science*, 25, 1087-1106.
- CHOI, M.-S., WOO, M.-O., KOH, E.-B., LEE, J., HAM, T.-H., SEO, H. S. & KOH, H.-J. 2012. Teosinte Branched 1 modulates tillering in rice plants. *Plant Cell Reports*, 31, 57-65.
- COOK, C. E., WHICHARD, L. P., TURNER, B., WALL, M. E. & EGLEY, G. H. 1966. Germination of Witchweed (*Striga lutea* Lour.): Isolation and Properties of a Potent Stimulant. *Science*, 154, 1189-1190.
- CRAWFORD, S., SHINOHARA, N., SIEBERER, T., WILLIAMSON, L., GEORGE, G., HEPWORTH, J., MÜLLER, D., DOMAGALSKA, M. A. & LEYSER, O. 2010. Strigolactones enhance competition between shoot branches by dampening auxin transport. *Development*, 137, 2905-2913.
- CURCI, P. L., AIESE CIGLIANO, R., ZULUAGA, D. L., JANNI, M., SANSEVERINO, W. & SONNANTE, G. 2017. Transcriptomic response of durum wheat to nitrogen starvation. *Scientific Reports*, 7, 1176.
- DAI, X., SINHAROY, S., UDVARDI, M. & ZHAO, P. X. 2013. PlantTFcat: an online plant transcription factor and transcriptional regulator categorization and analysis tool. *BMC Bioinformatics*, 14, 321.
- DARWINKEL, A. 1978. Patterns of tillering and grain production of winter wheat at a wide range of plant densities. *Netherlands Journal of Agricultural Science*, 383-398.
- DE JONG, M., GEORGE, G., ONGARO, V., WILLIAMSON, L., WILLETTS, B., LJUNG, K., MCCULLOCH, H. & LEYSER, O. 2014. Auxin and Strigolactone Signaling Are Required for Modulation of Arabidopsis Shoot Branching by Nitrogen Supply. *Plant Physiology*, 166, 384-395.
- DE SAINT GERMAIN, A., LIGEROT, Y., DUN, E. A., PILLOT, J. P., ROSS, J. J., BEVERIDGE, C. A. & RAMEAU, C. 2013. Strigolactones stimulate internode elongation independently of gibberellins. *Plant Physiology*, 163, 1012-1025.
- DING, C., YOU, J., CHEN, L., WANG, S. & DING, Y. 2014. Nitrogen fertilizer increases spikelet number per panicle by enhancing cytokinin synthesis in rice. *Plant Cell Reports*, 33, 363-371.
- DOEBLEY, J. F., GAUT, B. S. & SMITH, B. D. 2006. The Molecular Genetics of Crop Domestication. *Cell*, 127, 1309-1321.
- DOMAGALSKA, M. A. & LEYSER, O. 2011. Signal integration in the control of shoot branching. *Nature Reviews Molecular Cell Biology*, 12, 211.
- DREW, M. C. & SAKER, L. R. 1984. Uptake and long-distance transport of phosphate, potassium and chloride in relation to internal ion concentrations in barley: evidence of non-allosteric regulation. *Planta*, 160, 500-507.
- DUAN, E., WANG, Y., LI, X., LIN, Q., ZHANG, T., WANG, Y., ZHOU, C., ZHANG, H., JIANG, L., WANG, J., LEI, C., ZHANG, X., GUO, X., WANG, H. & WAN, J. 2019a. OsSHI1 Regulates Plant Architecture Through Modulating the Transcriptional Activity of IPA1 in Rice. *The Plant Cell*, 31, 1026-1042.
- DUAN, J., YU, H., YUAN, K., LIAO, Z., MENG, X., JING, Y., LIU, G., CHU, J. & LI, J. 2019b. Strigolactone promotes cytokinin degradation through transcriptional activation of *CYTOKININ OXIDASE/DEHYDROGENASE 9* in rice. *PNAS*, 116, 14319.

- DUN, E. A., DE SAINT GERMAIN, A., RAMEAU, C. & BEVERIDGE, C. A. 2012. Antagonistic Action of Strigolactone and Cytokinin in Bud Outgrowth Control. *Plant Physiology*, 158, 487–498.
- ELHANI, S., MARTOS, V., RHARRABTI, Y., ROYO, C. & GARCÍA DEL MORAL, L. F. 2007. Contribution of main stem and tillers to durum wheat (*Triticum turgidum* L. var. durum) grain yield and its components grown in Mediterranean environments. *Field Crops Research*, 103, 25-35.
- EVERS, J. & VOS, J. 2013. Modeling branching in cereals. *Frontiers in Plant Science*, 4, 399.
- EVERS, J. B., VOS, J., ANDRIEU, B. & STRUIK, P. C. 2006. Cessation of tillering in spring wheat in relation to light interception and red : far-red ratio. *Annals of Botany*, 97, 649-658.
- FANG, Z., BAI, G., HUANG, W., WANG, Z., WANG, X. & ZHANG, M. 2017. The Rice Peptide Transporter *OsNPF7.3* Is Induced by Organic Nitrogen, and Contributes to Nitrogen Allocation and Grain Yield. *Frontiers in Plant Science*, 8, 1338.
- FANG, Z., JI, Y., HU, J., GUO, R., SUN, S. & WANG, X. 2020. Strigolactones and Brassinosteroids Antagonistically Regulate the Stability of the D53–OsBZR1 Complex to Determine *FC1* Expression in Rice Tillering. *Molecular Plant*, 13, 586-597.
- FANG, Z., XIA, K., YANG, X., GROTEMEYER, M. S., MEIER, S., RENTSCH, D., XU, X. & ZHANG, M. 2013. Altered expression of the PTR/NRT1 homologue *OsPTR9* affects nitrogen utilization efficiency, growth and grain yield in rice. *Plant Biotechnology Journal*, 11, 446-58.
- FELEMBAN, A., BRAGUY, J., ZURBRIGGEN, M. D. & AL-BABILI, S. 2019. Apocarotenoids Involved in Plant Development and Stress Response. *Frontiers in Plant Science*, 10, 1168.
- FICHTNER, F., BARBIER, F. F., FEIL, R., WATANABE, M., ANNUNZIATA, M. G., CHABIKWA, T. G., HÖFGEN, R., STITT, M., BEVERIDGE, C. A. & LUNN, J. E. 2017. Trehalose 6-phosphate is involved in triggering axillary bud outgrowth in garden pea (*Pisum sativum* L.). *The Plant Journal*, 92, 611-623.
- FICHTNER, F. & LUNN, J. E. 2021. The Role of Trehalose 6-Phosphate (Tre6P) in Plant Metabolism and Development. *Annual Review of Plant Biology*, 72, 737-760.
- FIGUEROA, C. M., FEIL, R., ISHIHARA, H., WATANABE, M., KÖLLING, K., KRAUSE, U., HÖHNE, M., ENCKE, B., PLAXTON, W. C., ZEEMAN, S. C., LI, Z., SCHULZE, W. X., HOEFGEN, R., STITT, M. & LUNN, J. E. 2016. Trehalose 6–phosphate coordinates organic and amino acid metabolism with carbon availability. *The Plant Journal*, 85, 410-423.
- FINLAYSON, S. A., KRISHNAREDDY, S. R., KEBROM, T. H. & CASAL, J. J. 2010. Phytochrome regulation of branching in Arabidopsis. *Plant Physiology*, 152, 1914-1927.
- FOO, E., MORRIS, S. E., PARMENTER, K., YOUNG, N., WANG, H., JONES, A., RAMEAU, C., TURNBULL, C. G. N. & BEVERIDGE, C. A. 2007. Feedback Regulation of Xylem Cytokinin Content Is Conserved in Pea and Arabidopsis. *Plant Physiology*, 143, 1418-1428.
- FOO, E., YONEYAMA, K., HUGILL, C. J., QUITTENDEN, L. J. & REID, J. B. 2013. Strigolactones and the Regulation of Pea Symbioses in Response to Nitrate and Phosphate Deficiency. *Molecular Plant*, 6, 76-87.
- FRASER, J., DOUGHERTY, C. & LANGER, R. 1982. Dynamics of tiller populations of standard height and semi-dwarf wheats. *New Zealand Journal of Agricultural Research*, 25, 321-328.

- GAUDINIER, A., RODRIGUEZ-MEDINA, J., ZHANG, L., OLSON, A., LISERON-MONFILS, C., BÅGMAN, A.-M., FORET, J., ABBITT, S., TANG, M., LI, B., RUNCIE, D. E., KLIEBENSTEIN, D. J., SHEN, B., FRANK, M. J., WARE, D. & BRADY, S. M. 2018. Transcriptional regulation of nitrogen-associated metabolism and growth. *Nature*, 563, 259-264.
- GAUFICHON, L., ROTHSTEIN, S. J. & SUZUKI, A. 2015. Asparagine Metabolic Pathways in Arabidopsis. *Plant and Cell Physiology*, 57, 675-689.
- GOBENA, D., SHIMELS, M., RICH, P. J., RUYTER-SPIRA, C., BOUWMEESTER, H., KANUGANTI, S., MENGISTE, T. & EJETA, G. 2017. Mutation in sorghum *LOW GERMINATION STIMULANT 1* alters strigolactones and causes Striga resistance. *PNAS*, 114, 4471-4476.
- GOMEZ-ROLDAN, V., FERMAS, S., BREWER, P. B., PUECH-PAGÈS, V., DUN, E. A., PILLOT, J.-P., LETISSE, F., MATUSOVA, R., DANOUN, S., PORTAIS, J.-C., BOUWMEESTER, H., BÉCARD, G., BEVERIDGE, C. A., RAMEAU, C. & ROCHANGE, S. F. 2008. Strigolactone inhibition of shoot branching. *Nature*, 455, 189-194.
- GONZÁLEZ-GRANDÍO, E., PAJORO, A., FRANCO-ZORRILLA, J. M., TARANCÓN, C., IMMINK, R. G. H. & CUBAS, P. 2017. Abscisic acid signaling is controlled by a BRANCHED1/HD-ZIP I cascade in Arabidopsis axillary buds. *PNAS*, 114, E245-E254.
- GRAS, D. E., VIDAL, E. A., UNDURRAGA, S. F., RIVERAS, E., MORENO, S., DOMINGUEZ-FIGUEROA, J., ALABADI, D., BLÁZQUEZ, M. A., MEDINA, J. & GUTIÉRREZ, R. A. 2018. SMZ/SNZ and gibberellin signaling are required for nitrate-elicited delay of flowering time in *Arabidopsis thaliana*. *Journal of Experimental Botany*, 69, 619-631.
- GUAN, J. C., KOCH, K. E., SUZUKI, M., WU, S., LATSHAW, S., PETRUFF, T., GOULET, C., KLEE, H. J. & MCCARTY, D. R. 2012. Diverse roles of strigolactone signaling in maize architecture and the uncoupling of a branching-specific subnetwork. *Plant Physiology*, 160, 1303-1317.
- HA, C. V., LEYVA-GONZÁLEZ, M. A., OSAKABE, Y., TRAN, U. T., NISHIYAMA, R., WATANABE, Y., TANAKA, M., SEKI, M., YAMAGUCHI, S., DONG, N. V., YAMAGUCHI-SHINOZAKI, K., SHINOZAKI, K., HERRERA-ESTRELLA, L. & TRAN, L. S. 2014. Positive regulatory role of strigolactone in plant responses to drought and salt stress. *PNAS*, 111, 851-856.
- HARASIM, E., WESOLOWSKI, M., KWIATKOWSKI, C., HARASIM, P., STANIAK, M. & FELEDYN-SZEWCZYK, B. 2016. The contribution of yield components in determining the productivity of winter wheat (*Triticum aestivum* L.). *Acta Agrobotanica*, 69.
- HARRISON, P. J. & BUGG, T. D. 2014. Enzymology of the carotenoid cleavage dioxygenases: reaction mechanisms, inhibition and biochemical roles. *Archives of Biochemistry and Biophysics*, 544, 105-111.
- HE, X., QU, B., LI, W., ZHAO, X., TENG, W., MA, W., REN, Y., LI, B., LI, Z. & TONG, Y. 2015. The Nitrate-Inducible NAC Transcription Factor TaNAC2-5A Controls Nitrate Response and Increases Wheat Yield *Plant Physiology*, 169, 1991-2005.
- HIROSE, N., TAKEI, K., KUROHA, T., KAMADA-NOBUSADA, T., HAYASHI, H. & SAKAKIBARA, H. 2008. Regulation of cytokinin biosynthesis, compartmentalization and translocation. *Journal of Experimental Botany*, 59, 75-83.
- HU, B., WANG, W., OU, S., TANG, J., LI, H., CHE, R., ZHANG, Z., CHAI, X., WANG, H., WANG, Y., LIANG, C., LIU, L., PIAO, Z., DENG, Q., DENG, K., XU, C., LIANG, Y., ZHANG, L., LI, L. & CHU, C. 2015. Variation in NRT1.1B contributes to nitrate-use divergence between rice subspecies. *Nature Genetics*, 47, 834-838.

- ISHIDA, K., YAMASHINO, T., YOKOYAMA, A. & MIZUNO, T. 2008. Three type-B response regulators, ARR1, ARR10 and ARR12, play essential but redundant roles in cytokinin signal transduction throughout the life cycle of *Arabidopsis thaliana*. *Plant and Cell Physiology*, 49, 47-57.
- ISHIKAWA, S., MAEKAWA, M., ARITE, T., ONISHI, K., TAKAMURE, I. & KYOZUKA, J. 2005. Suppression of tiller bud activity in tillering dwarf mutants of rice. *Plant and Cell Physiology*, 46, 79-86.
- JAMIL, M., KANAMPIU, F. K., KARAYA, H., CHARNIKHOVA, T. & BOUWMEESTER, H. J. 2012. *Striga hermonthica* parasitism in maize in response to N and P fertilisers. *Field Crops Research*, 134, 1-10.
- Jl, Y., HUANG, W., WU, B., FANG, Z. & WANG, X. 2020. The amino acid transporter AAP1 mediates growth and grain yield by regulating neutral amino acid uptake and reallocation in *Oryza sativa*. *Journal of experimental botany*, 71, 4763-4777.
- JIANG, J., MA, S., YE, N., JIANG, M., CAO, J. & ZHANG, J. 2017. WRKY transcription factors in plant responses to stresses. *Journal of Integrative Plant Biology*, 59, 86-101.
- JIANG, L., LIU, X., XIONG, G., LIU, H., CHEN, F., WANG, L., MENG, X., LIU, G., YU, H., YUAN, Y., YI, W., ZHAO, L., MA, H., HE, Y., WU, Z., MELCHER, K., QIAN, Q., XU, H. E., WANG, Y. & LI, J. 2013. DWARF 53 acts as a repressor of strigolactone signalling in rice. *Nature*, 504, 401-405.
- JIN, J., TIAN, F., YANG, D.-C., MENG, Y.-Q., KONG, L., LUO, J. & GAO, G. 2016. PlantTFDB 4.0: toward a central hub for transcription factors and regulatory interactions in plants. *Nucleic Acids Research*, 45, D1040-D1045.
- KAMADA-NOBUSADA, T., MAKITA, N., KOJIMA, M. & SAKAKIBARA, H. 2013. Nitrogen-Dependent Regulation of De Novo Cytokinin Biosynthesis in Rice: The Role of Glutamine Metabolism as an Additional Signal. *Plant and Cell Physiology*, 54, 1881-1893.
- KAUR, H., CHOWRASIA, S., GAUR, V. S. & MONDAL, T. K. 2021. Allantoin: Emerging Role in Plant Abiotic Stress Tolerance. *Plant Molecular Biology Reporter*, 39, 648-661.
- KEBROM, T. H. 2017. A Growing Stem Inhibits Bud Outgrowth – The Overlooked Theory of Apical Dominance. *Frontiers in Plant Science*, 8, 1874.
- KEBROM, T. H., BURSON, B. L. & FINLAYSON, S. A. 2006. Phytochrome B represses *Teosinte Branched1* expression and induces sorghum axillary bud outgrowth in response to light signals. *Plant Physiology*, 140, 1109-1117.
- KEBROM, T. H., CHANDLER, P. M., SWAIN, S. M., KING, R. W., RICHARDS, R. A. & SPIELMEYER, W. 2012. Inhibition of Tiller Bud Outgrowth in the tin Mutant of Wheat Is Associated with Precocious Internode Development. *Plant Physiology*, 160, 308-318.
- KEBROM, T. H. & MULLET, J. E. 2016. Transcriptome Profiling of Tiller Buds Provides New Insights into PhyB Regulation of Tillering and Indeterminate Growth in Sorghum. *Plant Physiology*, 170, 2232-2250.
- KEBROM, T. H., SPIELMEYER, W. & FINNEGAN, E. J. 2013. Grasses provide new insights into regulation of shoot branching. *Trends in Plant Science*, 18, 41-48.
- KERSEY, P. J., ALLEN, J. E., ALLOT, A., BARBA, M., BODDU, S., BOLT, B. J., CARVALHO-SILVA, D., CHRISTENSEN, M., DAVIS, P., GRABMUELLER, C., KUMAR, N., LIU, Z., MAUREL, T., MOORE, B., MCDOWALL, M. D., MAHESWARI, U., NAAMATI, G., NEWMAN, V., ONG, C. K., PAULINI, M., PEDRO, H., PERRY, E., RUSSELL, M., SPARROW, H., TAPANARI, E.,

- TAYLOR, K., VULLO, A., WILLIAMS, G., ZADISSIA, A., OLSON, A., STEIN, J., WEI, S., TELLO-RUIZ, M., WARE, D., LUCIANI, A., POTTER, S., FINN, R. D., URBAN, M., HAMMOND-KOSACK, K. E., BOLSER, D. M., DE SILVA, N., HOWE, K. L., LANGRIDGE, N., MASLEN, G., STAINES, D. M. & YATES, A. 2018. Ensembl Genomes 2018: an integrated omics infrastructure for non-vertebrate species. *Nucleic Acids Research*, 46, D802-D808.
- KHUSH, G. S. 1999. Green revolution: preparing for the 21st century. *Genome*, 42, 646-655.
- KIBA, T., INABA, J., KUDO, T., UEDA, N., KONISHI, M., MITSUDA, N., TAKIGUCHI, Y., KONDOU, Y., YOSHIZUMI, T., OHME-TAKAGI, M., MATSUI, M., YANO, K., YANAGISAWA, S. & SAKAKIBARA, H. 2018. Repression of Nitrogen Starvation Responses by Members of the Arabidopsis GARP-Type Transcription Factor NIGT1/HRS1 Subfamily. *The Plant Cell*, 30, 925-945.
- KIBA, T., KUDO, T., KOJIMA, M. & SAKAKIBARA, H. 2010. Hormonal control of nitrogen acquisition: roles of auxin, abscisic acid, and cytokinin. *Journal of Experimental Botany*, 62, 1399-1409.
- KIBA, T., TAKEI, K., KOJIMA, M. & SAKAKIBARA, H. 2013. Side-chain modification of cytokinins controls shoot growth in Arabidopsis. *Developmental Cell*, 27, 452-461.
- KIM, D., LANGMEAD, B. & SALZBERG, S. L. 2015. HISAT: a fast spliced aligner with low memory requirements. *Nature Methods*, 12, 357-360.
- KOBAE, Y., KAMEOKA, H., SUGIMURA, Y., SAITO, K., OHTOMO, R., FUJIWARA, T. & KYOZUKA, J. 2018. Strigolactone Biosynthesis Genes of Rice are Required for the Punctual Entry of Arbuscular Mycorrhizal Fungi into the Roots. *Plant and Cell Physiology*, 544-553.
- KOBAYASHI, K., MASUDA, T., TAKAMIYA, K. & OHTA, H. 2006. Membrane lipid alteration during phosphate starvation is regulated by phosphate signaling and auxin/cytokinin cross-talk. *The Plant Journal*, 47, 238-248.
- KOHLER, W., CHARNIKHOVA, T., LIU, Q., BOURS, R., DOMAGALSKA, M. A., BEGUERIE, S., VERSTAPPEN, F., LEYSER, O., BOUWMEESTER, H. & RUYTER-SPIRA, C. 2011. Strigolactones are transported through the xylem and play a key role in shoot architectural response to phosphate deficiency in nonarbuscular mycorrhizal host Arabidopsis. *Plant Physiology*, 155, 974-987.
- KOPYLOVA, E., NOÉ, L. & TOUZET, H. 2012. SortMeRNA: fast and accurate filtering of ribosomal RNAs in metatranscriptomic data. *Bioinformatics*, 28, 3211-3217.
- KRASILEVA, K. V., VASQUEZ-GROSS, H. A., HOWELL, T., BAILEY, P., PARAISO, F., CLISSOLD, L., SIMMONDS, J., RAMIREZ-GONZALEZ, R. H., WANG, X., BORRILL, P., FOSKER, C., AYLING, S., PHILLIPS, A. L., UAUY, C. & DUBCOVSKY, J. 2017. Uncovering hidden variation in polyploid wheat. *PNAS*, 114, E913-E921.
- KRETZSCHMAR, T., KOHLER, W., SASSE, J., BORGHI, L., SCHLEGEL, M., BACHELIER, J. B., REINHARDT, D., BOURS, R., BOUWMEESTER, H. J. & MARTINOIA, E. 2012. A petunia ABC protein controls strigolactone-dependent symbiotic signalling and branching. *Nature*, 483, 341-344.
- KUDO, T., KIBA, T. & SAKAKIBARA, H. 2010. Metabolism and long-distance translocation of cytokinins. *Journal of Integrative Plant Biology*, 52, 53-60.
- KURAKAWA, T., UEDA, N., MAEKAWA, M., KOBAYASHI, K., KOJIMA, M., NAGATO, Y., SAKAKIBARA, H. & KYOZUKA, J. 2007. Direct control of shoot meristem activity by a cytokinin-activating enzyme. *Nature*, 445, 652-655.

- KUROHA, T., TOKUNAGA, H., KOJIMA, M., UEDA, N., ISHIDA, T., NAGAWA, S., FUKUDA, H., SUGIMOTO, K. & SAKAKIBARA, H. 2009. Functional Analyses of LONELY GUY Cytokinin-Activating Enzymes Reveal the Importance of the Direct Activation Pathway in Arabidopsis *The Plant Cell*, 21, 3152-3169.
- LEE, D. K., REDILLAS, M., JUNG, H., CHOI, S., KIM, Y. S. & KIM, J. K. 2018. A Nitrogen Molecular Sensing System, Comprised of the *ALLANTOINASE* and *UREIDE PERMEASE 1* Genes, Can Be Used to Monitor N Status in Rice. *Frontiers in Plant Science*, 9, 444.
- LEE, Y. H., FOSTER, J., CHEN, J., VOLL, L. M., WEBER, A. P. & TEGEDER, M. 2007. AAP1 transports uncharged amino acids into roots of Arabidopsis. *The Plant Journal*, 50, 305-319.
- LENG, Y., GAO, Y., CHEN, L., YANG, Y., HUANG, L., DAI, L., REN, D., XU, Q., ZHANG, Y., PONCE, K., HU, J., SHEN, L., ZHANG, G., CHEN, G., DONG, G., GAO, Z., GUO, L., YE, G., QIAN, Q., ZHU, L. & ZENG, D. 2020. Using *Heading date 1* preponderant alleles from indica cultivars to breed high-yield, high-quality japonica rice varieties for cultivation in south China. *Plant Biotechnology Journal*, 18, 119-128.
- LÉRAN, S., MUÑOS, S., BRACHET, C., TILLARD, P., GOJON, A. & LACOMBE, B. 2013. Arabidopsis NRT1.1 is a bidirectional transporter involved in root-to-shoot nitrate translocation. *Molecular Plant*, 6, 1984-7.
- LEWIS, J. M., MACKINTOSH, C. A., SHIN, S., GILDING, E., KRAVCHENKO, S., BALDRIDGE, G., ZEYEN, R. & MUEHLBAUER, G. J. 2008. Overexpression of the maize *Teosinte Branched1* gene in wheat suppresses tiller development. *Plant Cell Reports*, 27, 1217-1225.
- LEYVA-GONZÁLEZ, M. A., IBARRA-LACLETTE, E., CRUZ-RAMÍREZ, A. & HERRERA-ESTRELLA, L. 2012. Functional and transcriptome analysis reveals an acclimatization strategy for abiotic stress tolerance mediated by Arabidopsis NF-YA family members. *PLOS ONE*, 7, e48138.
- LI, C., CAO, W. & DAI, T. 2001. Dynamic characteristics of floret primordium development in wheat. *Field Crops Research*, 71, 71-76.
- LI, J.-Y., FU, Y.-L., PIKE, S. M., BAO, J., TIAN, W., ZHANG, Y., CHEN, C.-Z., ZHANG, Y., LI, H.-M., HUANG, J., LI, L.-G., SCHROEDER, J. I., GASSMANN, W. & GONG, J.-M. 2010. The Arabidopsis Nitrate Transporter NRT1.8 Functions in Nitrate Removal from the Xylem Sap and Mediates Cadmium Tolerance *The Plant Cell*, 22, 1633-1646.
- LI, X., XIA, K., LIANG, Z., CHEN, K., GAO, C. & ZHANG, M. 2016. MicroRNA393 is involved in nitrogen-promoted rice tillering through regulation of auxin signal transduction in axillary buds. *Scientific Reports*, 6, 32158.
- LIAO, Y., SMYTH, G. K. & SHI, W. 2013. featureCounts: an efficient general purpose program for assigning sequence reads to genomic features. *Bioinformatics*, 30, 923-930.
- LIAO, Z., YU, H., DUAN, J., YUAN, K., YU, C., MENG, X., KOU, L., CHEN, M., JING, Y., LIU, G., SMITH, S. M. & LI, J. 2019. SLR1 inhibits MOC1 degradation to coordinate tiller number and plant height in rice. *Nature Communications*, 10, 2738.
- LIN, H., WANG, R., QIAN, Q., YAN, M., MENG, X., FU, Z., YAN, C., JIANG, B., SU, Z., LI, J. & WANG, Y. 2009. DWARF27, an Iron-Containing Protein Required for the Biosynthesis of Strigolactones, Regulates Rice Tiller Bud Outgrowth. *The Plant Cell*, 21, 1512-1525.
- LIN, Y.-L. & TSAY, Y.-F. 2017. Influence of differing nitrate and nitrogen availability on flowering control in Arabidopsis. *Journal of Experimental Botany*, 68, 2603-2609.

- LIU, J., CHENG, X., LIU, P. & SUN, J. 2017. miR156-Targeted SBP-Box Transcription Factors Interact with DWARF53 to Regulate *TEOSINTE BRANCHED1* and *BARREN STALK1* Expression in Bread Wheat. *Plant Physiology*, 174, 1931-1948.
- LIU, Q., HARBERD, NICHOLAS P. & FU, X. 2016. SQUAMOSA Promoter Binding Protein-like Transcription Factors: Targets for Improving Cereal Grain Yield. *Molecular Plant*, 9, 765-767.
- LIU, T., LI, Y., REN, J., QIAN, Y., YANG, X., DUAN, W. & HOU, X. 2013. Nitrate or NaCl regulates floral induction in *Arabidopsis thaliana*. *Biologia*, 68, 215-222.
- LO, S.-F., YANG, S.-Y., CHEN, K.-T., HSING, Y.-I., ZEEVAART, J. A. D., CHEN, L.-J. & YU, S.-M. 2008. A Novel Class of Gibberellin 2-Oxidases Control Semidwarfism, Tillering, and Root Development in Rice. *The Plant Cell*, 20, 2603-2618.
- LÓPEZ-RÁEZ, J. A., CHARNIKHOVA, T., GÓMEZ-ROLDÁN, V., MATUSOVA, R., KOHLEN, W., DE VOS, R., VERSTAPPEN, F., PUECH-PAGES, V., BÉCARD, G., MULDER, P. & BOUWMEESTER, H. 2008. Tomato strigolactones are derived from carotenoids and their biosynthesis is promoted by phosphate starvation. *New Phytologist*, 178, 863-874.
- LOVE, M. I., HUBER, W. & ANDERS, S. 2014. Moderated estimation of fold change and dispersion for RNA-seq data with DESeq2. *Genome Biology*, 15, 550.
- LU, K., WU, B., WANG, J., ZHU, W., NIE, H., QIAN, J., HUANG, W. & FANG, Z. 2018. Blocking amino acid transporter Os AAP 3 improves grain yield by promoting outgrowth buds and increasing tiller number in rice. *Plant Biotechnology Journal*, 16, 1710-1722.
- LU, Z., YU, H., XIONG, G., WANG, J., JIAO, Y., LIU, G., JING, Y., MENG, X., HU, X., QIAN, Q., FU, X., WANG, Y. & LI, J. 2013. Genome-Wide Binding Analysis of the Transcription Activator IDEAL PLANT ARCHITECTURE1 Reveals a Complex Network Regulating Rice Plant Architecture. *The Plant Cell*, 25, 3743-3759.
- LUO, L., PAN, S., LIU, X., WANG, H. & XU, G. 2017. Nitrogen deficiency inhibits cell division-determined elongation, but not initiation, of rice tiller buds. *Israel Journal of Plant Sciences*, 64, 32-40.
- LUO, L., QIN, R., LIU, T., YU, M., YANG, T. & XU, G. 2018a. OsASN1 Plays a Critical Role in Asparagine-Dependent Rice Development. *International journal of molecular sciences*, 20, 130.
- LUO, L., TAKAHASHI, M., KAMEOKA, H., QIN, R., SHIGA, T., KANNO, Y., SEO, M., ITO, M., XU, G. & KYOZUKA, J. 2019. Developmental analysis of the early steps in strigolactone-mediated axillary bud dormancy in rice. *The Plant Journal*, 97, 1006-1021.
- LUO, L., WANG, H., LIU, X., HU, J., ZHU, X., PAN, S., QIN, R., WANG, Y., ZHAO, P., FAN, X. & XU, G. 2018b. Strigolactones affect the translocation of nitrogen in rice. *Plant Science*, 270, 190-197.
- LUO, L., ZHANG, Y. & XU, G. 2020. How does nitrogen shape plant architecture? *Journal of Experimental Botany*, 71, 4415-4427.
- MA, H., DUAN, J., KE, J., HE, Y., GU, X., XU, T.-H., YU, H., WANG, Y., BRUNZELLE, J. S., JIANG, Y., ROTHBART, S. B., XU, H. E., LI, J. & MELCHER, K. 2017. A D53 repression motif induces oligomerization of TOPLESS corepressors and promotes assembly of a corepressor-nucleosome complex. *Science Advances*, 3, e1601217.
- MAEDA, Y., KONISHI, M., KIBA, T., SAKURABA, Y., SAWAKI, N., KURAI, T., UEDA, Y., SAKAKIBARA, H. & YANAGISAWA, S. 2018. A NIGT1-centred transcriptional cascade

- regulates nitrate signalling and incorporates phosphorus starvation signals in Arabidopsis. *Nature Communications*, 9, 1376.
- MALONEY, V. J., PARK, J.-Y., UNDA, F. & MANSFIELD, S. D. 2015. Sucrose phosphate synthase and sucrose phosphate phosphatase interact in planta and promote plant growth and biomass accumulation. *Journal of Experimental Botany*, 66, 4383-4394.
- MARRO, N., LIDOY, J., CHICO, M. Á., RIAL, C., GARCÍA, J., VARELA, R. M., MACÍAS, F. A., POZO, M. J., JANOUŠKOVÁ, M. & LÓPEZ-RÁEZ, J. A. 2022. Strigolactones: New players in the nitrogen–phosphorus signalling interplay. *Plant, Cell & Environment*, 45, 512-527.
- MARTIN, M. 2011. Cutadapt removes adapter sequences from high-throughput sequencing reads. *EMBnet.journal*, 17, 10-12.
- MARZEC, M. & MELZER, M. 2018. Regulation of Root Development and Architecture by Strigolactones under Optimal and Nutrient Deficiency Conditions. *International Journal of Molecular Sciences*, 19, 1887.
- MARZEC, M., SITUMORANG, A., BREWER, P. B. & BRĄSZEWSKA, A. 2020. Diverse Roles of MAX1 Homologues in Rice. *Genes*, 11, 1348.
- MASHIGUCHI, K., SASAKI, E., SHIMADA, Y., NAGAE, M., UENO, K., NAKANO, T., YONEYAMA, K., SUZUKI, Y. & ASAMI, T. 2009. Feedback-regulation of strigolactone biosynthetic genes and strigolactone-regulated genes in Arabidopsis. *Bioscience, Biotechnology, and Biochemistry*, 73, 2460-2465.
- MASHIGUCHI, K., SETO, Y. & YAMAGUCHI, S. 2021. Strigolactone biosynthesis, transport and perception. *The Plant Journal*, 105, 335-350.
- MASON, M. G., ROSS, J. J., BABST, B. A., WIENCLAW, B. N. & BEVERIDGE, C. A. 2014. Sugar demand, not auxin, is the initial regulator of apical dominance. *PNAS*, 111, 6092-6097.
- MATUSOVA, R., RANI, K., VERSTAPPEN, F. W., FRANSSSEN, M. C., BEALE, M. H. & BOUWMEESTER, H. J. 2005. The strigolactone germination stimulants of the plant-parasitic *Striga* and *Orobanche* spp. are derived from the carotenoid pathway. *Plant Physiology*, 139, 920-34.
- MCCALLUM, C. M., COMAI, L., GREENE, E. A. & HENIKOFF, S. 2000. Targeted screening for induced mutations. *Nature Biotechnology*, 18, 455-457.
- MCMMASTER, G. S. 2005. Phytomers, phyllochrons, phenology and temperate cereal development. *The Journal of Agricultural Science*, 143, 137-150.
- MCSTEEN, P. & LEYSER, O. 2005. SHOOT BRANCHING. *Annual Review of Plant Biology*, 56, 353-374.
- MEHRABI, F. & SEPASKHAH, A. R. 2022. Leaf Nitrogen, Based on SPAD Chlorophyll Reading Can Determine Agronomic Parameters of Winter Wheat. *International Journal of Plant Production*, 16, 77-91.
- MENG, X., WANG, X., ZHANG, Z., XIONG, S., WEI, Y., GUO, J., ZHANG, J., WANG, L., MA, X. & TEGEDER, M. 2021. Transcriptomic, proteomic, and physiological studies reveal key players in wheat nitrogen use efficiency under both high and low nitrogen supply. *Journal of Experimental Botany*, 72, 4435-4456.
- MESSING, S. A. J., GABELLI, S. B., ECHEVERRIA, I., VOGEL, J. T., GUAN, J. C., TAN, B. C., KLEE, H. J., MCCARTY, D. R. & AMZEL, L. M. 2010. Structural Insights into Maize Viviparous14, a Key Enzyme in the Biosynthesis of the Phytohormone Abscisic Acid. *The Plant Cell*, 22, 2970-2980.

- MINAKUCHI, K., KAMEOKA, H., YASUNO, N., UMEHARA, M., LUO, L., KOBAYASHI, K., HANADA, A., UENO, K., ASAMI, T., YAMAGUCHI, S. & KYOZUKA, J. 2010. FINE CULM1 (FC1) Works Downstream of Strigolactones to Inhibit the Outgrowth of Axillary Buds in Rice. *Plant and Cell Physiology*, 51, 1127-1135.
- MITCHELL, J. H., REBETZKE, G. J., CHAPMAN, S. C. & FUKAI, S. 2013. Evaluation of reduced-tillering (*tin*) wheat lines in managed, terminal water deficit environments. *Journal of experimental botany*, 64, 3439-3451.
- MIYAWAKI, K., MATSUMOTO-KITANO, M. & KAKIMOTO, T. 2004. Expression of cytokinin biosynthetic isopentenyltransferase genes in Arabidopsis: tissue specificity and regulation by auxin, cytokinin, and nitrate. *The Plant Journal*, 37, 128-138.
- MÜLLER, B. & SHEEN, J. 2007. Advances in cytokinin signaling. *Science*, 318, 68-69.
- MÜLLER, D., WALDIE, T., MIYAWAKI, K., TO, J. P., MELNYK, C. W., KIEBER, J. J., KAKIMOTO, T. & LEYSER, O. 2015. Cytokinin is required for escape but not release from auxin mediated apical dominance. *The Plant Journal*, 82, 874-886.
- NAKAMURA, Y. 2013. Phosphate starvation and membrane lipid remodeling in seed plants. *Progress in Lipid Research*, 52, 43-50.
- NOGUERO, M. & LACOMBE, B. 2016. Transporters Involved in Root Nitrate Uptake and Sensing by Arabidopsis. *Frontiers in Plant Science*, 7, 1391.
- OHASHI, M., ISHIYAMA, K., KOJIMA, S., KOJIMA, M., SAKAKIBARA, H., YAMAYA, T. & HAYAKAWA, T. 2017. Lack of Cytosolic Glutamine Synthetase1;2 Activity Reduces Nitrogen-Dependent Biosynthesis of Cytokinin Required for Axillary Bud Outgrowth in Rice Seedlings. *Plant and Cell Physiology*, 58, 679-690.
- OHASHI, M., ISHIYAMA, K., KOJIMA, S., KONISHI, N., NAKANO, K., KANNO, K., HAYAKAWA, T. & YAMAYA, T. 2015a. Asparagine Synthetase1, but not Asparagine Synthetase2, is Responsible for the Biosynthesis of Asparagine Following the Supply of Ammonium to Rice Roots. *Plant and Cell Physiology*, 56, 769-778.
- OHASHI, M., ISHIYAMA, K., KOJIMA, S., KONISHI, N., SASAKI, K., MIYAO, M., HAYAKAWA, T. & YAMAYA, T. 2018. Outgrowth of Rice Tillers Requires Availability of Glutamine in the Basal Portions of Shoots. *Rice*, 11, 31.
- OHASHI, M., ISHIYAMA, K., KUSANO, M., FUKUSHIMA, A., KOJIMA, S., HANADA, A., KANNO, K., HAYAKAWA, T., SETO, Y. & KYOZUKA, J. 2015b. Lack of cytosolic glutamine synthetase1; 2 in vascular tissues of axillary buds causes severe reduction in their outgrowth and disorder of metabolic balance in rice seedlings. *The Plant Journal*, 81, 347-356.
- OLAS, J. J., VAN DINGENEN, J., ABEL, C., DZIAŁO, M. A., FEIL, R., KRAPP, A., SCHLERETH, A. & WAHL, V. 2019. Nitrate acts at the Arabidopsis thaliana shoot apical meristem to regulate flowering time. *New Phytologist*, 223, 814-827.
- OLDROYD, G. E. D. & LEYSER, O. 2020. A plant's diet, surviving in a variable nutrient environment. *Science*, 368, 6486.
- OSUGI, A., KOJIMA, M., TAKEBAYASHI, Y., UEDA, N., KIBA, T. & SAKAKIBARA, H. 2017. Systemic transport of trans-zeatin and its precursor have differing roles in Arabidopsis shoots. *Nature Plants*, 3, 17112.
- PALTA, J. A., FILLERY, I. R. & REBETZKE, G. J. 2007. Restricted-tillering wheat does not lead to greater investment in roots and early nitrogen uptake. *Field Crops Research*, 104, 52-59.

- PAUL, M. J. & FOYER, C. H. 2001. Sink regulation of photosynthesis. *Journal of Experimental Botany*, 52, 1383-1400.
- PEARCE, S., KIPPES, N., CHEN, A., DEBERNARDI, J. M. & DUBCOVSKY, J. 2016. RNA-seq studies using wheat *PHYTOCHROME B* and *PHYTOCHROME C* mutants reveal shared and specific functions in the regulation of flowering and shade-avoidance pathways. *BMC Plant Biology*, 16, 141.
- PEDROTTI, L., WEISTE, C., NÄGELE, T., WOLF, E., LORENZIN, F., DIETRICH, K., MAIR, A., WECKWERTH, W., TEIGE, M., BAENA-GONZÁLEZ, E. & DRÖGE-LASER, W. 2018. Snf1-RELATED KINASE1-Controlled C/S1-bZIP Signaling Activates Alternative Mitochondrial Metabolic Pathways to Ensure Plant Survival in Extended Darkness. *The Plant Cell*, 30, 495-509.
- POITOUT, A., CRABOS, A., PETŘÍK, I., NOVÁK, O., KROUK, G., LACOMBE, B. & RUFFEL, S. 2018. Responses to Systemic Nitrogen Signaling in Arabidopsis Roots Involve trans-Zeatin in Shoots. *The Plant Cell*, 30, 1243-1257.
- POWER, J. F. & ALESSI, J. 1978. Tiller development and yield of standard and semidwarf spring wheat varieties as affected by nitrogen fertilizer. *The Journal of Agricultural Science*, 90, 97-108.
- PRIYA, R. & SIVA, R. 2014. Phylogenetic analysis and evolutionary studies of plant carotenoid cleavage dioxygenase gene. *Gene*, 548, 223-233.
- PRUSINKIEWICZ, P., CRAWFORD, S., SMITH, R. S., LJUNG, K., BENNETT, T., ONGARO, V. & LEYSER, O. 2009. Control of bud activation by an auxin transport switch. *PNAS*, 106, 17431-17436.
- QU, B., HE, X., WANG, J., ZHAO, Y., TENG, W., SHAO, A., ZHAO, X., MA, W., WANG, J., LI, B., LI, Z. & TONG, Y. 2015. A wheat CCAAT box-binding transcription factor increases the grain yield of wheat with less fertilizer input. *Plant Physiology*, 167, 411-23.
- RAMAKERS, C., RUIJTER, J. M., DEPREZ, R. H. & MOORMAN, A. F. 2003. Assumption-free analysis of quantitative real-time polymerase chain reaction (PCR) data. *Neurosci Lett*, 339, 62-6.
- RAMEAU, C., BERTHELOOT, J., LEDUC, N., ANDRIEU, B., FOUCHER, F. & SAKR, S. 2015. Multiple pathways regulate shoot branching. *Frontiers in Plant Science*, 5, 741.
- RAMÍREZ-GONZÁLEZ, R. H., BORRILL, P., LANG, D., HARRINGTON, S. A., BRINTON, J., VENTURINI, L., DAVEY, M., JACOBS, J., VAN EX, F., PASHA, A., KHEDIKAR, Y., ROBINSON, S. J., CORY, A. T., FLORIO, T., CONCIA, L., JUERY, C., SCHOONBEEK, H., STEUERNAGEL, B., XIANG, D., RIDOUT, C. J., CHALHOUB, B., MAYER, K. F. X., BENHAMED, M., LATRASSE, D., BENDAHMANE, A., WULFF, B. B. H., APPELS, R., TIWARI, V., DATLA, R., CHOULET, F., POZNIAK, C. J., PROVART, N. J., SHARPE, A. G., PAUX, E., SPANNAGL, M., BRÄUTIGAM, A. & UAUY, C. 2018. The transcriptional landscape of polyploid wheat. *Science*, 361, 6403.
- RAUDVERE, U., KOLBERG, L., KUZMIN, I., ARAK, T., ADLER, P., PETERSON, H. & VILO, J. 2019. g:Profiler: a web server for functional enrichment analysis and conversions of gene lists (2019 update). *Nucleic Acids Research*, 47, W191-W198.
- REDILLAS, M. C. F. R., BANG, S. W., LEE, D.-K., KIM, Y. S., JUNG, H., CHUNG, P. J., SUH, J.-W. & KIM, J.-K. 2019. Allantoin accumulation through overexpression of *ureide permease1* improves rice growth under limited nitrogen conditions. *Plant Biotechnology Journal*, 17, 1289-1301.

- RIEU, I. & POWERS, S. J. 2009. Real-Time Quantitative RT-PCR: Design, Calculations, and Statistics. *The Plant Cell*, 21, 1031–1033.
- ROY, S. 2016. Function of MYB domain transcription factors in abiotic stress and epigenetic control of stress response in plant genome. *Plant Signaling & Behavior*, 11, e1117723.
- RUAN, W., GUO, M., WU, P. & YI, K. 2017. Phosphate starvation induced *OsPHR4* mediates Pi-signaling and homeostasis in rice. *Plant Molecular Biology*, 93, 327-340.
- RUBIN, G., TOHGE, T., MATSUDA, F., SAITO, K. & SCHEIBLE, W.-R. D. 2009. Members of the LBD Family of Transcription Factors Repress Anthocyanin Synthesis and Affect Additional Nitrogen Responses in Arabidopsis. *The Plant Cell*, 21, 3567-3584.
- RUYTER-SPIRA, C., KOHLEN, W., CHARNIKHOVA, T., VAN ZEIJL, A., VAN BEZOUWEN, L., DE RUIJTER, N., CARDOSO, C., LOPEZ-RAEZ, J. A., MATUSOVA, R., BOURS, R., VERSTAPPEN, F. & BOUWMEESTER, H. 2011. Physiological Effects of the Synthetic Strigolactone Analog GR24 on Root System Architecture in Arabidopsis: Another Belowground Role for Strigolactones?. *Plant Physiology*, 155, 721-734.
- SADRAS, V. O. & SLAFER, G. A. 2012. Environmental modulation of yield components in cereals: Heritabilities reveal a hierarchy of phenotypic plasticities. *Field Crops Research*, 127, 215-224.
- SAKAKIBARA, H. 2021. Cytokinin biosynthesis and transport for systemic nitrogen signaling. *The Plant Journal*, 105, 421-430.
- SAKAKIBARA, H., TAKEI, K. & HIROSE, N. 2006. Interactions between nitrogen and cytokinin in the regulation of metabolism and development. *Trends in Plant Science*, 11, 440-448.
- SAKAMOTO, T. & MATSUOKA, M. 2004. Generating high-yielding varieties by genetic manipulation of plant architecture. *Current Opinion in Biotechnology*, 15, 144-147.
- SAKR, S., WANG, M., DÉDALDÉCHAMP, F., PEREZ-GARCIA, M. D., OGÉ, L., HAMAMA, L. & ATANASSOVA, R. 2018. The Sugar-Signaling Hub: Overview of Regulators and Interaction with the Hormonal and Metabolic Network. *International Journal of Molecular Sciences*, 19, 2506.
- SANTORO, V., SCHIAVON, M., VISENTIN, I., CONSTÁN-AGUILAR, C., CARDINALE, F. & CELI, L. 2021. Strigolactones affect phosphorus acquisition strategies in tomato plants. *Plant, Cell & Environment*, 44, 3628-3642.
- SASSE, J., SIMON, S., GÜBELI, C., LIU, G.-W., CHENG, X., FRIML, J., BOUWMEESTER, H., MARTINOIA, E. & BORGHI, L. 2015. Asymmetric localizations of the ABC transporter PaPDR1 trace paths of directional strigolactone transport. *Current Biology*, 25, 647-655.
- SATO, T., MAEKAWA, S., KONISHI, M., YOSHIOKA, N., SASAKI, Y., MAEDA, H., ISHIDA, T., KATO, Y., YAMAGUCHI, J. & YANAGISAWA, S. 2017. Direct transcriptional activation of BT genes by NLP transcription factors is a key component of the nitrate response in Arabidopsis. *Biochemical and Biophysical Research Communications*, 483, 380-386.
- SCHÄFER, M., BRÜTTING, C., MEZA-CANALES, I. D., GROßKINSKY, D. K., VANKOVA, R., BALDWIN, I. T. & MELDAU, S. 2015. The role of cis-zeatin-type cytokinins in plant growth regulation and mediating responses to environmental interactions. *Journal of Experimental Botany*, 66, 4873-84.
- SEALE, M., BENNETT, T. & LEYSER, O. 2017. BRC1 expression regulates bud activation potential but is not necessary or sufficient for bud growth inhibition in Arabidopsis. *Development*, 144, 1661-1673.

- SEMAGN, K., BABU, R., HEARNE, S. & OLSEN, M. 2014. Single nucleotide polymorphism genotyping using Kompetitive Allele Specific PCR (KASP): overview of the technology and its application in crop improvement. *Molecular Breeding*, 33, 1-14.
- SETO, Y., SADO, A., ASAMI, K., HANADA, A., UMEHARA, M., AKIYAMA, K. & YAMAGUCHI, S. 2014. Carlactone is an endogenous biosynthetic precursor for strigolactones. *PNAS*, 111, 1640-1645.
- SHABEK, N., TICCHIARELLI, F., MAO, H., HINDS, T. R., LEYSER, O. & ZHENG, N. 2018. Structural plasticity of D3-D14 ubiquitin ligase in strigolactone signalling. *Nature*, 563, 652-656.
- SHARMA, R. 1995. Tiller mortality and its relationship to grain yield in spring wheat. *Field Crops Research*, 41, 55-60.
- SHINDO, M., SHIMOMURA, K., YAMAGUCHI, S. & UMEHARA, M. 2018. Upregulation of *DWARF27* is associated with increased strigolactone levels under sulfur deficiency in rice. *Plant Direct*, 2, e00050.
- SHINOHARA, N., TAYLOR, C. & LEYSER, O. 2013. Strigolactone Can Promote or Inhibit Shoot Branching by Triggering Rapid Depletion of the Auxin Efflux Protein PIN1 from the Plasma Membrane. *PLOS Biology*, 11, e1001474.
- SHIRATAKE, K., NOTAGUCHI, M., MAKINO, H., SAWAI, Y. & BORGHI, L. 2019. Petunia PLEIOTROPIC DRUG RESISTANCE 1 Is a Strigolactone Short-Distance Transporter with Long-Distance Outcomes. *Plant and Cell Physiology*, 60, 1722-1733.
- SIAME, B. A., WEERASURIYA, Y., WOOD, K., EJETA, G. & BUTLER, L. G. 1993. Isolation of strigol, a germination stimulant for *Striga asiatica*, from host plants. *Journal of Agricultural and Food Chemistry*, 41, 1486-1491.
- SLAFER, G., CALDERINI, D., MIRALLES, D., REYNOLDS, M., RAJARAM, S. & MCNAB, A. Increasing yield potential in wheat: Breaking the barriers. Proceedings CIMMYT International Symposium: Generation of yield components and compensation in wheat: opportunities for further increasing yield potential. Mexico: CIMMYT, 1996. 101-133.
- SLAFER, G. A., SAVIN, R. & SADRAS, V. O. 2014. Coarse and fine regulation of wheat yield components in response to genotype and environment. *Field Crops Research*, 157, 71-83.
- SMART, C. M. 1994. Gene expression during leaf senescence. *New phytologist*, 126, 419-448.
- SONG, W., LI, J., SUN, H., HUANG, S., GONG, X., MA, Q., ZHANG, Y. & XU, G. 2013. Increased photosynthetic capacity in response to nitrate is correlated with enhanced cytokinin levels in rice cultivar with high responsiveness to nitrogen nutrients. *Plant and Soil*, 373, 981-993.
- SONG, X., LU, Z., YU, H., SHAO, G., XIONG, J., MENG, X., JING, Y., LIU, G., XIONG, G., DUAN, J., YAO, X.-F., LIU, C.-M., LI, H., WANG, Y. & LI, J. 2017. IPA1 functions as a downstream transcription factor repressed by D53 in strigolactone signaling in rice. *Cell Research*, 27, 1128-1141.
- SOREFAN, K., BOOKER, J., HAUROGNÉ, K., GOUSSOT, M., BAINBRIDGE, K., FOO, E., CHATFIELD, S., WARD, S., BEVERIDGE, C., RAMEAU, C. & LEYSER, O. 2003. MAX4 and RMS1 are orthologous dioxygenase-like genes that regulate shoot branching in Arabidopsis and pea. *Genes & Development*, 17, 1469-1474.
- SOUNDAPPAN, I., BENNETT, T., MORFFY, N., LIANG, Y., STANGA, J. P., ABBAS, A., LEYSER, O. & NELSON, D. C. 2015. SMAX1-LIKE/D53 Family Members Enable Distinct MAX2-

- Dependent Responses to Strigolactones and Karrikins in Arabidopsis. *The Plant Cell*, 27, 3143-3159.
- SPARKES, D., HOLME, S. & GAJU, O. 2006. Does light quality initiate tiller death in wheat? *European Journal of Agronomy*, 24, 212-217.
- STEIN, O. & GRANOT, D. 2018. Plant Fructokinases: Evolutionary, Developmental, and Metabolic Aspects in Sink Tissues. *Frontiers in Plant Science*, 9, 339.
- STORTENBEKER, N. & BEMER, M. 2018. The SAUR gene family: the plant's toolbox for adaptation of growth and development. *Journal of Experimental Botany*, 70, 17-27.
- SULTANA, N., ISLAM, S., JUHASZ, A., YANG, R., SHE, M., ALHABBAR, Z., ZHANG, J. & MA, W. 2020. Transcriptomic Study for Identification of Major Nitrogen Stress Responsive Genes in Australian Bread Wheat Cultivars. *Frontiers in Genetics*, 11, 583785.
- SUN, H., GUO, X., QI, X., FENG, F., XIE, X., ZHANG, Y. & ZHAO, Q. 2021. SPL14/17 act downstream of strigolactone signalling to modulate rice root elongation in response to nitrate supply. *The Plant Journal*, 106, 649-660.
- SUN, H., TAO, J., LIU, S., HUANG, S., CHEN, S., XIE, X., YONEYAMA, K., ZHANG, Y. & XU, G. 2014. Strigolactones are involved in phosphate- and nitrate-deficiency-induced root development and auxin transport in rice. *Journal of Experimental Botany*, 65, 6735-6746.
- SUN, Y., LUO, W., JAIN, A., LIU, L., AI, H., LIU, X., FENG, B., ZHANG, L., ZHANG, Z., GUOHUA, X. & SUN, S. 2018. OsPHR3 affects the traits governing nitrogen homeostasis in rice. *BMC Plant Biology*, 18, 241.
- SUPEK, F., BOŠNJAK, M., ŠKUNCA, N. & ŠMUC, T. 2011. REVIGO Summarizes and Visualizes Long Lists of Gene Ontology Terms. *PLOS ONE*, 6, e21800.
- TAKEDA, T., SUWA, Y., SUZUKI, M., KITANO, H., UEGUCHI-TANAKA, M., ASHIKARI, M., MATSUOKA, M. & UEGUCHI, C. 2003. The OStB1 gene negatively regulates lateral branching in rice. *The Plant Journal*, 33, 513-520.
- TAKEI, K., UEDA, N., AOKI, K., KUROMORI, T., HIRAYAMA, T., SHINOZAKI, K., YAMAYA, T. & SAKAKIBARA, H. 2004a. AtIPT3 is a key determinant of nitrate-dependent cytokinin biosynthesis in Arabidopsis. *Plant and Cell Physiology*, 45, 1053-1062.
- TAKEI, K., YAMAYA, T. & SAKAKIBARA, H. 2004b. Arabidopsis CYP735A1 and CYP735A2 encode cytokinin hydroxylases that catalyze the biosynthesis of trans-zeatin. *Journal of Biological Chemistry*, 279, 41866-41872.
- TARANCÓN, C., GONZÁLEZ-GRANDÍO, E., OLIVEROS, J. C., NICOLAS, M. & CUBAS, P. 2017. A Conserved Carbon Starvation Response Underlies Bud Dormancy in Woody and Herbaceous Species. *Frontiers in Plant Science*, 8, 788.
- TEGEDER, M. & MASCLAUX-DAUBRESSE, C. 2018. Source and sink mechanisms of nitrogen transport and use. *New Phytologist*, 217, 35-53.
- TEPLOVA, I., VESELOV, S. & KUDOYAROVA, G. 1998. Changes in ABA and IAA content in the roots and shoots of wheat seedlings under nitrogen deficiency. In: BOX, J. E. (ed.) *Root Demographics and Their Efficiencies in Sustainable Agriculture, Grasslands and Forest Ecosystems: Proceedings of the 5th Symposium of the International Society of Root Research, held 14–18 July 1996 at Madren Conference Center, Clemson University, Clemson, South Carolina, USA*. Dordrecht: Springer Netherlands.

- THIMANN, K. V. & SKOOG, F. 1933. Studies on the Growth Hormone of Plants. III. The Inhibiting Action of the Growth Substance on Bud Development. *Proceedings of the National Academy of Sciences of the United States of America*, 19, 714-716.
- TOYOTA, M., TSUTSUI, I., KUSUTANI, A. & ASANUMA, K.-I. 2001. Initiation and development of spikelets and florets in wheat as influenced by shading and nitrogen supply at the spikelet phase. *Plant Production Science*, 4, 283-290.
- TREVASKIS, B., HEMMING, M. N., DENNIS, E. S. & PEACOCK, W. J. 2007. The molecular basis of vernalization-induced flowering in cereals. *Trends in Plant Science*, 12, 352-357.
- TSAI, Y. C., WEIR, N. R., HILL, K., ZHANG, W., KIM, H. J., SHIU, S. H., SCHALLER, G. E. & KIEBER, J. J. 2012. Characterization of genes involved in cytokinin signaling and metabolism from rice. *Plant Physiology*, 158, 1666-84.
- UAUY, C., WULFF, B. B. H. & DUBCOVSKY, J. 2017. Combining Traditional Mutagenesis with New High-Throughput Sequencing and Genome Editing to Reveal Hidden Variation in Polyploid Wheat. *Annual Review of Genetics*, 51, 435-454.
- UEDA, Y., KONISHI, M. & YANAGISAWA, S. 2017. Molecular basis of the nitrogen response in plants. *Soil Science and Plant Nutrition*, 63, 329-341.
- UEDA, Y., OHTSUKI, N., KADOTA, K., TEZUKA, A., NAGANO, A. J., KADOWAKI, T., KIM, Y., MIYAO, M. & YANAGISAWA, S. 2020. Gene regulatory network and its constituent transcription factors that control nitrogen-deficiency responses in rice. *New Phytologist*, 227, 1434-1452.
- UMEHARA, M., HANADA, A., MAGOME, H., TAKEDA-KAMIYA, N. & YAMAGUCHI, S. 2010. Contribution of Strigolactones to the Inhibition of Tiller Bud Outgrowth under Phosphate Deficiency in Rice. *Plant and Cell Physiology*, 51, 1118-1126.
- UMEHARA, M., HANADA, A., YOSHIDA, S., AKIYAMA, K., ARITE, T., TAKEDA-KAMIYA, N., MAGOME, H., KAMIYA, Y., SHIRASU, K., YONEYAMA, K., KYOZUKA, J. & YAMAGUCHI, S. 2008. Inhibition of shoot branching by new terpenoid plant hormones. *Nature*, 455, 195-200.
- URRIOLA, J. & RATHORE, K. S. 2015. Overexpression of a glutamine synthetase gene affects growth and development in sorghum. *Transgenic Research*, 24, 397-407.
- VAN RONGEN, M., BENNETT, T., TICCHIARELLI, F. & LEYSER, O. 2019. Connective auxin transport contributes to strigolactone-mediated shoot branching control independent of the transcription factor BRC1. *PLOS Genetics*, 15, e1008023.
- VASANTHA, S., SHEKINAH, D. E., GUPTA, C. & RAKKIYAPPAN, P. 2012. Tiller production, regulation and senescence in sugarcane (*Saccharum* species hybrid) genotypes. *Sugar Tech*, 14, 156-160.
- VEGA-ARREGUÍN, J. C., IBARRA-LACLETTE, E., JIMÉNEZ-MORAILA, B., MARTÍNEZ, O., VIELLE-CALZADA, J. P., HERRERA-ESTRELLA, L. & HERRERA-ESTRELLA, A. 2009. Deep sampling of the Palomero maize transcriptome by a high throughput strategy of pyrosequencing. *BMC Genomics*, 10, 299.
- VERWOERD, T. C., DEKKER, B. M. & HOEKEMA, A. 1989. A small-scale procedure for the rapid isolation of plant RNAs. *Nucleic Acids Res*, 17, 2362.
- VIDAL, E. A., MOYANO, T. C., CANALES, J. & GUTIÉRREZ, R. A. 2014. Nitrogen control of developmental phase transitions in *Arabidopsis thaliana*. *Journal of Experimental Botany*, 65, 5611-5618.

- WAKABAYASHI, T., YASUHARA, R., MIURA, K., TAKIKAWA, H., MIZUTANI, M. & SUGIMOTO, Y. 2021. Specific methylation of (11R)-carlactonoic acid by an Arabidopsis SABATH methyltransferase. *Planta*, 254, 88.
- WALDIE, T. & LEYSER, O. 2018. Cytokinin Targets Auxin Transport to Promote Shoot Branching. *Plant Physiology*, 177, 803–818.
- WALKER, C. H. & BENNETT, T. 2018. Forbidden fruit: dominance relationships and the control of shoot architecture. *Annual Plant Reviews*, 1, 1.
- WAN, Y., WANG, Y., SHI, Z., RENTSCH, D., WARD, J. L., HASSALL, K., SPARKS, C. A., HUTTLY, A. K., BUCHNER, P., POWERS, S., SHEWRY, P. R. & HAWKESFORD, M. J. 2021. Wheat amino acid transporters highly expressed in grain cells regulate amino acid accumulation in grain. *PLOS ONE*, 16, e0246763.
- WANG, B., SMITH, S. M. & LI, J. 2018a. Genetic Regulation of Shoot Architecture. *Annual Review of Plant Biology*, 69, 437-468.
- WANG, H., EGGERT, K., HAJIREZAEI, M. R., VON WIRÉN, N., SCHWEIZER, P., CHEN, W., CHARNIKHOVA, T., BOUWMEESTER, H., SEILER, C., KUHLMANN, M. & SREENIVASULU, N. 2018b. Abscisic acid influences tillering by modulation of strigolactones in barley. *Journal of Experimental Botany*, 69, 3883-3898.
- WANG, H., WAN, Y., BUCHNER, P., KING, R., MA, H. & HAWKESFORD, M. J. 2020a. Phylogeny and gene expression of the complete NITRATE TRANSPORTER 1/PEPTIDE TRANSPORTER FAMILY in *Triticum aestivum*. *Journal of Experimental Botany*, 71, 4531-4546.
- WANG, H., ZHANG, Y., NORRIS, A. & JIANG, C.-Z. 2022a. S1-bZIP Transcription Factors Play Important Roles in the Regulation of Fruit Quality and Stress Response. *Frontiers in Plant Science*, 12, 802802.
- WANG, J., LU, K., NIE, H., ZENG, Q., WU, B., QIAN, J. & FANG, Z. 2018c. Rice nitrate transporter OsNPF7.2 positively regulates tiller number and grain yield. *Rice*, 11, 12.
- WANG, J., SONG, K., SUN, L., QIN, Q., SUN, Y., PAN, J. & XUE, Y. 2019a. Morphological and Transcriptome Analysis of Wheat Seedlings Response to Low Nitrogen Stress. *Plants (Basel, Switzerland)*, 8, 98.
- WANG, J., WAN, R., NIE, H., XUE, S. & FANG, Z. 2022b. OsNPF5.16, a nitrate transporter gene with natural variation, is essential for rice growth and yield. *The Crop Journal*, 10, 397-406.
- WANG, J., WU, B., LU, K., WEI, Q., QIAN, J., CHEN, Y. & FANG, Z. 2019b. The Amino Acid Permease 5 (OsAAP5) Regulates Tiller Number and Grain Yield in Rice. *Plant Physiology*, 180, 1031-1045.
- WANG, L., SUN, S., JIN, J., FU, D., YANG, X., WENG, X., XU, C., LI, X., XIAO, J. & ZHANG, Q. 2015a. Coordinated regulation of vegetative and reproductive branching in rice. *PNAS*, 112, 15504-15509.
- WANG, L., WANG, B., JIANG, L., LIU, X., LI, X., LU, Z., MENG, X., WANG, Y., SMITH, S. M. & LI, J. 2015b. Strigolactone Signaling in Arabidopsis Regulates Shoot Development by Targeting D53-Like SMXL Repressor Proteins for Ubiquitination and Degradation. *The Plant Cell*, 27, 3128-3142.
- WANG, L., WANG, B., YU, H., GUO, H., LIN, T., KOU, L., WANG, A., SHAO, N., MA, H., XIONG, G., LI, X., YANG, J., CHU, J. & LI, J. 2020b. Transcriptional regulation of strigolactone signalling in Arabidopsis. *Nature*, 583, 277-281.

- WANG, M., LE MOIGNE, M.-A., BERTHELOOT, J., CRESPEL, L., PEREZ-GARCIA, M.-D., OGÉ, L., DEMOTES-MAINARD, S., HAMAMA, L., DAVIÈRE, J.-M. & SAKR, S. 2019c. BRANCHED1: A Key Hub of Shoot Branching. *Frontiers in Plant Science*, 10, 76.
- WANG, W., HU, B., YUAN, D., LIU, Y., CHE, R., HU, Y., OU, S., LIU, Y., ZHANG, Z., WANG, H., LI, H., JIANG, Z., ZHANG, Z., GAO, X., QIU, Y., MENG, X., LIU, Y., BAI, Y., LIANG, Y., WANG, Y., ZHANG, L., LI, L., SODMERGEN, JING, H., LI, J. & CHU, C. 2018d. Expression of the Nitrate Transporter Gene *OsNRT1.1A/OsNPF6.3* Confers High Yield and Early Maturation in Rice. *The Plant Cell*, 30, 638-651.
- WANG, X., NIU, Y. & ZHENG, Y. 2021. Multiple Functions of MYB Transcription Factors in Abiotic Stress Responses. *International Journal of Molecular Sciences*, 22, 6125.
- WANG, Y. & BOUWMEESTER, H. J. 2018. Structural diversity in the strigolactones. *Journal of Experimental Botany*, 69, 2219-2230.
- WANG, Y., LU, J., REN, T., HUSSAIN, S., GUO, C., WANG, S., CONG, R. & LI, X. 2017. Effects of nitrogen and tiller type on grain yield and physiological responses in rice. *AoB Plants*, 9, 2.
- WANG, Y., SHANG, L., YU, H., ZENG, L., HU, J., NI, S., RAO, Y., LI, S., CHU, J., MENG, X., WANG, L., HU, P., YAN, J., KANG, S., QU, M., LIN, H., WANG, T., WANG, Q., HU, X., CHEN, H., WANG, B., GAO, Z., GUO, L., ZENG, D., ZHU, X., XIONG, G., LI, J. & QIAN, Q. 2020c. A Strigolactone Biosynthesis Gene Contributed to the Green Revolution in Rice. *Molecular Plant*, 13, 923-932.
- WATERHOUSE, A., BERTONI, M., BIENERT, S., STUDER, G., TAURIELLO, G., GUMIENNY, R., HEER, F. T., DE BEER, T. A P., REMPFER, C., BORDOLI, L., LEPORE, R. & SCHWEDE, T. 2018. SWISS-MODEL: homology modelling of protein structures and complexes. *Nucleic Acids Research*, 46, W296-W303.
- WATERS, M. T., BREWER, P. B., BUSSELL, J. D., SMITH, S. M. & BEVERIDGE, C. A. 2012. The Arabidopsis Ortholog of Rice DWARF27 Acts Upstream of MAX1 in the Control of Plant Development by Strigolactones. *Plant Physiology*, 159, 1073-1085.
- WATERS, M. T., GUTJAHR, C., BENNETT, T. & NELSON, D. C. 2017. Strigolactone Signaling and Evolution. *Annual Review of Plant Biology*, 68, 291-322.
- WEN, Z., MEI, Y., ZHOU, J., CUI, Y., WANG, D. & WANG, N.-N. 2019. *SAUR49* Can Positively Regulate Leaf Senescence by Suppressing SSPP in Arabidopsis. *Plant and Cell Physiology*, 61, 644-658.
- WHELDON, C. D., HAMON-JOSSE, M., LUND, H., YONEYAMA, K. & BENNETT, T. 2022. Environmental strigolactone drives early growth responses to neighboring plants and soil volume in pea. *Current Biology*, 32, 1-8.
- WHIPPLE, C. J., KEBROM, T. H., WEBER, A. L., YANG, F., HALL, D., MEELEY, R., SCHMIDT, R., DOEBLEY, J., BRUTNELL, T. P. & JACKSON, D. P. 2011. grassy tillers1 promotes apical dominance in maize and responds to shade signals in the grasses. *PNAS*, 108, E506-E512.
- WU, K., WANG, S., SONG, W., ZHANG, J., WANG, Y., LIU, Q., YU, J., YE, Y., LI, S., CHEN, J., ZHAO, Y., WANG, J., WU, X., WANG, M., ZHANG, Y., LIU, B., WU, Y., HARBERD, N. P. & FU, X. 2020. Enhanced sustainable green revolution yield via nitrogen-responsive chromatin modulation in rice. *Science*, 367, 6478.
- WU, S. & LI, Y. 2021. A Unique Sulfotransferase-Involving Strigolactone Biosynthetic Route in Sorghum. *Frontiers in Plant Science*, 12, 793459.

- XIE, K., WU, C. & XIONG, L. 2006. Genomic Organization, Differential Expression, and Interaction of SQUAMOSA Promoter-Binding-Like Transcription Factors and microRNA156 in Rice. *Plant Physiology*, 142, 280–293.
- XIE, Q., MAYES, S. & SPARKES, D. L. 2016. Optimizing tiller production and survival for grain yield improvement in a bread wheat× spelt mapping population. *Annals of Botany*, 117, 51-66.
- XIE, X., WANG, G., YANG, L., CHENG, T., GAO, J., WU, Y. & XIA, Q. 2015a. Cloning and characterization of a novel *Nicotiana tabacum* ABC transporter involved in shoot branching. *Physiologia Plantarum*, 153, 299-306.
- XIE, X., YONEYAMA, K., KISUGI, T., NOMURA, T., AKIYAMA, K., ASAMI, T. & YONEYAMA, K. 2015b. Strigolactones are transported from roots to shoots, although not through the xylem. *Journal of Pesticide Science*, 40, 214-216.
- XU, H.-C., TIE, C., WANG, Z.-L. & HE, M.-R. 2015a. Physiological basis for the differences of productive capacity among tillers in winter wheat. *Journal of Integrative Agriculture*, 14, 1958-1970.
- XU, J., ZHA, M., LI, Y., DING, Y., CHEN, L., DING, C. & WANG, S. 2015b. The interaction between nitrogen availability and auxin, cytokinin, and strigolactone in the control of shoot branching in rice (*Oryza sativa* L.). *Plant Cell Reports*, 34, 1647-1662.
- XU, Q., CHEN, S., YUNJUAN, R., CHEN, S. & LIESCHE, J. 2018. Regulation of Sucrose Transporters and Phloem Loading in Response to Environmental Cues. *Plant Physiology*, 176, 930-945.
- YADAV, U. P., IVAKOV, A., FEIL, R., DUAN, G. Y., WALTHER, D., GIAVALISCO, P., PIQUES, M., CARILLO, P., HUBBERTEN, H.-M., STITT, M. & LUNN, J. E. 2014. The sucrose–trehalose 6-phosphate (Tre6P) nexus: specificity and mechanisms of sucrose signalling by Tre6P. *Journal of Experimental Botany*, 65, 1051-1068.
- YANG, H., POSTEL, S., KEMMERLING, B. & LUDEWIG, U. 2014. Altered growth and improved resistance of Arabidopsis against *Pseudomonas syringae* by overexpression of the basic amino acid transporter AtCAT1. *Plant, Cell & Environment*, 37, 1404-1414.
- YAO, R., MING, Z., YAN, L., LI, S., WANG, F., MA, S., YU, C., YANG, M., CHEN, L., CHEN, L., LI, Y., YAN, C., MIAO, D., SUN, Z., YAN, J., SUN, Y., WANG, L., CHU, J., FAN, S., HE, W., DENG, H., NAN, F., LI, J., RAO, Z., LOU, Z. & XIE, D. 2016. DWARF14 is a non-canonical hormone receptor for strigolactone. *Nature*, 536, 469-73.
- YAO, X., NIE, J., BAI, R. & SUI, X. 2020. Amino Acid Transporters in Plants: Identification and Function. *Plants (Basel, Switzerland)*, 9, 972.
- YOKOTA, T., SAKAI, H., OKUNO, K., YONEYAMA, K. & TAKEUCHI, Y. 1998. Alectrol and orobanchol, germination stimulants for *Orobancha minor*, from its host red clover. *Phytochemistry*, 49, 1967-1973.
- YONEYAMA, K., AKIYAMA, K., BREWER, P. B., MORI, N., KAWANO-KAWADA, M., HARUTA, S., NISHIWAKI, H., YAMAUCHI, S., XIE, X., UMEHARA, M., BEVERIDGE, C. A., YONEYAMA, K. & NOMURA, T. 2020a. Hydroxyl carlactone derivatives are predominant strigolactones in Arabidopsis. *Plant Direct*, 4, 1–14.
- YONEYAMA, K. & BREWER, P. B. 2021. Strigolactones, how are they synthesized to regulate plant growth and development? *Current Opinion in Plant Biology*, 63, 102072.

- YONEYAMA, K., KISUGI, T., XIE, X., ARAKAWA, R., EZAWA, T., NOMURA, T. & YONEYAMA, K. 2015. Shoot-derived signals other than auxin are involved in systemic regulation of strigolactone production in roots. *Planta*, 241, 687-698.
- YONEYAMA, K., MORI, N., SATO, T., YODA, A., XIE, X., OKAMOTO, M., IWANAGA, M., OHNISHI, T., NISHIWAKI, H., ASAMI, T., YOKOTA, T., AKIYAMA, K., YONEYAMA, K. & NOMURA, T. 2018a. Conversion of carlactone to carlactonoic acid is a conserved function of MAX1 homologs in strigolactone biosynthesis. *New Phytologist*, 218, 1522-1533.
- YONEYAMA, K., XIE, X., KIM, H. I., KISUGI, T., NOMURA, T., SEKIMOTO, H., YOKOTA, T. & YONEYAMA, K. 2012. How do nitrogen and phosphorus deficiencies affect strigolactone production and exudation? *Planta*, 235, 1197-1207.
- YONEYAMA, K., XIE, X., KUSUMOTO, D., SEKIMOTO, H., SUGIMOTO, Y., TAKEUCHI, Y. & YONEYAMA, K. 2007a. Nitrogen deficiency as well as phosphorus deficiency in sorghum promotes the production and exudation of 5-deoxystrigol, the host recognition signal for arbuscular mycorrhizal fungi and root parasites. *Planta*, 227, 125-132.
- YONEYAMA, K., XIE, X., NOMURA, T. & YONEYAMA, K. 2020b. Do Phosphate and Cytokinin Interact to Regulate Strigolactone Biosynthesis or Act Independently? *Frontiers in Plant Science*, 11, 438.
- YONEYAMA, K., XIE, X., NOMURA, T., YONEYAMA, K. & BENNETT, T. 2022. Supra-organismal regulation of strigolactone exudation and plant development in response to rhizospheric cues in rice. *Current Biology*, 32, 1-8.
- YONEYAMA, K., XIE, X., YONEYAMA, K., KISUGI, T., NOMURA, T., NAKATANI, Y., AKIYAMA, K. & MCERLEAN, C. S. P. 2018b. Which are the major players, canonical or non-canonical strigolactones? *Journal of Experimental Botany*, 69, 2231-2239.
- YONEYAMA, K., YONEYAMA, K., TAKEUCHI, Y. & SEKIMOTO, H. 2007b. Phosphorus deficiency in red clover promotes exudation of orobanchol, the signal for mycorrhizal symbionts and germination stimulant for root parasites. *Planta*, 225, 1031-1038.
- YU, S., PRATELLI, R., DENBOW, C. & PILOT, G. 2015. Suppressor mutations in the Glutamine Dumper1 protein dissociate disturbance in amino acid transport from other characteristics of the Gdu1D phenotype. *Frontiers in Plant Science*, 6, 593.
- ZHA, M., ZHAO, Y., WANG, Y., CHEN, B. & TAN, Z. 2022. Strigolactones and Cytokinin Interaction in Buds in the Control of Rice Tillering. *Frontiers in Plant Science*, 13, 837136.
- ZHANG, L., TAN, Q., LEE, R., TRETHERY, A., LEE, Y. H. & TEGEDER, M. 2010a. Altered xylem-phloem transfer of amino acids affects metabolism and leads to increased seed yield and oil content in Arabidopsis. *The Plant Cell*, 22, 3603-3620.
- ZHANG, S., LI, G., FANG, J., CHEN, W., JIANG, H., ZOU, J., LIU, X., ZHAO, X., LI, X., CHU, C., XIE, Q., JIANG, X. & ZHU, L. 2010b. The interactions among DWARF10, auxin and cytokinin underlie lateral bud outgrowth in rice. *Journal of Integrative Plant Biology*, 52, 626-38.
- ZHANG, S., ZHANG, Y., LI, K., YAN, M., ZHANG, J., YU, M., TANG, S., WANG, L., QU, H., LUO, L., XUAN, W. & XU, G. 2021. Nitrogen Mediates Flowering Time and Nitrogen Use Efficiency via Floral Regulators in Rice. *Current Biology*, 31, 671-683.e5.
- ZHANG, Y., LI, Z., MA, B., HOU, Q. & WAN, X. 2020. Phylogeny and Functions of LOB Domain Proteins in Plants. *International Journal of Molecular Sciences*, 21, 2278.

- ZHANG, Y., VAN DIJK, A. D. J., SCAFFIDI, A., FLEMATTI, G. R., HOFMANN, M., CHARNIKHOVA, T., VERSTAPPEN, F., HEPWORTH, J., VAN DER KROL, S., LEYSER, O., SMITH, S. M., ZWANENBURG, B., AL-BABILI, S., RUYTER-SPIRA, C. & BOUWMEESTER, H. J. 2014. Rice cytochrome P450 MAX1 homologs catalyze distinct steps in strigolactone biosynthesis. *Nature Chemical Biology*, 10, 1028-1033.
- ZHAO, H., LIN, K., MA, L., CHEN, Q., GAN, S. & LI, G. 2020. Arabidopsis NUCLEAR FACTOR Y A8 inhibits the juvenile-to-adult transition by activating transcription of MIR156s. *Journal of Experimental Botany*, 71, 4890-4902.
- ZHAO, L., LIU, F., CRAWFORD, N. M. & WANG, Y. 2018. Molecular Regulation of Nitrate Responses in Plants. *International Journal of Molecular Sciences*, 19, 2039.
- ZHAO, M., DING, H., ZHU, J.-K., ZHANG, F. & LI, W.-X. 2011. Involvement of miR169 in the nitrogen-starvation responses in Arabidopsis. *The New phytologist*, 190, 906-915.
- ZHENG, Y., JIAO, C., SUN, H., ROSLI, HERNAN G., POMBO, MARINA A., ZHANG, P., BANF, M., DAI, X., MARTIN, GREGORY B., GIOVANNONI, JAMES J., ZHAO, PATRICK X., RHEE, SEUNG Y. & FEI, Z. 2016. iTAK: A Program for Genome-wide Prediction and Classification of Plant Transcription Factors, Transcriptional Regulators, and Protein Kinases. *Molecular Plant*, 9, 1667-1670.
- ZHOU, F., LIN, Q., ZHU, L., REN, Y., ZHOU, K., SHABEK, N., WU, F., MAO, H., DONG, W., GAN, L., MA, W., GAO, H., CHEN, J., YANG, C., WANG, D., TAN, J., ZHANG, X., GUO, X., WANG, J., JIANG, L., LIU, X., CHEN, W., CHU, J., YAN, C., UENO, K., ITO, S., ASAMI, T., CHENG, Z., WANG, J., LEI, C., ZHAI, H., WU, C., WANG, H., ZHENG, N. & WAN, J. 2013. D14–SCFD3-dependent degradation of D53 regulates strigolactone signalling. *Nature*, 504, 406-410.
- ZOU, J., ZHANG, S., ZHANG, W., LI, G., CHEN, Z., ZHAI, W., ZHAO, X., PAN, X., XIE, Q. & ZHU, L. 2006. The rice *HIGH-TILLERING DWARF1* encoding an ortholog of Arabidopsis MAX3 is required for negative regulation of the outgrowth of axillary buds. *The Plant Journal*, 48, 687-698.